

Some pages of this thesis may have been removed for copyright restrictions.

If you have discovered material in Aston Research Explorer which is unlawful e.g. breaches copyright, (either yours or that of a third party) or any other law, including but not limited to those relating to patent, trademark, confidentiality, data protection, obscenity, defamation, libel, then please read our [Takedown policy](#) and contact the service immediately (openaccess@aston.ac.uk)

Liposomes: A Multifaceted Delivery System

Sameer Joshi
Doctor of Philosophy

ASTON UNIVERSITY
February 2017
©

©Sameer Joshi, 2017

Sameer Joshi asserts his moral right to be identified as the author of this thesis.

This copy of the thesis has been supplied in condition that anyone who consults it is understood to recognise that its copyright rests with its author and that no quotation from the thesis and no information derived from it may be published without appropriate permission or acknowledgement.

Aston University

Liposomes: A multifaceted delivery system

Sameer Joshi

Doctor of Philosophy

2017

Summary

In the past two decades, liposomes have been employed extensively as vehicles to modify and enhance the delivery of drugs, vaccines, and biomolecules. This highly versatile drug delivery system lends itself to a plethora of applications, providing both safety and efficacy. Within this thesis, the potential of liposomes to deliver challenging drugs has been explored, including the co-delivery of drugs of divergent solubility and an anti-respiratory syncytial virus (RSV) peptide.

Prior to the formulation development, the HPLC based method for simultaneous analysis of the drugs metformin HCl and glipizide was developed and validated. The formulation development initially considered the production of multi-lamellar vesicles using the conventional thin film hydration method, where the effect of lipid chain length and cholesterol content on liposome attributes was considered. After optimising the concentration of cholesterol, the capacity of liposomes to load drugs was determined by a pilot escalation study for both the drugs. The synergistic effect of drugs on *in-vitro* drug release was studied using USP-IV dissolution apparatus. Furthermore, the similar composition of lipids was used to prepare liposomes with the emerging technique, microfluidics. Here, for the first time, simultaneous co-encapsulation of hydrophilic and lipophilic drug was demonstrated. Following the optimisation of microfluidics process parameters necessary for the production of small unilamellar liposomes with narrow polydispersity index (PDI), the effect of single or co-drug encapsulation on particle characteristics and drug encapsulation was investigated, with a subsequent pilot drug escalation study to determine the drug loading capacity of liposomes produced by microfluidics. Finally, *in-vitro* studies were performed to study the synergistic effect of simultaneously co-encapsulated drugs. Also, the potential of the 1,2-disteroyl-*sn*-glycero-phosphocholine (DSPC): cholesterol formulation as a carrier of anti-RSV protein and the empty formulation itself as anti-RSV agent were investigated using bio-analytical techniques.

The co-encapsulation of drugs of divergent solubility was achieved by both the conventional thin film hydration and the emerging microfluidics technology. However, microfluidics proved advantageous with regards to time required for liposome production, one-step production of small unilamellar vesicles (SUV), narrow PDI and effective drug encapsulation with lower amounts of lipids. The liposomes of DSPC: cholesterol were also discovered to be a potential carrier of anti-RSV peptide, as well as potential anti-RSV agent itself, compared with the reported gold nanoparticles (GNPs).

Keywords: Liposomes, co-encapsulation, microfluidics, thin-film hydration, RSV

Acknowledgement

First, I want to thank my Aai (Mother), Papa (Father) and my lovely wife Neha for being backbone of my ambitions. I also want to thank all my family back home in India, my wonderful sisters, brother-in-law, father-in-law, mother-in-law and my cousins Shubhada and Aniket for supporting in every need. Nonetheless, I want to thank my lovely nieces and nephews, who maintained joy within me all the time. I also want to thank my friends Victoria, Faraz, Kishore and Gopal from Nottingham for their support.

At Aston University, first I want to thank Prof. Yvonne Perrie for accommodating me in her innovative research group, for her incredible guidance, support and care. I would like to extend my thanks to Dr. Daniel Kirby for his incredible guidance as well as for being such a wonderful, supportive and friendly supervisor. Also, I would like to thank Aston University for the sponsorship, overseas scholarship as well as for the overseas travel grant. Many thank to my research group, Prof. Afzal R Mohommed and people within the lab MB328. Many thank to the technical team, Jit, Christine and Tom for helping me in materials and equipments. Many thank to M.Pharm students Aziz and Talha for their great work. Many thanks to Elisabeth Kastner for her support in the microfluidics work. Many thank to Ehsan for the scientific discussions. Nonetheless, many thanks to Swapnil, Shital, Pranav, Alpesh, Ali, Hamad, Jas, Peter and Fraser for being wonderful buddies; you have engraved many moments of joy and happiness.

At Alabama State University (USA), I first want to thank Prof. Shree Ram Singh for the wonderful opportunity and for his support throughout my stay in the USA. Nonetheless, I want to thank Dr. Vida Dennis, Dr. Komal Vig, Dr. Swapnil Bawage, Dr. Atul Chaudhari, Dr. Pooja Tiwari, and Dr. Rade Banganzi for their support during my work at Alabama State University. I also want to thank CNBR, Alabama State University for sponsoring my research as well as stay in the USA.

I also want thank Dr. Christopher Parmenter from the University of Nottingham for his support in cryo-TEM analysis.

Finally but not for the last time, I want thank Yvonne for being my supervisor. I owe a lot to you. You were truly an inspiring, supportive and caring. I will always feel honoured of being your student, solemnly thank you Yvonne.

Thank you
Sameer Joshi

*“Whole of science is nothing more than
a refinement of the everyday thinking.”*

*Albert Einstein
1879-1955*

Publications

1. Joshi S, Hussain MT, Roces CB, Anderluzzi G, Kastner E, Salmaso S, Kirby DJ, Perrie Y. Microfluidics based manufacture of liposomes simultaneously entrapping hydrophilic and lipophilic drugs. *International journal of pharmaceutics*. 2016 Nov 30; 514(1):160-8.
2. S Joshi, D Kirby, Y Perrie, S R Singh. Novel nano-biomaterials for inhibition of respiratory syncytialvirus. *TechConnect World Innovation Conference and Expo, Technical Proceedings of the 2017, Volume 3, p. 75-78.*

Conference abstracts

1. Sameer Joshi, Daniel Kirby, Defang Ouyang, Yvonne Perrie (2014) Co-encapsulation of drugs of different solubility within liposomal drug delivery systems. *Research day (Birmingham, UK)*. Accepted 19/05/2014.
2. Sameer Joshi, Daniel Kirby, Defang Ouyang, Yvonne Perrie (2014) Liposomal drug delivery of anti-diabetic drugs metformin and glipizide. *From drug discovery to drug delivery from drug discovery to drug delivery (Athens, Greece)*. Accepted 13/10/2014.
3. Sameer Joshi, Daniel Kirby, Defang Ouyang, Yvonne Perrie (2014) Encapsulation of contrast solubility drugs in liposomal drug delivery system. *Innovations in Encapsulation (London, UK)*. Accepted 16/10/2014.
4. Sameer Joshi, Daniel Kirby, Yvonne Perrie (2015) Co-encapsulation of anti-diabetic drugs using a liposomal drug delivery system. *UKICRS (Nottingham, UK)* 05/03/2015.
5. Sameer Joshi, Daniel Kirby, Yvonne Perrie (2015) Liposomal drug delivery of anti-diabetic drugs. *CRS (Edinburgh, UK)*. Accepted 06/04/2015.
6. Sameer Joshi, Daniel Kirby, Yvonne Perrie (2015) A novel approach to co-encapsulate contrast solubility drugs in liposomal drug delivery systems. *Research day (Birmingham, UK)*. Accepted 07/05/2015.
7. Sameer Joshi, Daniel Kirby, Yvonne Perrie (2015) A novel approach to co-encapsulate contrast solubility drugs in liposomal drug delivery systems. *APS-Pharmsci (Nottingham, UK)*. Accepted 10/06/2015.
8. Sameer Joshi, Daniel Kirby, Yvonne Perrie (2015) Microfluidics for preparation of liposomes encapsulating the anti-diabetic drug metformin. *ILS (London, UK)*. Accepted 08/12/2015.

9. Sameer Joshi, Daniel Kirby, Yvonne Perrie (2016) Microfluidics based liposomal co-encapsulation of drugs of divergent solubility. CRS (Seattle, USA). Accepted 18/05/2016.
10. Sameer Joshi, Daniel Kirby, Yvonne Perrie, Shree Singh (2016). Nanobio-materials for inhibition of respiratory syncytial virus. APS Pharmsci (Glasgow, UK) Accepted 23/06/2016.
11. Sameer Joshi, Daniel Kirby, Yvonne Perrie, (2016). Microfluidics based encapsulation of hydrophilic drug APS Pharmsci (Glasgow, UK). Accepted 08/07/2016.

Content

Summary	2
Acknowledgement	3
Publications.....	5
Conference abstracts	5
Content	7
List of figures.....	12
List of tables	23
Abbreviations	25
Chapter 1: Realising the potential of liposomes: a carrier for chemical and biological molecules	27
1 Introduction to delivery systems	28
1.1 Liposomes	29
1.1.1 Classification of liposomes.....	33
1.1.2 Considerations in building liposomes.....	34
1.1.2.1 Mechanism of liposome vesicle production.....	35
1.1.2.2 Effect of transition temperature in bilayer formation	38
1.1.2.3 Role of cholesterol in liposome formation, stability and activity.....	42
1.1.2.4 Solubility of the payload	44
1.1.2.5 Vesicle properties contributing towards liposomal structure and behaviour	45
1.1.2.6 Surface charge	48
1.1.2.7 Steric Hindrance.....	48
1.1.3 Method of liposome production.....	49
1.1.3.1 Thin film hydration.....	50
1.1.3.2 Microfluidics.....	53
1.1.4 Characterisation of liposomes	56
1.1.4.1 Size and surface analysis.....	56
1.1.4.2 Drug encapsulation and release	58
1.1.4.3 Phase transition studies.....	60
1.1.4.4 Microbial assay	61
1.1.5 Applications of liposomes	61
1.2 Other particulate systems for the delivery of chemical and biological substances.....	64
1.3 Current challenges in pharmaceutical industry.....	65

1.4 Aim and Objectives	67
Chapter 2: Materials and methods	69
2.1 Materials and chemicals	70
2.2 Methods of liposome production	73
2.2.1 Thin film hydration.....	73
2.2.2 Probe sonication	74
2.2.3 Protein loading.....	74
2.2.4 Microfluidics based one step SUV production	75
2.3 Purification of liposomes, separation of unloaded analyte and quantification of loading	77
2.3.1 Centrifugation	77
2.3.2 Dialysis	77
2.3.3 Spin columns	78
2.4 Characterisation of liposomes	79
2.4.1 Laser diffraction	79
2.4.2 Dynamic light scattering	79
2.4.3 Surface charge measurement.....	80
2.4.4 Determination of unknown concentration using calibration curve	80
2.4.4.1 High performance liquid chromatography (HPLC)	81
2.4.4.2 Bicinchoninic acid (BCA) assay	82
2.4.5 Removal of residual solvent and quantification	82
2.4.6 <i>In-vitro</i> drug release.....	83
2.4.7 Microscopic analysis of liposomes.....	84
2.4.7.1 Confocal microscopy for the visualisation of MLV	84
2.4.7.2 Cryo-electron microscopy for the visualisation of SUV	85
2.4.7.3 Fluorescence microscopy for the visualisation of RF-482	85
2.4.7.3 Electron microscopy for the analysis of peptide loaded liposomes.....	86
2.5 Production and analysis of gold nanoparticles (GNPs).....	86
2.5.1 Functionalisation of gold nanoparticles	86
2.5.2 Particle characteristics	87
2.5.3 UV/visible-spectrophotometry for the confirmation of conjugation.....	87
2.5.4 Quantification of GNPs-Peptide conjugation	88
2.6 Analysis of RSV inhibition.....	88
2.6.1 Cell culture and subculture	88

2.6.3 Cell viability assay/MTT assay.....	89
2.6.4 Fluorescence microscopy for cell imaging.....	90
2.6.5 Immunofluorescence imaging.....	90
2.6.6 Plaque assay.....	91
2.6.7 Quantitative polymerase chain reaction (qPCR) analysis.....	92
2.7 Statistical analysis.....	93
Chapter 3: Method development for the simultaneous quantification of metformin and glipizide.....	94
3.1 Introduction.....	95
3.2 Method development.....	98
3.2.1 Physicochemical properties of drug.....	98
3.2.2 Selection of diluents and determination of analytical wavelength (λ max).....	99
3.2.3 Selection of column, mode of elution and mobile phase.....	100
3.2.4 Impact of ion-pairing agent and pH on separation of compounds.....	102
3.3 Method validation.....	107
3.3.1 Specificity.....	107
3.3.2 Accuracy.....	107
3.3.3 Linearity.....	108
3.3.4 Precision.....	110
3.3.5 Intermediate precision.....	112
3.3.6 Limit of detection (LOD) and limit of quantification (LOQ).....	113
3.4 Development of drug release methods using USP-4 based SOTAX dissolution apparatus with flow through cell (FTC).....	114
3.4.1 USP-4 dissolution apparatus.....	114
3.4.2 Efficacy of the dialysis membrane for the passage of drug.....	118
3.4.3 Selection of release medium for the <i>in-vitro</i> release of liposomal drugs.....	118
3.4.4 <i>In-vitro</i> release of liposome encapsulated drugs.....	119
3.5 Conclusion.....	123
Chapter 4: Formulation of liposomes co-encapsulating hydrophilic and lipophilic drugs.....	124
4.1 Introduction.....	125
4.2 Aim and objectives.....	126
4.3 Results and discussion.....	126
4.3.1 Selection of drugs for co-encapsulation.....	126

4.3.2 Selection of lipids	127
4.3.3 Influence of cholesterol concentration on MLV particle characteristics.....	133
4.3.4 Stability testing of DSPC liposomes	135
4.3.5 Liposome encapsulation of drugs and short-term drug retention study	138
4.3.6 Effect of drug encapsulation on particle characteristics	148
4.3.7 Co-encapsulation of metformin and glipizide in MLV	152
4.3.7.1 Drug escalation study	155
4.3.8 Co-encapsulation of metformin and glipizide in SUV	157
4.3.9 <i>In-vitro</i> drug release from MLV and SUV	160
4.4 Conclusion.....	166
Chapter 5: Microfluidics based manufacture of liposomes co-encapsulating hydrophilic and lipophilic drugs.....	168
5.1 Introduction	169
5.2 Aim and objectives.....	172
5.3 Results and discussion	173
5.3.1 Optimisation of microfluidics method parameters	173
5.3.2 Separation of non-encapsulated drug and removal of residual solvent	179
5.3.3 Microfluidics assisted liposomal co-encapsulation of two divergent solubility drugs	182
5.3.4 The role of drug concentration in drug loading.....	184
5.3.5 Microscopic elucidation of small unilamellar liposomes.....	187
5.3.6 <i>In-vitro</i> release study of liposome encapsulated and co-encapsulated glipizide and metformin.....	190
5.3.7 Influence of liposomal size on <i>in-vitro</i> drug release.....	194
5.4 Conclusions	198
Chapter 6: Liposomes for the inhibition of respiratory syncytial virus	200
6.1 Introduction	201
6.2 Aim and objectives.....	205
6.3 Results and discussion	206
6.3.1 Conjugation of gold nanoparticles and peptide RF-482	206
6.3.3 Conjugation of liposomes and peptide RF-482.....	208
6.3.4 Evaluation of column efficiency to separate the non-conjugated protein	214
6.3.5 Quantification of conjugation.....	215

6.3.6 Cell toxicity analysis	216
6.3.7 Investigation of viral inhibition	219
6.4 Conclusion	227
Chapter 7: Overall discussion and conclusion	228
7.1 RP-HPLC based simultaneous determination of metformin and glipizide	229
7.2 Production of liposomes co-encapsulating drugs of divergent solubility	230
7.3 Microfluidics based simultaneous co-encapsulation of lipophilic and hydrophilic drugs	232
7.4 Liposomal inhibition of respiratory syncytial virus	234
7.5 Overall conclusion	236
7.6 Future work	237
References	240

List of figures

Chapter 1

Figure 1.1 Liposomes made up where hydrophilic core is surrounded by lipid bilayer. Liposomes exist as unilamellar or multi-lamellar structures (Kastner et al., 2015).	30
Figure 1.2 Classification of liposomes based on their size. SUV and LUV can be prepared from MLV using techniques like sonication (for SUV), thawing (LUV),etc (Kastner et al., 2015).	34
Figure 1.3 a) Arrangement of a single molecule of lipid to lipid bilayer. b) Diagrammatic illustration of the mechanism of liposomal vesicle formation.....	37
Figure 1.4 Diagrammatic illustration of effect of change in the transition temperature on the lipid bilayer. (modified from (Monteiro et al., 2014)).	41
Figure 1.5 a) Steroid ring in its structure makes it more promising to makes it prominent in its activity. b)3D structure of cholesterol.The 3D structure adopted from Avanti Polar (AvantiPolar, 2014).	43
Figure 1.6 Compartmentalisation of the drugs into the liposomes with respective solubility.	45
Figure 1.7 Structural representation of possible structure for a range packing parameter value.	47
Figure 1.8 Classification of methods of liposome production. (Modified from (Dua et al., 2012).	50
Figure 1.9 Diagrammatic illustration of thin film hydration process for liposome production (Bangham et al., 1965).....	52

Figure 1.10 Microscopic image of a staggered herringbone micro-mixer engraved in patterns on a channel floor. 55

Chapter 2

Figure 2.1 Thin-film hydration method for the production of MLV. Lipophilic drug was combined with lipids in the organic phase and hydrophilic drug was added during hydration of thin lipid film. 73

Figure 2.2 Illustration of thin film hydration based SUV production and loading of fusion protein RF-482. 75

Figure 2.3 Diagrammatic illustration of microfluidic chip inlet and outlet and a microscopic image of cycles of herringbone micromixer.(modified from (Kastner et al., 2014))..... 76

Chapter 3

Figure 3.1 Schematic representation of an HPLC assembly. Three major sections of the HPLC are mobile phase, stationary phase and the detector. Pumps and injectors are equally important but their functioning are dependent on the quality of mobile phase and sample matrix respectively. 97

Figure 3.2 Representation of divergent nature of glipizide and metformin through their physicochemical properties. 99

Figure 3.3 Chromatogram representing preliminary analysis of glipizide and metformin. Analysis performed on Shimadzu HPLC at 233 nm using Phenomenex Luna C-18 column and acetonitrile:

PBS (65 : 35 v/v) mobile phase. Y-axis = Area Under Curve (AUC) (Dependent of concentration of analyte) and X-Axis = Minutes (Retention time representing interaction of analyte with the stationary phase when dissolved in given mobile phase and flow rate)..... 102

Figure 3.4 Chromatogram representing preliminary analysis of glipizide and metformin. Analysis performed on Shimadzu HPLC at 233 nm using Phenomenex Luna C-18 column and acetonitrile: PBS (65 : 35 v/v) mobile phase. Y-axis = Area Under Curve (AUC) (Dependent of concentration of analyte) and X-Axis = Minutes (Retention time representing interaction of analyte with the stationary phase when dissolved in given mobile phase and flow rate)..... 103

Figure 3.5 Chromatogram representing preliminary analysis of glipizide and metformin. The effect of pH on the separation of analyte. Analysis performed on Shimadzu HPLC at 233 nm using Phenomenex Luna C-18 column and acetonitrile: PBS (65: 35 v/v, aq. pH 5.75) mobile phase. a) glipizide RT=2.3 minutes, b) metformin RT= 1.5 minutes, c) metformin at 1.5 and glipizide at 2.3 minutes. Y-axis = Area Under Curve (AUC) (Dependent of concentration of analyte) and X-Axis = Minutes (Retention time representing interaction of analyte with the stationary phase when dissolved in given mobile phase and flow rate)..... 105

Figure 3.6 $R^2 \geq 0.995$ representing linearity obtained from the detector response to the analyte concentrations. a) Linearity of metformin concentration range 50 $\mu\text{g/mL}$ to 250 $\mu\text{g/mL}$; b) Linearity of glipizide concentration range 20 $\mu\text{g/mL}$ to 100 $\mu\text{g/mL}$. (AUC= Area under curve). 109

Figure 3.7 Percent $RSD \leq 0.5\%$ representing preciseness of the method. Values obtained from the detector response to the analytes concentration. a) % RSD for 3 different concentrations of

metformin representing concentration precision. b) % RSD for 3 different concentrations of glipizide representing concentration precision. (AUC= Area under Curve) 111

Figure 3.8 Type of FTC (a) Large and (b) small FTC. The FTC can be used in (c) Closed loop system and (d) open loop systems. Adopted from (Fotaki, 2011). Copyright 2011 The United States Pharmacopoeia. The FTC can be used in (c) Closed loop system and (d) open loop systems. 116

Figure 3.9 Schematic representation of USP-4 closed loop system. Adapter, flow-cell and reservoir are the 3 main components of the closed loop system used for studying in-vitro drug release..... 117

Figure 3.10 Chromatogram representing the analysis of released drug from liposomes into simulated biological dissolution media. The HPLC-UV method developed (section 3.3) for the quantification of drug encapsulation was applied for this analysis. Y-axis = Area Under Curve (AUC) (Dependent of concentration of analyte) and X-Axis = Minutes (Retention time representing interaction of analyte with the stationary phase when dissolved in given mobile phase and flow rate). 121

Figure 3.11 Chromatogram representing the analysis of released drug from liposomes into PBS (pH 7.4). The HPLC-UV method developed (section 3.3) for the quantification of drug encapsulation was applied for this analysis. Y-axis = Area Under Curve (AUC) (Dependent of concentration of analyte) and X-Axis = Minutes (Retention time representing interaction of analyte with the stationary phase when dissolved in given mobile phase and flow rate). 122

Chapter 4

Figure 4.1 Chemical structures of selected drug for co-encapsulation. A) Metformin hydrochloride (Water Soluble), B) Glipizide (Poorly water soluble), C) Simvastatin (Poorly water soluble). Sketches drawn and transferred from web.chemdoodle.com..... 128

Figure 4.2 Chemical structures of selected drug for co-encapsulation. A) PC (L- α -lysophosphatidylcholine), B) DSPC (1,2-distearoyl-sn-glycero-3-phosphocholine), C) Cholesterol. Sketches adopted from the website of Avanti polar lipids Inc..... 130

Figure 4.3 Comparison of size results obtained from analysis of PC:Chol and DSPC:Chol formulations prepared by thin film hydration method. PBS (pH 7.4) was used as hydration medium for these formulations (N=3 \pm SD)..... 132

Figure 4.4 Comparison of the vesicle size from liposomes containing increased cholesterol concentration. DSPC:Cholesterol 5:1 and 5:2 w/w formulations. Results are expressed as the means of four experiments (N=3 \pm SD). 134

Figure 4.5 Comparison of particle characteristics obtained from analysis of formulation prepared with drug and with two cholesterol concentrations. Samples were stored at three different stability conditions. a & b) Size and zeta potential analysis respectively, representing the formulation with ratio of DSPC:Cholesterol, 5:1 w/w (N= 3 \pm SD). c&d) Size and zeta potential analysis respectively, representing the formulation with ratio of DSPC:Cholesterol, 5:2 w/w (N= 3 \pm SD). 137

Figure 4.6 Comparison of data obtained from HPLC analysis of formulations prepared with the metformin, glipizide and simvastatin. a & b) percent drug entrapped and percent recovery,

respectively, representing the formulation with ratio of DSPC:Cholesterol, 5:1 w/w (N= 3 ± SD).
 c & d) percent drug entrapped and percent recovery, respectively, representing the formulation
 with ratio of DSPC:Cholesterol, 5:2 w/w (N= 3 ± SD). 140

Figure 4.7 Drug retention study performed with the metformin and glipizide samples. Samples
 were stored at three different environmental conditions to investigate the leakage of the drug
 due to environmental factors. a & b) Metformin loading representing two different
 formulations with ratio of DSPC:Cholesterol, 5:1 w/w (N= 3 ± SD) and DSPC:Cholesterol, 5:2
 w/w (N= 3 ± SD). c & d) Glipizide loading representing two different formulations with ratio of
 DSPC:Cholesterol, 5:1 w/w (N= 3 ± SD) and DSPC:Cholesterol, 5:2 w/w (N= 3 ± SD) respectively.
 146

Figure 4.8 Comparison of particle characteristics obtained from analysis of formulation
 prepared with the drug metformin and with two cholesterol concentrations. Samples were
 stored at three different stability conditions. a & b) Size and zeta potential analysis representing
 formulations with ratio of DSPC:Cholesterol, 5:1 w/w (N= 3 ± SD). c & d) Size and zeta potential
 analysis representing formulations with ratio of DSPC:Cholesterol, 5:2 w/w (N= 3 ± SD). 150

Figure 4.9 Comparison of particle characteristics obtained from analysis of formulation
 prepared with the drug glipizide and with two cholesterol concentrations. Samples were stored
 at three different stability conditions. a & b) Size and zeta potential analysis representing
 formulations with ratio of DSPC:Cholesterol, 5:1 w/w (N= 3 ± SD). c & d) Size and zeta potential
 analysis representing formulations with ratio of DSPC:Cholesterol, 5:2 w/w (N= 3 ± SD). 151

Figure 4.10 Co-encapsulation of divergent solubility drugs into multi-lamellar liposomes. Comparison of effect of single and co-drug encapsulation on percent drug loading. a) % drug loading and b) size analysis representing the formulation with ratio of DSPC:cholesterol, 5:2 w/w (N=3, ± SD). 154

Figure 4.11 Investigation of effect of drug amount escalation on a)%drug loading, b) % drug encapsulation and c) particle size, representing the formulation with ratio of DSPC:Cholesterol, 5 : 2 w/w (n=3, ±SD). 156

Figure 4.12 Co-encapsulation of divergent solubility drugs into small unilamellar liposomes. Comparison of effect of single and co-drug encapsulation on a) percent drug loading (**: suggesting $p < 0.05$, t-test) & b) particle size, representing the formulation with ratio of DSPC:cholesterol, 5:2 w/w (N=3, ± SD). 159

Figure 4.13 In-vitro release of glipizide and metformin in MLV. a) Drug release under physiological conditions from various formulations in aqueous buffer, pH = 7.4, at 37°C. b) Cumulative drug release (mg) representing data response under zero order model. c) Log cumulative percent drug remaining representing response under first order model. d) Cumulative percent drug release plotted using Higuchi model of drug release. (N=3, ± SD). 162

Figure 4.14 In-vitro release of glipizide and metformin in SUV. a) Drug release under physiological conditions from various formulations in aqueous buffer, pH = 7.4, at 37°C. b) Cumulative drug release (mg) representing data response under zero order model. c) Log cumulative percent drug remaining representing response under first order model. d) Cumulative percent drug release plotted using Higuchi model of drug release. (N=3, ± SD). 165

Chapter 5

Figure 5.1 Illustration of the process of liposomal suspension production using microfluidics device. At different TFR (mL/min) solvent and aqueous phase run at different FRR through microfluidics channel having staggered herringbone micromixer. The resultant is a liposomal suspension having no drug, single drug or co-drug encapsulated.	171
Figure 5.2 Comparison of the particle characteristics of DSPC:Cholesterol (5:2, w/w) liposomes produced by microfluidics at different flow rate ratios (FRR) and total flow rates (TFR) with a total sample volume 1.0 mL. Results represent mean \pm SD, n = 3. (OR= organic, AQ= Aqueous, PDI= Poly dispersity index).....	174
Figure 5.3 For total sample volume 1.6 mL including 0.6 mL waste volume, selection of flow rate and flow rate ratio for the production of DSPC: Cholesterol liposomes produced by microfluidics. Results represent mean \pm SD, n = 3.	176
Figure 5.4 Effect of sample volume on particle size. a) Particle size when the total sample 1.0 mL b) Particle size when the total sample volume 1.6 mL. (n=3).	177
Figure 5.5 Comparison of DSPC:Cholesterol (5:2, w/w) liposomes z-average diameter, pdi and drug loading for liposomes with glipizide loading within the bilayer, with metformin loading within the aqueous phase, liposomes containing both glipizide and metformin and liposomes without drug present. Results represent mean \pm SD, N=4.	183
Figure 5.6 The relation between lipophilicity (log P) and drug encapsulation. Liposomal composition= DSPC:Cholesterol (5:2 w/w) with/without glipizide and metformin hydrochloride. (MET-CO: Metformin co-encapsulated, GPZ-CO: Glipizide co-encapsulated).	184

Figure 5.7 The role of drug concentration in drug loading for glipizide and metformin. Samples were prepared on microfluidic device and tested for percent loading using RP-HPLC (UV detector). a) % drug loading with respect to the drug concentrations. b) Drug loading presented as amount of drug loaded for respective drug concentration. (N=4, \pm SD). 186

Figure 5.8 DSPC:Cholesterol (5:2, w/w) liposomes produced by microfluidics imaged by Cryo-TEM. A) Liposomes without drug incorporated, B) liposomes with glipizide loading within the bilayer, C) liposomes with metformin loading within the aqueous phase, D) liposome containing both glipizide and metformin. 189

Figure 5.9 USP-4 aided study *in-vitro* release of glipizide and metformin in SUV. a) Drug release under physiological conditions from various formulations in aqueous buffer, pH = 7.4, at 37°C. b) Cumulative drug release (mg) representing data response under zero order model. c) Log cumulative percent drug remaining representing response under first order model. d) Cumulative percent drug release plotted using Higuchi model of drug release. (N=3, \pm SD).... 192

Figure 5.10 Drug release under physiological conditions from various formulations in aqueous buffer, pH = 7.4, at 37°C (n=4 \pm SD). Comparison of drug release kinetics of the MV as well as SUV prepared by thin film hydration (TFH) and the SUV prepared by microfluidics. a) glipizide encapsulated individually, b) metformin encapsulated individually, c) glipizide co-encapsulated, d) metformin co-encapsulated. 196

Chapter 6

Figure 6.1 Diagrammatic illustration of the structure of respiratory syncytial virus (RSV), a member of the Paramyxo virus community and Pneumoviridae subfamily. (image modified from (Redmond, 2013)) .	202
Figure 6.2 Diagrammatic illustration of the amino acid regions of the RSV fusion protein precursor F0 from which the peptide RF482 is derived.	205
Figure 6.3 DLS analysis of non-functionalised and functionalised hours. The line at the bottom (size 85.85 ± 1.5 nm) represents non-functionalised nanoparticles; whereas top line (size 58.14 ± 0.3 nm) represents functionalised gold nanoparticles. (n=3 \pm SD).	207
Figure 6.4 UV/Visible scan of GNPs and FG NPs.	208
Figure 6.5 DLS measurement of liposomes before and after RF-482 conjugation. (n=3 \pm SD)....	209
Figure 6.6 Fluorescence microscopy analysis liposomes conjugated with FITC labelled peptide RF-482 (Green). (a) 10X magnification and (b) at 40X magnification.....	212
Figure 6.7 Transmission electron microscopy analysis. Comparison between (a) empty liposomes and (b) RF-482 peptide associated liposomes Images taken at 50X magnification and 60kv HT.	213
Figure 6.8 Analysis of column efficiency to separate non conjugated protein.....	214
Figure 6.9 Liposomal conjugation with peptide RF-482 determined by BCA assay. Results presented as peptide conjugated determined after separation of non-conjugated peptide. (n=3 \pm SD).....	216

Figure 6.10 Toxicity profiling of peptide RF-482, Liposomes and RF-482 conjugated liposomes as well as GNPs and FGPNs presented through cell viability count performed using MTT assay (section 2.6.3). (72 hours, n=3 ±SD)..... 218

Figure 6.11 Screening of Peptide, Liposomes and gold nanoparticles with and without peptide conjugated against RSV. Plaques were counted and the mean count of each sample was compared against control to determine the percent inhibition. (n=3 ±SD)..... 221

Figure 6.12 Fluorescence microscopy analysis. FITC (Green): RSV and DAPI (Blue): HEP-2 Cell nucleus. In liposomes and RF-482 liposomes the blue colour represents survived cells and green colour represents presence of RSV. 223

Figure 6.13 Screening of RSV-F gene amplicon dilution with water as negative control. Water represents blank or sample with no gene amplicon. Blue line: indicating the threshold of virus sample has higher gene amplicon than the gene amplicon of standard 10^4 . Comparison of viral gene amplicon (V) and Peptide (P1 & P2), Liposomes (L1 & L2), Functionalised liposomes (LP1 & LP2), gold nanoparticles (N2) and functionalized gold nanoparticles (NP2). (* and ** in the figure represents $p < 0.05$ and $p < 0.01$ respectively)..... 226

List of tables

Chapter 1

Table 1.1 Examples of marketed liposomal formulations.	31
Table 1.2 Examples of lipids along their full form, molecular structure, molecular weight (MW) and transition temperature (Tc).	40
Table 1.3 Overview of applications of liposomes in science.	62

Chapter 2

Table 2.1 Method parameters of gas chromatographic method used for residual solvent analysis.	83
--	----

Chapter 3

Table 3.1 SOP for the RP-HPLC method for glipizide and metformin analysis.	106
Table 3.2 Percent recovery of metformin and glipizide representing accuracy of the RP-HPLC method (n=3).	108
Table 3.3 Percent recovery representing the ruggedness of the analytical method for both metformin and glipizide (n=3).	112
Table 3.4 Different dissolution apparatus currently in use mentioned in USP.	114
Table 3.5 Testing efficacy of the dialysis tubing for the drug passage (n=1).	118
Table 3.6 Simulated biological fluid to use as dissolution media to study the release of liposome encapsulated drugs. (Adopted from (Marques et al., 2011)).	120

Chapter 4

Table 4.1 Composition of formulations prepared for the preliminary study of effect of cholesterol concentration, type of lipid and hydration media.....	131
Table 4.2 Properties of hydrophilic and lipophilic drugs used in the liposomal formulations...	139
Table 4.3 Particle characteristics of drug loaded liposomes (N=3, \pm SD).....	141
Table 4.4 Zeta potential of empty and drug loaded liposomes. Results represent mean \pm SD, n = 3.	160

Chapter 5

Table 5.1 Liposomal systems in clinical use.....	170
Table 5.2 Analysis of metformin loaded liposomes subjected to dialysis as well as spin column filtration. All the experiments were performed in triplicates (n=3).....	180
Table 5.3 Analysis of glipizide loaded liposomes subjected to dialysis as well as spin column filtration. All the experiments were performed in triplicates (n=3).....	180
Table 5.4 Kinetic values of release of glipizide and metformin from liposomal formulations using the correlation coefficient parameter.....	193

Abbreviations

ANNOVA	Analysis Of Variance
API	Active Pharmaceutical Ingredient
AUC	Area Under Curve
BBB	Blood Brain Barrier
BCA-Assay	Bicinchonic Acid Assay
CHOL	Cholesterol
DAPI	4',6-Diamidino-2-Phenylindole
DLS	Dynamic Light Scattering
DNA	Deoxyribonucleic acid
DSC	Differential Scanning Colorimetry
DSPC	1,2-Disteroyl- <i>sn</i> -Glycero-Phosphocholine
EMA	European Medicines Authority
EPC	Egg-Phosphocholine
EPR	Enhanced permeability and retention
FBS	Fetal Bovine Serum
FDA	Food Drug Administration
FGNP	Functionalised Gold Nanoparticles
FITC	Fluorescein Isothiocyanate
FRR	Flow Rate Ratio
FTC	Flow through cell
GC	Gas Chromatography
GNP	Gold Nanoparticles
GPZ	Glipizide
HBSS	Hank's Balanced Salt Solution
HEP-2	Human Epidermoid Type-2
HLB	Hydrophilic Lipophilic Balance
ICH	international conference on harmonization
LOD	Limit Of Detection

LOQ	Limit of Quantification
LUV	Large Unilamellar Vesicles
MEM	Minimum Essential Medium
MET HCl	Metformin Hydrochloride
MLV	Multilamellar Vesicles
MPS	mononuclear phagocyte system
MTT	3-(4, 5-Dimethyl-thiazol-2-yl)-2, 5-Diphenyl-Tetrazolium-Bromide
MWCO	molecular weight cut-off
NP-HPLC	Normal Phase-HPLC
NMR	Nuclear Magnetic Resonance
PBS	Phosphate Buffered Saline
PDI	Polydispersity Index
PDMS	Poly-dimethyl-siloxane
qRT-PCR	Quantitative-Realtime-Polymerase Chain Reaction
RF-482 Peptide	Anti-Respiratory Syncytial Virus Fusion Peptide
RNA	Ribonucleic Acid
RP-HPLC	Reversed Phase Chromatography
RSD	Relative Standard Deviation
RSV	Respiratory Syncytial Virus
SANS	Small Angle X-Ray Scattering
SAXS	Small Angle Neutron Scattering
SD	Standard Deviation
SHM	Staggered Herringbone Micromixer
SUV	Small Unilamellar Vesicles
T _c	Transition Temperature
TEM	Transmission Electron Microscopy
TFR	Total Flow Rate
TLC	Thin Layer Chromatography
USP-4	United State Pharmacopoeia Dissolution Apparatus-4
VMD	Volume Mean Diameter

Chapter 1: Realising the potential of liposomes: a carrier for chemical and biological molecules

1 Introduction to delivery systems

To improve the therapeutic profile and efficacy of drugs, various carrier systems have been developed, including nano-particulate systems to microelectronic carriers (Balmayor et al., 2011). These systems can be used for a wide range of delivery routes, from topical delivery through to crossing the blood brain barrier (BBB), with the aim of targeted, timed and dose specific delivery of chemical and biological molecules.

The aim of delivery systems is to enhance the delivery of active pharmaceutical ingredients to the target site and overcome limitations in the stability and/or solubility of the ingredient. There are various designs, methodologies and process optimisations involved in the development of these drug delivery systems; for example, 1) transdermal delivery systems, 2) colloidal carriers and 3) drug-conjugates and prodrug technology. Furthermore, technical development of these novel drug delivery systems (NDDS) involves the use of methodologies such as hot melt extrusion (e.g. Bioadhesive hot-melt extruded film (Repka et al., 2002)), dry powder inhalers (e.g. drug delivery to the respiratory tract using dry powder inhaler (Timsina et al., 1994)), lyophilisation (e.g. lyophilised paclitaxel magnetoliposomes (Zhang et al., 2005)) and microfluidisation (e.g. Preparation of nano-emulsions (Tadros et al., 2004)). Of these various systems, colloidal carriers of drugs, peptides and genes have been the choice for many researchers, due to advantages including their ease in cell penetration and protection against biodegradation (Hung, 2006).

Nanoparticles and nanotechnology generally refers to the particles that have one or more dimensions between approximately 1 and 100 nm; however, the US Food and Drug Administration (FDA) consider 1000 nm as the upper limit for screening of materials for

consideration as nanotechnology and a key consideration is their small size and high surface area to volume ratio. Due to their size, nanoparticles tend to be more accessible to target sites within the body and less susceptible to recognition and removal by the mononuclear phagocyte system (MPS) after administration. Examples of nanoparticles commonly used within pharmaceutical research include liposomes, niosomes, and the metal/polymeric nanoparticles.

1.1 Liposomes

Liposomes were first discovered by (Bangham et al., 1965), who described these ‘Bangosomes’ as swollen phospholipid systems. The term ‘liposome’ was subsequently adopted, which came from a combination of two Greek words, ‘lipos’ and ‘soma’, meaning ‘fat’ and ‘body’, respectively (Çağdaş et al., 2014). The application of liposomes in drug and vaccine delivery was first proposed in the 1970s by Gregoriadis (Gregoriadis et al., 1971; Gregoriadis and Ryman, 1972a) and their medical uses became perceptible during the 1990s; the European Medicines Agency (EMA) approved the first liposomal drug product, ‘AmBisome’, with the active ingredient amphotericin-B for human use in 1990, and subsequently the FDA approved it in 1997 (Cornier et al., 2016). It is produced as small negatively charged liposomes, containing the lipophilic drug Amphotericin B, used against systemic fungal infections.

Since these early developments, countless researchers have studied and looked to commercialise liposome drug delivery systems, with more than a dozen liposomal formulations already marketed (Table 1.1). Whilst previous dosage forms were dose limited due to toxicity

and poor aqueous solubility, incorporation into liposomes allows for targeted delivery (e.g. Doxil) and improved solubility (e.g. AmBisome) and, due to this formulation approach, larger and longer dosage regimens are now possible with reduced toxicity (Lasic, 1998). Liposomes are composed of lipids, that when forced into an aqueous environment, align to form bilayered vesicles, which can be single or multi-lamellar in nature (Figure 1.1).



Figure 1.1 Liposomes made up where hydrophilic core is surrounded by lipid bilayer. Liposomes exist as unilamellar or multi-lamellar structures (Kastner et al., 2015).

Table 1.1 Examples of marketed liposomal formulations.

No	Product	Drug	Therapeutic use	Lipids
1	Ambisome	Amphotericin B	Antifungal (fungal infections and leishmaniasis)	Hydrogenated soy PC(HSPC), 1,2-dioctadecanoyl- <i>sn</i> -glycero-3-phospho-(1'- <i>rac</i> -glycerol) (DSPG), cholesterol
2	Myocet	Doxorubicin	Anti-cancer (leukemia, lymphoma, and different types of carcinoma as well as soft tissue sarcomas)	Egg PC (EPC) and cholesterol
3	Doxil	Doxorubicin	Anti-cancer (leukemia, lymphoma, and different types of carcinoma as well as soft tissue sarcomas)	HSPC, cholesterol and PEG 2000
4	Caelyx	Doxorubicin	Anti-cancer (leukemia, lymphoma, and different types of carcinoma as well as soft tissue sarcomas)	HSPC, cholesterol and PEG 2000
5	LipoDox	Doxorubicin	Anti-cancer (leukemia, lymphoma, and different types of carcinoma as well as soft tissue sarcomas)	1,2-distearoyl- <i>sn</i> -glycero-3-phosphocholine (DSPC), cholesterol, PEG 2000-DSPE
	Thermodox	Doxorubicin	Anti-cancer (leukemia, lymphoma, and different types of carcinoma as well as soft tissue sarcomas)	1,2-dipalmitoyl- <i>sn</i> -glycero-3-phosphocholine (DPPC), mono steroyl PC (MSPC) and DSPC and cholesterol
7	DaunoXome	Daunorubicin	Anti-cancer (leukemia, lymphoma, and different types of carcinoma as well as soft tissue sarcomas)	
8	Marqibo	Vincristine	Anti-cancer (leukaemia, lymphoma, myeloma, breast, head as well as neck cancer)	Egg sphingomyelin and cholesterol
9	Visudyne	Verteporfin	Macular degeneration (To eliminate the abnormal blood vessels in the eye).	BPD-MA:EPG:1,2-dimyristoyl- <i>sn</i> -glycero-3-phosphocholine (DMPC)

10	DepoCyt	Cytarabine	Anti-cancer (myeloid leukemia, acute lymphocytic leukemia, chronic myelogenous leukemia, and non-Hodgkin's lymphoma)	1,2-dioleoyl- <i>sn</i> -glycero-3-phosphocholine (DOPC), 1,2-dihexadecanoyl- <i>sn</i> -glycero-3-phospho-(1'- <i>rac</i> -glycerol)(DPPG) and cholesterol
11	DepoDur	Morphine sulphate	Opioid Analgesic	DOPC, DPPG and cholesterol
12	Arikace	Amikacin	Bacterial infections (joint infections, intra-abdominal infections, meningitis, pneumonia, sepsis, as well as urinary tract	DPPC and cholesterol
13	Lipoplatin	Cisplatin	Anti-cancer (testicular, ovarian , breast, bladder, head, neck , cervical cancer and lung cancer)	DPPG, Soy PC, cholesterol and PEG2000-DSPE
14	LEP-ETU	Paclitaxel	Anti-cancer (Kaposi sarcoma and ovarian, breast, lung, cervical as well as pancreatic cancer)	DOPE and cholesterol
15	Epaxal	Hepatitis A vaccine	Hepatitis A	DOPC and 1,2-dioleoyl- <i>sn</i> -glycero-3-phosphoethanolamine (DOPE)
16	Inflexal V	Influenza vaccine	Influenza	DOPC and DOPE

1.1.1 Classification of liposomes

Liposomes can be classified in a range of ways. Based on the interaction of liposomes with cell and other blood components, liposomes are broadly classified into five categories: 1) conventional liposomes; 2) pH sensitive liposomes; 3) cationic liposomes; 4) immuno-liposomes; and 5) non-interactive sterically stabilised liposomes (also known as long circulating liposomes)(Storm and Crommelin, 1998b). Sterically stabilised liposomes are prepared by using long-chain polymers in the lipid bilayer of liposomes (Bakker-Woudenberg et al., 2005). These polymers form a coat on the surface and help in blocking opsonin adsorption as well as penetration (Sharma and Sharma, 1997). This reduced opsonisation results in slower uptake of these long circulating liposomes by mononuclear phagocytes (MPS). Hence, these types of liposomes are different from conventional liposomes because of their extended half-life *in vivo* (Chonn and Cullis, 1995; Ricci et al., 2000).

Liposomes can be prepared in the range of approximately 50 nm to several microns and can be single or multi-lamellar in nature. Both the size and number of lamella or lipid bilayer can influence drug entrapment efficiency within liposomes. Therefore, based on their size and structure liposomes are classified into three major categories: 1) multilamellar vesicles (MLV); 2) large unilamellar vesicles (LUV); 3) small unilamellar vesicles (SUV) (Figure 1.2).



Figure 1.2 Classification of liposomes based on their size. SUV and LUV can be prepared from MLV using techniques like sonication (for SUV), thawing (LUV), etc (Kastner et al., 2015).

1.1.2 Considerations in building liposomes

Lipids are molecules made up of prominently hydrocarbon moieties, having molecular weights ranging from 150 to 3000 (Small, 1981). This hydrocarbon portion of the lipid molecule could be aliphatic or aromatic (cyclic), and normally they have one or two carbon chains. Three chained lipids are also available and these are known as triacylglycerols (Perrie and Rades, 2012b; Small, 1981). *Fahy et al* (2005) have defined a lipid as hydrophobic or amphiphilic small molecules that may originate entirely or in part by carbonium-based condensation of thioesters and/or carbocation-based condensation of isoprene units (Fahy et al., 2005). Examples of carbonium-based condensation of thioesters are fatty acids and polyketides, whereas carbocation-based condensation of isoprene units includes phenols and sterols. Depending on the chemically functional backbone, lipids could be categorised as polyketides, acylglycerols, sphingolipids, prenols, or saccharolipids (Fahy et al., 2005). Moreover, lipids may be categorised into two main categories; simple and complex lipids (Fahy et al., 2005). Simple lipids contain elements C, H and O in their structure, whereas complex lipids include extra elements like phosphorous, sulfur and nitrogen in their structure. Phospholipids are the most common type of lipids used in

liposome preparation, due to the variability of head group, degree of hydrocarbon chain saturation and variability in chain length, which provides a wide range of options in the formulation of liposomes.

1.1.2.1 Mechanism of liposome vesicle production

Phospholipids have two hydrophobic tails and a hydrophilic head. Liposomes are generally produced upon hydration of thin lipid films or lipid cakes and layers of liquid crystalline bilayers fluidise and swell. These hydrated bilayers detach and self-transform to a large multi lamellar vesicle upon mechanical agitation.

The process of vesicle formation is largely dependent of energy input. Basically, an energy is associated with a patch of thin film where the phospholipids are layered (Figure 1.3a) and the energy associated with the thin film is higher towards the edges and near the hydrophobic tails. The significance of the energy effect minimises when these hydrophobic tails get exposed to the hydration media and forms a spherical vesicle (Patil and Jadhav, 2014). During the process of vesicle formation, the 'bending energy' is responsible for the bending of the lipid layer into the disc shape and this causes an increase in the total energy of the system (Patil and Jadhav, 2014); this, at a subsequent stage, starts decreasing and vanishes upon vesicle formation after attachment of the bilayer edges (Patil and Jadhav, 2014).

In other words, phospholipids are molecules, which can be dissolved in organic solvent but form stacks of lipid upon removal of the solvent (Lasic and Barenholz, 1996). As described in Figure 1.3b, these stacks upon hydration swell and with the help of bending energy turn into multi-lamellar vesicles (MLV).

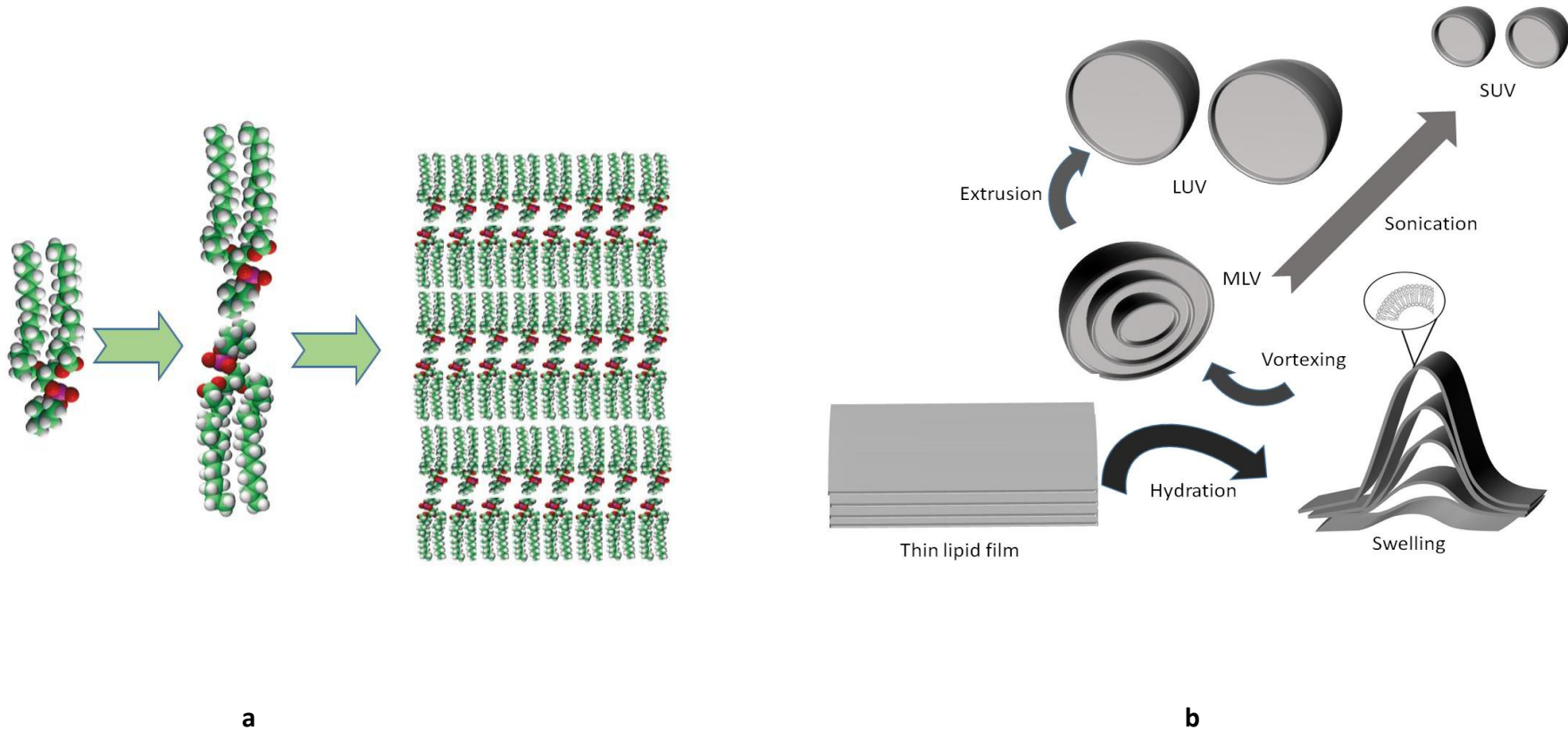


Figure 1.3 a) Arrangement of a single molecule of lipid to lipid bilayer. b) Diagrammatic illustration of the mechanism of liposomal vesicle formation.

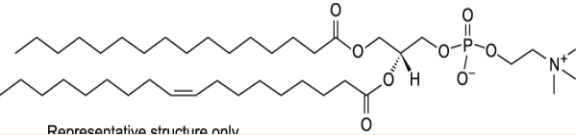
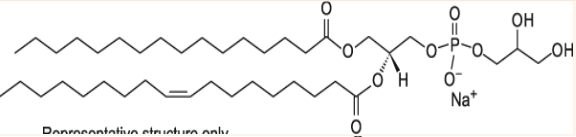
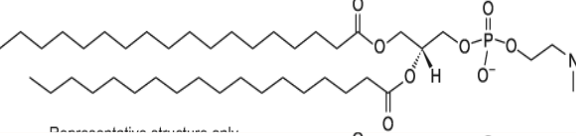
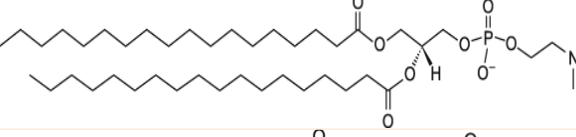
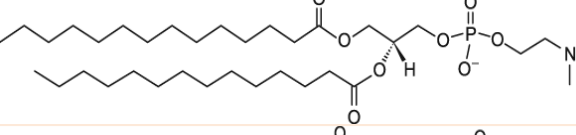
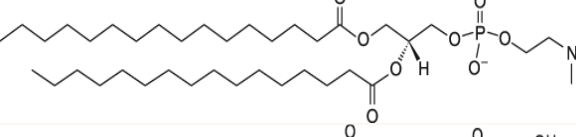
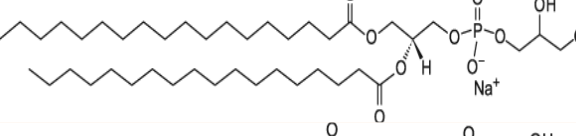
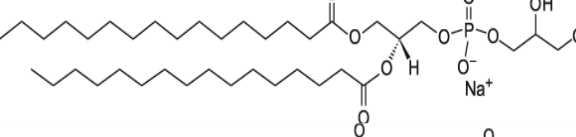
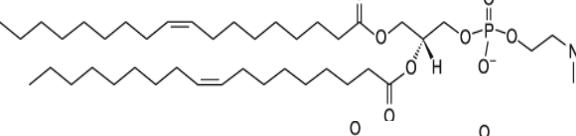
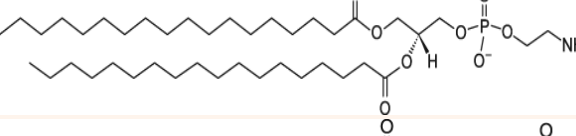
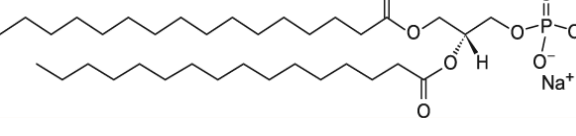
1.1.2.2 Effect of transition temperature in bilayer formation

There are two key components within liposomes: phospholipids (normally a phosphatidyl choline) and cholesterol. Phospholipids are available with a range of fatty acid chains and this impacts on the resulting liposome characteristics. Indeed, the physico-chemical characteristics of liposomes is principally determined by their lipid, as well as other constituents and formulation techniques, which include size reduction methods to produce smaller, more homogeneous liposome suspensions. Traditional examples include sonication, whereby disruptive energy causes large vesicles to rearrange into smaller ones, and size-extrusion, in which vesicles are forced through defined pore sizes. As shown in Figure 1.4, lipids are composed of two main sections: a hydrophobic section and a hydrophilic head-group. Due to the hydrophobic and hydrophilic nature of the tail and head respectively, the polar head group is directed outwards and the non-polar tails form the inner bilayer phase. Due to this biphasic nature, both water soluble and lipophilic drugs can be loaded into liposome systems. Table 1.2 lists a selection of phospholipids and their characteristics.

As can be seen from Table 1.2, increasing the hydrophobic chain length of lipids increases their transition temperature. Transition temperature (T_c) plays crucial role in formation, as well as membrane fluidity of liposomes (Mabrey and Sturtevant, 1976). The lipid transition temperature is the temperature where the lipid changes its phase from an ordered solid state of lipid to disordered liquid crystalline state (Figure 1.4). In the ordered solid state, the hydrocarbon chains are extended and packed; whereas in the disordered state, the chains are

randomly oriented. The T_c of lipid bilayers can be determined by calorimetric analysis; when a substance experiences a transition from a solid to a liquid state, the energy is gained by the system to break the intermolecular chains without causing a consistent increase in the temperature of the substance, and this change in phase can be observed as a sharp peak in the thermogram (Kolusheva et al., 2003). Microcal-high sensitivity calorimeter is widely used in determination of T_c , through calculation of change in temperature (ΔH_{cal}) and Van't Hoff enthalpies (ΔH_{vaf}). The position of peak representing excess heat capacity versus temperature is considered as the transition temperature (T_c) (Savva et al., 1999).

Table 1.2 Examples of lipids along their full form, molecular structure, molecular weight (MW) and transition temperature (Tc).

Lipid	Structure	MW	Tc, °C
Phosphatidylcholine (PC)	 <i>Representative structure only</i>	770.12	-2
Phosphatidylglycerol (PG)	 <i>Representative structure only</i>	782.28	-3
Hydrogenated phosphatidylcholine (HSPC)	 <i>Representative structure only</i>	783.77	53
1,2-disterol-sn-phosphatidylcholine (DSPC)	 <i>Representative structure only</i>	790.15	55
1,2—Dimyristoyl-sn-glycero-3-phosphatidyl choline (DMPC)	 <i>Representative structure only</i>	677.93	24
1,2—Dipalmitoyl-sn-glycero-3-phosphatidyl choline (DPPC)	 <i>Representative structure only</i>	734.04	41
Distearoyl-phosphatidylglycerol (DSPG)	 <i>Representative structure only</i>	801.06	55
Dipalmitoylphosphatidylglycerol (DPPG)	 <i>Representative structure only</i>	744.95	41
Dioleoylphosphatidylglycerol (DOPC)	 <i>Representative structure only</i>	786.11	-17
1,2-disteroyl-sn-glycero-3-phosphoethanolamine (DSPE)	 <i>Representative structure only</i>	748.07	74
1,2-dipalmitoyl-sn-glycero-3-phosphate (DPPA)	 <i>Representative structure only</i>	670.87	-20

The formation of liposomes can be described as a two-step process; the first step is bilayer formation and the second is the closing of the bilayer to form liposomes. The transition temperature of lipids is responsible for their phase change and lipids, when at temperatures above their transition temperature, will initially orientate into parallel alignment and form a sheet like structure (Figure 1.4); subsequently liposomes form by the bilayer sheet closing onto a vesicle structure to reduce tension (Antonietti and Förster, 2003).

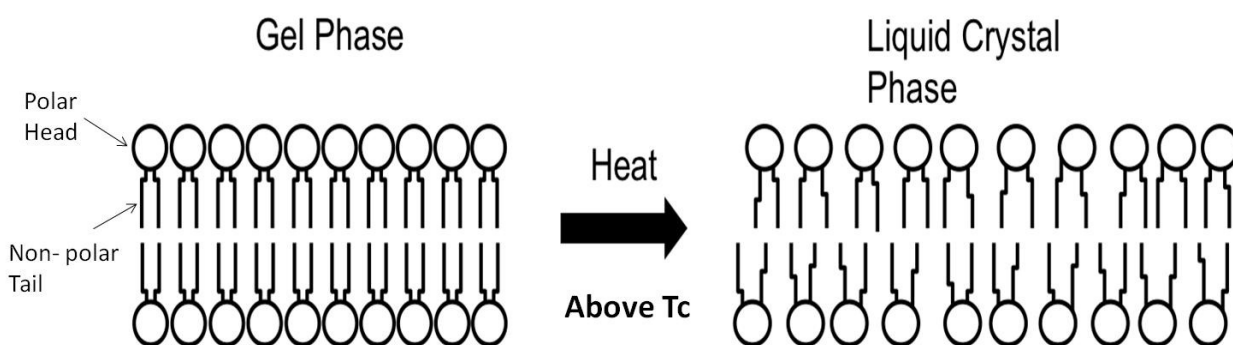


Figure 1.4 Diagrammatic illustration of effect of change in the transition temperature on the lipid bilayer. (modified from (Monteiro et al., 2014)).

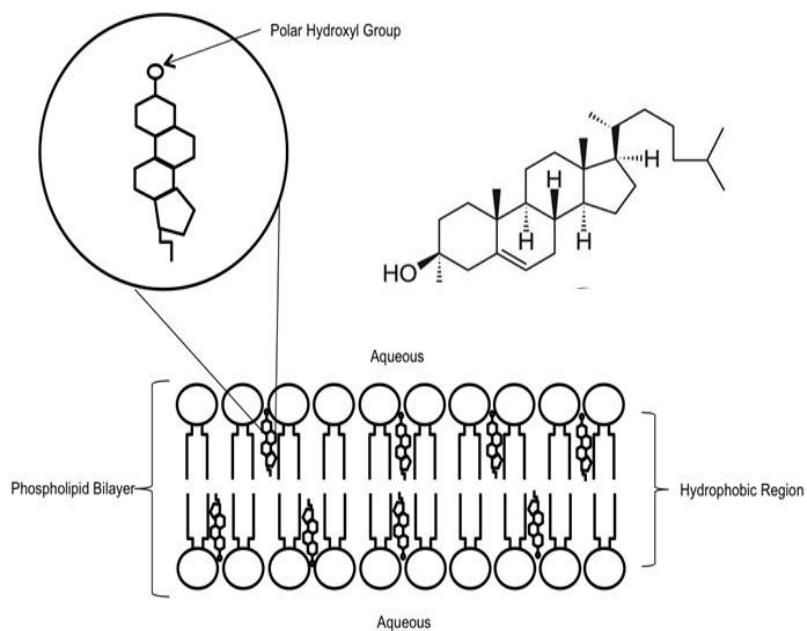
In the consideration of their application, the liposomal transition temperature is a key factor. Employing lipids with transition temperatures about body temperature ($>37^{\circ}\text{C}$) make lipid bilayers less prone to leakage and uptake by the MPS at physiological temperature (Gregoriadis et al., 1984). On the other hand, liposomes with lower T_c ($<37^{\circ}\text{C}$) are more susceptible to leakage at physiological temperature and may experience quick uptake by MPS or lose their original structure at that temperature (Bhandary et al., 2010; Sharma and Sharma, 1997). Commonly 1,2-disteroyl-sn-phosphatidylcholine (DSPC) is used to prepare liposomes (Table 1.2). The long saturated alkyl chains of DSPC result in a transition temperature of 55°C and this property of DSPC is beneficial for drug retention *in vivo* compared to 1,2-dipalmitoyl-sn-glycero-

3-phosphocholine (DPPC) (Webb et al., 1998). Furthermore, the long saturated chains of DSPC increase probability of high drug loading, especially for lipid soluble drugs (Anderson and Omri, 2004; Mohammed et al., 2004).

1.1.2.3 Role of cholesterol in liposome formation, stability and activity

In addition to the choice of phospholipid, cholesterol content is a key factor in liposome formulation. Cholesterol plays a vital role in animal cells, modulating physical as well as functional properties of the bilayer (Gallová et al., 2004). Cholesterol is a large lipophilic molecule with a very small polar region at the hydroxyl end. It is poorly water-soluble and incorporates itself between acyl chains of the phospholipid bilayer (Figure 1.5). Cholesterol is often incorporated into liposomes to improve bilayer fluidity and permeability (Socaciu et al., 2000) and brings profound changes to physical properties of membranes (Wang and Quinn, 2002). In particular, inclusion of cholesterol improves bilayer stability. Indeed, during early investigations of liposomes (Gregoriadis and Davis, 1979), it was discovered that the optimal concentration of cholesterol is 1:1 mol/mol, lipid:cholesterol, and not only increases the stability but also reduces permeability of the bilayer. The key factor making cholesterol more promising is its planar steroid ring (Figure 1.5), imparting a rigid structure to the molecule and this makes lipid-cholesterol interactions more prominent.

a)



b)

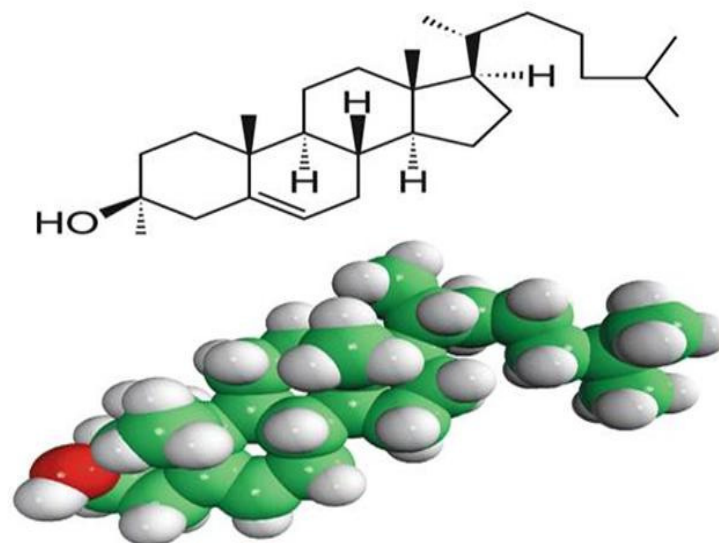


Figure 1.5 a) Steroid ring in its structure makes it more promising to makes it prominent in its activity. b) 3D structure of cholesterol. The 3D structure adopted from Avanti Polar (AvantiPolar, 2014).

Cholesterol provides rigidity to liposomal membranes (Mohammed et al., 2004; Nomura et al., 2005), but high concentrations of cholesterol may impact on the size of the vesicles (Nomura et al., 2005). The miscibility, as well as promising action of cholesterol depends on the polar head groups of lipid being used, in addition to the saturated or unsaturated nature of the lipid (Mohammed et al., 2004; Wang and Quinn, 2002). For example, research performed by Wang and Quinn (2002) describes the interaction of cholesterol with phospholipids and found it decreased in the order sphingomyelin > phosphatidylcholine > phosphatidylserine > phosphatidylethanolamine. Through these interactions, cholesterol actively participates in bilayer formation due to its relatively small head group. In the case of saturated phospholipids like phosphatidylethanolamine, the strong intermolecular interaction can result in elimination of cholesterol from the bilayer. However, in the case of unsaturated phosphatidylethanolamine, the intermolecular interaction is weak and, hence, there is non-lamellar phase formation (Wang and Quinn, 2002). Indeed, it has been observed that for the mixture containing cholesterol less than 30 mol %, the gel to liquid crystalline transition shifted towards the lower temperature i.e. from lamellar to non lamellar and began to increase for cholesterol proportions more than 30 mol % (Wang and Quinn, 2002).

1.1.2.4 Solubility of the payload

Due to their biphasic nature, liposomes can deliver both water soluble and lipid soluble drugs by a range of routes, including the intravenous route (Douroumis and Fahr, 2012). However, with respect to analyte encapsulation, the solubility of the analyte is an important aspect of liposomal encapsulation, with lipophilic molecules encapsulated into the lipid bilayer and the

hydrophilic moieties into the hydrophilic core of the liposomes (Figure 1.6). On the other hand, the solubility of the encapsulated drug can also control release rate from the liposomes; during the *in-vitro* studies, the analyte with least water solubility elutes slower than the analyte with greater solubility. If the drug is loaded passively, then the encapsulation of the lipophilic drug is higher with slow drug release and vice versa for the hydrophilic drug.



Figure 1.6 Compartmentalisation of the drugs into the liposomes with respective solubility.

1.1.2.5 Vesicle properties contributing towards liposomal structure and behaviour

Changes in size directly affect entrapment efficiency and, thereby, drug delivery (Kazi et al., 2010). For intravenous injection of liposomes, it is important to reduce the size range between 100 nm to 200 nm (Allen et al., 1988). This range of vesicle size is small enough to enter inflamed areas of tissues and tumour sites and the small size is less prone to clearance by the macrophages in the MPS and, thus, tend to reside longer in the blood (Gregoriadis et al., 1996; Waterhouse et al., 2005). A key factor controlling vesicle size is the method of manufacture, as already discussed. However, there are various other contributing factors that can influence

vesicle size. The incorporation of drugs within bilayer vesicles can influence their properties; for example, in recent studies by *Essa* (2010), mannitol was taken as water soluble drug, whereas estradiol was selected as poorly water soluble drug, and it was observed that hydrophilic drug can increase the size by approximately 6.5 %, whereas lipophilic drug increased the vesicle size by 35 % of the size of empty liposomes. The influence of encapsulation of lipophilic drug was possibly due to the interaction with the head groups or due to the mutual repulsion, whereas the influence of hydrophilic drug encapsulation was insignificant (*Essa*, 2010a).

Another factor influencing vesicle size is the packing of vesicles. Geometry of amphiphiles can be analysed by determining the critical packing parameter (CPP). CPP is a dimensionless number illustrating tendency of any amphiphiles to form micellar or vesicular aggregates. CPP values below 0.5 indicate the spherical micelle formation and $CPP=1$ indicates formation of vesicles. However CPP above 1 gives indication of reverse micelle formation. The increase in alkyl chain length would result in an increased CPP and, hence, minimal permissible vesicle size increases (*Uchegbu and Florence, 1995; Uchegbu and Vyas, 1998a*). Also, the molecular structure of the amphiphiles can influence the assembly of lipids as well as crystalline phase formation. Amphiphiles have two major non-polar (A_{np}) and polar (A_p) areas. When these areas are stable, the stable bilayer is formed, whereas an imbalance (i.e. CPP less than $\frac{1}{2}$ and more than 1) in A_{np} and A_p gives random aggregated structures (*Figure 1.7*).

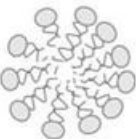
			Critical Packing parameter
		Spherical micell	$<1/3$
		Worm like micell	$1/3$ to $1/2$
		Vesicle	$1/2$ to 1
		Plane bilayer	-1
		Inverted micell	>-1

Figure 1.7 Structural representation of possible structure for a range packing parameter value.

Bigger vesicles form when small head and long chain length molecules are used (Bayindir and Yuksel, 2010). Indeed, the type and amount of lipid play a vital role in vesicle size as well as entrapment efficiency. A well-defined structure of liposomes is determined by the arrangement of lipid molecules and this appropriate arrangement of lipid molecules depends on the interaction between the non-polar lipid tails directed away from the polar head groups placed in contact with the water. This results in optimisation of surface area and brings reduction in surface energy due to increases in hydrophobicity, which leads to smaller particle size (Kazi et

al., 2010; Yoshioka et al., 1994). Therefore, the vesicle size is directly proportional to the hydrophobicity (Uchegbu and Florence, 1995).

1.1.2.6 Surface charge

Daneshpouret. al. (2011) have recently shown that the addition of the negatively charged lipid phosphatidyl serine (PS) in the formulations has a substantial effect on both the size as well as zeta potential of the liposomes, regardless of the PC or cholesterol content employed (Daneshpour et al., 2011). On the other hand, *Felgner et. al* (1994) mentioned that cationic liposomes were able to deliver contents by fusion with cells (Daneshpour et al., 2011; Felgner et al., 1994; Mohammed et al., 2004). The presence of charge increases the distance between consecutive bilayers in multilamellar vesicle structure (Kazi et al., 2010). However, charges are sometimes necessary to avoid aggregation (Uchegbu and Florence, 1995). Also, in recent research, it was found that addition of negative charges make niosomes (non-ionic surfactant vesicles) less stable (Fang et al., 2001). Therefore, it is important to know vesicle charge, not only for stability purposes, but also for the *in-vivo* activity.

1.1.2.7 Steric Hindrance

The presence of appropriate coats such as polyethylene glycol (PEG) or carboxymethylchitin (CMC) on the surface of liposomes can sterically hinder opsonin (an antibody producing immune response) adsorption, thereby resulting in reduced uptake by MPS. The molecules of water forms the organised vesicle via hydrogen bonding to the ether oxygen molecules of the

PEG, and these tightly bound water molecules form a film around the vesicle, repelling the protein interactions. This covering of the PEG on the surface of the vesicle could increase the hydrodynamic size, prevent aggregation, favour the formation of mono-dispersed liposomal suspension and increase the enhanced permeation and retention (EPR) effect due to prolonged circulation (Bozzuto and Molinari, 2015). Hence, sterically stabilised liposomes are more stable in the blood stream than conventional liposomes (Sharma and Sharma, 1997).

1.1.3 Method of liposome production

Although liposomes were discovered nearly half century ago, the developments in preparation of these vesicles is still limited and in need advanced research. A variety of methods are described in an exhaustive number of reviews (Akbarzadeh et al., 2013; Bramwell and Perrie, 2005; Dua et al., 2012; Mansoori et al., 2012; Perrie et al., 2008; Perrie and Rades, 2012a; Sharma and Sharma, 1997; Storm and Crommelin, 1998a; Wagner and Vorauer-Uhl, 2010) and there are nearly half a dozen methods of liposome preparation available in pharmaceutical and cosmetic research (Figure 1.8).

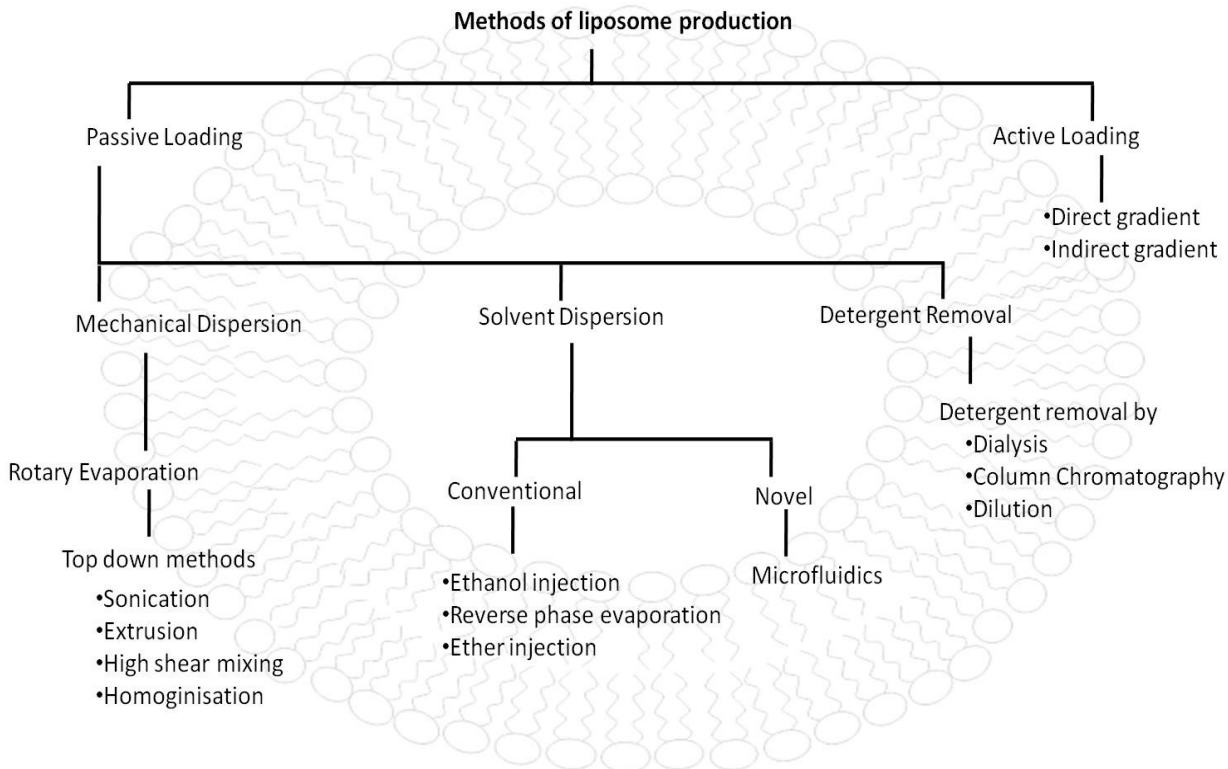


Figure 1.8 Classification of methods of liposome production. (Modified from (Dua et al., 2012).

1.1.3.1 Thin film hydration

Production of multilamellar liposomes by a thin film preparation followed by hydration was first achieved by *Bangham et al.* (Bangham et al., 1965). However, carrying forward this research, a range of methods have been established for the preparation of liposomes. Preparation of multilamellar liposomes can be achieved remarkably simply. Briefly, lipids are dissolved in the organic solvents to form a thin film on the wall of a round bottom flask by rotary evaporation under maintained and reduced pressure. When mixtures of lipids are used, then those lipids must be amply mixed in the organic solvents before subjecting to the rotary

evaporation. Water or any other aqueous buffer is then added to the round bottom flask and the lipids get hydrated at a temperature above the transition temperature (Figure 1.9). This method is based on the principle of passive loading and a maximum 50 % of lipophilic drug and upto 15 % hydrophilic drug loading has been reported in past research (Cullis et al., 1989). Size reduction of these vesicles can be achieved by various methods (Figure 1.9) and probe sonication is the most common approach used in laboratory research. This method uses sonic energy to rupture the bilayer and form small unilamellar liposomes. However, possible contamination with titanium particles from the probe is one of the disadvantages of this method. Centrifugation of the sonicated suspension is an approach to remove these titanium particulates.

As discussed earlier in this chapter, MLV exhibit particle diameters above 1 μm . Due to uneven number of lamellas, these large particle diameters bring heterogeneity in the particle size distribution and may develop multi compartmentalisation (Hope et al., 1993). Extrusion is one of the many techniques available to overcome this issue; during the process of extrusion, a moderate amount of pressure is applied to force the liposomes through a mesh of defined pore size. During the passage through the mesh, the MLVs deform and reseal. Multiple numbers of passes of the same liposomal suspension through this extrusion assembly reflects on the particle size distribution, where the multiple extrusion as well as the pore size reduced the particle size from 1 μm to 100 nm (Hope et al., 1993; Hunter and Frisken, 1998).



Figure 1.9 Diagrammatic illustration of thin film hydration process for liposome production (Bangham et al., 1965).

1.1.3.2 Microfluidics

Microfluidics is one of the recently emerging technologies that allows reproducible mixing on the nanolitre scale in milliseconds to seconds (Kastner et al., 2014) and is cost-effective in liposome production. Microfluidics is based on laminar fluid flow and involves diffusion mixing; where the nano-precipitation and nanoparticles production can be achieved in a single step using micro-mixing (Bally et al., 2012). There are different types of micromixers involved in current microfluidic research and most common are the T & Y shaped mixromixers, parallel lamination micromixers, sequential micromixers and droplet generators (Erbacher et al., 1999; Gobby et al., 2001; Kastner et al., 2014; Lee et al., 2003; Quevedo et al., 2005). The T and Y shaped micromixers are slower than other types but due to ease of operation they are widely used. The parallel lamination micromixers enhance the mixing efficiency by increasing the surface area and reducing the diffusion length. However, the sequential micro-mixer works on rearrangements of fluid streams; whereas the droplet mixromixer generates droplets using electric field.

Microfluidics is a novel method to prepare liposomes that are reproducible, in a one-step and high throughput method compared to the traditional thin film hydration method (Hood et al., 2014). Microfluidics is presented by a low Reynold's number ('Re'), which is a non-dimensional number to determine whether the flow is turbulent or laminar. A threshold value for this is 2000 and 'Re' below 2000 is considered as laminar flow. This 'Re' can be expressed as follow.

$$Re = \frac{\rho V \omega^2}{\mu}$$

Equation 1.1

Here μ is the viscosity of the fluid, ρ is the density, V is velocity scale and $\dot{\omega}^2$ is the diameter of the pipeline. Microfluidics allows distinct mixing organised exclusively by interfacial diffusion, where multiple flow streams get injected into a microchannel (Pradhan et al., 2008). It is a promising way to obtain a mono-disperse population of particles (Belliveau et al., 2012). The small width of the short length microfluidic channels is the reason for the fast mixing (Riahi et al., 2015). The diffusive mixing time plays a vital role in particle size distribution and rate of particle formation, whilst the channel width ($\dot{\omega}^2$), diffusivity (D) of the solvent in the core stream, and the ratio of the core stream flow rate to the total flow rate of the surrounding streams (R) also contribute (Lo et al., 2010).

$$T_{\text{mix}} = \dot{\omega}^2 / 9D(1+1/R^2)$$

Equation 1.2

Microfluidics is based on laminar fluid flow and involves diffusion mixing. Flow rates, aqueous to solvent ratios, total sample volumes and waste volumes can be manipulated as needed. A provision in the form of a heating block is provided under the microfluidic chip to create a special environment for high transition temperature lipids. The device can be divided in 3 different sections, namely a syringe holder assembly, a chip holder and a chip. The syringe holding assembly is designed to hold two syringes; one filled with solvents, in which lipids and/or drug is dissolved, and another filled with buffer, in which drug may be dissolved. The suspension is dispensed through an outlet of the cartridge connected to chip holder. One side of this chip holder is metal, with 2-inlets as well as one outlet, whilst the other side is a separate plastic cover to hold the chip within this metal case. The third and important part of the microfluidic device is the chip. The chip is engraved with two channels, one for the buffer and other for the solvent. These channels carry different solution and mix at a particular point from

which mixture of these two solutions elutes from an outlet on the other end. Also, a staggered herringbone micromixer (SHM) is a micro-mixer engraved in patterns on the bottom of the channel (Figure 1.10). This initiates turbulent mixing a series of repetitive flow profiles (Stroock et al., 2002).



Figure 1.10 Microscopic image of a staggered herringbone micro-mixer engraved in patterns on a channel floor.

Briefly, the method involves mixing of buffer and solvent phases coming from two different 300 μm diameter channels joined at a point in a planar chip. From the point of joining, the fully solvated lipids self-assemble as liposomes when the two phases interdiffuse (Pradhan et al., 2008). Preparation of liposomes by a microfluidic device is based on 2 important parameters; namely flow rate ratio (FRR) and total flow rate (TFR) (Kastner et al., 2014).

1.1.4 Characterisation of liposomes

The quality of the liposomal formulation is determined by the size, shape, zeta-potential, entrapment efficiency and quantitative analysis of the amount of lipid, cholesterol as well as other excipient, such as α -tocopherol, etc. For this, use of techniques such as dynamic or diffraction light scattering, microscopy, high performance liquid chromatography (HPLC) and UV/Visible-spectrophotometry is common. However, further and detailed analysis includes liposomal lamellarity, geometry of lipid and lipid bilayer and the role of cholesterol in liposomal assembly. This can be performed by the use of small-angle x-ray scattering (SAXS) or small angle neutron scattering (SANS), Fourier transform infra-red spectroscopy (FT-IR) differential scanning calorimetry (DSC) and Langmuir–Blodgett trough.

1.1.4.1 Size and surface analysis

When analysing liposomal drug delivery systems, size is considered as a critical parameter; the lower the size of liposomes, the better the bioavailability of drugs as the size of liposomes significantly affects the absorptions and thereby the bioavailability (Ong et al., 2016). There are different techniques used to reduce size of liposomes (e.g. sonication, extrusion and microfluidisation) and dynamic and diffraction light scattering are the best available tools for liposomal size analysis. It is fast and reasonably accurate, although factors such as particle aggregation and multiple scattering could affect particle size measurements. The diffusion caused due to the Brownian motion of the particle/liposomes measured by these techniques.

Microscopy is another tool for the structural elucidation of liposomes. There are various microscopic techniques available in current research, depending on the size of liposomes, but generally scanning electron microscopy (SEM) and transmission electron microscopy (TEM) are the most commonly used. Size analysis of MLVs is possible with optical microscope. However, for analysis of SUV and LUV below 1 μm , the SEM and TEM are suitable. Also, for lipid bilayer analysis or drug entrapment analysis, fluorescent or confocal microscopy is used. Sample preparation is a crucial stage of microscopic analysis. For example, Bibi et. al. (2011) described three ways of sample preparation for microscopic study;

- 1) Using a cover-slip as a conventional way of microscopic study
- 2) Using a micro-slide: here an external micro-slide mounted on top of a normal glass-slide with glue(Bibi et al., 2011). This idea of sample preparation keeps the sample safe from mechanical damage, and the end of the microscopic slides can be sealed, which prevent sample from drying..
- 3) Using a frame seal chamber: this strategy of sample preparation gives greater chance for better resolution, with advantages similar to the micro-slide, where sample drying can be avoided.

Another consideration in the characterisation of liposomes is their surface potential. The zeta potential is a quantification of the relative electrostatic potential due to surface charge density on the surface of the particle, conductivity of the solvent and depends on the velocity of particles mobility in electric field. The change in frequency of a moving particle is measured

when an electric field is applied across the cell. This change in frequency is usually a result of charges on the particles.

To consider the liposomal structure, *Bhalerao et al.* (2003) have described a ^{31}P -NMR method to determine lamellarity of liposomes (Bhalerao and Raje Harshal, 2003). They have used Mn^{2+} ions from magnesium chloride (MnCl_2), which interact with the periphery of the outmost bilayer, resulting in enlarged peak. This reduced signal then can be used to correlate with the lamellarity of the liposomes. In general, a 50% reduction in NMR signal may be interpreted as unilamellar liposomes, whilst a 25% reduction in the signal intensity of the original NMR signal suggests two bilayers of liposome. *Ristori et al.* (2005) have studied physicochemical characterisation of cationic liposomes loaded with sugar-based carboranes. Carboranes are famous for their anti-cancer neutron capture therapy and liposomes are famous for non-toxic drug delivery (Ristori et al., 2005). Using SAXS and SANS, the size, shape and bilayer composition of liposomes has been studied. The targeting effect toward the nucleus by cationic lipids and the availability of the sugar moieties on the liposome surface, were the major constructive properties of this loaded liposomes that were established (Ristori et al., 2005). The data obtained from X-ray or neutron scattering can reveal if any subtle changes occurred in the bilayer of the liposomes.

1.1.4.2 Drug encapsulation and release

Target specific and controlled drug release represents one of the many key attributes of liposomes. To consider drug loading, a range of methods are used to quantify the drug. For example, *Mohammed et al.* (2004) in their research have determined entrapment efficiency of ibuprofen within MLV by measuring non-incorporated drug separated by centrifugation, then

analysed by UV-spectroscopy and validated by HPLC (Mohammed et al., 2004). In general, the drug entrapment efficiency can be calculated with the following formula (Mitra et al., 2013).

$$\% \text{ Entrapment efficiency} = \frac{\text{Entrapped drug}}{\text{Total drug}} \times 100 \quad \text{Equation 1.3}$$

The method mentioned by *Mohammad et al.* (2004) also includes incubation of drug loaded liposomes in phosphate saline buffer (PBS) at 37°C in a water bath with constant agitation. At constant intervals, samples were removed and analysed spectrophotometrically to determine amount of drug release in a particular time interval (Mohammed et al., 2004).

Use of dialysis for *in vitro* drug release has been widely adopted at laboratory scale research (Cosco et al., 2012; Kastner et al., 2015; Laouini et al., 2012). Appropriate dialysis membrane selection is a key factor in this study, since the pore size of the membrane determines the separation and the membrane should be free to active ingredients and there must not be any adsorption of active ingredient. The molecular weight cut-off (MWCO) specifications must be taken into consideration and this depends on the average molecular mass of molecules in the solution (Paul et al., 2013). In other words, MWCO is the smallest average molecular mass of the standard molecule which will not diffuse across the membrane. Sample molecules larger than the pores remain on the sample side, whereas sample molecules smaller than the pore size cross the membrane. A dialysis bag containing a few millilitres of liposomal suspension can be placed in a receptor compartment at 37°C by tying it hermetically and under constant stirring. The receptor compartment must be closed in order to avoid evaporation of contents

present. At particular and predetermined time intervals, samples are withdrawn from the receptor compartment (i.e. the media outside the dialysis tube) and analysed spectrophotometrically or chromatographically. Sink conditions are maintained by the addition of fresh buffer to the receiver phase. However, the method needs skills as well as extreme care of the dialysis tubing to avoid contamination and sample loss. Precise and rugged experimental arrangement is the doorstep to achieve precision in multiple experimental outcomes. The percent drug release then can be calculated using the equation below.

$$\% \text{ Release} = \frac{\text{Drug Released}}{\text{Loaded Drug}} \times 100 \quad \text{Equation 1.4}$$

1.1.4.3 Phase transition studies

DSC is the technique used widely to determine the phase transition behaviour of the lipid. This is useful to know the phase transition temperature of the lipid, as it is necessary to hydrate the lipid suspension above its transition temperature to form liposomes. Along with this use, it is beneficial to record the activity of cholesterol when present in the formulation. As mentioned earlier, presence of cholesterol more than 30 mole % can completely diminish the phase transition temperature and makes the lipid bilayer less prone to leakage (Wang and Quinn, 2002).

In typical DSC experiment, the liposome formulation with recorded weight is placed into the an aluminium pan, followed by sealing with an aluminium lid. The cuvette was then mounted in to

the DSC chamber and heated from 20 to 200°C at the heating rate of 10°C/min in nitrogen atmosphere (Bhalerao and Raje Harshal, 2003). Another method described a DSC approach for the commonly used lipid distearoyl phosphatidylcholine (DSPC) (Terada et al., 2006). Here, 50 microlitre of suspension is placed for DSC analysis at 3°C /minute from ambient temperature to 75 °C.

1.1.4.4 Microbial assay

The total microbial count (TMC) determination is performed and this is done using the plate count method. Selection of appropriate media is crucial here. The method mentioned in United States Pharmacopoeia (*USP*)-29, <61>, states that for a fluid specimen that consists of a true solution or a suspension in water or a hydroalcoholic vehicle containing less than 30 % of alcohol, the specimen is suspended in pH 7.2 PBS (Pharmacopoeia, 2002). This sample is then analysed by appropriate method e.g. plate method where the numbers of colonies are counted from two plates and the average of this is reported as results.

1.1.5 Applications of liposomes

The structural as well as physiological characteristics of the liposomes are diverse and so are their applications. Liposomes with their broad range of applications are involved in the multidisciplinary research. More than a dozen fields in the science have applications of liposomes (Table 1.3).

Table 1.3 Overview of applications of liposomes in science.

Number	Discipline	Application
1	Arithmetic	Studying bilayer elasticity the topology of two dimensional structures can be explored in 3-dimensioal space(Sackmann, 1995)
2	Physics and biophysics	Softening, hardening, aggregation, elasticity and fractals, phase-transition, permeability (Blok et al., 1975; Sackmann, 1995)
3	Chemistry and biochemistry	Artificial photosynthesis, micro and nano-compartmentalisation, catalysis and photochemistry (Landfester and Ostafin, 2008; Lipowsky and Sackmann, 1995)
4	Physical chemistry	Colloidal chemistry, aggregation forces (inter and intra), DLVO(Lipowsky and Sackmann, 1995; Sabin et al., 2006)
5	Pharmaceutics	Pharmacodynamics, colloidal suspension compounding. (Perrie and Rades, 2012a)
6	Medicine and pharmacology	Therapeutics and diagnostics(Rahman et al., 1985)
7	Biology and microbiology	Cell function, fusion as well as recognition and representation of artificial biological membrane (Gregoriadis, 1993)

These liposome vehicles can be tailored in variety of applications such as:

- 1) distribution: passive or active targeting of the molecules by site specification or site avoidance(Perrie and Rades, 2012a);
- 2) duration: liposomes can act as a reservoir, helping towards delayed or controlled release of molecules(Kastner et al., 2015);
- 3) protection: it is a shell that protects molecules such as proteins and peptides from biological degradation(Vabbilisetty and Sun, 2014);
- 4) internalisation: liposomes due to their size and/or surface characteristics can be internalised into the cells and deliver the active ingredient (Hadjidemetriou et al., 2015);

5) amplification: liposomes can work as immunological adjuvant vaccines (Schwendener, 2014).

Liposomal applications in medicine and pharmacology can be separated as diagnostic and therapeutic applications. Liposomes containing drug or marker can be used as a tool to study cell interactions, recognition or mechanism of action of certain molecules. In the case of drugs with limited therapeutic index, their toxicity can be lowered by using liposomes as a carrier giving a temporal and spatial effect to the delivery of the drug molecules. In other words, liposomes can be used to alter the bio-distribution and pharmacokinetics. For example, the clinically approved oncological agent doxorubicin, demonstrated reduced toxicity with better therapeutic outcome when packaged within liposomes (O'Brien et al., 2004). Some other medicinal benefits of liposomes include improved solubility of poorly water soluble drugs, passive targeting to the immune system cells, and sustained release upon systemic or local administration, site bypassing and better tissue penetration. Indeed, applications of liposomes in the biochemical field are prolific and liposomes have remarkably influenced the understanding of membrane proteins and cell functions. Many processes such as exo-and endocytosis, transportation to and from golgi apparatus, internalisation or fusion and neurotransmission are largely dependent on travel of the vesicles. Hence, vesicles are the biggest source of internal communication.

Indeed, liposomes can be used depending on the need of research. Due to the structural attributes, liposomes can be used in combinational therapy. Drugs prescribed in combinational

therapy, such as metformin and glipizide, gemcitabine and tamoxifen, doxorubicin and paclitaxel, irinotecan and fluxoridine, etc. (Cosco et al., 2012; Liu et al., 2014; Tardi et al., 2007) can be compartmentalised depending on the solubility of the analyte; i.e. a lipophilic drug can be encapsulated into the phospholipid bilayer and at the same time a hydrophilic drug can be encapsulated into the hydrophilic core of the liposomes. Similarly, for the delivery of the biomolecules such as proteins and peptides, liposomes are advantageous. Depending on the characteristics of the peptide, this can be encapsulated or attached to the surface of the liposomes e.g. Trans-activating transcriptional peptide can be attached to the surface of liposomes (Hadjidemetriou et al., 2015; Torchilin et al., 2001; Vabbilisetty and Sun, 2014).

1.2 Other particulate systems for the delivery of chemical and biological substances

Similar to liposomes, niosomes are bilayered vesicles constructed from the non-ionic surfactants. They offer advantages over other vesicle forming structures, as they have relatively economical production and can offer enhanced stability (Vora et al., 1998). There are different types of non-ionic surfactants that can be used in the formulation of niosomes, ranging from fatty alcohols, ethers, esters and poloxamers (Karim et al., 2010). Surfactants with hydrophilic lipophilic balance (HLB) between 14 and 17 can't form vesicles due to high aqueous solubility, but with optimised cholesterol concentration can produce vesicles from these surfactants (Seleci et al., 2016). These surfactants, as well as the cholesterol, can help to attain the required shape and can be particularly useful for those surfactants with a HLB around 10 (Marianecci et al., 2014). Common surfactants used in the formulation of niosomes include Spans, Tweens,

Brij, Steryl alcohol and Poloxamers and the choice of surfactant can impact upon the properties of the vesicles, including their size, tapped volume, and surface charge (Diljyot, 2012). As with other nano and microparticles, niosomes have been used in controlled release preparations and have shown to be able to target a range of organs, such as the skin, brain, liver, respiratory system, ocular systems and certain tumours (Uchegbu and Vyas, 1998b). Niosomes have also shown promise as drug carriers for dermal indications. This includes acting as a local anaesthetic, use in psoriasis and as a skin tone lightener in the cosmetics industry. Metal or polymeric particles have been involved in the mimicking or altering the biological process (Singh and Lillard, 2009). Most of these particle based delivery systems are biodegradable, designed for drug delivery and stabilising molecules like proteins, peptides and DNA (Singh and Lillard, 2009). In oncological studies, it was found that these particles can get accumulated at target site and show the depot effect depending on the make-up of the carrier and provide a constant supply of the loaded active ingredient (Desai et al., 1997). Metal nanoparticles came into focus as imaging agent and diagnostic biosensors (Arvizo et al., 2011; Mody et al., 2010), but metal particles such as gold nanoparticles have been shown to have a role in the transport of an anti-cancer agents (Chen et al., 2008).

1.3 Current challenges in pharmaceutical industry

As mentioned earlier, liposomes are the most common and investigated delivery systems used for delivery of variety of chemical and biological molecules (Lasic, 1993; Perrie and Rades, 2012a). The first generation of liposomes experienced rapid clearance by MPS due to structural

imperfections but the optimisation made longer circulation and enhanced EPR effect (Sawant and Torchilin, 2012). Although the optimisation increased the availability of molecule and enhanced EPR effect, the endocytosed material is prone to degradation by acidic environment in the lysosol and the enzymes. This results in the reduced biological activity of molecules that are sensitive, for example peptides and peptidic drugs (Connor and Huang, 1986).

Furthermore, prolonged retention at the target site would not be important if the drug is rapidly lost on storage. The correct choice of lipid and formulation component would be a solution, but optimisation of component concentration and process parameters is equally important, especially for hydrophilic drugs, as they may suffer low membrane permeation and low retention (Cullis et al., 1989).

Studies have described that discovery of new drugs is not sufficient for the growth of therapeutic excellence; therefore, developments in delivery of existing drugs is necessary (Kalepu and Nekkanti, 2015). 40 % of the marketed drugs are hydrophilic and, therefore, remaining are the significant number of marketable drugs are poorly water soluble (Kalepu and Nekkanti, 2015). Hence, the pharmaceutical market is significantly interested in developing strategies to deliver poorly water soluble molecules.

Moreover, recent research has exploited the co-delivery of hydrophilic and lipophilic drugs (Cosco et al., 2012; Tardi et al., 2007). Surprisingly, very little research has been reported about

the delivery of multiple drugs in one liposomal formulation. This may be a result of challenges associated with encapsulation, stability and release of two therapeutic agents in one liposomal composition (Tardi et al., 2007).

Liposomes are not only preferred in the pharmaceutical but also in the biopharmaceuticals (Van Slooten et al., 2001). Liposome based vaccines such as hepatitis C virus vaccine, tuberculosis vaccine, etc. are being evaluated extensively (Schwendener, 2014; Schwendener et al., 2010; van Dissel et al., 2014). Similar to other deadly diseases, respiratory syncytial virus (RSV) is affecting millions of children and adult around the world (AR et al., 2005a; Borchers et al., 2013; Rappuoli et al., 2011). First line of treatment for treatment of RSV infection is use of bronchodilators such as α and/or β adrenergic agonist (Borchers et al., 2013) but there is no active prophylaxis available for this virus. Recently, anti-RSV peptide RF-482 found capable of inhibiting the virus (Singh et al., 2014) and this anti-RSV peptide was carried by gold nanoparticles (GNPs). Considering available RSV inhibitor and potential of liposomes in vaccine development, liposome based vaccine against RSV could be safe and effective candidate.

1.4 Aim and Objectives

Given the need of optimal use of liposomal structural benefits, the overall aim of this thesis was to investigate the role of liposomes to enhance the delivery of different classes of drugs (small active pharmaceutical ingredients and bio-molecules). To achieve this, the objectives of the thesis were:

1. Develop appropriate methodical tools for the preparation, quantification and characterisation of a range of liposomal formulations.
2. Investigate the role of liposomes for the delivery of hydrophilic and low solubility drugs alone and as part of a combination therapy.
3. Investigate and develop a new high-throughput one-step process for the manufacture of liposomes simultaneously entrapping hydrophilic and lipophilic drugs.
4. Investigate potential of liposomes to deliver peptides and exploit their use to control RSV infection.

Chapter 2: Materials and methods

2.1 Materials and chemicals

*All the materials, chemicals used were of analytical grade.

Material/Chemical/Instrument	Vendor/Supplier
1,1'-dioctadecyl-3,3,3'-tetramethylindocarbocyanine perchlorate (Dil C)	Sigma-Aldrich Company Ltd. (Poole, UK)
1,2-distearoylphosphatidylcholine (DSPC)	Avanti Polar Lipids, Inc. (Alabaster, AL)
1-Ethyl-3-(3-dimethylaminopropyl)carbodiimide (EDC)	Sigma-Aldrich, St. Louis, MO, USA
12-Well Plates	Life Technologies, CA, USA
1X PBS: 0.01M Phosphate buffered saline, pH 7.4	Life Technologies, CA, USA
75 cm ² Flasks	Life Technologies, CA, USA
8-well chamber slides	Life Technologies, CA, USA
96-well Reaction plates	Life Technologies, CA, USA
Acetonitrile	Fisher Scientific UK (Loughborough, UK)
BCA-assay Kit	Thermo scientific, Rockford, IL, USA
Cell counter	Thermo scientific, Rockford, IL, USA
Centrifugation tubes for MLV	Sigma-Aldrich Company Ltd., Poole, UK
Centrifuge Apparatus	DJB Labcare Ltd,. Buckinghamshire UK
Chloroform	Fisher Scientific, Loughborough, UK
Cholesterol	Sigma-Aldrich Company Ltd., Poole, UK
Confocal Microscope	Leica Microsystems, Milton Keynes, UK
Cryo-Electron Microscope	Tecnai 12 G2 electron microscope (FEI, Eindhoven, USA).
Crystal Violet	Life Technologies, CA, USA
DAPI	Life Technologies, Carlsbad, CA, USA
Dialysis Tubing/Membrane	Medicell membranes Ltd, London, UK
Diffraction light scattering-Sympatec-HELOS	Sympatec, Bury, UK
Dulbecco's Modified Eagle's Media (DMEM)	Life Technologies, CA, USA
dye MTT (3-(4, 5-dimethyl-thiazol-2-yl)-2, 5-diphenyl-tetrazolium bromide)	Promega Corp, Madison, WI, USA
Dynamic light scattering-Malvern-ZS-Nano	Zetasizer Nano-S, Malvern instruments, Westborough, MA, USA

Dynamic light scattering-Malvern-ZS-Nano	Malvern Instruments, Worcestershire, UK
Egg-Phosphotidyl Choline (PC)	Avanti Polar Lipids, Inc., Alabaster, AL
Electron Microscope	EM10A/B, ZEISS, Germany.
Ethanol	Fisher Scientific, Loughborough, UK
Fetal Bovine Serum (FBS)	Life Technologies, CA, USA
Filter Units-Ultracel- 50K	Millipore Ireland Ltd., Cork, Ireland
FITC (goat)	Life Technologies, CA, USA
FITC-labelled-RF-482	Bachem Americas Inc., Santa, Clara, CA, USA
Fluorescence Microscope	Nikon Inc. Melville, NY, USA
Gas Chromatography (GC) CSI 200	Cambridge Scientific Instruments Ltd, Witchford, UK
GC column	GC column TRACE, 15 m x 0.25 mm x 0.25 µm
Glipizide	Discovery Chemicals, UK
Gold Nanoparticles (GNPs)	Nanopartz™, Loveland, CO, USA
Hank's balanced salt solution (HBSS)	Life Technologies, CA, USA
High performance liquid chromatography (HPLC)	Shimadzu 2010-HT, Milton Keynes, UK
HPLC-column	Phenomenex, Macclesfield, UK
Human epidermoid type-2 (HEP-2) cells	American Type Culture Collection (ATCC®, Manassas, VA, USA)
Kanamycin	Sigma-Aldrich Co., St Louis, MO, USA
Metformin	Sigma-Aldrich Co. St Louis, MO, USA
Methanol	Fisher Scientific, Loughborough, UK
Methyl Cellulose	Sigma-Aldrich Co., St Louis, MO, USA
NanoAssemblr™ benchtop	Precision Nanosystems, Agronomy Rd, Vancouver
Microslide	Cam lab, Cambridge, UK
Minimum Essential Medium (MEM)	Life Technologies, CA, USA
Ortho-phosphoric acid	Sigma-Aldrich Company Ltd., Poole, UK
Osmium Tetroxide (4 % Solution)	Electron Microscopy Sciences, Hatfield, PA, USA.

Paraformaldehyde-glutaraldehyde	Sigma-Aldrich Co., St Louis, MO, USA
Penicillin	Sigma-Aldrich Co., St Louis, MO, USA
Peptide RF-482	Bachem Americas Inc., Santa, Clara, CA, USA
Phosphate Buffered Saline (PBS)	Sigma-Aldrich Company Ltd., Poole, UK
Plastic syringes	Sigma-Aldrich Company Ltd., Poole, UK
Plate reader	TECAN™, Morrisville, NC, USA
Primers(forward & reverse) and Probes	Life Technologies, CA, USA
Probe Sonicator	MSE Ltd., London, UK
Real-time PCR instrument	Biosystems® ViiA™ 7 real time PCR ,Life Technologies, CA, USA.
Respiratory Syncytial Virus (RSV)	American Type Culture Collection (ATCC®, Manassas, VA, USA)
RNA-Extraction Kit	Life Technologies, CA, USA
DNA-Extraction Kit	Qiagen, Germantown, MD, USA
RNA-Free Water	Qiagen, Germantown, MD, USA
Rota evaporator	BuchiLabortechnik GmbH, Essen, GE
Rota Evaporator	Roavaps, Atkinson, NH, USA.
Simvastatin	Sigma-Aldrich Company Ltd., Poole, UK
Spin Columns	Sartorius AG, Goettingen, Germany
Streptomycin	Sigma-Aldrich Co. St Louis, MO, USA
SuperScript II	Life Technologies, CA, USA
TaqMan® Master Mix 2	Life Technologies, CA, USA
USP-4 SOTAX, FTC	SOTAX AG, Switzerland
UV-Visible Spectrophotometer	Beckman Coulter spectrophotometer, Brea, CA, USA
Water	Milli-Q, MB-328, Aston University
β-mercaptoethanol	Sigma-Aldrich Co., St Louis, MO, USA

2.2 Methods of liposome production

2.2.1 Thin film hydration

Multi-lamellar vesicles (MLVs) were prepared using the conventional thin film hydration method (Bangham et al., 1965) (Figure 2.1). Briefly, the lipid components (DSPC cholesterol, 5:1 Or 5:2 w/w) were dissolved in an organic solvent mixture of chloroform and methanol (9:1 v/v) with the addition of lipophilic drug, followed by solvent evaporation to obtain a thin dry film. To remove the solvent residue, the film was then flushed with Nitrogen (N₂). The film was then hydrated with 2.0 mL phosphate saline buffer (PBS) with the addition of hydrophilic drug and vortexed for 1 minute, which produces a milky suspension, suggesting detachment of lipids from the wall of the round bottom flask. The milky suspension was then heated for 30 minutes at the temperature above the 'T_c' of lipid used and at an interval of 10 minutes the sample was vortexed for 1 minute. This step-by-step treatment to the thin film of lipids resulted in the formation of MLVs, which were prepared at two different DSPC-cholesterol ratios of 5:1 and 5:2 w/w, respectively.



Figure 2.1 Thin-film hydration method for the production of MLV. Lipophilic drug was combined with lipids in the organic phase and hydrophilic drug was added during hydration of thin lipid film.

2.2.2 Probe sonication

Probe sonication is one of the many methods to reduce the size of MLVs produced by the thin film hydration method. Time of sonication and amplitude at which sonication is performed are the factors responsible for the size reduction of MLV. Titanium probe was used for this size reduction. The probe was immersed into the milky MLV suspension and the sonication was performed maintaining the temperature above the transition temperature of the lipid. A change in colour (i.e. from milky to a clear suspension) was observed during the process of the sonication. The suspension was cooled for 20 minutes prior to the next treatment. Probe sonication leaves debris of the probe immersed into the suspension (Mizuguchi et al., 2015); therefore, the debris was removed before analysing the size of the obtained vesicles.

2.2.3 Protein loading

The fusion protein RF-482 is a small and heat sensitive protein (39 amino acids, molecular weight: 4361.8, theoretical iso-electric point: 4.95, net charge: -2, atomic formula: $C_{192}H_{303}N_{53}O_{63}$ and total number of atoms 611). Therefore, a slight modification was done in the thin film hydration method (Figure 2.2), where in spite of the hydrophilic nature of the protein, it was not added to the hydration buffer but was added post sonication when SUVs were obtained. Briefly, a predetermined concentration of protein was added to the SUV suspension and mounted on a shaker for 30 minutes. This was done to facilitate the fusion of protein on to the liposomal surface.



Figure 2.2 Illustration of thin film hydration based SUV production and loading of fusion protein RF-482.

2.2.4 Microfluidics based one step SUV production

Liposomes were manufactured using a microfluidic device manufactured by Precision NanoSystems Inc., Vancouver, Canada, using a microfluidic chip with a 300 micron Staggered Herringbone Micromixer (Figure 2.3). The design introduces a turbulent flow in a micro-channels by subjecting the fluid to a repetitive series of rotational flow profiles, which is achieved by alteration of the grooves as a function of the axial position in the channel (Stroock et al., 2002). Other parts of this bench top instrument include plastic syringes, which carry buffer and solvent that are pumped into the microfluidic channels by moveable stages. The movement of these stages can be programmed through a computer based program, which also control TFR, FRR, initial as well as end waste volumes.

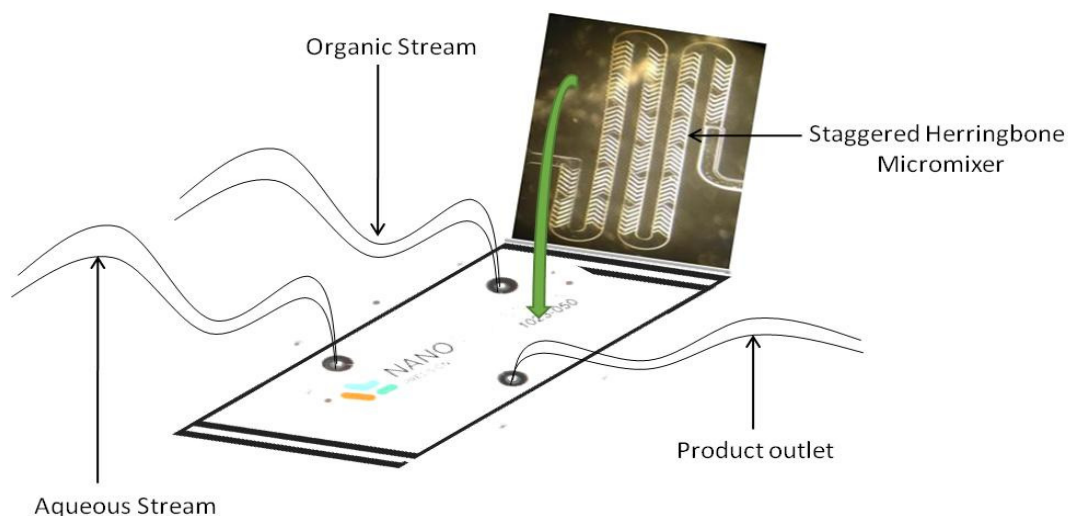


Figure 2.3 Diagrammatic illustration of microfluidic chip inlet and outlet and a microscopic image of cycles of herringbone micromixer.(modified from (Kastner et al., 2014)).

The aqueous buffer used in all studies was PBS, 10 mM, pH 7.4. The flow rate ratio (FRR) between the aqueous and solvent stream was varied from 5:1 to 1:1 (aq:solvent ratio) and the total flow rate (TFR) was varied from 5 to 15 mL/min. Through this method, liposome formation and incorporation of the drugs was performed simultaneously by addition of the drug into the appropriate phase; within these studies, the lipophilic drug glipizide (anti-diabetic, molecular weight: 445.6 gm/mol, pKa: 12.4, logP: -1.8) was dissolved in the solvent, whilst the hydrophilic drug metformin (anti-diabetic, molecular weight: 165.7 gm/mol, pKa: 5.6, logP: 1.9) was dissolved in PBS prior to microfluidic mixing. The liposome formulations were collected from the chamber outlet and dialysed using dialysis tubing (Section 2.3.2) at room temperature against PBS buffer for removal of residual solvent as well as the non-loaded drug.

2.3 Purification of liposomes, separation of unloaded analyte and quantification of loading

2.3.1 Centrifugation

For the purpose of purification to remove the titanium debris after the size of MLV was reduced by probe sonication, as well as separation of non-entrapped drug, liposomes were subjected to centrifugation. Each sample was centrifuged at 2500 rpm for 30 minutes and this procedure repeated twice by re-suspending the same sample in PBS. Without disturbing the pellet, visual observation was performed to check for the presence of unusual or unexpected supernatant.

For water soluble drugs, the centrifugation process is simple and involves centrifugation of liposomal suspension directly and analysis of non-entrapped drug present in supernatant. For lipid soluble drugs, media preparation is needed, which depends on the extent of its water solubility. In the case of metformin, 1.0 mL of the suspension was centrifuged directly. As the solubility of glipizide in PBS is 37 mg/L, the suspension was diluted in 40 mL PBS to achieve maximum solubility of glipizide and to avoid its sedimentation along with liposomes.

2.3.2 Dialysis

Empty as well as drug loaded liposomes were dialysed using (3500Da) membrane for 15 minute for the removal of residual solvent as well the non-encapsulated drug. The dialysis tubing (Medicell membranes Ltd, London, UK) was soaked under running water to remove the traces of preservatives. The tubing was cut into 10 cm length pieces and secured with clips on both

ends ensuring no sample leakage. The 60 mL PBS outside the dialysis tubing and the sample inside the tubing was then analysed by HPLC for quantification of drug and the residual solvent.

2.3.3 Spin columns

Although the process of dialysis is used widely for the removal of solvent as well as the free drug, it requires skilled operation and is prone to environmental contamination. Therefore, as an alternative approach, disposable spin columns (Sartorius-Vivaspin 2, Surrey, UK) were tested for the removal of residual solvent as well as the non-encapsulated drug. Here, the membrane of the spin column was pre-soaked with water and centrifuged at 2000 rpm for 5 minutes. Following this, the required volume (1.0 mL) of sample was placed in to the spin column and then centrifuged for 15 minutes at 3000 rpm. The sample was washed once again with 1.0 mL PBS for 15 minutes at 3000 rpm to achieve the maximum removal of non-encapsulated drug as well as residual solvents. The eluent as well as the sample inside the spin column was then tested for quantification of drug using HPLC and the residual solvent using GC.

To separate unloaded peptide RF-482, a similar approach was used. The peptide was removed using centrifugal filter units (Ultracel- 50K, Millipore Ireland Ltd., Cork, Ireland). The eluent as well as the sample inside the spin column was then tested for quantification of unloaded and loaded peptide, respectively, using the BCA assay (Section 2.4.4.2).

2.4 Characterisation of liposomes

2.4.1 Laser diffraction

Characterisation of MLVs was performed using laser diffraction method (Sympatec-HELOS, Sympatec, Bury, UK), using samples within an optical concentration range of 15-25 %. The size was reported as volume mean diameter (VMD) and the particle size distribution is reported in terms of span value. The span value was generated using equation 2.1 based on the particle distribution percentile ($D_{0.1}$, $D_{0.5}$ and $D_{0.9}$) (Kirby et al., 2008).

$$Span = \frac{D_{0.9} - D_{0.1}}{D_{0.5}} \quad \text{Equation 2.1}$$

2.4.2 Dynamic light scattering

Characterisation of small unilamellar vesicles (SUVs) was performed using dynamic light scattering (Malvern Zetasizer Nano-ZS). Intensity based mean particle size was reported as Z-average for the monomodal distribution. In the case of multimodal distribution, the Z-average was reported based on the intensity as well as the size based distribution of vesicles. The sample analysis was carried out at 25°C and in the attenuation range of 6 to 10. To achieve this attenuation range the sample was diluted with water. The width of particle distribution was reported as polydispersity index (PDI).

2.4.3 Surface charge measurement

Characterisation of the surface charge of the vesicles was performed using particle electrophoresis (Malvern Zetasizer Nano-ZS). In this instrument uses laser doppler micro-electrophoresis to measure zeta-potential. Briefly, the velocity of particles according to their zeta-potential is measured, as a result of an dc electric field being applied across the sample.

The sample was diluted 1:100 in diluted PBS (1 in 300).

2.4.4 Determination of unknown concentration using calibration curve

Using area under curve (AUC) (HPLC) and absorbance (BCA assay), percent recovery of the unknown concentration of drug and peptide was determined statistically by using a calibration curve. Intensity was considered as the response (y) from the detector, which is directly proportional to the concentration (x) of analyte present in the unknown solution. Linearity of standards as well as its slope (c) and intercept (m) also contribute in determination of sample concentration. It was observed that the ' R^2 ' value, which is measure of linearity between detector signals and sample concentration, is >0.99 . This shows good correlation between detector signals and sample concentration.

For both HPLC and BCA assays, the quantification of unknown concentration was performed by plotting a calibration curve which was presented as a linear function of concentration of API or peptide.

2.4.4.1 High performance liquid chromatography (HPLC)

A validated HPLC method was used to determine the entrapped and non-entrapped drug. Briefly, simultaneous quantification of metformin and glipizide (both liposome entrapped and non-entrapped) was performed using reversed-phase high performance liquid chromatography (RP-HPLC, Shimadzu 2010-HT, Milton Keynes, UK) connected with an ultra-violet detector at 233 nm to allow simultaneous quantification of both drugs. Isocratic elution was performed using a mobile phase composition of acetonitrile:PBS (65:35, pH 5.75) at constant flow rate of 1.0 mL/minute, using a Luna column (C-18, 5 μ , i.d. 150 X 4.6 mm) from Phenomenex (Macclesfield, UK)(Kar and Choudhury, 2009). Mobile phase acetonitrile: PBS (65:35, pH 5.75) was used as sample diluent. However, to determine drug encapsulated into the liposome, the liposomes were dissolved in ethanol followed by a second dilution with the mobile phase.

Considering analyte properties and foreseeing the co-encapsulation of drugs, the method was developed in-house and validated following ICH guidelines (FDA, 1994). The method development and validation is further described in chapter3. Briefly, the determination of loading was performed by separating non-entrapped drug. This was done by centrifugation for the MLV and by dialysis for the SUV. The percent encapsulation and non-encapsulation was then determined by using equations 2.2 &2.3, whilst the percentage recovery of the drug was calculated by equation 2.4.

$$\% \text{ Encapsulation} = \frac{\text{Amount of drug in the sample (i. e. in liposome)} \times 100}{\text{Amount of drug used initially}} \quad \text{Equation 2. 2}$$

$$\% \text{ Non - encapsulation} = \frac{\text{Amount of drug in the sample (i. e. outside liposome)} \times 100}{\text{Amount of drug used initially}} \quad \text{Equation 2. 3}$$

$$\%Recovery = \frac{(\text{Amount of drug encapsulated} + \text{Amount of drug non - encapsulated}) \times 100}{\text{Amount of drug used initially}} \quad \text{Equation 2.4}$$

2.4.4.2 Bicinchoninic acid (BCA) assay

After separation of liposome associated and non-associated peptide molecules (RF-482), the eluent and the liposome suspension were tested for peptide presence by BCA assay, using a Micro BCA assay kit (Thermo scientific, Rockford, IL, USA). PBS (pH 7.4) was used as sample diluent. However, ethanol (Fisher scientific, Fair lawn, NJ, USA) was used to separate liposome associated protein and this was further diluted with PBS. Five standards of peptide RF-482 were prepared for linearity and calibration curve. Working reagent was prepared following the protocol provided (Thermo scientific, Rockford, IL, USA). 150 μ L of standards and samples were added to the 96-well plate. To all the standards and samples, 150 μ L of working reagent was added and incubated for 2 hours, after which the plate was cooled to room temperature and tested for peptide quantification using a plate reader (TECANTM, Morrisville, NC, USA) at 562 nm. Apart from the standards and samples, ethanol, buffer as well as 'empty' liposomes were tested for BCA interference. Percent loaded protein, unloaded protein and percent recovery of the protein was calculated using the same equations 2.2, 2.3 & 2.4, respectively.

2.4.5 Removal of residual solvent and quantification

Two different approaches, dialysis and using spin columns, were used to remove residual solvent in the SUV suspension obtained from the microfluidic device. 'Empty' as well as drug

loaded liposomes were dialysed using (3500Da) membrane (Medicell membranes Ltd., London, UK) for 15 minutes for the removal of residual solvent as well the non-encapsulated drug. Dialysis was performed using PBS (composition: phosphate buffer 0.01 M, 0.0027 M potassium chloride and 0.137 M sodium chloride, pH 7.4). On the other hand, disposable spin columns (Sartorius-Vivaspin 2, Surrey, UK) were also used for the removal of residual solvent as well the non-encapsulated drug.

Gas chromatography (200 series gas chromatograph, Ellutia, Cambs, UK) was used to test the presence of residual solvents in liposome samples obtained from the microfluidic device. The specifications of the method are described in table 2.1.

Table 2.1 Method parameters of gas chromatographic method used for residual solvent analysis.

Specification	Description
Gas chromatography	200 series gas chromatogrph, Ellutia, Cambs, UK)
Column	Capillary column. Dimensions:15 m x 0.25 mm x 0.25 µm. 1.5 µm film thickness.
Carrier gas	Hydrogen
Injector temperature	210°C
Detector temperature	280°C
Over temperature	Oven temperature was controlled by a 5-ramp temperature elevation program. The temperature was initially set at 45°C for 3 min, elevated to 250C at the rate of 20°C/min.

2.4.6 *In-vitro* drug release

The majority of *in-vitro* drug release studies are based upon dialysis of liposomal formulation against large volumes of buffers or other simulated media at physiological temperatures; yet, this excess buffer could lead to leakage of drug out of liposomes (Shabbits et al., 2002).

The CE7smart USP-4 system (SOTAX AG, Switzerland) was used to create an incubating environment for the release of drug encapsulated within liposomes. The method is widely used for the drug release study of novel drug delivery systems (Burgess et al., 2004; Siewert et al., 2003). Dialysed samples were subjected for the drug release. Briefly, the method is based on a dialysis adaptor placed in a flow-cell. Through this flow-cell, PBS (pH 7.4) was used in a closed loop system and was circulated at constant temperature ($37 \pm 1^\circ\text{C}$) at a constant flow of 8.0 mL/minute. The method was developed in-house and the release of drug was quantified using the validated HPLC method for the individual and simultaneous determination of glipizide and metformin. Samples were withdrawn at time intervals of 10, 30, 60, 90, 120, 180, 360, 540, 720 and 1440 minutes. The setup of the USP-4 and its operation is described further in chapter 3.

2.4.7 Microscopic analysis of liposomes

2.4.7.1 Confocal microscopy for the visualisation of MLV

1,1'-dioctadecyl-3,3,3,3'-tetramethylindocarbocyanine perchlorate (DiI C), a lipophilic dye, was used for this analysis. Liposomes were produced using the thin film hydration method (section 2.2.1), with the addition of 0.2 mole % of the DiI C dye. This dye has excitation wavelength 540 - 552 nm and emission wavelength 565 - 640 nm. When in the emission wavelength, the dye emits a red colour. A microslide (Cam lab, Cambridge, UK) was mounted on a clean glass slide to avoid the possible squeezing of liposomes caused by the usage of conventional coverslip. 10 μL of the suspension of DiI C dye encapsulated liposomes was then injected in to the microslide

using a micropipette. Due to the lipophilic nature of the dye, it was expected to be encapsulated into the bilayer of liposomes, thereby allowing imaging of the multiple red coloured layers of the MLV.

2.4.7.2 Cryo-electron microscopy for the visualisation of SUV

All the samples were freshly prepared on the day of analysis. Empty, single and co-drug loaded liposomes were prepared using the method described before (section 2.2). A 3 μ L aliquot of each sample was placed onto a pre-cleaned lacey carbon coated grid and flash frozen by plunging into liquid ethane cooled by liquid nitrogen. Samples were stored in liquid nitrogen and conveyed to a cryo-holder and observed under the electron microscope at liquid nitrogen temperatures. Grids were observed using Tecnai 12 G2 electron microscope (FEI, Eindhoven) at 80 kV and the evaluation was performed in the magnification range of 40000 X to 135000 X.

2.4.7.3 Fluorescence microscopy for the visualisation of RF-482

Fluorescein isothiocyanate FITC labelled peptide RF-482 was used to demonstrate the association of peptide with liposomes. Liposomes were produced using the method described in section 2.2.3. The unloaded fluorescent peptide was removed by using filter units (Ultracel-50K, Millipore Ireland Ltd., Cork, Ireland) and centrifugation. A drop of SUV suspension was then placed on a glass slide and dried in a desiccator, which was covered to avoid the interference of light with the fluorescent peptide. The slide with the dried SUV was then

observed under FITC channel of the Nikon Ti Eclipse fluorescence microscope (Nikon Inc. Melville, NY, USA).

2.4.7.3 Electron microscopy for the analysis of peptide loaded liposomes

Osmium tetroxide is commonly used for the fixative stain for cells; since the liposome structure resembles cell structure, a similar fixative staining was performed. Briefly, a drop of each liposome sample was placed on to the carbon film mesh copper grid and the excess suspension was removed using filter paper. Staining was performed using 4 % osmium tetroxide solution. Images were captured using high resolution electron microscope (EM10A/B, ZEISS, Germany).

2.5 Production and analysis of gold nanoparticles (GNPs)

2.5.1 Functionalisation of gold nanoparticles

Using apre-developed and validated protocol for the functionalisation of GNPs (Tiwari et al., 2014), 50 nm in sized carboxyl-polymer coated spherical GNPs (Nanopartz™, Loveland, CO, USA), were functionalised with RF-482 (Bachem Americas Inc., Santa Clara, CA, USA) with the aid of 1-Ethyl-3-(3-dimethylaminopropyl) carbodiimide (EDC, Sigma Aldrich, St. Louis, MO, USA) chemistry. The carboxylated GNPs were conjugated by mixing with peptide (17 mM) and EDC followed by shaking on an auto-shaker for an hour. The peptide concentration was higher than free carboxyl groups on the GNPs. The whole solution was then centrifuged at 18000 rpm for 60 min to separate unbound protein and repeated once for maximum removal of unbound

protein. Finally, the pellet of functionalised GNPs was re-suspended in sterile deionised water up to 5 mL.

The copyrights of the functionalisation are reserved but available information confirms that the peptide was first reacted to [(2-amino-ethoxy)-ethoxy]-acetic acid (H-AEEAc) by N-terminal addition reaction and conjugation of this to the GNPs was facilitated by the carboxyl group (-COOH) of the polymer coated on the surface of the GNPs (Singh et al., 2014).

2.5.2 Particle characteristics

Dynamic light scattering (DLS) (Zetasizer Nano-S, Malvern instruments, Westborough, MA, USA) was used for size determination of GNPs, F-GNPs, empty and RF-482 encapsulated liposomes. Zeta potential was determined using laser Doppler velocimetry (Zetasizer Nano-S, Malvern instruments, Westborough, MA, USA). The analysis was performed for both GNPs and FGPNs. Samples were diluted 1:100 in distilled water for both size and surface charge analysis.

2.5.3 UV/visible-spectrophotometry for the confirmation of conjugation

GNPs functionalisation was evaluated by UV/Vis spectrophotometry (Beckman Coulter spectrophotometer, Brea, CA, USA). Confirmation of conjugation of peptide with GNPs was made upon the data analysis of DLS as well as UV/Visible spectrometry (Beckman Coulter spectrophotometer, Brea, CA, USA); Chithraniet al. (2006) have reported that the functionalisation of GNPs can be confirmed by a shift in λ_{max} (Chithrani et al., 2006b).

2.5.4 Quantification of GNPs-Peptide conjugation

As mentioned earlier in section 2.5.1, the peptide concentration was higher than free carboxyl groups on the GNPs; therefore, the whole sample was then centrifuged at 18000 rpm for 60 min to separate unbound protein and repeated again for maximum removal of unbound protein. Finally, the pellet of functionalised GNPs was re-suspended in sterile deionised water up to 5 mL. The supernatant obtained after F-GNPs washing was subjected to BCA assay and tested for quantification of protein conjugated with GNPs, using an indirect approach by quantifying non-conjugated protein.

2.6 Analysis of RSV inhibition

The evaluation of GNPs and functionalised GNPs was established to prove their potential of inhibiting RSV (Tiwari et al., 2014). Following the established protocols of the GNPs conjugate system, the liposomes alone as well as liposomes loaded with peptide was evaluated for their potential to inhibit RSV.

2.6.1 Cell culture and subculture

Human epidermoid type-2 (HEP-2) cells (American Type Culture Collection (ATCC), Manassas, VA 20110 USA) were used throughout this study. Cells stored into the liquid nitrogen vapour phase were sub-cultured using the protocol provided by the supplier. Cells were thawed and centrifuged at 1500 rpm for 5 minutes to remove the organic solvent in the medium. The pellet was re-suspended using growth medium (MEM-10) supplemented with 2 mM L-Glutamine, 10%

FBS, 75U/mL Penicillin, 100 µg/mL Kanamycin as well as 75 µg/mL Streptomycin and stored in 75 cm² flask inside the incubator at 37°C in 5 % CO₂ environment. The flask was microscopically observed after 48 hours for the confluence. Upon observing the required confluence, the medium was discarded and the cells were detached from the wall of the flask using Trypsin0.53mM EDTA. The cell suspension was removed carefully and the flask was washed with the medium for maximum removal of the cells. The cell suspension was then centrifuged at 1500 rpm for 5 minutes and the cells re-suspended using MEM-10. The cells suspended in the medium were counted and sub-cultured if needed or preserved in liquid nitrogen vapour phase.2.6.2 Cell count

Cells prior to experimentation/ sub-culture/ storage were counted using a cell counter (countess-II FL, automated cell counter, ThermoFisher scientific, NY, USA). 10 µL of trypan blue (ThermoFisher scientific, NY, USA) and 10 µL of the sample was mixed and pipetted into the disposable chamber slide (Countess cell counting chamber slide, ThermoFisher scientific, NY, USA). The slide was inserted into the instrument and readings of cell count were noted for further use.

2.6.3 Cell viability assay/MTT assay

Human epidermoid type-2 (HEP-2) cells were proliferated using minimum essential medium (MEM) supplemented with 10 % foetal bovine serum (FBS), 2 mM L-glutamine, 75 U/mL penicillin, 100 mg/mL kanamycin and 75 mg/mL streptomycin. Empty and functionalised liposomes as well as peptide RF-482 was tested for the cell toxicity by using dye MTT (3-(4, 5-

dimethyl-thiazol-2-yl)-2, 5-diphenyl-tetrazolium bromide). The reduction assay was performed using CellTiter 96® Non-Radioactive cell proliferation assay kit (Promega, Madison, WI, USA). 25,000 cells per well were seeded using MEM-10 (10% FBS). Two different concentrations of peptide RF-482, empty liposomes and functionalised liposomes were tested for their celltoxicity 72 hours post incubation. MTT assay was performed as per protocol provided (Promega, Madison, WI, USA). The absorbance was measured at 570 nm using the plate reader (TECAN™, Morrisville, NC, USA).

2.6.4 Fluorescence microscopy for cell imaging

FITC labelled peptide RF-482 was used to demonstrate the association of peptide with liposomes. However, to study the RSV inhibition, 30000 cells per well were chambered into an 8 chambered slide. Cells were incubated with peptide RF-482, empty liposomes and functionalised liposomes for 48 h, followed by fixing in paraformaldehyde-glutaraldehyde and buffer (PBS) wash. The nuclei were stained using 4', 6-Diamidino-2-phenylindole (DAPI) and cell membranes were stained using Cell Mask™ (Life Technologies, Carlsbad, CA, USA). Using the DAPI and FITC channel of the Nikon Ti Eclipse fluorescence microscope (Nikon Inc. Melville, NY, USA), all the slide chambers were imaged.

2.6.5 Immunofluorescence imaging

Viral fusion inhibition was observed under fluorescence microscopy. 30,000 Hep-2 cells were grown in 250 µL/ well - 8 well chamber slides for 24-48h (with >80 % confluency). These cells were infected with RSV-Peptide/GNPs/FGNPs/liposome/RF-482 encapsulated liposomes,

followed by incubation for 48-72 Hrs at 37°C in a humidified 5% CO₂ atmosphere. Uninfected cells were then removed using 1X PBS washing and infected ones were fixed with methanol and permeabilised with cooled acetone for 1 minute at -20°C. Primary antibody was then added followed by removal of unattached antibody and addition of secondary antibody antibody-FITC (goat). Similar washing was performed to remove unused secondary antibody, followed by staining using DAPI (ProLong[®] Gold Antifade Reagents with DAPI, Life Technology). A cover-slip was fixed over the slide before observing under microscope.

2.6.6 Plaque assay

The plaque assay is one of the most common and reliable method of determination of viral/antiviral activity by counting plaques in the cell culture. The plaque assay was performed using HEP-2 cells (1.5×10^5 /well) proliferated in MEM-10 for 48hours to achieve maximum confluency. A predetermined titre of RSV was used for the experiments. Mixtures of RSV and peptide/empty liposome/conjugated liposome/GNPs/FGNPs were prepared in Dulbecco's modified eagle's media (DMEM) prior to the infection. Post-infection, the cells were covered by immobilising overlaying medium (1.6 % methyl cellulose) and subsequently incubated for 5 days at 37°C in 5 % CO₂ environment. On the 5th day, the overlaying medium was removed and the monolayer was fixed with cold methanol at -20°C followed by staining with 0.1 % crystal violet solution. Plaques were counted to determine the viral or antiviral activity.

2.6.7 Quantitative polymerase chain reaction (qPCR) analysis

The whole experiment consisted of a set of small experiments starting from cell culture to gene quantification. To reduce the chances of cross-contamination, these small experiments were performed in different rooms. Similar to the plaque assay, this experiment was started by plating HEP-2 cells (1.5×10^5 /well). After 48 hours proliferation, the cells were treated with viral dilutions with and without peptide/empty liposomes/conjugated liposomes/GNPs/FGNPs. These treated cells were then incubated for 48 hours at 37°C in 5 % CO₂ environment. After 48 hours incubation, the cells were harvested for RNA extraction. From the extracted RNA, using manufacturer's protocols, 1 µg RNA was converted to cDNA using reverse transcriptase enzyme. The RSV-F gene specific primers, along with the probe as well the experimental procedures, were selected based on previously published research (Eroglu et al., 2013; Mentel et al., 2003). Each qPCR reaction was performed using a total reaction mixture volume of 20 µL, comprised of 2 µL cDNA, reverse and forward primers (both 1 µL each), 2 µL probe, 10 µL of TaqMan Master Mix and nuclease free water. Water as a negative control and RSV-F gene amplicon dilutions (10^2 to 10^8) were used as standards to prepare a calibration curve. The qPCR for each sample was run in duplicate on Applied Biosystems® ViiA™ 7 real time PCR (Life Technologies).

2.7 Statistical analysis

Unless stated otherwise, the results were calculated as mean \pm standard deviation (SD). T-test alone or ANOVA followed by Dunnett's post hoc analysis was performed for comparison and significance was acknowledged for p values less than 0.05. All the calculations were made using Graphpad version-6 (GraphPad Inc., La Jolla, CA).

Chapter 3: Method development for the simultaneous quantification of metformin and glipizide

3.1 Introduction

Pharmaceutical analysis is a key element in the formulation of medicines and an important task within this is analytical assay development and validation. A wide range of instrumental techniques are in use to meet regulatory requirements, including spectroscopy and chromatography; these two techniques are the major tools for the qualitative, as well as quantitative analysis of APIs within products (Lawrence, 2008; Rozet et al., 2007). The present focus of the analytical method development is towards the development of precise, fast, reproducible, easy and cost effective methods. From the origins of pharmaceutical analysis, analytical assay methods have been included in the compendia of pharmacopoeias to characterise the purity of bulk drugs by finalising the limits of their active ingredient content. In recent years, the assay methods in the pharmacopeial monographs comprise in titrimetry, spectrophotometry, chromatography, capillary electrophoresis as well as the electro analytical methods (Pharmacopoeia, 2002).

Of these methods, chromatography is considered as one of the most reliable tools for drug detection and quantification. Chromatography has a broad history, and has been practiced in several forms, ranging from thin layer chromatography (TLC) to Ultra performance liquid chromatography (UPLC). Based on the physical sources which bring the mobile phase and the stationary phase together, chromatography is classified into two parts; first is planar chromatography, where the stationary phase is supported onto a plane or plate or paper and the mobile phase is driven by capillary action, gravity, pressure or electric field; the second is column chromatography, where the mobile phase is driven through the column by pressure,

gravity or electric field (Giddings, 1991). HPLC is the advanced type of column chromatography; in short, a mobile phase carrying drug for detection gets forced at high pressure through the column and the compound elutes according to its affinity towards the stationary phase (Snyder et al., 1979). Mainly, there are four different types of HPLC methods, namely normal phase-HPLC (NP-HPLC), reverse-phase-HPLC (RP-HPLC), size exclusion chromatography and ion-exchange chromatography. RP-HPLC is widely used in pharmaceuticals, as well as biomedical research, and is recognised for its excellent resolution, experimental ease, high recoveries and excellent reproducibility (Aguilar, 2004). Of the two, RP-HPLC is the most preferred, not only for the bulk drug analysis but also for the main compound analysis. Due to the non-polar nature of the stationary phase, molecule separation occurs according to their hydrophobicity. The elution of the compound can either be isocratic elution, where the concentration of organic phase is constant, or gradient elution, where the concentration of the organic solvent changes according to the programmed time (Aguilar, 2004). The assembly of RP-HPLC involves mobile phase, injector, pump, column, detector, instrument control and waste (Figure 3.1).

A wide range of detectors are used in chromatographic science. However, the most widely used detector for RP-HPLC is ultra-violet (UV) detector e.g. UV/Visible detector, fluorescence detector etc. In this work, the RP-HPLC with UV detector was used for qualitative and quantitative analysis.

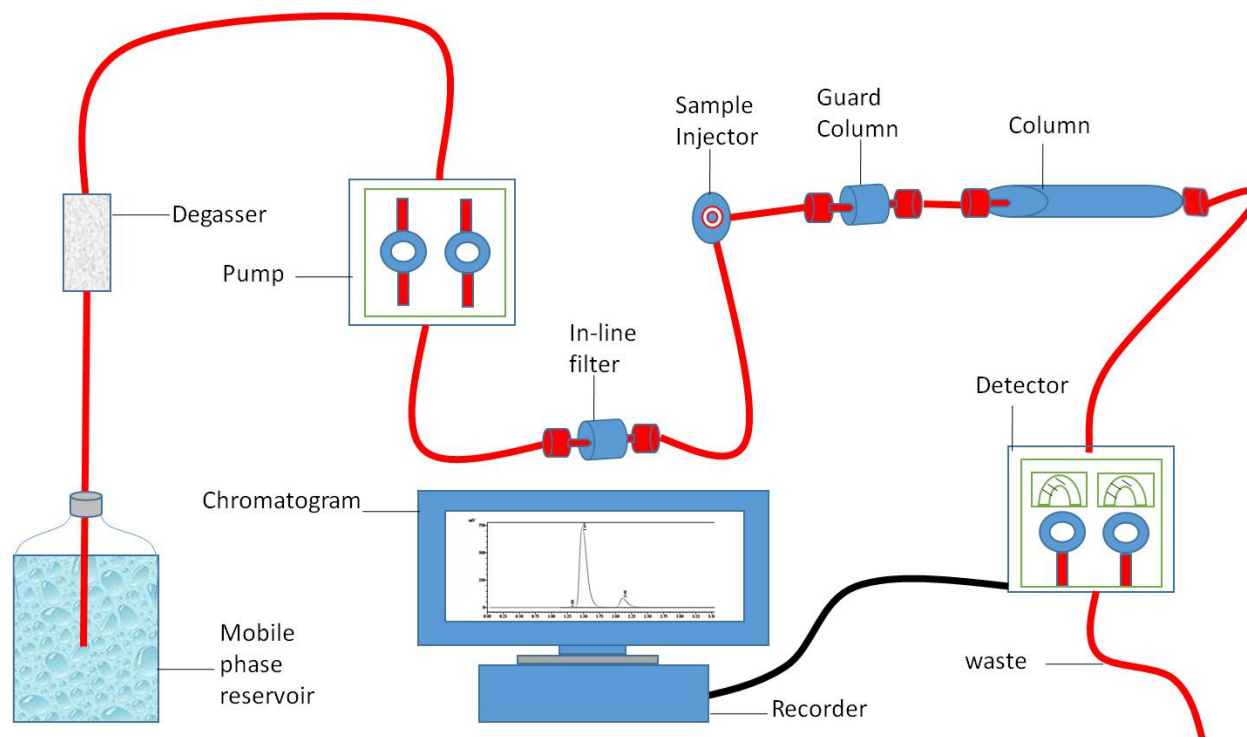


Figure 3.1 Schematic representation of an HPLC assembly. Three major sections of the HPLC are mobile phase, stationary phase and the detector. Pumps and injectors are equally important but their functioning are dependent on the quality of mobile phase and sample matrix respectively.

The aim of the work presented in this chapter was to develop and validate an HPLC assay for simultaneous detection of glipizide and metformin to allow quantification of drug loading within liposomes. To consider drug release from these liposomes, a USP-4 dissolution based method was developed and used in combination with HPLC to determine the release of single or co-encapsulated drugs.

3.2 Method development

3.2.1 Physicochemical properties of drug

The basic criterion for HPLC assay development is to study the physicochemical properties of the drug substance that could influence the chromatographic separation, which involves consideration of the solubility, pKa and Log P of the drugs. Metformin has a pKa value of 12.4, whereas that of glipizide is 5.6 (Figure 3.2). Similarly, log P represents drug lipophilicity (P) and is the partition coefficient of the molecule in a water-octanol system; metformin and glipizide represent log P values of -1.8 and 1.9, respectively (Figure 3.2). Subsequently, metformin is practically insoluble in organic solvent and glipizide is a poorly water soluble drug. Therefore, simultaneous determination of these compounds with divergent properties is challenging (Snyder et al., 1979; Snyder et al., 2012).

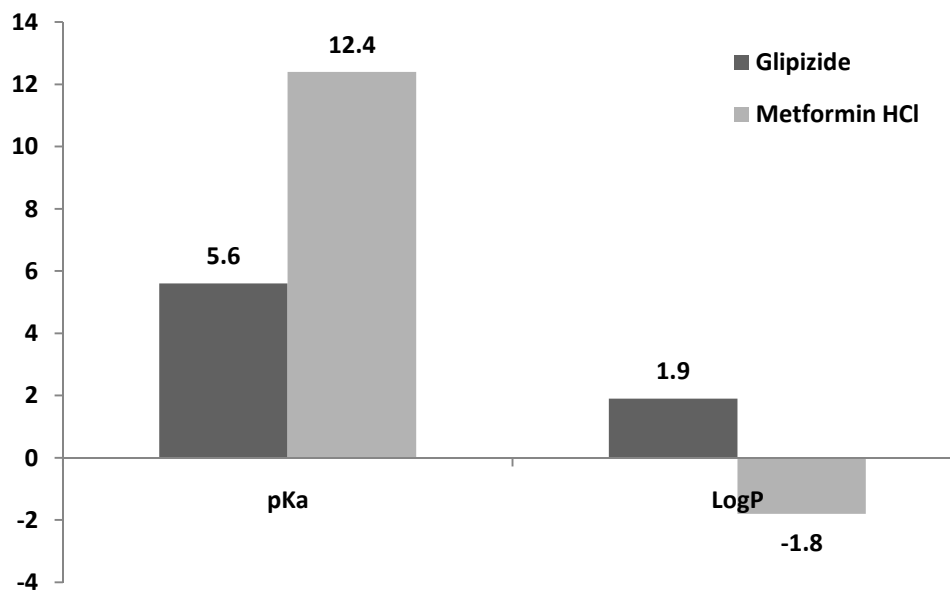


Figure 3.2 Representation of divergent nature of glipizide and metformin through their physicochemical properties.

3.2.2 Selection of diluents and determination of analytical wavelength (λ max)

The selection of solvent is a crucial part in this particular analysis development, due to the divergent solubility of the two drugs for analysis, with metformin requiring an aqueous media and, due to the poor water solubility of glipizide, use of organic solvent was preferred. Phosphate buffer is widely used due to its pKa values, prominent hydrophilic effect and better stability. In RP-HPLC, water is considered as a poor solvent but acetonitrile is well known for its organic modifier activity. Furthermore, acetonitrile has a low UV-cut off of 190 nm, which allows detection of compounds at lower wavelength. Apart from these properties of acetonitrile, an important characteristic is that it is less viscous than methanol and less bubble formation is observed when mixed with water; this reduces the back pressure on the RP-HPLC

system. Considering the above factors, a mixture of acetonitrile and phosphate buffered saline (65:35 v/v) was chosen as the diluent.

The maximum absorption wavelength (λ_{max}), was determined using UV-Visible spectrophotometer (Thermo Scientific Genesys 10S). For this qualitative analysis, two solutions of the two drugs were prepared separately at three different concentrations. Upon the spectrophotometric analysis, it was observed that both the drugs possess similar λ_{max} of 233 nm (results not shown).

3.2.3 Selection of column, mode of elution and mobile phase

Metformin is a polar molecule (Wanjari et al., 2008), which has led to researchers preferring ion-pair extraction or capillary electrophoresis for its separation from the matrix (Lai and Feng, 2006; Song et al., 1998). In contrast, Glipizide belongs to anarylsulfonylurea, which is relatively non polar (Lebovitz, 1985). Having this information about both the drugs, it was challenging to develop a RP-HPLC method for the separation of polar and non-polar molecules on the same column. Silica surface with octadecylsilane ligands are widely used in analytical separation with minor changes in the mobile phase (Ihara et al., 2006). Therefore, a Phenomenex Luna C-18 column with the dimensions i.d. 250 X 4.6 mm, particle size 5 μm and pore size 100 Å was chosen for the separation.

Before selecting elution mode, it is necessary to understand the capacity factor (k'), also termed the capacity ratio, which is a measure of the retention time of the peak, independent of geometry of the column or flow rate of the mobile phase. If the retention of the final peak has k' less than 5, then it is considered as weak retention (Schellinger and Carr, 2006). Considering the presence of a polar (metformin) and relatively non-polar (glipizide) molecule in the sample matrix, there was possibility of weak retention. To avoid interference of possible weak retention and baseline impediment, it is recommended to use isocratic elution. Given the versatility of acetonitrile and the hydrophilic effect as well as stability of phosphate buffer, it was preferred to have a mixture of these as mobile phase for the RP-HPLC separation. Therefore, the diluent (acetonitrile:PBS, 65:35 v/v) used earlier for spectrophotometric analysis, was finalised to be used for the RP-HPLC separation.

To test the above selection, preliminary analysis was performed at 233 nm on Shimadzu HPLC with UV detector using Phenomenex Luna C-18 column (150 X 4.6 mm, 5 μ m, 100 Å), and acetonitrile:PBS (65:35 v/v) mobile phase. There were two chromatographic peaks observed within 5 minutes. It was concluded that the 1st and 2nd peaks possibly represents metformin and glipizide, respectively; however, the peaks were not well separated (Figure 3.3).

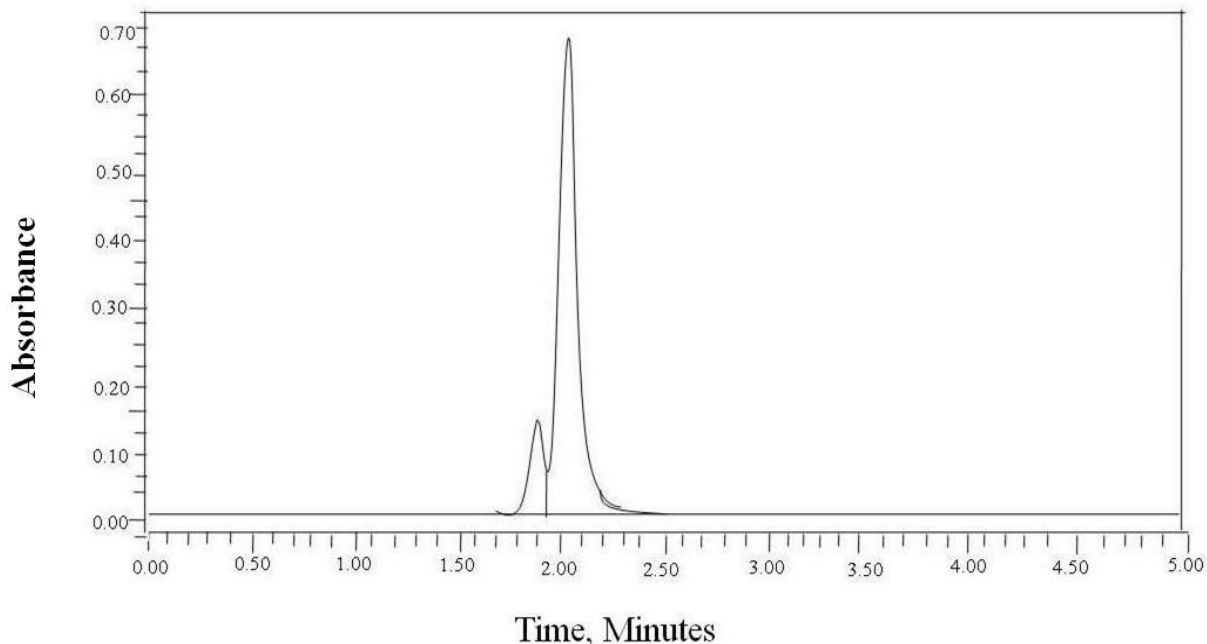


Figure 3.3 Chromatogram representing preliminary analysis of glipizide and metformin. Analysis performed on Shimadzu HPLC at 233 nm using Phenomenex Luna C-18 column and acetonitrile: PBS (65 : 35 v/v) mobile phase. Y-axis = Area Under Curve (AUC) (Dependent of concentration of analyte) and X-Axis = Minutes (Retention time representing interaction of analyte with the stationary phase when dissolved in given mobile phase and flow rate).

3.2.4 Impact of ion-pairing agent and pH on separation of compounds

Given that the mechanism of HPLC is primarily based on the hydrophobic interactions of the analyte and the stationary phase, use of an ion pairing agent can be used to promote retention of polar compounds such as metformin (e.g. phosphoric acid). Whilst, the exact mechanism of action is under debate, it has been shown that ion-pairing agents enhance retention of such molecules (Tinner, 2016). In terms of ion-pairing agents, a variety of ion-pairing agents are available e.g phosphoric acid, tri-fluoroacetic acid, penta-fluoroacetic acid etc. Using ortho-phosphoric acid, the pH of the aqueous portion of the mobile phase was adjusted to acidic. An

experiment similar to section 3.2.3 was performed with increased metformin and glipizide concentration for better peak height, but the pH of the mobile phase was adjusted to 6.75. Using this set up, both peak separation and peak resolution was improved (Figure 3.4).

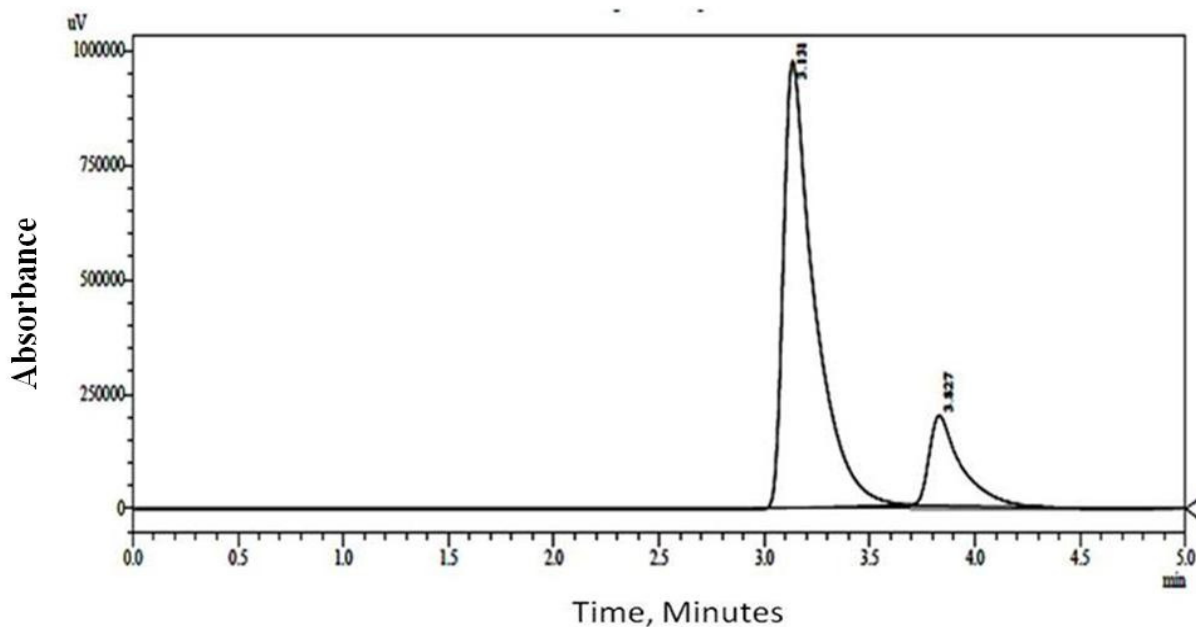


Figure 3.4 Chromatogram representing preliminary analysis of glipizide and metformin. Analysis performed on Shimadzu HPLC at 233 nm using Phenomenex Luna C-18 column and acetonitrile: PBS (65 : 35 v/v) mobile phase. Y-axis = Area Under Curve (AUC) (Dependent of concentration of analyte) and X-Axis = Minutes (Retention time representing interaction of analyte with the stationary phase when dissolved in given mobile phase and flow rate).

In section 3.2.3, it was observed that the smaller peak eluting first is metformin, whereas here it was observed that the smaller peak represents glipizide and the bigger peak represents metformin. This was confirmed by running a single analyte of the same concentration (Figure 3.4).

To further consider the impact of pH on peak separation, the pH was further reduced from 6.75 (Figure 3.4) to pH 5.75 for both the drugs independently and simultaneously (Figure 3.5). This reduction in pH promoted improved separation and a reduction in retention time to 1.5 and 2.4

minutes for metformin and glipizide, respectively (Figure 3.5). The retention of analyte in a mobile phase running on a stationary phase is dependent on the pH of the mobile phase, due to the impact on ionisation (Equation 3.1 and 3.2).



At the low pH, the concentration of the H⁺ ions causes an equilibrium shift and, hence, at higher pH the acidic analytes elute more rapidly (Fallon et al., 1987). Hence, both metformin and glipizide, which are weak acids and strong base respectively, elute slowly at higher pH of 6.75 (Figure 3.4) and rapidly at lower pH of 5.75 (Figure 3.5).

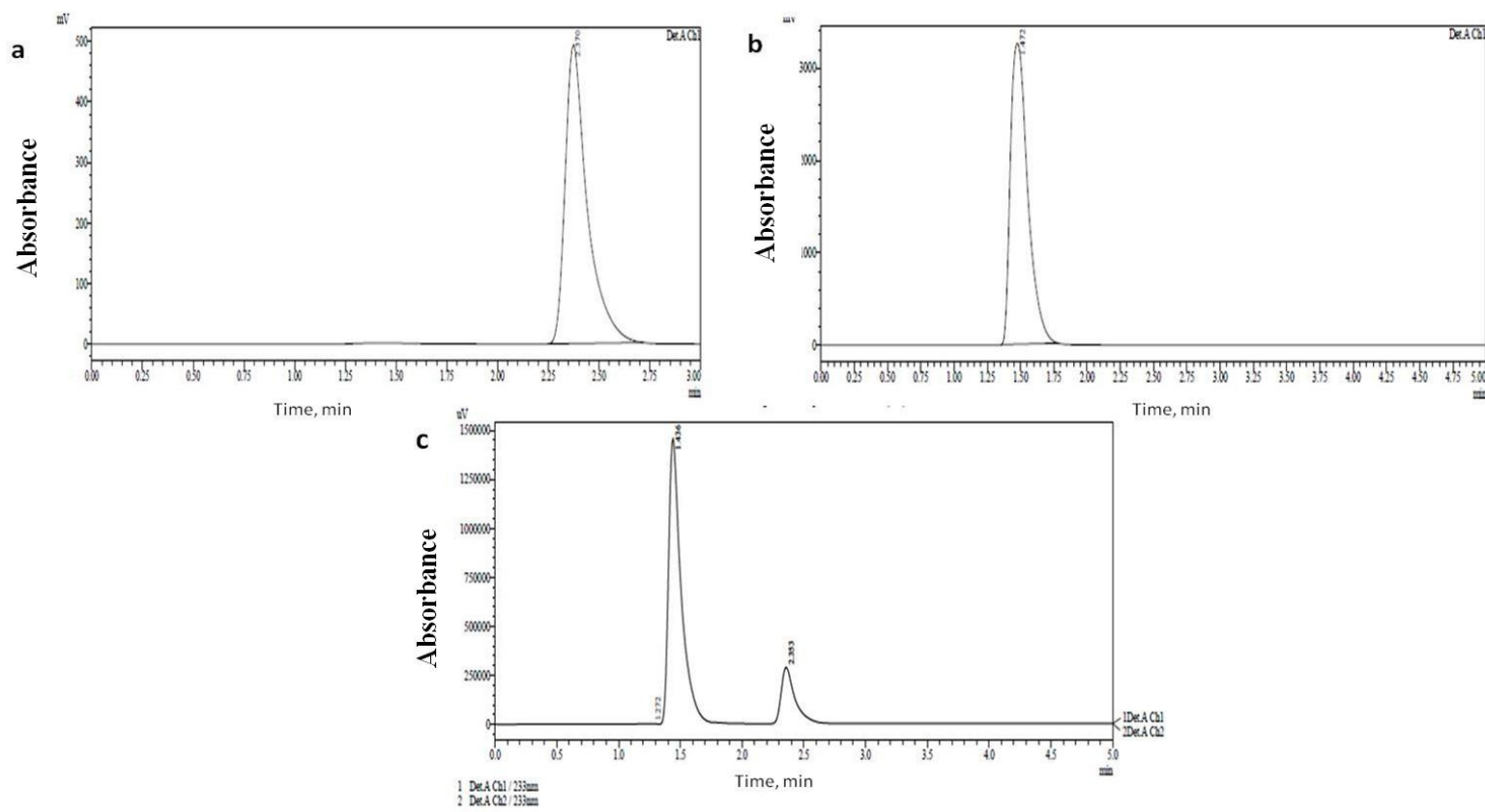


Figure 3.5 Chromatogram representing preliminary analysis of glipizide and metformin. The effect of pH on the separation of analyte. Analysis performed on Shimadzu HPLC at 233 nm using Phenomenex Luna C-18 column and acetonitrile: PBS (65: 35 v/v, aq. pH 5.75) mobile phase. a) glipizide RT=2.3 minutes, b) metformin RT= 1.5 minutes, c) metformin at 1.5 and glipizide at 2.3 minutes. Y-axis = Area Under Curve (AUC) (Dependent of concentration of analyte) and X-Axis = Minutes (Retention time representing interaction of analyte with the stationary phase when dissolved in given mobile phase and flow rate).

Based on these studies, a final HPLC protocol for the simultaneous analysis of both glipizide and metformin was developed, as outlined in Table 3.1.

Table 3.1 SOP for the RP-HPLC method for glipizide and metformin analysis.

RP-HPLC Assay	
Aim: Simultaneous determination of glipizide and metformin using RP-HPLC.	
Method parameters	
Chemicals:	Glipizide and metformin, phosphate buffered saline (PBS), acetonitrile (ACN), ortho-phosphoric acid, milli-Q water.
Column:	C18, 5 micron particle size, i.d. 150 × 4.6 mm, Pore size 100 Å
Mobile phase:	Adjust the pH of PBS to 5.75. Then mix acetonitrile and PBS with adjusted pH in a proportion 65:35 v/v. Degas for 5 minutes before use.
Diluent:	Use mobile phase as diluent.
Column Temperature:	Room Temperature
Sample Temperature:	Room Temperature
Flow:	1.0 mL / minute
Run time:	5 minutes
Wavelength:	233 nm
Detector:	Ultra-violet (UV)
Retention time:	Metformin-1.5 minutes, Glipizide-2.3 minutes.

3.3 Method validation

The international conference on harmonization (ICH) recognises accuracy, precision, repeatability, intermediate-precision, specificity, limit of quantitation and detection as well as linearity as major parameters for the HPLC method validation (FDA, 1994). Therefore, the method developed for the analysis of glipizide and metformin, as outlined in Table 3.1, was tested for these validation parameters.

3.3.1 Specificity

Specificity confirms no interference of the external components to the analyte with good chromatographic resolution (FDA, 1994). To confirm this, the chromatograms for each drug alone and in combination were generated (Figure 3.5). Apart from the sample analyte solutions, the buffer, as well as pH adjusted mobile phase and acetonitrile was injected separately. Neither single component analysis nor multi component analysis has observed interference of the extraneous entities (Figure 3.5).

3.3.2 Accuracy

Accuracy represents how close the experimental concentration is to the true concentration of the analyte (FDA, 1994). Five samples of different concentration were prepared in triplicates and tested for the recovery, as outlined in Table 3.2. For concentrations of both drugs, the recovery observed was >95 % (Table 3.2).

Table 3.2 Percent recovery of metformin and glipizide representing accuracy of the RP-HPLC method (n=3).

Metformin				Glipizide			
Standard	Concentration (µg/mL)	Found concentration (µg/mL)	% Recovery	Standard	Concentration (µg/mL)	Found concentration (µg/mL)	% Recovery
1	100	97.8	97.8	1	20	19.8	98.8
		± 0.3	± 0.3			± 0.3	± 0.2
2	200	191.4	95.7	2	30	30	100
		± 0.5	± 0.2			± 0.2	± 0.1
3	300	311.5	103.8	3	40	40.4	100.9
		± 0.5	± 0.2			± 0.2	± 0.2
4	400	411.8	102.9	4	50	50.3	100.6
		± 0.5	± 0.3			± 0.5	± 0.3
5	500	487.6	97.5	5	60	56.6	99.3
		± 1.0	± 0.2			± 0.6	± 0.3

3.3.3 Linearity

In validating the assay method, it is recommended that samples used to determine the recovery must be used for the purpose of linearity determination (FDA, 1994), i.e. samples should demonstrate that the recovery is within limits and satisfy the requirement of linearity (Jain et al., 2011). Therefore, five different concentrations of glipizide and metformin were used to consider linearity and accuracy. The accuracy represented for both drugs in table 3.3 was obtained from a linear calibration curve with $R^2 \geq 0.995$ (Figure 3.6).

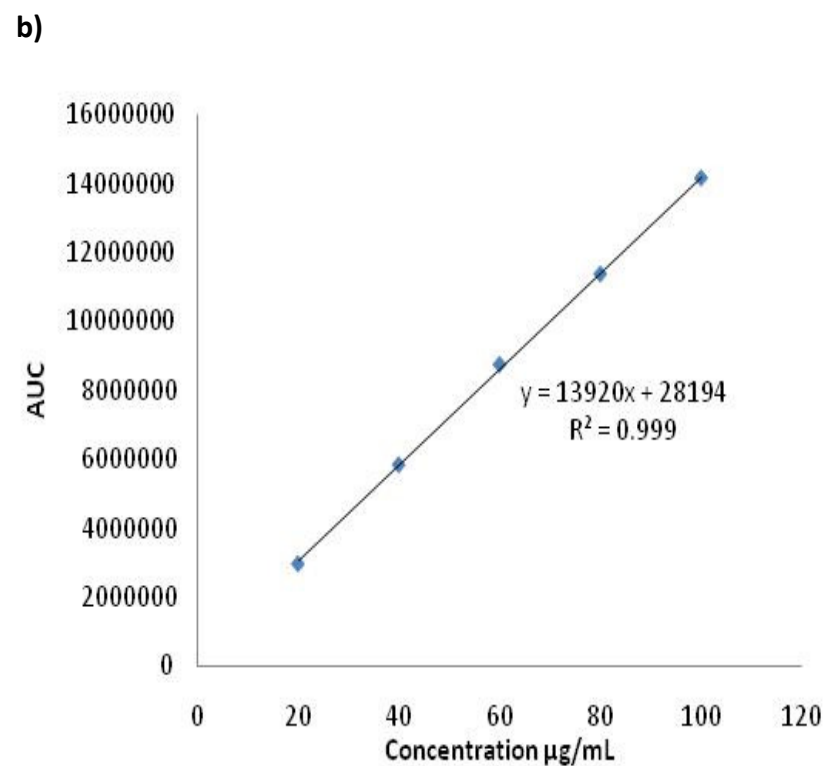
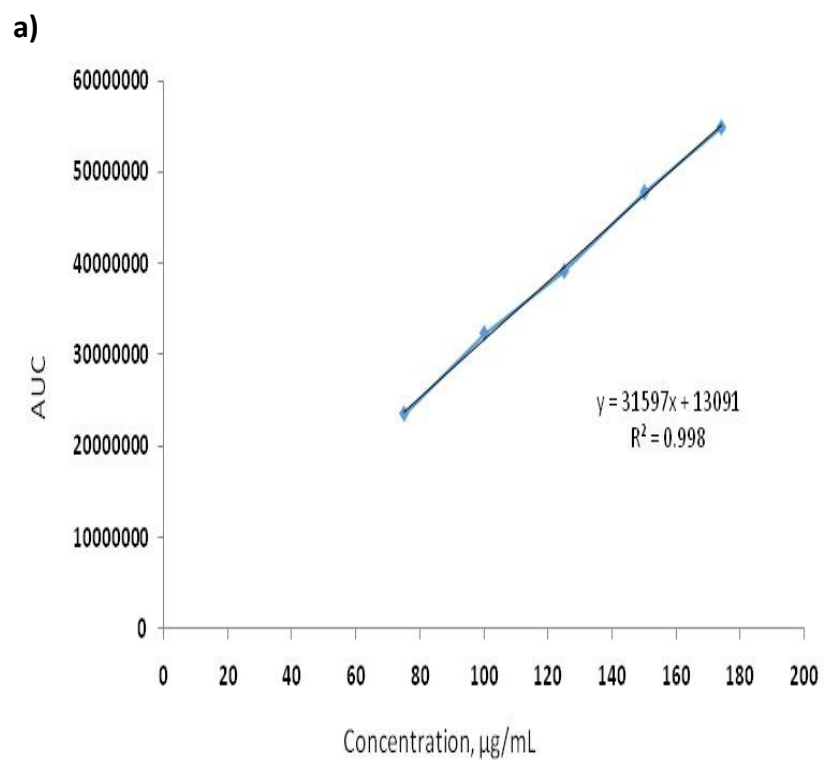


Figure 3.6 $R^2 \geq 0.995$ representing linearity obtained from the detector response to the analyte concentrations. a) Linearity of metformin concentration range 50 $\mu\text{g/mL}$ to 250 $\mu\text{g/mL}$; b) Linearity of glipizide concentration range 20 $\mu\text{g/mL}$ to 100 $\mu\text{g/mL}$. (AUC= Area under curve)

3.3.4 Precision

When a number of measurements are made under similar analytical conditions, the closeness of the measurements represents method precision (FDA, 1994). Precision is recommended to be calculated from the samples satisfying the requirement of linearity and accuracy. The fulfilment of the precision requirement is determined by percent relative standard deviation (% RSD) and it is recommended to be less than 0.5 %.

$$\% RSD = \frac{\text{Standard deviation}}{\text{Mean area of standard}} \times 100 \quad \text{Equation 3.3}$$

Three concentrations of both glipizide and metformin were prepared in pentaplicates. The closeness of value of those pentaplicate samples was then tested by determining % RSD from the average value. It was observed that both glipizide and metformin can be precisely determined using this RP-HPLC assay, as for both the drugs the % RSD was <0.5 % (Figure 3.7).

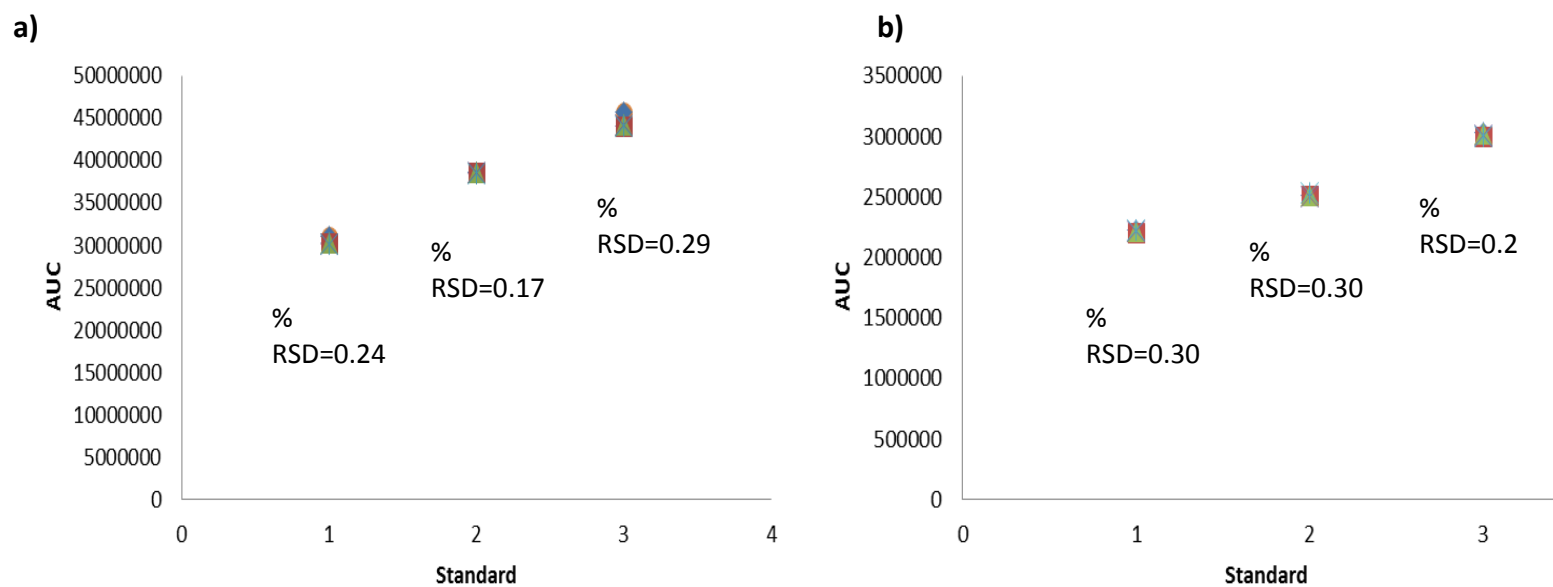


Figure 3.7 Percent $RSD \leq 0.5\%$ representing preciseness of the method. Values obtained from the detector response to the analytes concentration. a) % RSD for 3 different concentrations of metformin representing concentration precision. b) % RSD for 3 different concentrations of glipizide representing concentration precision. (AUC= Area under Curve)

3.3.5 Intermediate precision

Intermediate precision is also referred to as ruggedness. Determination of accuracy on different occasions is considered as intermediate precision (FDA, 1994). Therefore, experiments were performed during two different weeks and the data was collected. On both occasions, the recovery of both glipizide and metformin for all five samples was found >95 % (Table 3.3). This confirms the ruggedness of the method.

Table 3.3 Percent recovery representing the ruggedness of the analytical method for both metformin and glipizide (n=3).

Metformin				Glipizide			
Standard	Concentration (µg/mL)	Found concentration (µg/mL)	% Recovery	Standard	Concentration (µg/mL)	Found concentration (µg/mL)	% Recovery
1	100	97.6 ± 0.3	97.6 ± 0.3	1	20	19.2 ± 0.4	96 ± 0.3
2	200	193.5 ± 0.5	96.8 ± 0.2	2	30	31.1 ± 0.2	103.7 ± 0.4
3	300	304.5 ± 0.4	101.5 ± 0.4	3	40	39.8 ± 0.2	99.5 ± 0.2
4	400	403.8 ± 0.5	101 ± 0.3	4	50	49.5 ± 0.2	99 ± 0.2
5	500	492.6 ± 1.0	98.5 ± 0.2	5	60	58.6 ± 0.4	97.7 ± 0.3

3.3.6 Limit of detection (LOD) and limit of quantification (LOQ)

These parameters of the validation are also known as sensitivity of the method (Jain et al., 2011). LOD and LOQ are the two vital parameters of method validation and can be determined by plotting a calibration curve using different concentrations of the analyte. Using area under curve (AUC) percent recovery of standards, as well as unknown concentration of each drug was determined statistically. The AUC considered as response (y) is directly proportional to the concentration(x) of analyte present in the unknown solution. Linearity of standards as well as its slope (c) and intercept (m) also contribute in determination of sample concentration. Equation 3.4 represents the equation to calculate concentration (x) of sample (Nagaraja et al., 1999).

$$y = mx + c \quad \text{Equation 3.4}$$

As a part of drug analysis it is equally important to determine limit of detection (LOD) and limit of quantification (LOQ), using equations 3.5 and 3.6, respectively:

$$LOD = (3 \times \delta) \div s \quad \text{Equation 3.5}$$

$$LOQ = (10 \times \delta) \div s \quad \text{Equation 3.6}$$

Where δ is the standard deviation of standard deviation of y-intercept and s is slope (Chorachoo et al., 2013; Jamadar et al., 2011). Using the data obtained from the calibration curve (Figure 3.6), the LOD and LOQ of glipizide were calculated to be 2.2 μg and 6.6 μg , respectively, whereas for metformin these were 20.2 μg and 61.4 μg , respectively.

3.4 Development of drug release methods using USP-4 based SOTAX dissolution apparatus with flow through cell (FTC)

3.4.1 USP-4 dissolution apparatus

Dissolution testing is derived from the disintegration testing. Official dissolution testing was adopted in the British pharmacopoeia (BP) in 1945, followed by the United States pharmacopoeia (USP) in 1950. In the early development of dissolution testing, various methods were proposed (e.g. Basket stirrer method, beaker method and Vliet's method), before the introduction in the 1970s of the first two USP dissolution apparatus, the paddle and basket. In the past two decades, there has been further expansion of compendial dissolution testing apparatus for a variety of applications (Table 3.4)

Table 3.4 Different dissolution apparatus currently in use mentioned in USP.

USP dissolution apparatus	Name
USP-1	Basket
USP-2	Paddle
USP-3	Reciprocating cylinder
USP-4	Flow through
USP-5	Paddle over disk
USP-6	Cylinder
USP-7	Reciprocating holder

Among these various dissolution testing systems, USP-4 is recommended for the analysis of *in-vitro* drug release from liposomes (Bhardwaj and Burgess, 2010; Yuan et al., 2016). USP-4 was first included in the USP in 1957 (chapter <711> dissolution), and has since been adopted by the

European pharmacopoeia (Ph. Eur.) (Ph.Eur. 2.9.3) and Japanese pharmacopoeia (JP) (JP, XV, 6.10 dissolution test).

The FTC are marketed into two different dimensions: a large cell (22.6 mm-internal diameter) and a small cell (12 mm-i.d.) (Fotaki, 2011). These provide 19 mL and 8 mL volume for the dissolution testing (Figure 3.9A&B). Depending on the purpose of analysis, these FTC then can be used in two different systems: open loop or closed loop system (Figure 3.8C&D).

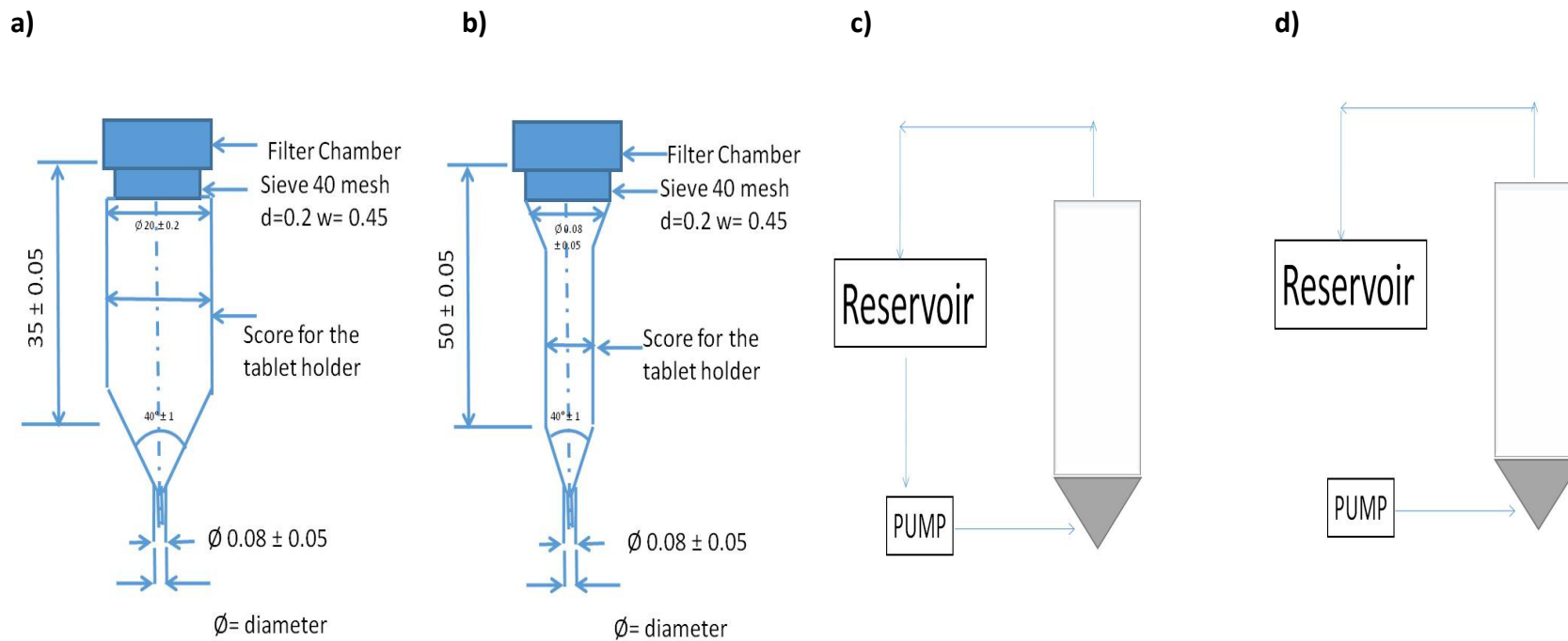


Figure 3.8 Type of FTC (a) Large and (b) small FTC. The FTC can be used in (c) Closed loop system and (d) open loop systems. Adopted from (Fotaki, 2011). Copyright 2011, The United States Pharmacopoeia. The FTC can be used in (c) Closed loop system and (d) open loop systems.

In this research, the CE7 smart USP-4 system (SOTAX AG, Switzerland) was used to create an incubating environment for the release of drug encapsulated within liposomes. The method is widely used for drug release studies from novel drug delivery systems (Burgess et al., 2004; Siewert et al., 2003). To measure drug release, samples were subjected to dialysis; briefly, the method is based on a dialysis adaptor placed in a flow-cell. Through this flow-cell, PBS (pH 7.4) was used in a closed loop system and was circulated at constant temperature ($37 \pm 1^\circ\text{C}$) at a constant flow of 8.0 mL/minute (Figure 3.9).

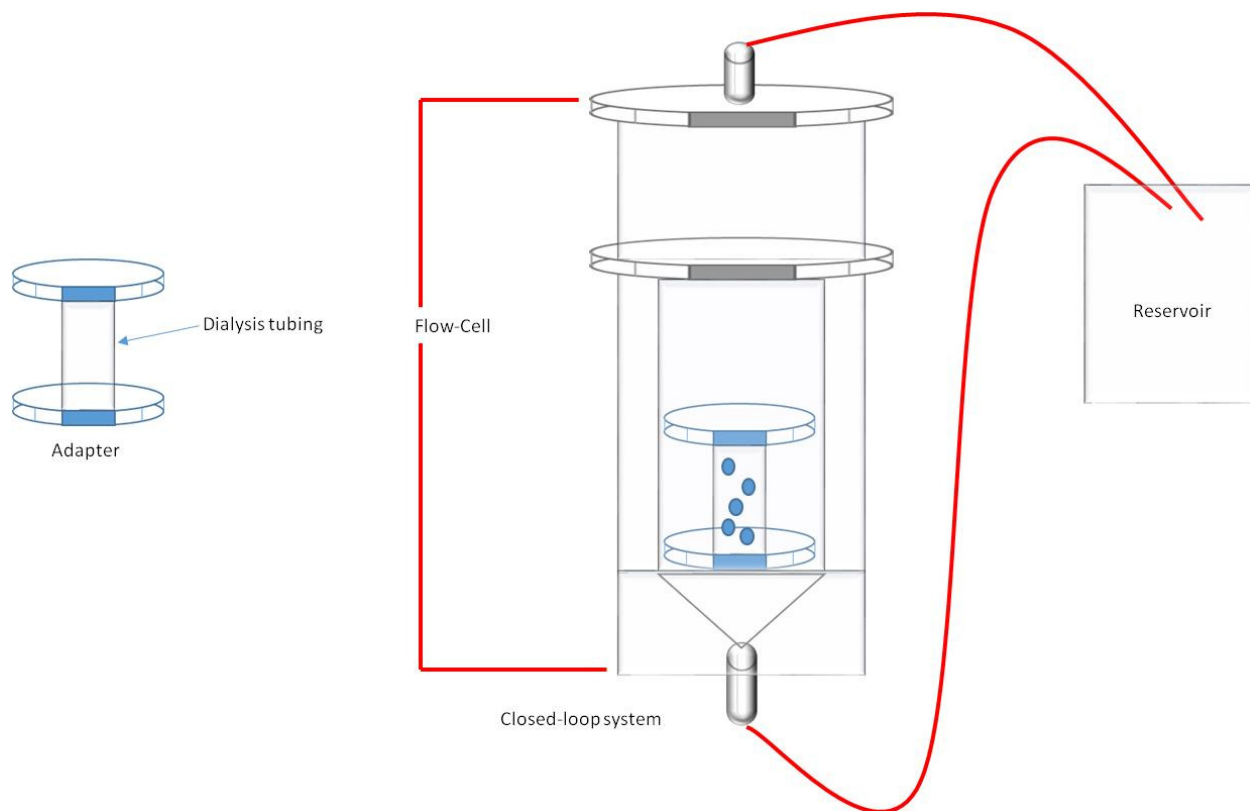


Figure 3.9 Schematic representation of USP-4 closed loop system. Adapter, flow-cell and reservoir are the 3 main components of the closed loop system used for studying in-vitro drug release.

3.4.2 Efficacy of the dialysis membrane for the passage of drug

As seen in the previous section, the assembly for *in-vitro* release drug study of liposomes has an adapter inside the FTC. To hold the liposomal suspension into this adapter, this advanced setting was wrapped by a dialysis membrane. To determine the efficacy of this system with the liposomes being developed, a predetermined concentration of both drugs was initially investigated to ensure effective 'free' drug removal. It was observed for both the drugs that >90% of the drug was diffused through the membrane in the initial 10 minute interval and complete removal was achieved within 20 minutes (Table 3.5).

Table 3.5 Testing efficacy of the dialysis tubing for the drug passage (n=1).

Time interval	% Metformin released	% Glipizide released
10 Minute	96.6	93.4
20 Minute	101.2	102.4
30 Minute	102.1	102.6

3.4.3 Selection of release medium for the *in-vitro* release of liposomal drugs

In the GI tract, the duodenum and jejunum are ideal for the absorption of fats, whereas the colon is ideal for water, electrolytes as well as short-chain fatty acids. Therefore, it is expected that liposomal absorption can be achieved in the small and large intestine, especially in the duodenum, jejunum and colon. The pH of the duodenum and jejunum is neutral to slightly

basic. Therefore, preliminary studies were conducted using neutral to slightly basic release media.

To study the effect of salts and pH, the release of drug was studied initially in two different mediums: simulated media (Table 3.6) and PBS (composition: phosphate buffer 0.01 M, 0.0027 M potassium chloride and 0.137 M sodium chloride, pH 7.4).

3.4.4 *In-vitro* release of liposome encapsulated drugs

Liposomal drug release studies have often been performed using a large amount of buffers and it was also observed that excess buffer often results in inaccurate analysis due to leakage of drug(s) (Shabbits et al., 2002). Therefore, the *in-vitro* drug release was studied using USP-4, FTC based closed loop system (SOTAX, SOTAX Ltd., London, UK). The USP-4 is well known for versatility, and has distinct advantages such as requiring low volume of media, precise as well as auto-temperature control and most important is the adaptor, which is especially designed for the submicron sized delivery systems.

To develop a protocol for analysis of drug released from liposome in release media, initial trials were undertaken using individual drugs. The initial observations were aimed to spot peaks of active analyte; this was done to study the interference of the media or method. Release of drug is not only triggered by the pH of the environment but also by the presence of salts in the fed and fasted state. Recently *Marques. et. al.* (Marques et al., 2011) have described the simulated

biological fluids that may be used as dissolution media. Therefore, initial trials of liposomal drug were decided to be taken into simulated medium resembling colonic as well as duodenum and jejunum environment (Table 3.6).

Table 3.6 Simulated biological fluid to use as dissolution media to study the release of liposome encapsulated drugs. (Adopted from (Marques et al., 2011)).

Simulated colonic fluid	
Composition	Amount (g/L)
Potassium chloride	0.2
Sodium chloride	8
Potassium phosphate monobasic	0.24
Sodium phosphate dibasic	1.44
pH	7

Although peaks of metformin and glipizide were spotted with good resolution, there was interference of the dissolution media observed during the chromatographic analysis (Figure 3.10). An alternative approach to the simulated fluid was use of buffer solution at the required pH. Therefore, PBS solution of pH 7.4 was used for further trials, since there was no interference caused by the dissolution medium. Both metformin and glipizide peaks were detected on the same retention time as observed during drug loading quantification (Figure 3.11). Further, the drug release was quantified using RP-HPLC (section 2.6.) and reported as % release relative to amount of drug entrapped within liposomes.

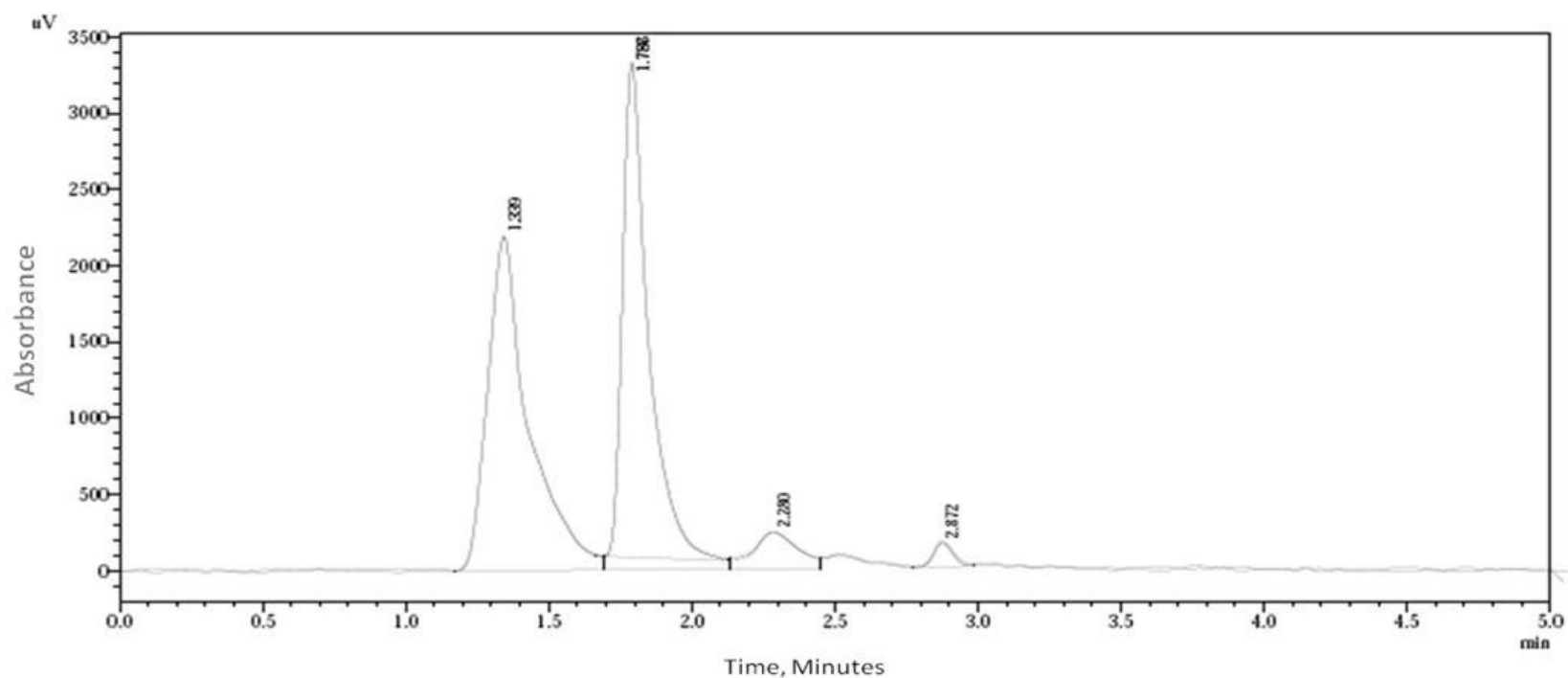


Figure 3.10 Chromatogram representing the analysis of released drug from liposomes into simulated biological dissolution media. The HPLC-UV method developed (section 3.3) for the quantification of drug encapsulation was applied for this analysis. Y-axis = Area Under Curve (AUC) (Dependent of concentration of analyte) and X-Axis = Minutes (Retention time representing interaction of analyte with the stationary phase when dissolved in given mobile phase and flow rate).

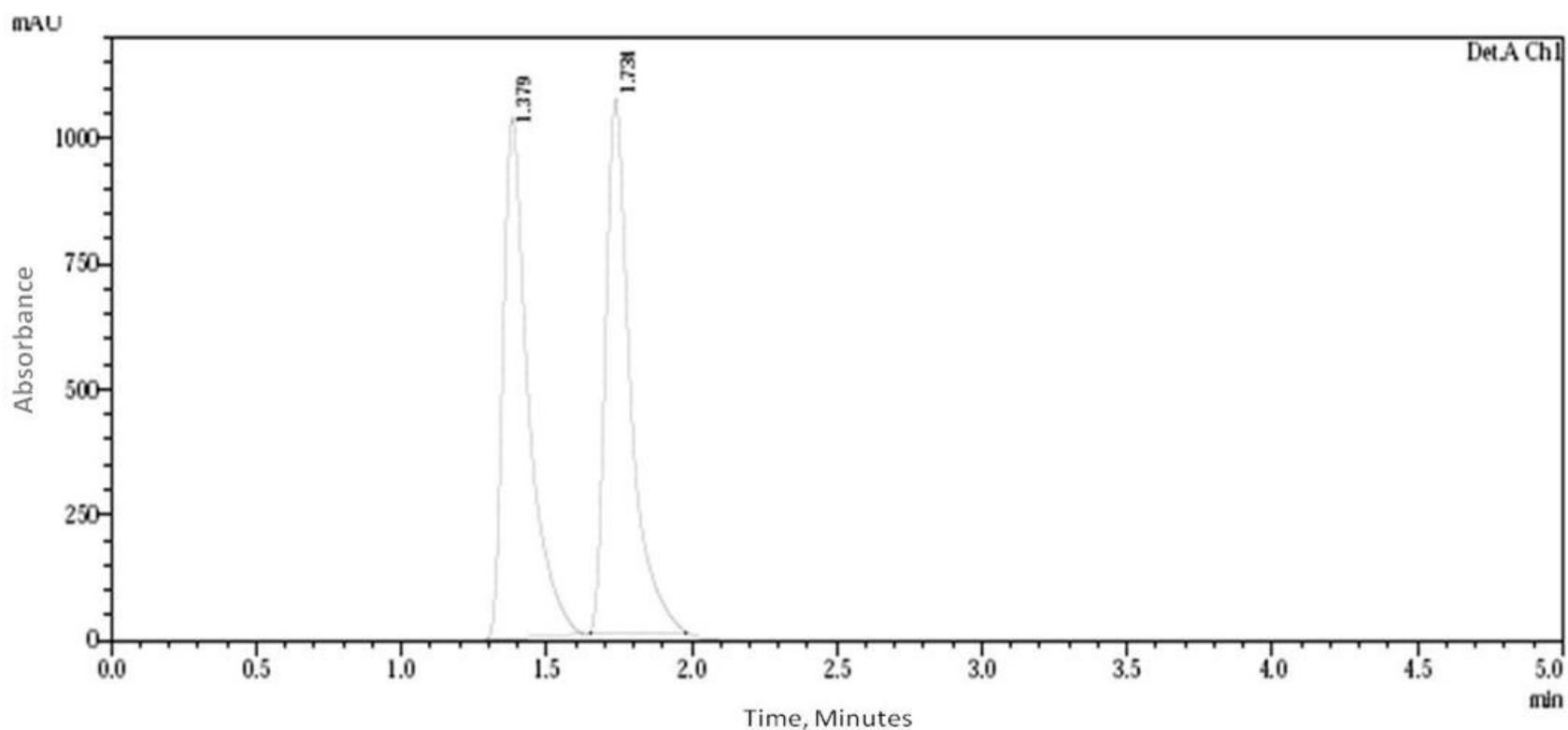


Figure 3.11 Chromatogram representing the analysis of released drug from liposomes into PBS (pH 7.4). The HPLC-UV method developed (section 3.3) for the quantification of drug encapsulation was applied for this analysis. Y-axis = Area Under Curve (AUC) (Dependent of concentration of analyte) and X-Axis = Minutes (Retention time representing interaction of analyte with the stationary phase when dissolved in given mobile phase and flow rate).

3.5 Conclusion

Due to the divergent nature of both molecules, to develop a method for simultaneous determination was a challenging task. The developed RP-HPLC method is based on isocratic elution, which makes the method simple and retention time observed for both drugs is less than 3 minutes. The validation was carried out using ICH guidelines and this method has fulfilled all the validation requirements recommended by ICH. In short, the method is easy, precise, accurate, selective as well as sensitive. Also, this method of simultaneous determination of glipizide and metformin has been found to be effectively rugged and robust for both the drug determination.

The simulated biological dissolution medium failed to meet the qualitative criteria for the chromatographic analysis of released drug. However, with PBS (pH 7.4) it was possible to maintain the intrinsic environment.

Chapter 4: Formulation of liposomes co-encapsulating hydrophilic and lipophilic drugs

4.1 Introduction

Administration of multiple drugs simultaneously is usually possible with conventional dosage forms (e.g. tablets, capsules and liquids). However, their controlled delivery using novel drug delivery systems (e.g. liposomes, niosomes, polymer nanoparticles, etc.) has received limited attention. Therefore, the research reported within this chapter focused on co-encapsulation of drugs with divergent solubilities within liposomes. At present, although marketed liposome products have been prepared with either hydrophilic or lipophilic active ingredients encapsulated, currently there are no products on the market taking advantage of the potential to encapsulate both hydrophilic and lipophilic active ingredients in the same vesicles. Indeed, there is very limited research present about this concept of co-encapsulation.

Co-encapsulation is an innovative approach, making liposomes a multi-drug carrier. In recent years, co-encapsulation has been reported for two drugs of divergent solubility inside liposomes (Cosco et al., 2012; Liu et al., 2014; Tardi et al., 2007). For example, *Cosco et al.* (2012) demonstrated liposomal co-encapsulation of gemcitabine (a water soluble drug) and tamoxifen (a lipid soluble drug), whereas, *Tardi et al.* (2007) and *Liu et al.* (2014) have shown co-encapsulation of irinotecan-floxuridine and doxorubicin-paclitaxel, respectively. In each of these studies, the method used was the thin film hydration method. However, to enhance the loading of the hydrophilic drug, a pH gradient was created. It can be seen from the drugs selected, these studies were mainly done with oncological agents and supplements the potential of this co-encapsulation in cancer research. However, the potential of liposomes to co-encapsulate drugs could also create a novel way of delivering drugs of divergent solubility

which are prescribed in combinational therapy, such as the above mentioned gemcitabine and tamoxifen, or metformin and glipizide, which can be prepared in a single dosage form and could improve patient concordance (Collier, 2012).

4.2 Aim and objectives

The aim of this work was to develop a formulation co-encapsulating divergent solubility drugs in liposomes manufactured by the conventional thin film hydration method. To achieve this, the objectives were to:

1. Optimise the lipid concentration to be used for co-encapsulation;
2. Study the impact of single and co-drug encapsulation on drug encapsulation efficiency;
3. Study the drug retention capacity of liposomes encapsulating one or two drugs together;
4. Study the *in-vitro* drug release behaviour of drugs individually and simultaneously encapsulated.

4.3 Results and discussion

4.3.1 Selection of drugs for co-encapsulation

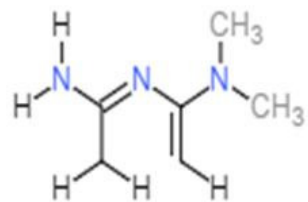
As mentioned above, drugs prescribed in combinational therapy and with contrasting solubility are ideal for this concept of co-encapsulation. Diabetes is a principal risk factor for those patients with cardiovascular (CVS) disease (Dokken, 2008) and the 'statins' are given as a preventive intervention (Ebrahim et al., 2014; Taylor et al., 2013). Statins such as simvastatin,

atorvastatin, etc., are prescribed in combination with metformin for the diabetic patients suffering from cardiovascular disorders. Therefore drugs considered for co-loading within liposomes were:

- Metformin hydrochloride (Figure 4.1A) is water soluble and highly prescribed drug for treating type-2 diabetes (Setter et al., 2003). It is a water soluble compound and will be entrapped in the hydrophilic core of liposomes or niosomes. Metformin belongs to the biguanide anti-diabetic agents (Vigneri and Goldfine, 1987). Metformin is used in combination therapy glipizide and marketed products are available e.g. the tablet formulation '*Metaglip*'.
- Glipizide (Figure 4.1B) is a poorly water soluble drug and a potent hyperglycemic drug from the family of sulfonylureas (Prendergast, 1983). Glipizide and metformin have contrast solubility and are used in combinational therapy.
- Simvastatin (Figure 1C) is a poorly soluble drug and has no drug-drug interactions with the metformin. Therefore, two combinations metformin-glipizide and metformin-simvastatin were selected for preliminary investigations.

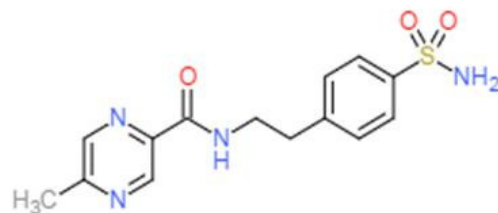
4.3.2 Selection of lipids

Lipids are molecules made up of prominently hydrocarbon moieties and having molecular weights ranging from 150 to 3000 (Small, 1981). The hydrocarbon portion of the lipid molecule can be aliphatic or aromatic (cyclic) and can be of single chain or have multiple chains, with phospholipids and spingolipids having two hydrocarbon chains and triaclycerols having three chains (Perrie and Rades, 2012b; Small, 1981).

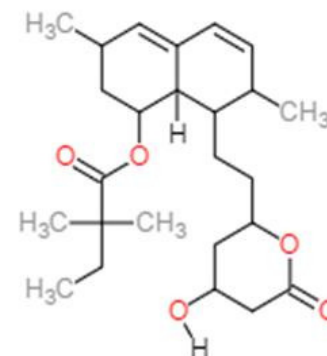


. HCl

Metformin Hydrochloride
(A)



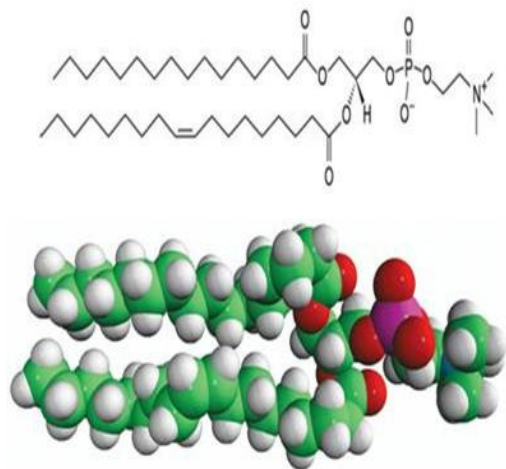
Glipizide
(B)



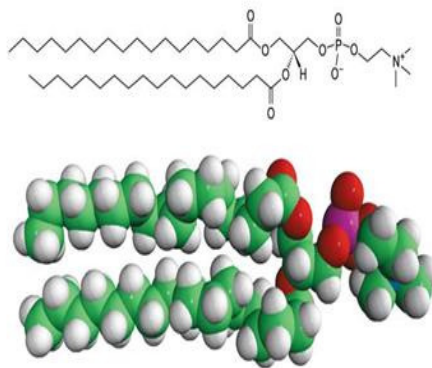
Simvastatin
(C)

Figure 4.1 Chemical structures of selected drug for co-encapsulation. A) Metformin hydrochloride (Water Soluble), B) Glipizide (Poorly water soluble), C) Simvastatin (Poorly water soluble). Sketches drawn and transferred from web.chemdoodle.com

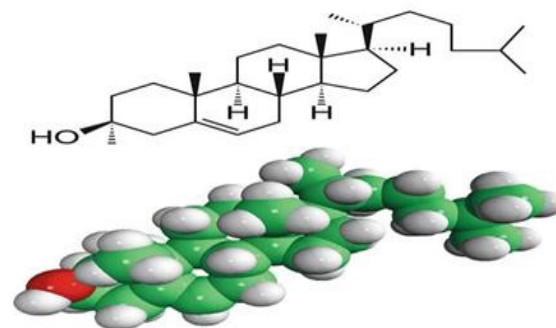
Phospholipids are amphiphilic in nature and have both hydrophobic and hydrophilic parts within their structure, thus supporting the formation of lipid bilayers. Due to variability in their head group, degree of saturation of fatty esters and variability in chain length, phospholipids can be used to formulate a range of liposome systems. Phospholipids as a group are lipids with one or more phosphate groups. In the field of liposomes, both PC and DSPC are being used widely, since they form a predominant component of human cell membranes and because they are less prone to oxidation upon storage (Lasic, 1993). The polar head-group and non-polar tail of these lipids form structures resembling human cell membranes. Especially, due to the high transition temperature and longer chain length, 40 % of the marketed liposomal formulations have DSPC in the formulation (De Villiers et al., 2008). DSPC is a synthetic lipid having only saturated chains, whereas the Egg-yolk PC (EPC) is a natural PC-lipid with both saturated as well as unsaturated fatty acids in its structure. Therefore, during initial studies, liposomes were produced using the PC (Figure 4.2A) or DSPC (Figure 4.2B) and their particle characteristics compared (Table 4.1). Cholesterol (Figure 4.2C) is a major component of eukaryotic cell membrane. Cholesterol brings profound changes to physical properties of membranes (Wang and Quinn, 2002), e.g. as discussed in chapter 1 (Section 1.1.1.2).



A) PC



B) DSPC



C) Cholesterol

Figure 4.2 Chemical structures of selected drug for co-encapsulation. A) PC (L- α -lysophosphatidylcholine), B) DSPC (1,2-distearoyl-sn-glycero-3-phosphocholine), C) Cholesterol. Sketches adopted from the website of Avanti polar lipids Inc.

To consider the effect of lipid chain length, MLVs were prepared using the thin film hydration method (Bangham et al., 1965). Two different formulations were prepared in PBS (pH 7.4) with either PC or DSPC and cholesterol (Table 4.1). The increase in alkyl chain length could result in an increase in CPP and, hence, impact on the liposome characteristics, including vesicle size (Uchegbu and Florence, 1995; Uchegbu and Vyas, 1998a). Indeed, the formation of bigger vesicles has been shown to be directly proportional to the lipid chain length (Bayindir and Yuksel, 2010).

Table 4.1 Composition of formulations prepared for the preliminary study of effect of cholesterol concentration, type of lipid and hydration media.

Formulation	Concentration (w/w)	
	PC/DSPC	CHOL
PC:CHOL (PBS, pH 7.4)	5	2
DSPC:CHOL (PBS, pH 7.4)	5	2

Figure 4.3 shows the sizes of MLV liposomes prepared using PC:Chol ($7.5 \pm 1.2 \mu\text{m}$) are significantly ($p < 0.05$, t-test) smaller than their DSPC:Chol liposome counterparts ($11.5 \pm 2.2 \mu\text{m}$). This difference in size could be due to difference in their alkyl chain lengths (Figure 4.2). Furthermore, when taking into account the span value— which is measure of particle size distribution, where a span value >1.0 is considered as broader size distribution – here, both liposome formulations have a broad size distribution as the span value for PC:Chol liposomes is (Span: 1.6 ± 0.08) and DSPC:chol (Span: 2.0 ± 0.11) (results not shown). This heterogeneous size distribution is a common issue with liposomes formed by the lipid film hydration.

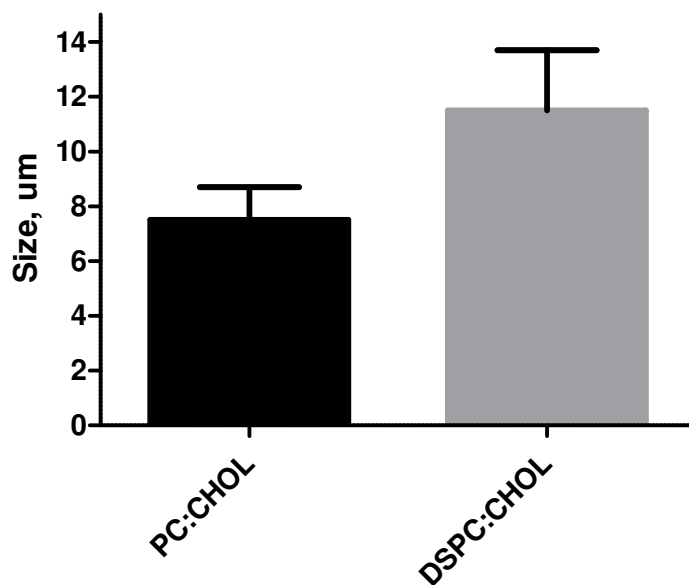


Figure 4.3 Comparison of size results obtained from analysis of PC:Chol and DSPC:Chol formulations prepared by thin film hydration method. PBS (pH 7.4) was used as hydration medium for these formulations (N=3± SD).

Transition temperature (T_c) plays a crucial role in the formation of liposomes, as well as their membrane fluidity (Mabrey and Sturtevant, 1976) and this is usually determined by differential scanning calorimetry (DSC). In the production of liposomes, liposome formation can only happen above the transition temperature of the lipid mixture. Lipids with $T_c > 37^\circ\text{C}$ make lipid bilayers less prone to leakage and uptake by mononuclear phagocyte system (MPS) at physiological temperature. On the other hand, liposomes produced with lipids having a T_c below physiological temperatures are more susceptible to leakage and clearance within the body, as they are more rapidly opsonised and taken up by MPS (Bhandary et al., 2010; Kirby et al., 1980; Sharma and Sharma, 1997). In addition to higher T_c lipids, the presence of cholesterol in the system can also improve membrane fluidity. Cholesterol concentrations of more than 30 molar % have been shown to eliminate the phase transition of lipid membranes, making them

less leaky on systemic administration (Mohammed et al., 2004; Sharma and Sharma, 1997; Wang and Quinn, 2002). Given this information, using DSPC will give more robust liposomes (due to its transition temperature (T_c) and saturated long chains) and the use of higher transition temperature lipid could be beneficial in terms of storage of formulations; therefore, DSPC was selected for continued studies.

4.3.3 Influence of cholesterol concentration on MLV particle characteristics

Cholesterol is a common component of liposome formulations, because cholesterol brings profound changes to physical properties of membranes (Wang and Quinn, 2002). In particular, inclusion of cholesterol improves bilayer stability. The key factor making cholesterol more promising is its planar steroid ring imparting a rigid structure to the molecule, which makes lipid-cholesterol interaction more prominent (Mohammed et al., 2004; Nomura et al., 2005). However, the impact of cholesterol content on MLV formulations has been controversial; it has been reported that the cholesterol content in the MLV formulations does not make any significant changes in the size and surface charge (Ali et al., 2010), whilst contrasting reports state that the addition of cholesterol to the lipid membrane reduces the Na^+ binding to the lipid head group, releasing the ions from the membrane interface to the water phase, resulting in significant reduction in surface charge (Magarkar et al., 2014), whereas it has also been suggested that high concentrations of cholesterol may impact on the size of the vesicles and possibly decrease the size by making the structure more rigid (Nomura et al., 2005). Therefore, to consider the impact of cholesterol concentration on liposome formulations, two ratios of

phospholipid:cholesterol were considered. Knowing that the absence of cholesterol makes the bilayer porous (Ali et al., 2010), presence of cholesterol condenses the bilayer by reducing permeability, and an excess of cholesterol can significantly influence bilayer loading (Bernsdorff et al., 1997); the cholesterol concentrations of 17 and 30 mol % were chosen for the formulation (based on previous studies, Ali et al. 2010)

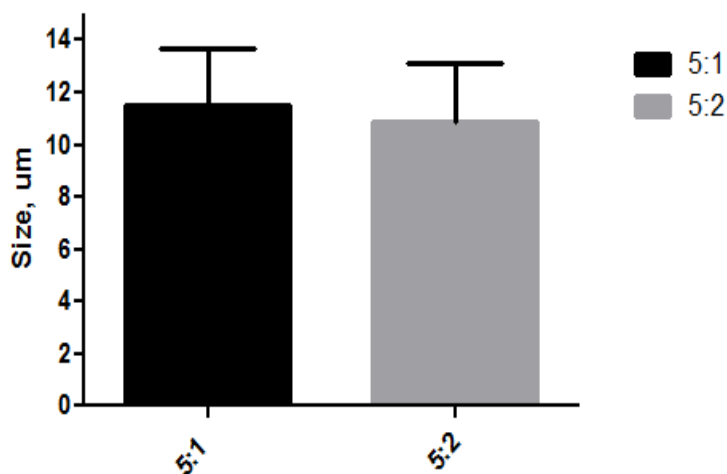


Figure 4.4 Comparison of the vesicle size from liposomes containing increased cholesterol concentration. DSPC:Cholesterol 5:1 and 5:2 w/w formulations. Results are expressed as the means of four experiments ($N=3 \pm SD$).

Confirming the findings of *Ali et al. (2010)*, the results in Figure 4.4 show that there was no significant difference ($p > 0.05$, t-test) in the size of liposomes prepared at different ratios of cholesterol (5:1 and 5:2). This is in contrast to the results reported by *Magarkar et al. (2014)* and *Nomura et al. (2005)*. Within their study, they attribute the reduction in size of liposomes prepared from Di-oleoyl-phosphatidylcholine (DOPC) and varying cholesterol concentration up to 40 mol % on increasing concentration of cholesterol. *Magarkar et al. (2014)* have also

proposed that the elevated concentration of cholesterol reduces the zeta potential of DSPC and 1-palmitoyl-2-oleoyl-sn-glycero-3-phosphocholine (POPC) membranes (Magarkar et al., 2014). PC and DSPC are zwitterionic lipids with net neutral surface charge. Zeta potential measures the potential difference between the dispersion medium (in this case PBS) and stationary layer of fluid attached to the liposomes; thus, resulting in a small negative charge on the vesicles. The charge on the liposomes of all formulations of both the lipids was neutral to very slightly negative (PC= -6.7 ± 1.2 mV (n=3), DSPC= -8.7 ± 2 mV (n=3)) with cholesterol having no notable impact.

4.3.4 Stability testing of DSPC liposomes

To investigate the stability of liposomes and to inform how these systems can be stored during forthcoming studies, the stability (in terms of liposome size and zeta potential) of DSPC liposomes was considered, as well as the effect of cholesterol concentration. Formulations were stored in three different stability chambers: 1) 4°C; 2) 25°C/60 % RH; and 3) 40°C/75% RH. The purpose of stability testing under different environmental conditions was to provide substantiation of how the quality of the formulation varies with time under the influence of different environmental factors, such as temperature and humidity. The samples were tested for size and zeta potential at intervals over 21 days.

It was observed for all the suspensions that for 21 days, the storage conditions have negligible effect on the liposome size or zeta potential (Figure 4.5 a, b, c &d). During the span of 28 days, there was no notable change in size or zeta potential observed for the suspensions stored at

4°C and 25°C/60% RH (Figure 4.5 a&c). However, significant increases ($p < 0.05$, ANOVA post hoc Dunnett's test) in size were observed after 21 days for the suspensions stored at 40°C/75% RH, with no change in the surface charge (Figure 4.5 a,b,c & d). These findings were the same, irrespective of the cholesterol concentration. Previous research has described that increasing the cholesterol concentration brings stability to the formulation, as instability was observed in the liposomal size for lower (<20 mol %) cholesterol concentrations (Bruglia et al., 2015). However, in this research no size change has been observed for two different formulations with varying cholesterol concentration.

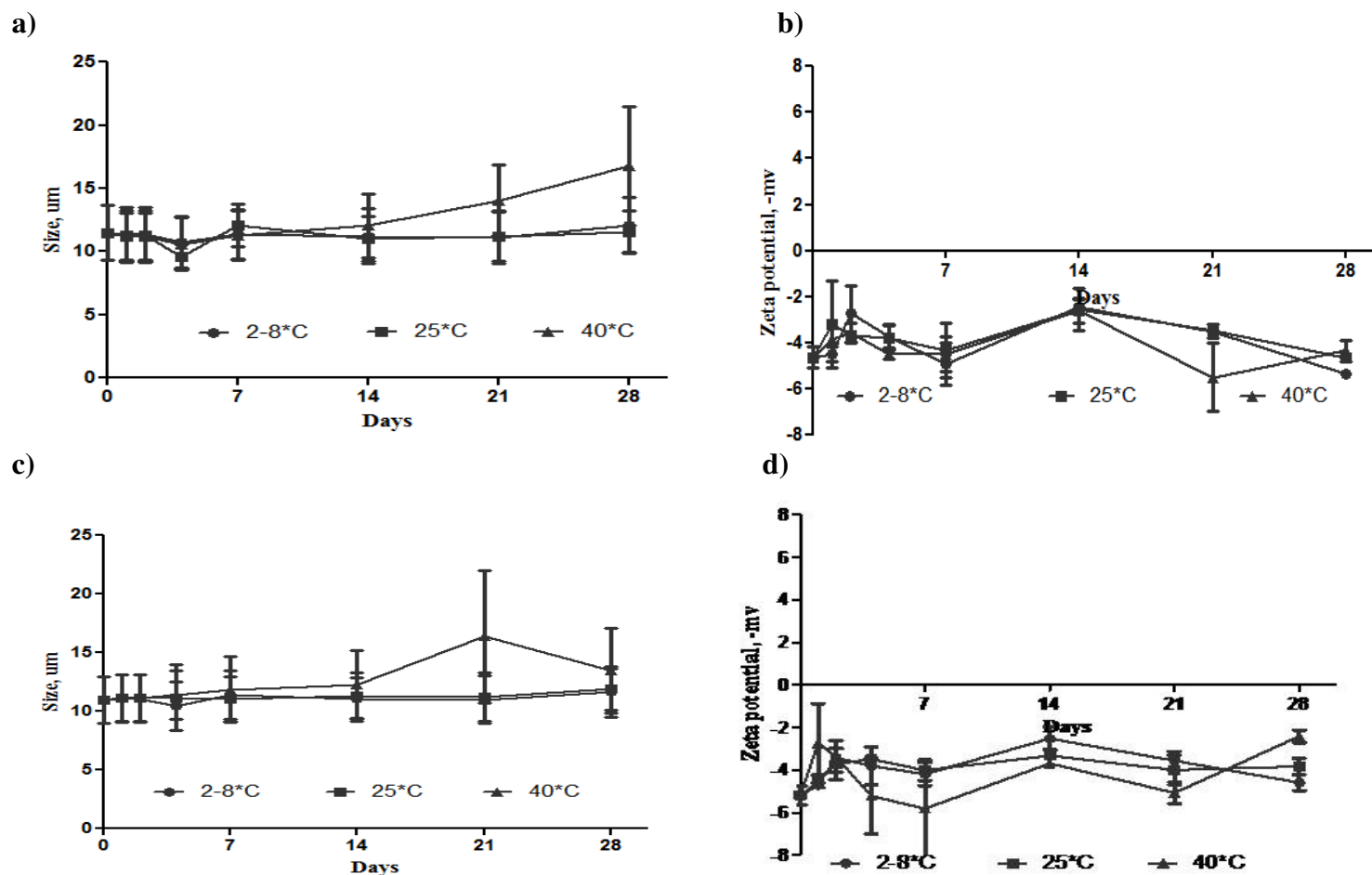


Figure 4.5 Comparison of particle characteristics obtained from analysis of formulation prepared with drug and with two cholesterol concentrations. Samples were stored at three different stability conditions. a & b) Size and zeta potential analysis respectively, representing the formulation with ratio of DSPC:Cholesterol, 5:1 w/w ($N = 3 \pm \text{SD}$). c & d) Size and zeta potential analysis respectively, representing the formulation with ratio of DSPC:Cholesterol, 5:2 w/w ($N = 3 \pm \text{SD}$).

4.3.5 Liposome encapsulation of drugs and short-term drug retention study

Liposomes at this stage of the research were loaded with metformin, glipizide and simvastatin individually. Determination of drug loading, and effect of the drug loading on particle characteristics, determines the development of the formulation (Essa, 2010b).

Lipid soluble drugs are expected to give high drug loading; however, it is dependent upon the nature of the drug and storage condition. The separation of encapsulated and non-encapsulated drug was achieved by centrifugation, based on a previously validated indirect approach to determine the entrapment efficiency of ibuprofen in MLV by measuring non-incorporated drug present in the hydration medium after separation by centrifugation (Mohammed et al., 2004). However, to study loss of drug and actual encapsulation, it is necessary to determine the drug recovery. This was achieved by determining the non-encapsulated drug (in the supernatant) as well as the encapsulated drug (in the liposomes). This quantification was done by using a validated HPLC method (Chapter3). One of the key elements of liposomal encapsulation of API is the determination of non-encapsulated and encapsulated drug as to determine the total drug recovery. In other words, it is the evaluation of drug encapsulation and drug loss. All three drugs were subjected to this evaluation process, where the encapsulation, non-encapsulation and drug loss was determined.

The passive encapsulation of drugs into liposomes is dependent of the properties of the drug to be encapsulated (Cullis et al., 1989). The hydrophilic drug, metformin, and the lipophilic drugs,

glipizide and simvastatin, were predicted for their percent encapsulation into the liposomes. The encapsulation is predicted here as a function of solubility, pH of buffer used, pKa and LogP values (Table 4.2). If the pKa of the drug is higher than the pH of the buffer used or <3 , then it possibly results in higher exaggerated drug loading (Lasic, 1993; Lasic and Barenholz, 1996). On the other hand, sensitivity in drug loading can be expected if the pKa ranges between 3 and 7 (Lasic and Barenholz, 1996). Drugs with log P value <1.7 are retained well in the hydrophilic core, whereas, the drugs with log P value >5 are retained well in the lipophilic bilayer. However, the drugs with LogP value between 1.7 and 5 can experience rapid loss from the lipid bilayer (Perrie and Rades, 2012a).

Table 4.2 Properties of hydrophilic and lipophilic drugs used in the liposomal formulations.

Parameter	Glipizide	Simvastatin	Metformin
Water Solubility (mg/mL)	0.03	0.01	Freely soluble as HCl
pH of buffer used	7.4	7.4	7.4
pKa	5.6	4.5	12.4
LogP	1.9	14.7	-1.8
Predicted % drug loading	5 to 50	5 to 50	1 to 15

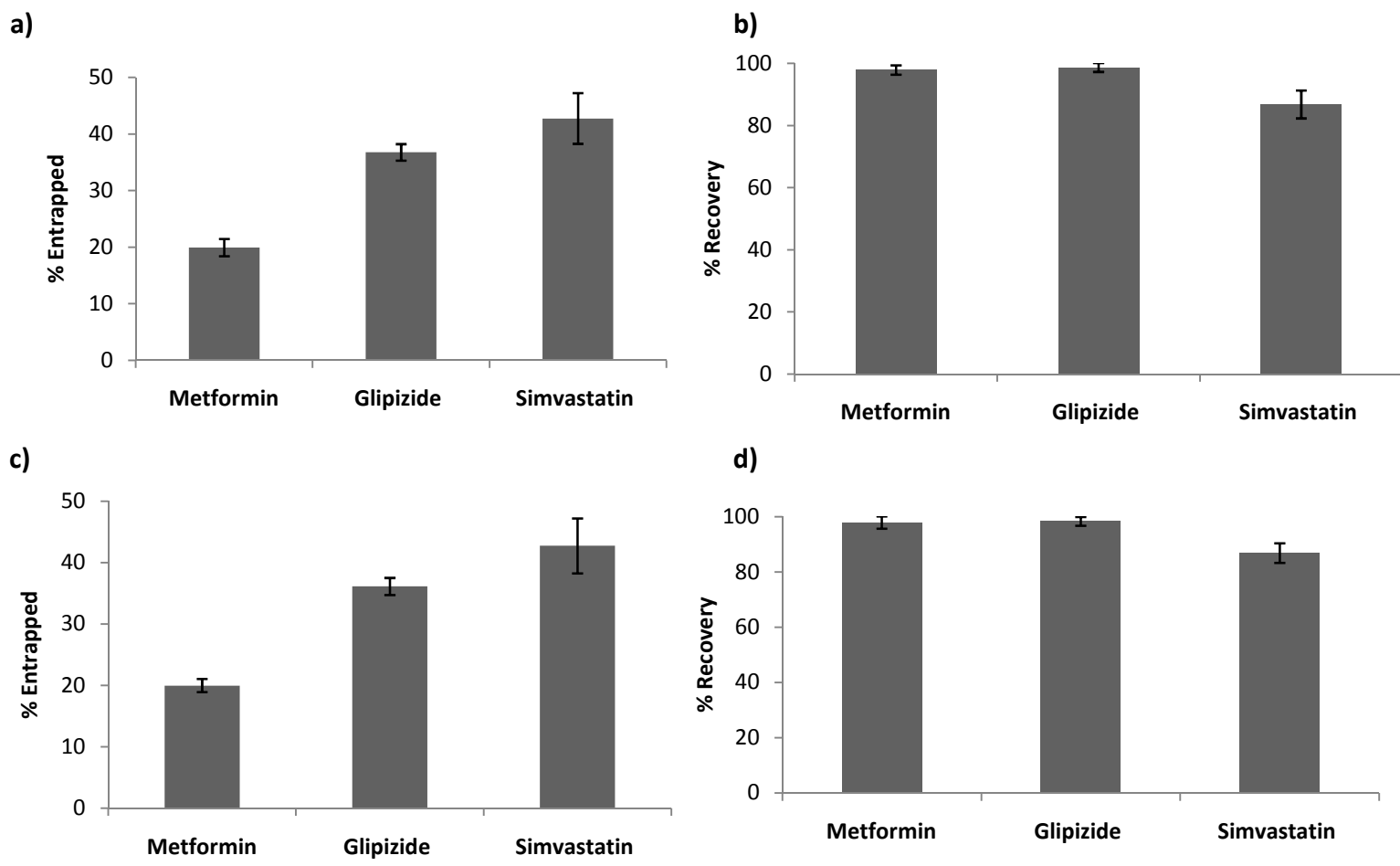


Figure 4.6 Comparison of data obtained from HPLC analysis of formulations prepared with the metformin, glipizide and simvastatin. a & b) percent drug entrapped and percent recovery, respectively, representing the formulation with ratio of DSPC:Cholesterol, 5:1 w/w (N= 3 ± SD). c & d) percent drug entrapped and percent recovery, respectively, representing the formulation with ratio of DSPC:Cholesterol, 5:2 w/w (N= 3 ± SD).

Table 4.3 Particle characteristics of drug loaded liposomes (N=3, \pm SD).

Lipids	Drug	Size, μm	Span	Zeta potential, mV
DSPC:Cholesterol (5:1 w/w)	Metformin	11.1 \pm 0.9	2.1 \pm 0.3	-5.6 \pm 2.1
	Glipizide	7.7 \pm 1.5	1.6 \pm 0.5	-6.8 \pm 0.9
	Simvastatin	15.3 \pm 4.4	2.7 \pm 0.9	-5.6 \pm 1.3
DSPC:Cholesterol (5:2 w/w)	Metformin	12.1 \pm 1.5	2.1 \pm 0.6	-5.9 \pm 1.5
	Glipizide	8.1 \pm 1.8	1.6 \pm 0.4	-5.9 \pm 0.8
	Simvastatin	9.3 \pm 4.4	2.1 \pm 0.5	-9.6 \pm 1.9

Metformin is a hydrophilic drug and passive encapsulation of hydrophilic drugs within liposomes is generally poor. It was reported that the percent encapsulation of most hydrophilic drugs subjected to passive encapsulation ranges between 1 to 15 % of the total weight of drug added (Cullis et al., 1989; Sharma and Sharma, 1997). In contrast, loading of poorly soluble drugs into the bilayer tends to be higher and reported in the range of 5 to 50 % (Cullis et al., 1989). The results in Figure 4.6 demonstrate that within the DSPC:Chol liposomes, metformin entrapment was approximately 20 % of the initial amount used (20 mg) irrespective to the cholesterol concentration used (Figure 4.6 a and c), with good total drug recovery noted (>95%; Figure 4.6 b and d). This is slightly higher than normally reported for hydrophilic drug loading within multilamellar vesicles and may result from bilayer interactions within the system. When considering loading within the bilayer, again there was no impact in terms of cholesterol content on drug loading with approximately 40 to 45 % for glipizide and simvastatin (Figure 4.6 a and c). However, whilst drug recovery for glipizide was again >95%, total drug recovery for simvastatin fell below normal acceptable ranges (Figure 4.6 b and d).

In terms of vesicle size, the results in Table 4.3 show that the lipophilic drug encapsulated liposomes are comparatively smaller at higher cholesterol concentration. In Figure 4.3 (section 4.3.3), although the effect of cholesterol was not significant on size of liposomes but at higher concentration of cholesterol the size of liposomes was found slightly reduced. Similarly, after encapsulation of drug the size of liposomes was not affected significantly by concentration of cholesterol but there was slight reduction in size at higher cholesterol concentration, this is possibly due to the nature of cholesterol which provides rigidity to the bilayer.

Also, it has previously been reported that the increase or decrease in cholesterol concentration along with lipophilic drug had no significant impact on size of vesicles (Atyabi et al., 2009). This is true in the case of the lipophilic drug glipizide, but in the case of simvastatin, the size of liposomes was not only significantly increased upon encapsulation of drug at 5:1 DSPC:Cholesterol concentration, but also significantly decreased upon increasing the cholesterol concentration. This is possibly due to the lipid lowering nature of the simvastatin and represents a highly unstable formulation. On the other hand, the size of liposomes encapsulated with hydrophilic drug metformin had no significant impact on size compared to empty liposome (Figure 4.3, section 4.3.3). Overall, there was no significant impact on size or surface charge of liposomes due to the encapsulation of metformin or glipizide.

Encapsulation of a lipophilic drugs within liposomes has been reported to be dependent on factors such as drug-lipid interaction, cholesterol content, size of the drug molecule and drug-to-lipid ratio (Ali et al., 2013). It was reported that the inclusion of 30 to 50 mol % cholesterol in phosphatidylcholine liposomes could potentially influence the drug loading in the bilayer by increasing the hydrophobicity of the bilayer interface (Bernsdorff et al., 1997). For example, DSPC has previously been shown to promote high drug loading due to its long chain structure, which may allow for enhanced hydrophobic interactions within the bilayer. This was demonstrated with the encapsulation of ibuprofen in the liposomes, which increased with increasing lipid chain length of the order dilignoceroyl phosphatidylcholine (D24PC) > DSPC > DMPC > PC (Mohammed et al., 2004).

From Figure 4.7, it can be seen that the percent loading of metformin was observed to be approximately 5 % higher than that of reported loading for hydrophilic drugs (Sharma and Sharma, 1997). It was reported that cholesterol reduces the moving of the phospholipid hydrocarbon chains, which helps to decrease the leakage of the encapsulated hydrophilic drugs and stabilises the lipid bilayer (Eloy et al., 2014; Manojlovic et al., 2008). Apart from this, it is also believed that the cholesterol suppresses the passage of water through the polar heads of the lipids, increasing lipid hydrophobicity; this could further result in the accumulation of the hydrophilic drug in this part of the liposomal structure (Eloy et al., 2014; Kępczyński et al., 2008). This phenomenon was first reported by *Subczynski et al* (1994), where it was reported that the inclusion of cholesterol not only influences polarity of the head groups, but also increased the hydrophobicity of the central region of the bilayer (Subczynski et al., 1994); this potentially results in stopping the leakage of entrapped water. The size of the sterol molecules measures half of the lipid molecule and, in the bilayer, the position of sterol molecules is towards the head groups (Richter et al., 1999); it was reported that for DSPC:Cholesterol the hydration effect starts at 5:1 (molar ratio) and reaches a crest at 2:1 (molar ratio), where the polar heads could form hydrogen bonds with the water or cholesterol (Deniz et al., 2010). Therefore, the drug loading of metformin via the passive entrapment method reported in Figure 4.6 may be a result of either some bilayer interaction of the metformin with the vesicles and/or the reduced loss of the drug from the MLV systems.

It was also reported that at low fractions of cholesterol in the formulations (below 33 mole %), the cholesterol molecules engage the half the area of the phosphocholine (PC) molecule and

considering this fact, no change in the size of the liposomes can be expected until a relatively high amount of cholesterol incorporation has happened (Melzak et al., 2012). Therefore, the amount of cholesterol used to produce empty or metformin or glipizide loaded liposomes was not sufficient enough to cause changes in the liposomal size.

The bulky appearance of cholesterol is the main reason of immobility of hydrophobic tails (Deol and Khuller, 1997) and this is the reason of high drug entrapment in the lipid bilayer. However, it was observed that a change in cholesterol concentration has not made any significant difference on drug loading. This may be because the formulation used, DSPC:Chol, 5:1 w/w, is minimum required concentration to achieve high drug loading. Formulations of both drugs were shown to have similar stability, with higher levels of cholesterol in the liposome formulation adding no advantage.

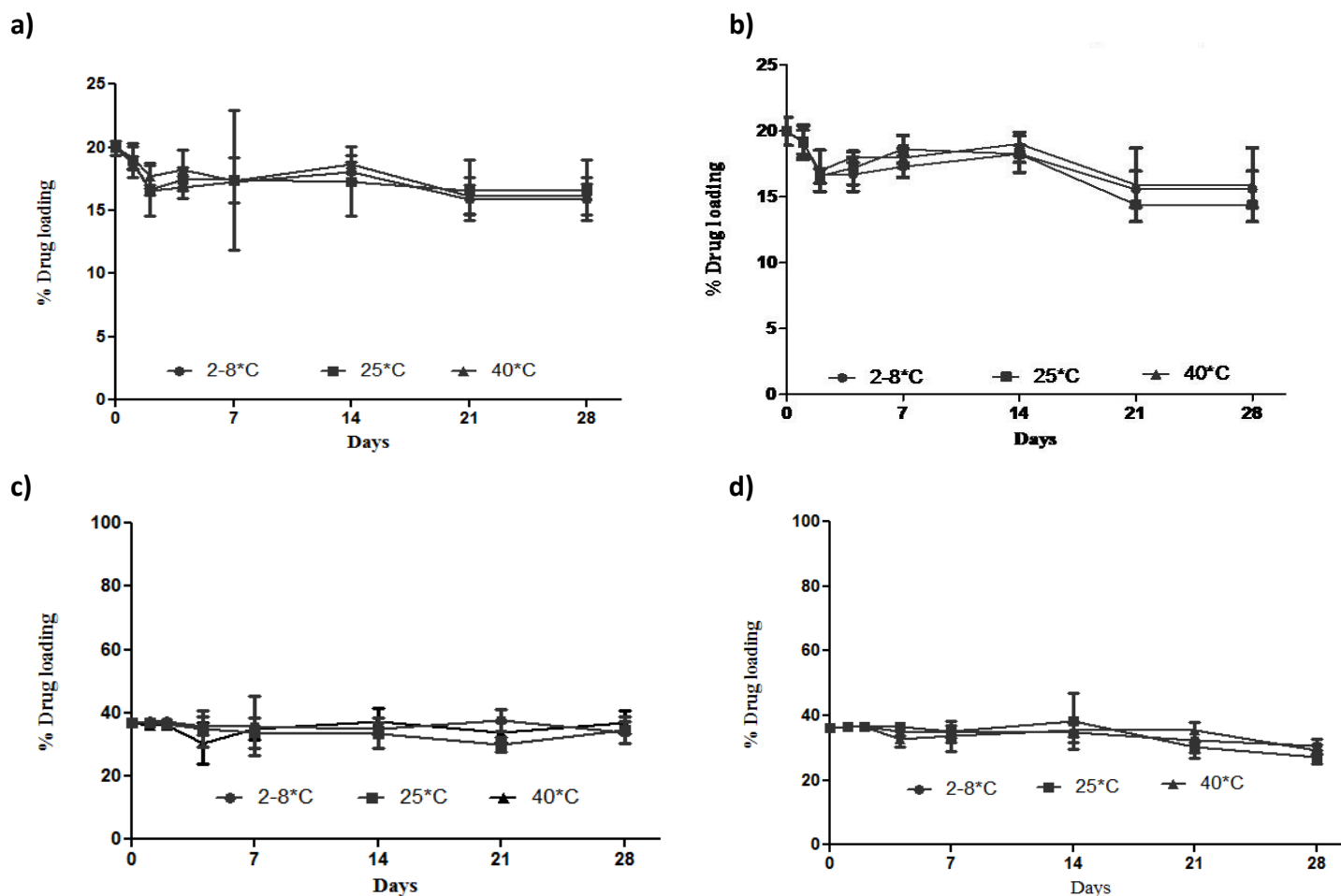


Figure 4.7 Drug retention study performed with the metformin and glipizide samples. Samples were stored at three different environmental conditions to investigate the leakage of the drug due to environmental factors. a & b) Metformin loading representing two different formulations with ratio of DSPC:Cholesterol, 5:1 w/w ($N= 3 \pm SD$) and DSPC:Cholesterol, 5:2 w/w ($N= 3 \pm SD$). c & d) Glipizide loading representing two different formulations with ratio of DSPC:Cholesterol, 5:1 w/w ($N= 3 \pm SD$) and DSPC:Cholesterol, 5:2 w/w ($N= 3 \pm SD$) respectively.

Figure 4.7 a & b considers the stability in terms of drug retention of the two different formulations (DSPC:Chol, 5:1 w/w and 5:2 w/w) incorporating metformin. Both the formulations show good drug retention over time. Over 28 days, the drug loss was found to be less than 7 %, which demonstrates their capability to withstand various temperature and humidity conditions (Figure 4.7). From a starting loading of 19.9 ± 0.6 % metformin for DSPC:Chol, 5:1 w/w, there was very little drug loss after 28 days when stored at 4°C (15.9 ± 1.2 %), 25°C (16.6 ± 2.4 %) and 40°C (16.1 ± 1.5 %) (Figure 4.7a), whereas for DSPC:Chol, 5:2, w/w, from a starting loading of 20.0 ± 1.1 % metformin, again there is very little drop in drug entrapment when stored at 4°C (15.6 ± 1.4 %), 25°C (14.4 ± 0.2 %) and 40°C (15.9 ± 2.8 %) (Figure 4.7b).

Similarly, the glipizide loaded liposomes prepared with different cholesterol content, exhibited very good encapsulation and, for DSPC:Chol, 5:1 w/w, from a starting loading of 36.8 ± 0.4 % glipizide, there was very little drug loss after 28 days when stored at 4°C (33.8 ± 3.5 %), 25°C (34.7 ± 4.2 %) and 40°C (37.0 ± 3.6 %) (Figure 4.7c). Similarly for DSPC:Chol, 5:2 w/w from a starting loading of 36.1 ± 0.4 % glipizide, very little drop in drug entrapment (4°C (30.4 ± 2.3 %), 25°C (27.2 ± 2.2 %) and 40°C (29.3 ± 1.6 %) (Figure 4.7d)) was noted.

In recent research performed on conventional liposomes versus PEGylated DSPC liposomes, *Muppidi et al. (2012)* have demonstrated that for an initial 28 days at lower temperature, the conventional liposomes were equally stable to the PEGylated liposomes and the instability of the higher temperature could be due to the swelling or aggregation of the liposomes (Muppidi et al., 2012). Therefore, from the above Figure 4.7, it can be concluded that the loss of drug at

higher temperature could be due increased fluidity within the bilayers and/or liposome fusion, resulting in drug permeation out of the liposomes.

4.3.6 Effect of drug encapsulation on particle characteristics

The size of the liposomes can also be an important indicator for the stability of liposomes, as whilst retention of drug is important, aggregation and precipitation of liposomes can also present issues in the use of the product. Similarly, zeta potential is sensitive to changes in pH; therefore, any significant change could cause a change in the cholesterol conformation (Sulkowskiet al., 2005), due to protonation potentially affecting stability, ultimately leading to flocculation and coagulation. Therefore, to study this, the size and zeta potential of liposomes loaded with either metformin or glipizide were also tracked over time when stored at: 4°C, 25°C/60 % RH and 40°C/75% RH (Figure 4.8 & 4.9).

Metformin containing liposomes prepared with DSPC:CHOL 5:1 w/w showed no significant change in size or zeta potential over the 28 days stability testing period ($p > 0.05$, ANOVA post hoc Dunnett's test)(Figure 4.8). From a starting size of $11.07 \pm 0.99 \mu\text{m}$, there was no significant change in size after 28 days when stored at 4°C ($10.01 \pm 1.8 \mu\text{m}$), 25°C ($11.6 \pm 1.6 \mu\text{m}$) and 40°C ($10.25 \pm 1.9 \mu\text{m}$) (Figure 4.8a). Similarly, the zeta potential remained around -2 to -6 mV irrespective of the temperature the vesicles were stored at (Figure 4.8b). With increasing concentration of cholesterol (DSPC:Chol 5:2w/w), the formulations were again stable with nosignificant change in size (Figure 4.8c) or zeta potential (Figure 4.8d) over the 28 days

stability testing period, with vesicles remaining around 10 microns in size and approximately -6 mV.

Similarly, glipizide containing liposomes showed no significant change in size or zeta potential over the 28 days stability testing period (Figure 4.9); with liposomes containing low levels of cholesterol (DSPC:Chol 5:1w/w) having a starting size of $7.7 \pm 1.5 \mu\text{m}$ on day zero to $10.01 \pm 1.8 \mu\text{m}$ (4°C), $7.6 \pm 0.7 \mu\text{m}$ (25°C) and $9.2 \pm 1.7 \mu\text{m}$ (40°C) (Figure 4.9a). The zeta potential again was around -6 mV, with no significant difference (Figure 4.9b). With increased cholesterol (DSPC:Chol 5:2w/w), again there was no significant change in size (Figure 4.9c) or zeta potential (Figure 4.9d) over the 28 days stability testing period.

One of the main reasons to induce charge on liposomal samples is to avoid aggregation. In this project, liposomes were not induced with charge and were prepared with neutral lipids. However, it was important to analyse the effect of formulation process or drug incorporation on liposomes, as incorporation of drug inside liposomes could produce charge on liposomes. As negatively charged liposomes have been reported to have a shorter half-life in blood (Immordino et al., 2006), such liposomes are not ideal for sustained release. From the results in figure 4.7, 4.8 and 4.9, it can be seen that the MLV systems loaded with either metformin or glipizide showed similar stability under the test conditions as liposomes without drug.

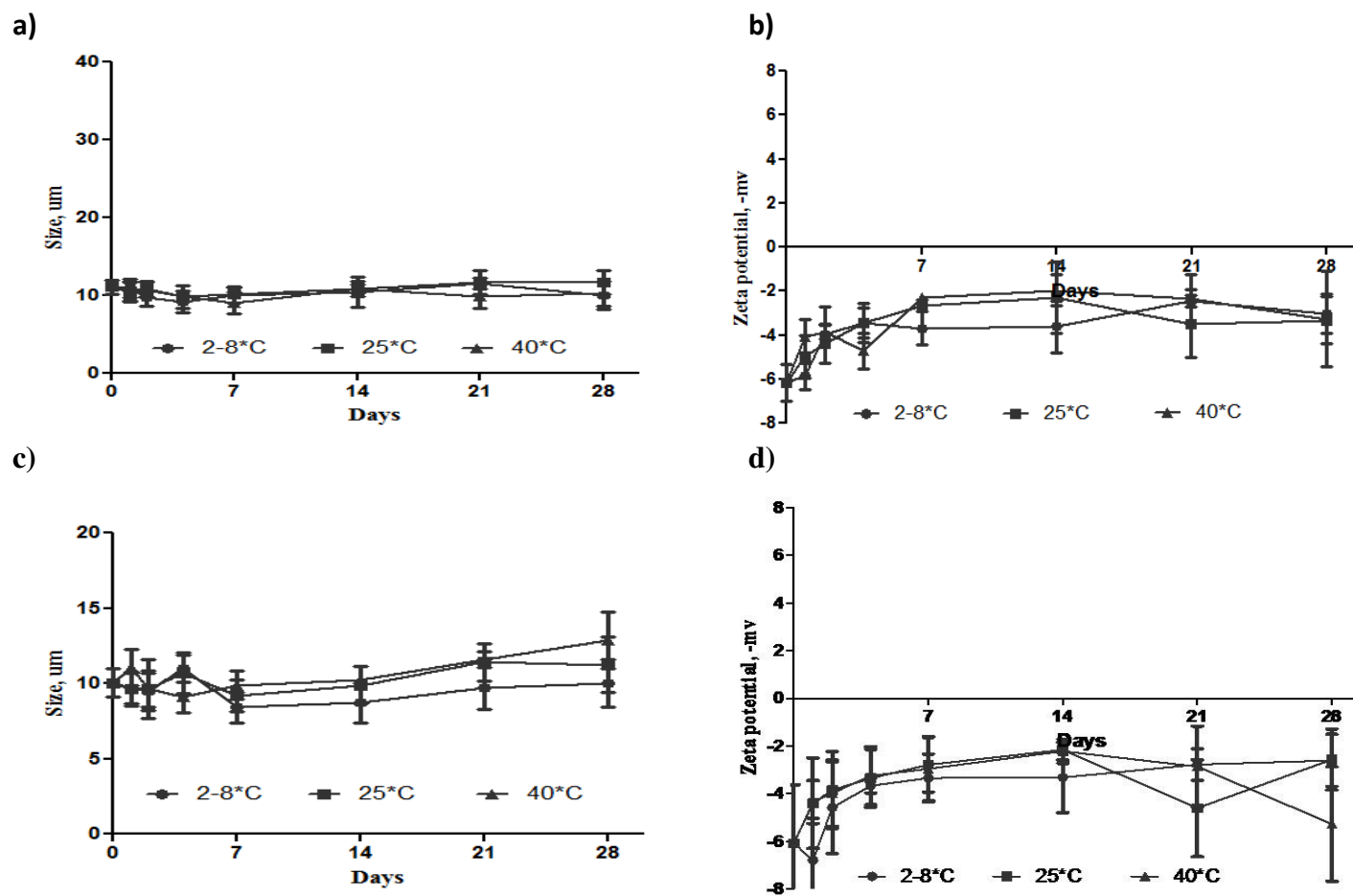


Figure 4.8 Comparison of particle characteristics obtained from analysis of formulation prepared with the drug metformin and with two cholesterol concentrations. Samples were stored at three different stability conditions. a & b) Size and zeta potential analysis representing formulations with ratio of DSPC:Cholesterol, 5:1 w/w ($N= 3 \pm \text{SD}$). c & d) Size and zeta potential analysis representing formulations with ratio of DSPC:Cholesterol, 5:2 w/w ($N= 3 \pm \text{SD}$).

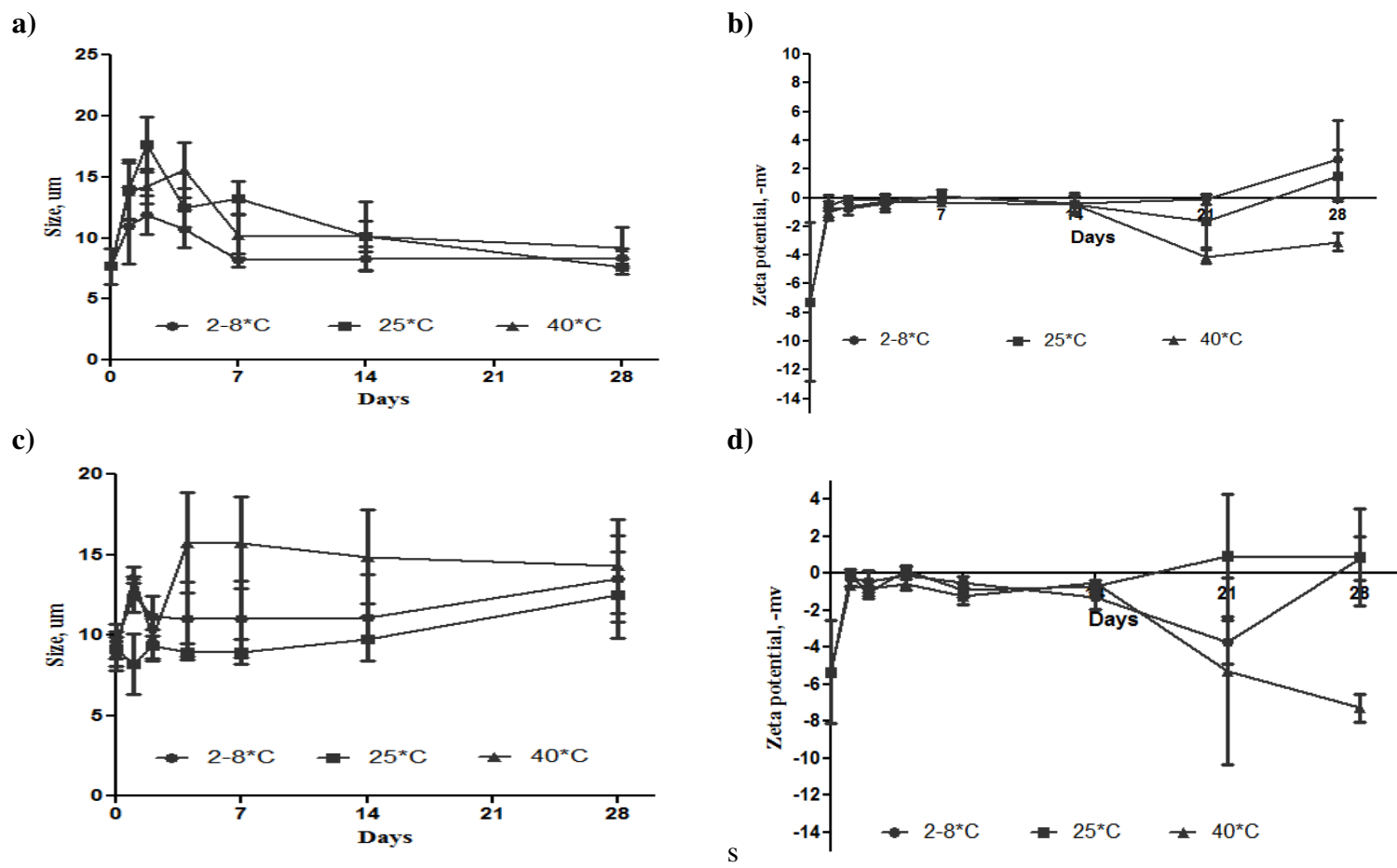


Figure 4.9 Comparison of particle characteristics obtained from analysis of formulation prepared with the drug glipizide and with two cholesterol concentrations. Samples were stored at three different stability conditions. a & b) Size and zeta potential analysis representing formulations with ratio of DSPC:Cholesterol, 5:1 w/w (N= 3 \pm SD). c & d) Size and zeta potential analysis representing formulations with ratio of DSPC:Cholesterol, 5:2 w/w (N= 3 \pm SD).

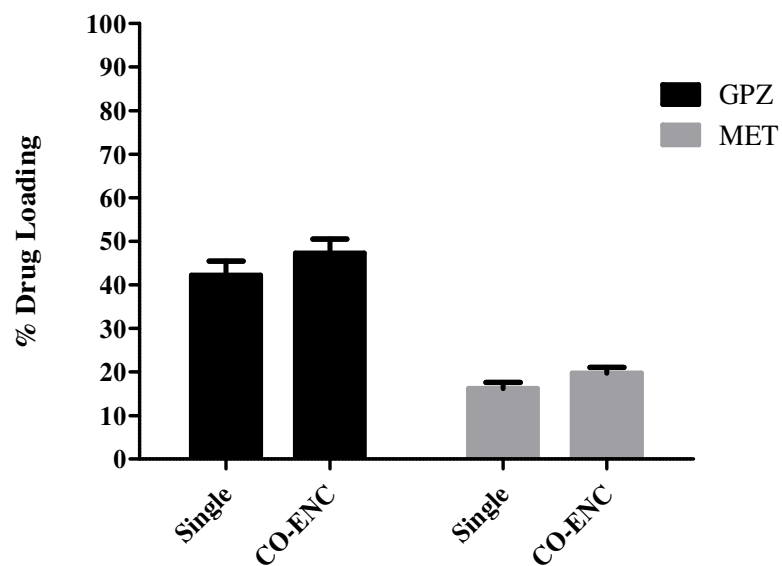
4.3.7 Co-encapsulation of metformin and glipizide in MLV

After confirming the stability of the empty and single drug loaded liposomal formulations, further efforts were taken to co-encapsulate drugs of divergent solubility and study the maximum possible encapsulation for each drug. From the previous studies, it was also confirmed that different cholesterol concentrations did not notably change the size, zeta potential and drug loading. Therefore, from here on, all experiments were performed with using DSPC:Cholesterol 5:2 w/w.

Formulations were prepared using the thin-film hydration method. All the samples were tested for size, zeta potential and drug encapsulation determination. Liposomes loaded with single drug were comparatively smaller than co-drug loaded liposomes; the average size for individually loaded glipizide and metformin liposomes was $9.6 \pm 1.1 \mu\text{m}$ and $10.9 \pm 2.2 \mu\text{m}$, respectively (Figure 4.10). However, after co-encapsulation of both glipizide and metformin, liposomes with a significantly larger average particle size ($13.6 \pm 0.5 \mu\text{m}$, $p < 0.05$, t-test) were produced. In all cases, there was no surface charge development observed, with the zeta potential for all samples being around neutral. The drug loading for individually loaded glipizide and metformin was $40.5 \pm 0.1\%$ and $21.0 \pm 0.1\%$, respectively. When co-encapsulated, the drug loading was calculated to be $41.5 \pm 0.9\%$ and $22.0 \pm 0.1\%$ for glipizide and metformin, respectively (Figure 4.10). It was observed that, when co-encapsulated, there was no significant difference in drug loading compared to liposomes where 1 drug alone was incorporated (Figure 4.10).

Similar to above observations, recently *Liu et al.* (2014) have reported co-encapsulation of doxorubicin and paclitaxel. The percent encapsulation of doxorubicin or paclitaxel alone or the co-encapsulation does not differ significantly. It was also observed in their research that upon co-encapsulation, the *in-vitro* drug release of lipophilic drug is slightly faster than that of released alone.

a)



b)

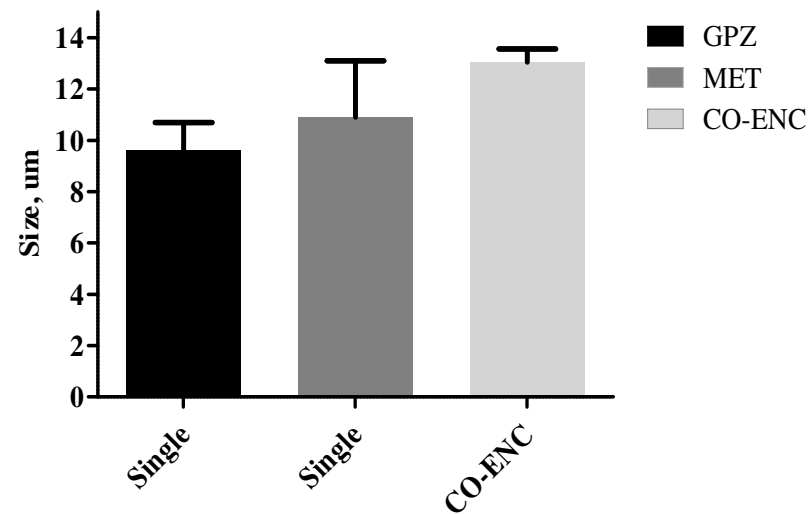


Figure 4.10 Co-encapsulation of divergent solubility drugs into multi-lamellar liposomes. Comparison of effect of single and co-drug encapsulation on percent drug loading. a) % drug loading and b) size analysis representing the formulation with ratio of DSPC:cholesterol, 5:2 w/w (N=3, \pm SD).

4.3.7.1 Drug escalation study

In addition to the particle characteristics and stability studies, the liposomal system (DSPC:Chol, 5:2 w/w) was evaluated for maximum drug encapsulation. Four different amounts of metformin (20, 40, 80 and 120 mg) and glipizide (10, 20, 30 and 50 mg) were chosen for this drug escalation study. Increases in the amount of metformin from 20 to 120 mg did not significantly influence the percent drug loading, with 20 to 29% loading and a maximum of 28 mg metformin loading achieved (Figure 4.11). Similarly, increasing the initial amount of glipizide from 10 to 50 mg again made no significant difference on the percent drug loading (46 to 56 %) with a maximum of 28.1 mg being loaded (Figure 4.11). This demonstrates that a weight ratio of 28:28:10:4 (DSPC:Chol:met:glip) can be achieved within appropriate lipid doses.

It is described earlier (section 4.3.5) that addition of cholesterol reduces the movement of phospholipid hydrocarbon chains, giving stability to the bilayer as well as reducing the loss of hydrophilic drug. *Eloy et al.* (2014) have reported that the encapsulation of hydrophilic drug is dependent of aqueous volume of liposomes as well as cholesterol concentration (*Eloy et al.*, 2014). Similarly, it was discussed in this chapter that the lipid chain length can also favour the drug encapsulation of lipophilic drug (*Mohammed et al.*, 2004), but it could also favour hydrophilic drug encapsulation, as longer lipid chains could generate greater van der Waal's forces, resulting in stronger adhesion, thereby less drug loss (*Hąc-Wydro et al.*, 2007; *Moghaddam et al.*, 2011). *Han et al.* (2012), have also reported the effect of chain length on encapsulation of hydrophilic drug Alendronate (*Han et al.*, 2012). Doxorubicin entrapment of approximately 14 %, with 1:1 (molar ratio) phosphocholine:Cholesterol MLV was also reported by *Cullis et al.* (*Cullis et al.*, 1989).

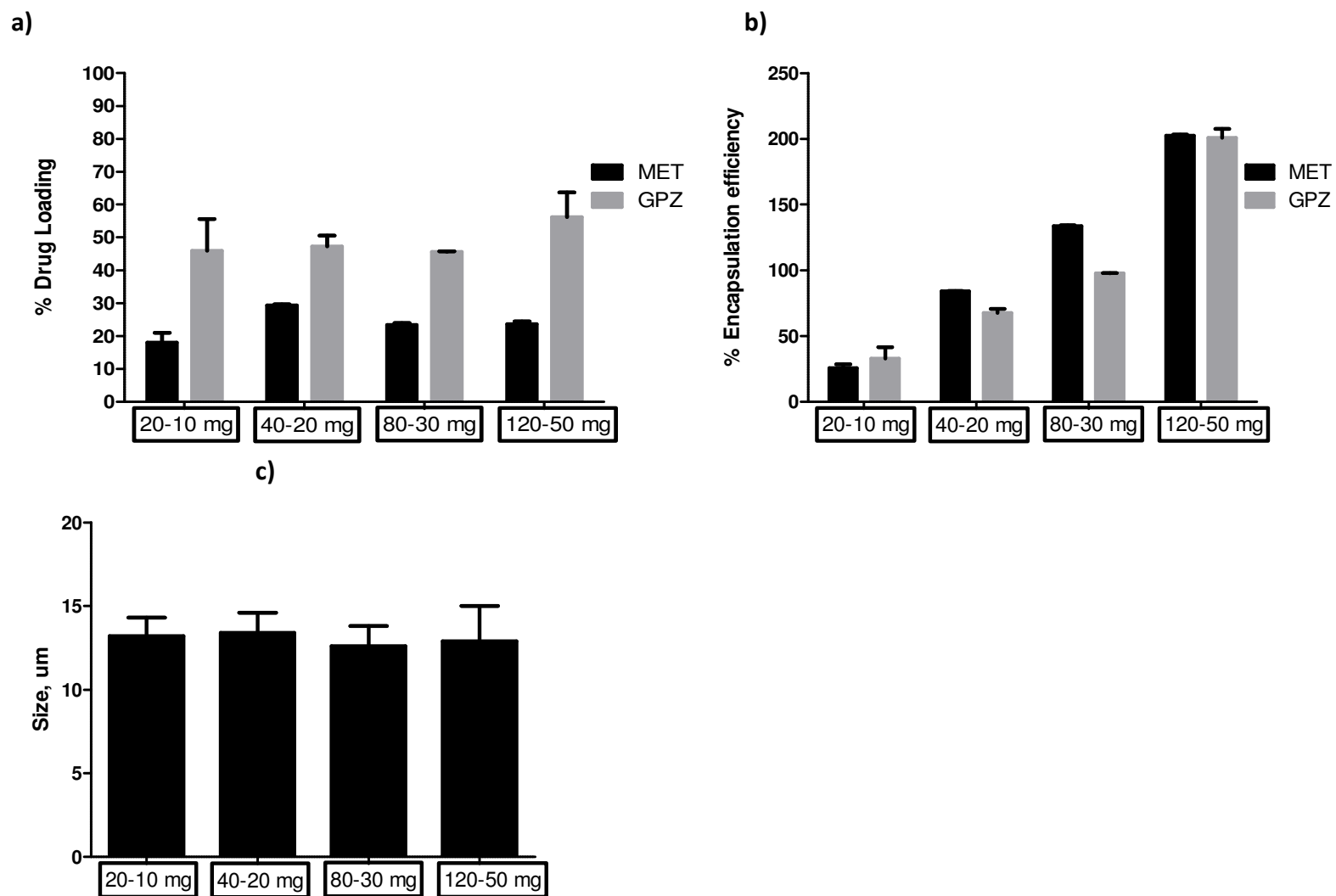


Figure 4.11 Investigation of effect of drug amount escalation on a) % drug loading, b) % drug encapsulation and c) particle size, representing the formulation with ratio of DSPC:Cholesterol, 5 : 2 w/w (n=3, ±SD).

4.3.8 Co-encapsulation of metformin and glipizide in SUV

Knowing that changes in size directly affect drug delivery (Kazi et al., 2010), and that smaller vesicles are less prone to clearance and reside longer in blood (Gregoriadis et al., 1996; Waterhouse et al., 2005), it was essential to reduce to the size of vesicles but co-encapsulate drugs at the same time. Therefore, MLV formulations were further subjected to probe sonication to reduce vesicle size and obtain SUV. Probe sonication is an easy and relatively quick method to produce SUV from MLV.

Formulations were prepared using the thin-film hydration method followed by probe sonication to obtain SUV. All the samples were tested for size, zeta potential and drug encapsulation determination. SUV liposomes loaded with single drug were comparatively smaller than co-drug loaded liposomes (Figure 4.12; the average size for individually loaded glipizide and metformin SUVs was 143.9 ± 8.1 nm (PDI: 0.3 ± 0.06) and 137.6 ± 8.1 nm (PDI: 0.2 ± 0.05), respectively (Figure 4.12). Co-drug loading in these systems made no notable impact on vesicle size, with vesicles 147.6 ± 5.5 nm (PDI: 0.3 ± 0.03) in size (Figure 4.12).

As discussed in chapter 1, liposomes are formed when the lipid layers are hydrated. The hydrated lipid sheets self assemble and form MLVs. Then, MLVs can be transformed to SUVs by sonication or extrusion. During the course of sonication, the field of sonic energy ruptures the bilayer and thereby forms SUVs. When the lipid bilayer is ruptured, the lipophilic drug entrapped into the bilayer becomes prone to leaving the bilayer and precipitates due to poor

water solubility. Similarly, this rupture of bilayer and removal of lipophilic drug creates the possibility for loss of co-entrapped hydrophilic drug. Therefore, size reduction using sonic energy can lead to reduction in drug entrapment. The sonication leads to formation of single compartment vesicles and, thereby, low internal volume, which directly affects the drug loading (Szoka and Papahadjopoulos, 1978).

Similarly, this may have affected the co-encapsulation of glipizide and metformin, as the drug loading for individually loaded glipizide and metformin was $32.6 \pm 0.4 \%$ and $15.1 \pm 0.1 \%$ respectively; however, when co-encapsulated, the drug loading was calculated to be $29.7 \pm 2.3 \%$ and $11.5 \pm 0.3 \%$, respectively (Figure 4.12). It was observed that, when co-encapsulated, there is a significant ($p < 0.05$, t-test) decrease in percent drug loading for both of the drugs (Figure 4.12).

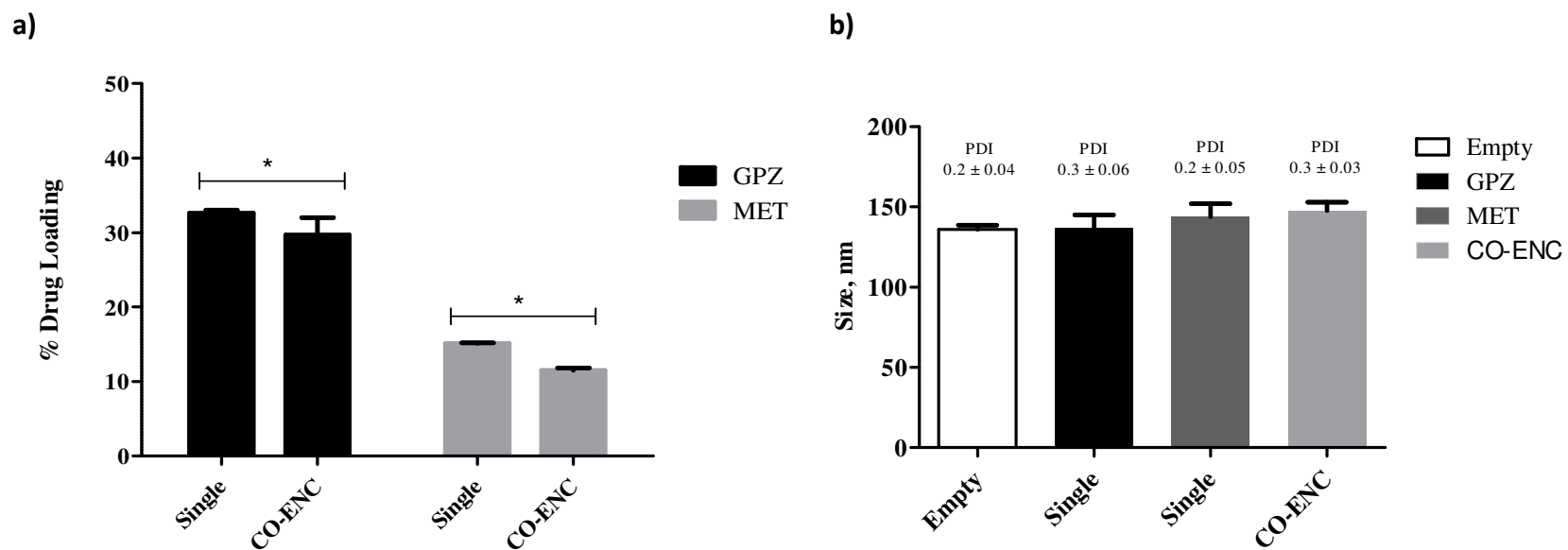


Figure 4.12 Co-encapsulation of divergent solubility drugs into small unilamellar liposomes. Comparison of effect of single and co-drug encapsulation on a) percent drug loading (*': suggesting $p < 0.05$, t-test) & b) particle size, representing the formulation with ratio of DSPC:cholesterol, 5:2 w/w (N=3, \pm SD).

In all cases, there was no surface charge development observed; the zeta potential for all samples was between 0.0 and -10 mV (Table 4.4).

Table 4.4 Zeta potential of empty and drug loaded liposomes. Results represent mean \pm SD, n = 3.

Sample	Zeta Potential, mV			
	MLV		SUV	
	DSPC:cholesterol (5:1 w/w)	DSPC:cholesterol (5:2 w/w)	DSPC:cholesterol (5:1 w/w)	DSPC:cholesterol (5:2 w/w)
Empty	-4.8 \pm 0.9	-6.9 \pm 1.3	-8.6 \pm 1.7	-8.8 \pm 2.1
Metformin	-5.6 \pm 2.1	-5.9 \pm 1.5	-9.6 \pm 2.2	-8.4 \pm 1.8
Glipizide	-6.8 \pm 0.9	-5.9 \pm 0.8	-8.8 \pm 1.9	-8.9 \pm 0.5
Co-drug	-9.5 \pm 0.9	-6.8 \pm 0.6	-8.8 \pm 1.9	-6.7 \pm 0.2

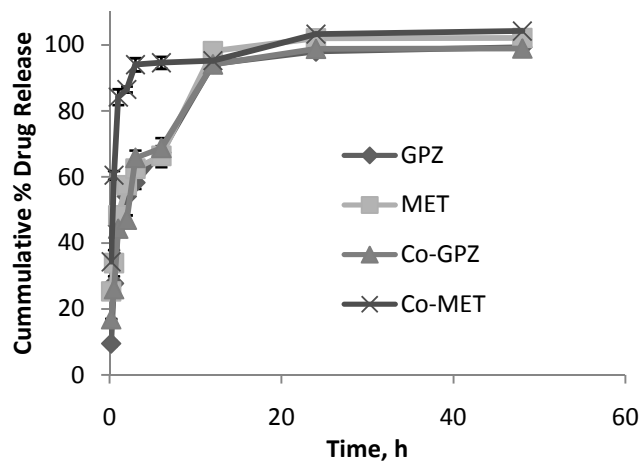
4.3.9 *In-vitro* drug release from MLV and SUV

Data from the *in-vitro* drug release can be used to predict and develop the *in-vivo* behaviour of the drug. There are numerous predictive methods used to study the *in-vitro* release, but model dependent methods (e.g. zero order, first order, Higuchi etc.) are common (Dash et al., 2010). To study the zero order release kinetics, the data obtained from *in vitro* drug release studies can be plotted as cumulative amount of drug released *versus* time; whereas log cumulative percent drug release *versus* time can be used to study the first order release kinetics. However, in Higuchi model, the release is square root of time dependent process which follows Fickian diffusion (Gohel et al., 2000).

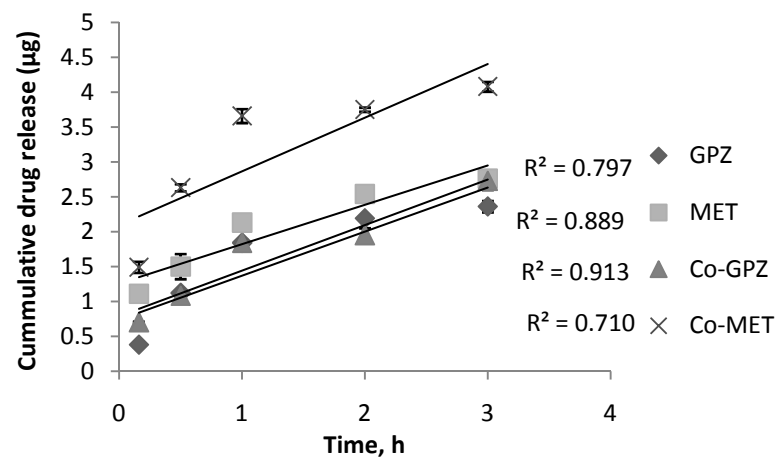
There are various models reported in past literature and it can be expected that any drug subjected for drug release would follow one or a mixture of these models (Ramteke et al., 2014). Out of these, zero order and first order kinetics are widely discussed. Zero order is the process that happens at a constant rate independent of drug concentration (Costa and Lobo, 2001), whereas first order is directly proportional to the drug concentration involved in the process (Jeong et al., 2000). However, drug in suspension can also experience diffusion where relationship between the cumulative percent drug released and square root of time is explored (Siepmann and Peppas, 2011).

Metformin, due to its hydrophilic nature, was expected to be released faster. Thus, almost 60 % metformin was released within first 120 minutes and > 90 % released in 6 hours. On the other hand, it was observed that the initial release of glipizide was very slow compared to metformin, but within 12 hours >90 % glipizide was released and quantified successfully (Figure 4.13). When plotted the cumulative percent drug released versus time (h), it was observed that the release of drug is faster in first few hours (Figure 4.13a). Therefore, the release was further studied considering zero, first and Higuchi model of release (Figure 4.13 b & C).

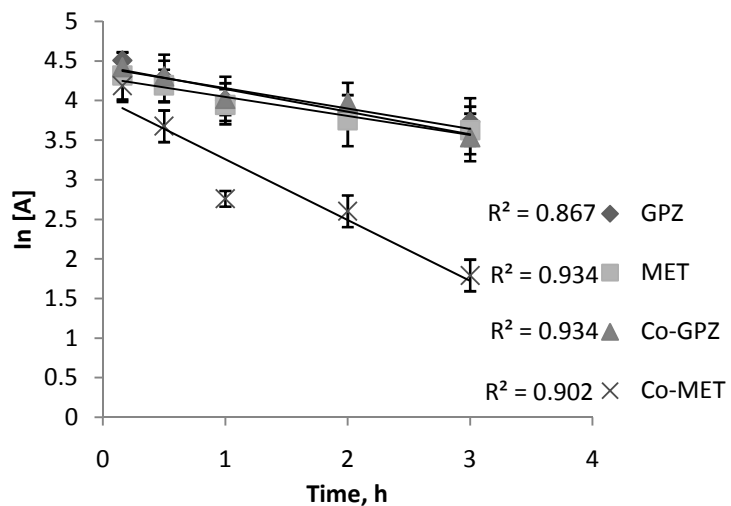
a)



b)



c)



d)

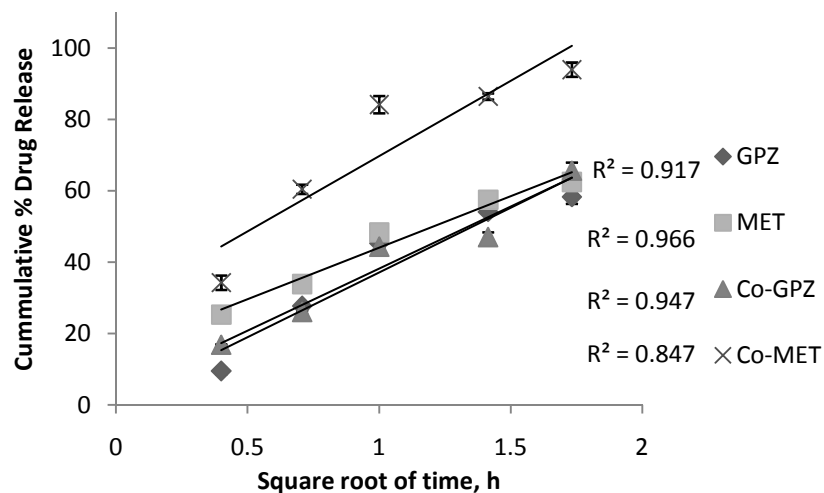


Figure 4.13 In-vitro release of glipizide and metformin in MLV. a) Drug release under physiological conditions from various formulations in aqueous buffer, pH = 7.4, at 37°C. b) Cumulative drug release (mg) representing data response under zero order model. c) Log cumulative percent drug remaining representing response under first order model. d) Cumulative percent drug release plotted using Higuchi model of drug release. (N=3, \pm SD).

The release data from all formulations (Figure 4.13a and 14a) was again treated according to zero-order (cumulative amount of drug released vs time; Figure 4.13b and 14b), first-order (log cumulative percentage of drug released vs time; Figure 4.13c and 14c) and Higuchi (cumulative amount of drug released vs square root of time; Figure 4.14d and 14d) models. It has been reported that other drugs that are encapsulated into the liposome follow zero or first order kinetics (Ali et al., 2010; Hathout et al., 2007; Nounou et al., 2006). However; from the R^2 values obtained from line of fit, it can be concluded that only when the metformin was co-entrapped with the glipizide has followed first order release but for all other samples there is strong correlation observed with Higuchi model compared to first order and zero order kinetics (Figure 4.13 c & b). However, in case of drug release from SUV obtained after sonication; where, all the metformin shown to fit good with Higuchi model but the glipizide shown to fit good with zero order having difference in R^2 values (Figure 4.14 b & d).

Release of drug from liposomes has previously been shown to be dependent on cholesterol concentration, and relatively slow release has been observed when propofol (lipophilic drug) has been encapsulated within liposomes incorporating 11, 20 and 33 mole % total cholesterol concentration (Ali et al., 2010). Therefore, concentration of cholesterol could be a possible reason for the slow release of glipizide. Recently published research on the release of co-encapsulated drug shows that the presence of lipophilic drug reduces the release rate of hydrophilic drug significantly (Cosco et al., 2012). However, here it was observed that, when co-loaded, the initial release rate was higher for both drugs; in the case of metformin hydrochloride, the release was increased approximately 3 times that of release of individually entrapped metformin. Similarly, with glipizide, the release was increased approximately two

times that of release of individually entrapped glipizide (Figure 4.15). This may be a result of a burst effect (Calvagno et al., 2007); i.e. initial release of glipizide increased fluidity of the bilayer, which in turn had a pronounced effect on metformin hydrochloride release, as well as glipizide release, to a lesser extent. The initial quick release of metformin is a result of its solubility in PBS, which, along with the driving forces, made it to diffuse at a higher rate compared to glipizide.

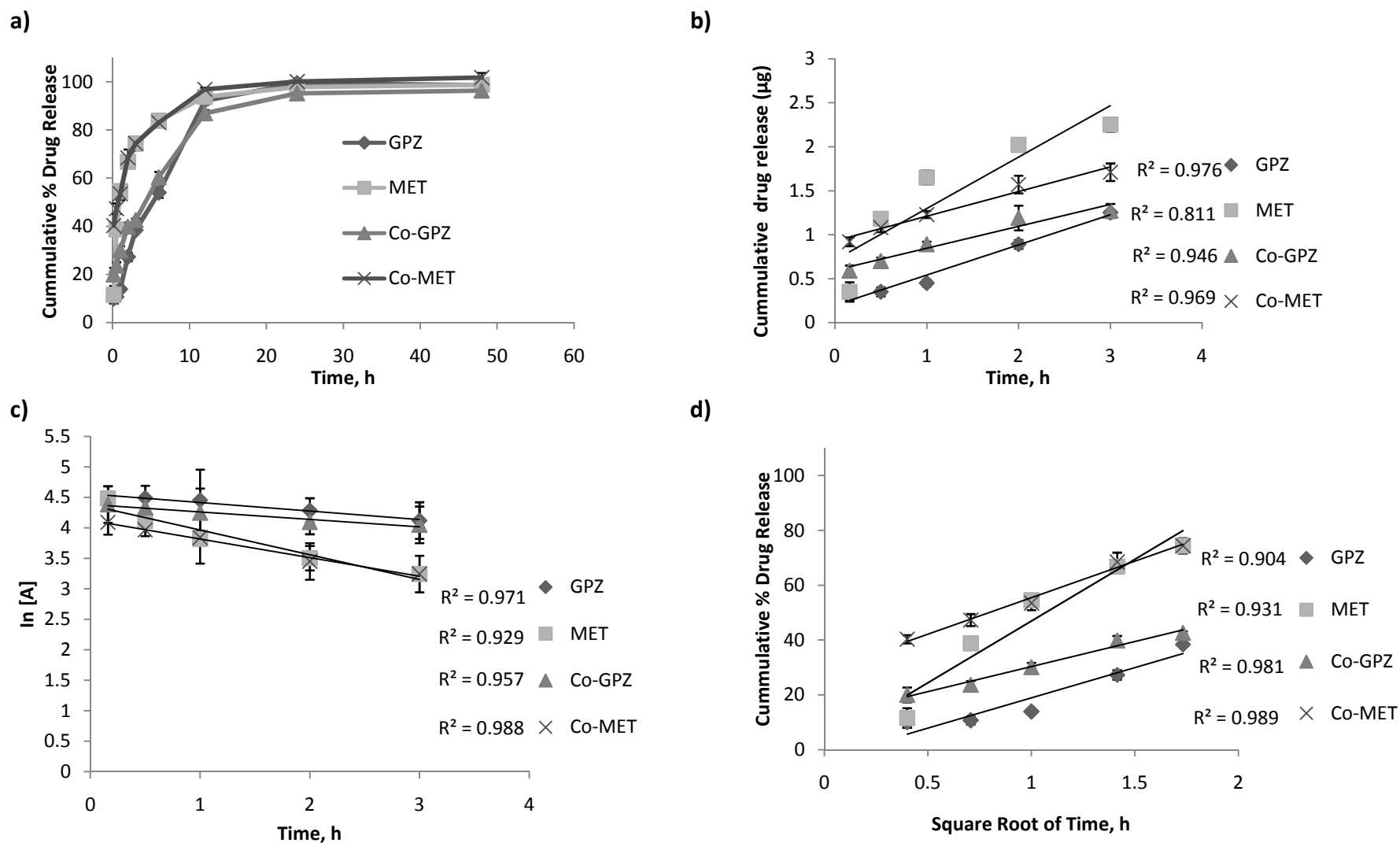


Figure 4.14 In-vitro release of glipizide and metformin in SUV. a) Drug release under physiological conditions from various formulations in aqueous buffer, pH = 7.4, at 37°C. b) Cumulative drug release (mg) representing data response under zero order model. c) Log cumulative percent drug remaining representing response under first order model. d) Cumulative percent drug release plotted using Higuchi model of drug release. (N=3, ± SD).

4.4 Conclusion

Liposomal size is important when there is possibility of clearance by RES (Gregoriadis, 1995). The RES opsonise MLV faster than SUV; hence, the rate of RES uptake increases with increases in size and SUV have a longer circulation profile than MLV (Gregoriadis and Davis, 1979; Sharma and Sharma, 1997). Therefore, in this chapter, individual and co-encapsulation of metformin and glipizide was comparatively evaluated in MLV and SUV. Also, the results reported in this chapter have given an overview about the effect of varying concentration of cholesterol.

In the case of the MLV formulation, individual encapsulation of metformin and glipizide brought no significant changes in the particle size, but the co-encapsulation increased the particle size significantly (approximately 44 %, $p < 0.05$, t-test). The stability of the lipid formulation, with or without drug, was assessed at different stability environment and only the formulation stored at the elevated temperature and humidity (40°C/ 75 % RH) showed a significant increase (approximately 52 %, $p < 0.05$, t-test) in the particle size of MLV (section 4.3.4). Drug escalation studies performed with metformin as well as glipizide has given an overall idea about the ability DSPC:Cholesterol 5:2 w/w system to accommodate the maximum possible amount of drug in the vesicle (section 4.3.5). From this study, it can also be concluded that approximately 40% glipizide and approximately 20% metformin gets encapsulated, no matter of the initial amount of drug. In the case of SUVs, no significant changes were observed in the particle characteristics due to individual or co-drug encapsulation (Figure 4.12b). However, a significant decrease (approximately 25 % and 45 %

reduction for glipizide and metformin respectively, $p < 0.05$, t-test) in % encapsulation of both the drugs has been observed after size reduction.

With respect to the drug release, there is a distinct pattern observed in drug release of both MLV and SUV. The release of drugs from MLV is comparatively slower than SUV; where the burst release was not prominent in MLV formulations. Most of the formulations show good fit with Higuchi release except the glipizide in SUV which fit good with zero order release and metformin when co-entrapped in MLV obeys first order release.

Chapter 5: Microfluidics based manufacture of liposomes co-encapsulating hydrophilic and lipophilic drugs

Publication related to this chapter:

Joshi, S., Hussain, M.T., Roces, C.B., Anderluzzi, G., Kastner, E., Salmaso, S., Kirby, D.J., Perrie, Y., 2016. Microfluidics based manufacture of liposomes simultaneously entrapping hydrophilic and lipophilic drugs. *International journal of pharmaceutics* 514, 160-168.

5.1 Introduction

The field of microfluidics had notable developments in the 1990s (Harrison et al., 1992) and, since then, over 10,000 papers have been published on the topic (ISI Web of Science 2016). Microfluidics, in general, considers the use of channels having at least one dimension in the micron size range and exploits the flow of liquid through these micron sized channels. However, the exact nature of microfluidics is open to interpretation; some researchers have considered it as a technology in the form of 'lab-on-chip', others have considered it as a science to study the flow of liquid through these micro-channels and microfluidics has been used for extraction, purification, labelling, fractionation, droplet preparation, environmental analysis and drug metabolism analysis (Abdelgawad et al., 2009; Nge et al., 2013; Yang et al., 2010). Glass, silicone and polymers like poly-dimethyl-siloxane (PDMS) have been used for microfluidics chip preparation. PDMS is a transparent elastic polymer used widely in microfluidic technology, due to cost-effectiveness and easy moulding of the material. However, silicone was the first material used for the fabrication of microfluidic devices and has subsequently been replaced by glass and PDMS (Nge et al., 2013). This was primarily due to the fact silicone is transparent to infrared but not to visible light. However, a combination of glass or polymer with silicone was proposed as an alternative to silicone only systems and this was found to be more applicable in biological detection (Washburn et al., 2009). On the other hand, PDMS was first introduced in 1990s (Effenhauser et al., 1997a; Effenhauser et al., 1997b) and at present it is the more preferable material for the academic laboratories, due to ease of handling, preparation and storage (Nge et al., 2013).

As outlined within Chapter 1, in the preparation of liposomes, there is a range of methods including the thin film hydration method (Bangham et al., 1965), ethanol injection (Pons et al., 1993) and hot-melt extrusion (Repka et al., 2007). However many of these methods have limited scalability, and in recent years microfluidics has been investigated as a potential production method for liposomes (Yu et al., 2009). For clinical application, liposomes with size < 100 nm are generally used, as shown in Table 5.1. This is due to this size range offering improved drug delivery and targeting by avoiding recognition and clearance by the mononuclear phagocyte system (MPS) (Gregoriadis, 1993; Perrie and Rades, 2012a).

Table 5.1 Liposomal systems in clinical use.

Product name	API	Vesicle size range, nm
Doxil	Doxorubicin	80-100
Myocet	Doxorubicin	150-190
Daunoxome	Daunorubicin	45-50
Ambisome	Amphotericin B	80-100
Marqibo	Vincristine	90-100

Formation of SUV is possible by two ways, either by preparing large vesicles followed by size reduction methods (e.g. homogenisation, microfluidisation, high-shear mixing and sonication) or by using advanced techniques to form SUV directly from lipid monomers. In the case of licensed products, the majority of the systems have been prepared by microfluidisation followed by lyophilisation to remove the water content in the final product (Dua et al., 2012) and this does not map well with current laboratory research, where the vast majority of work still adopts basic methods, such as the thin film hydration first

developed by (Bangham et al., 1965). To address this, new methods that allow for the rapid translation from bench to clinic are required, with microfluidics offering strong potential.



Figure 5.1 Illustration of the process of liposomal suspension production using microfluidics device. At different TFR (mL/min) solvent and aqueous phase run at different FRR through microfluidics channel having staggered herringbone micromixer. The resultant is a liposomal suspension having no drug, single drug or co-drug encapsulated.

Microfluidics is a novel method to prepare liposomes (Fig 5.1) that is reproducible, a one-step process and high throughput compared to the traditional thin film hydration method (Hood et al., 2014). More recently, microfluidics has been considered for the formulation of liposomes (Jahn et al., 2007; Kastner et al., 2014; Kastner et al., 2015). Microfluidics is presented by a low Reynold's number 'Re', which is a non-dimensional number to determine whether the flow is turbulent or laminar. A threshold value for this is 2000 and 'Re' below 2000 is considered as laminar flow. This 'Re' can be expressed as follow.

$$Re = \frac{\rho VD}{\mu}$$

Equation 5.1

Here μ is the viscosity of the fluid, ρ is the density, V is velocity scale and D is the diameter of the pipeline. It is a promising way to obtain a monodisperse population of particles (Belliveau et al., 2012). Microfluidics allows distinct mixing organised exclusively by interfacial diffusion where multiple flow streams get injected into a microchannel (Pradhan et al., 2008). In other words, this is based on laminar fluid flow and involves diffusion mixing. Liposome formation is energetically favourable at a point in the system where concentration of solvent/buffer reaches a position where lipid solubility is low (Jahn et al., 2004). Within the process, flow rates, aqueous to solvent ratios, total sample volumes, waste volumes can be manipulated as needed and should be optimised for a given system.

5.2 Aim and objectives

The work in this chapter aimed to prepare liposomes < 100 nm using microfluidics so as to effectively reduce the time and effort required in preparing liposomes with better drug encapsulation. To achieve this, the objectives were:

1. Optimisation of the microfluidics parameters for the manufacturing of liposomes.
2. Liposome purification by solvent and un-entrapped drug removal.
3. Studying effect of simultaneous drug encapsulation on percent encapsulation and simultaneous drug release.

To achieve this, initial studies focused on microfluidics parameter optimisation for the better quality and yield of SUV. This was followed by evaluation of effect of single and co-drug encapsulation on particle characteristics. Into the optimised SUV formulation, the

maximum possible drug encapsulation was then studied and finally *in-vitro* drug release was analysed for the maximum single and co-drug drug loaded formulations.

5.3 Results and discussion

5.3.1 Optimisation of microfluidics method parameters

An in depth investigation of the formulation is necessary when designing a colloidal carrier carrying two drugs of different physico-chemical properties. As described earlier in chapters 1 and 4, to consider encapsulation of two drugs of different solubility, DSPC, a long chain phospholipid, was used, as previous studies demonstrate that greater drug loading (Ali et al., 2010; Mohammed et al., 2004) and retention (Gregoriadis and Davis, 1979) can be achieved using long chain phospholipids. An optimised ratio of DSPC:Cholesterol 5:2 w/w was used as previously adopted in Chapter 4.

Initial studies investigated the impact of total flow rate (TFR) and flow rate ratio (FRR) on liposome attributes, given that previous studies have highlighted the importance of considering the effect of such parameters (Kastner et al., 2014). Liposomes produced after each run were tested for size and zeta potential analysis. At first, total sample volume of 1.0 mL including the waste volume was considered for the formulation (Figure 5.2).

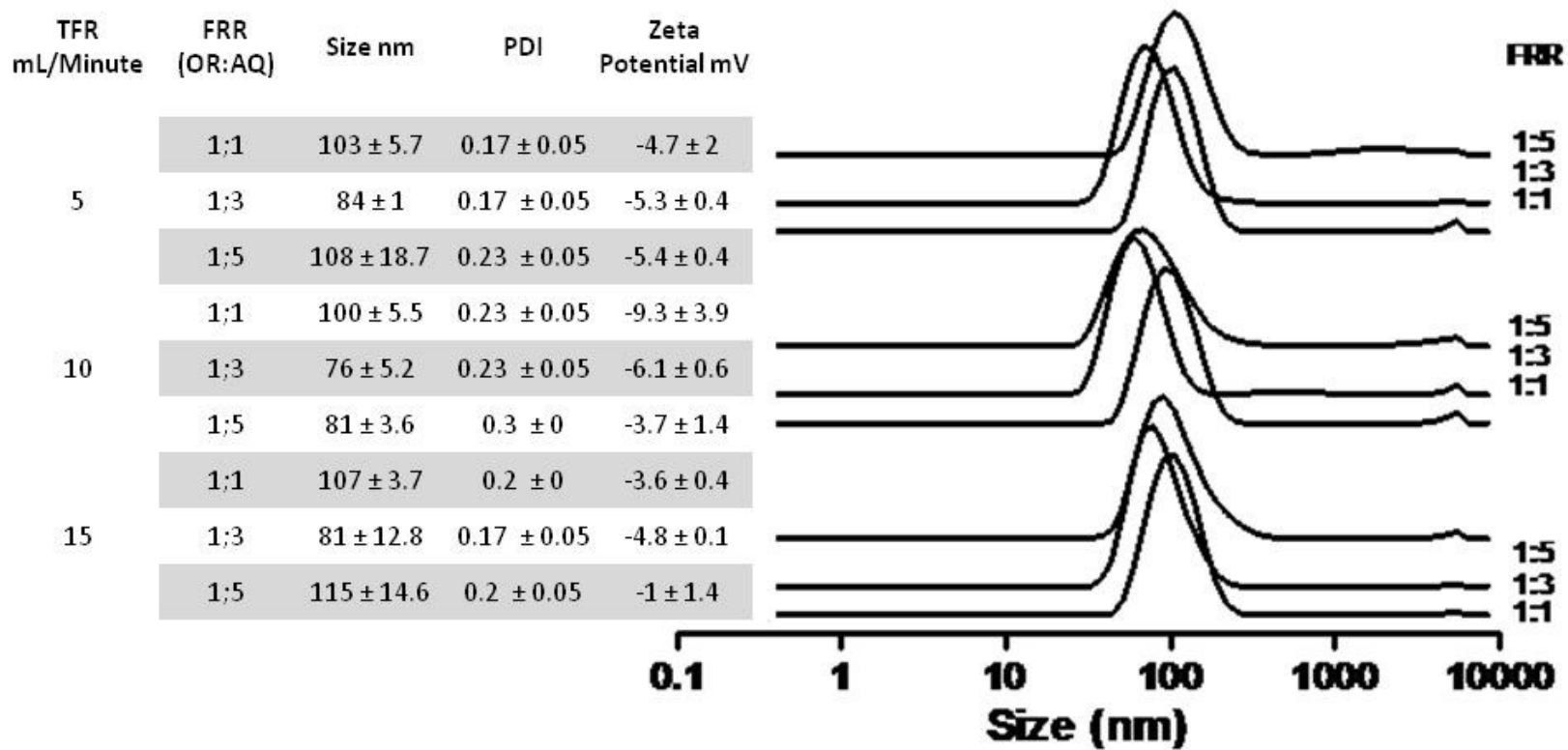


Figure 5.2 Comparison of the particle characteristics of DSPC:Cholesterol (5:2, w/w) liposomes produced by microfluidics at different flow rate ratios (FRR) and total flow rates (TFR) with a total sample volume 1.0 mL. Results represent mean ± SD, n = 3. (OR= organic, AQ= Aqueous, PDI= Poly dispersity index).

Although previous reports have shown that it is possible to control the size of liposomes with an increase in the aqueous stream volume (Kastner et al., 2015), it was not observed here with a sample volume of 1.0 mL. The results in figure 5.2 show that there is no notable trend observed at different TFR or FRR, with all parameters tested being able to produce liposomes in the range of 80 to 120 nm. The observed PDI for all samples is in the range of 0.1 to 0.2, which also indicates that a change in solvent to aqueous ratio has no effect on particle heterogeneity. It was concluded that possibly the use of a sample volume of 1.0 mL does not give enough time for mixing, whilst it can also be possible that, due to less waste volume (0.1 mL), the larger particles are becoming part of the sample volume. Therefore, it was decided to repeat the experiment with a larger sample (1.6 mL) and initial waste (0.6 mL) volume for subsequent experiments (Figure 5.3).

Unlike the 1.0 mL sample volume, a substantial trend has been observed after increasing the sample volume as well the initial waste volume, with these differences in particle size with two different sample and waste volumes described with a multidimensional surface plot (Figure 5.4). Here, a change in particle size was studied considering the two dimensions, namely FRR and TFR.

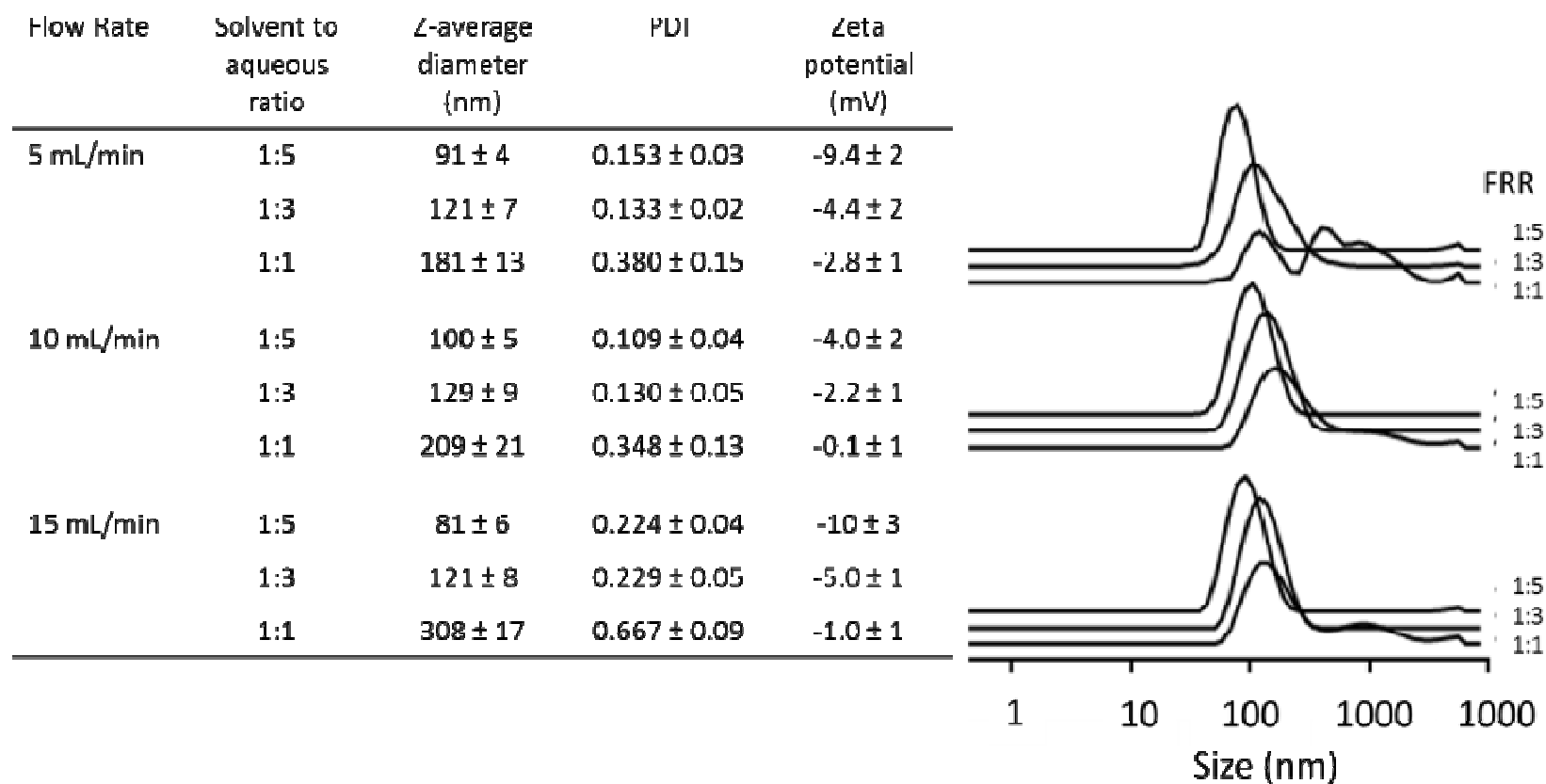


Figure 5.3 For total sample volume 1.6 mL including 0.6 mL waste volume, selection of flow rate and flow rate ratio for the production of DSPC: Cholesterol liposomes produced by microfluidics. Results represent mean ± SD, n = 3.

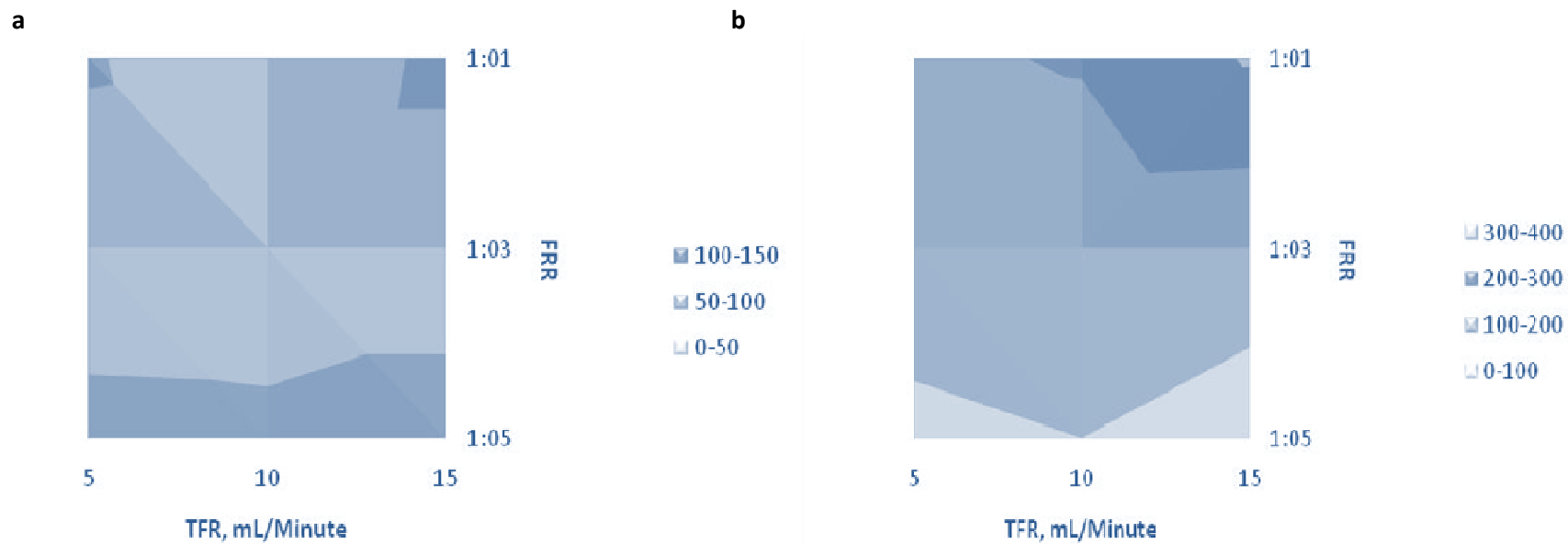


Figure 5.4 Effect of sample volume on particle size. a) Particle size when the total sample 1.0 mL b) Particle size when the total sample volume 1.6 mL. (n=3).

In the surface plot of a total volume of 1 mL (Figure 5.4a), a scattered particle size was observed at different TFR and FRR. Here, the particles were in the range of 50-150 nm and no effect was observed due to change in the TFR or FRR. However, unambiguous patterns were observed in the surface plot with the sample volume 1.6 mL (Figure 5.4b), where there is a decrease in particle size with an increase in TFR at any FRR. In other words, having more aqueous volume had a remarkable effect on particle size and it can be seen that particles are predicted in the range of 1-100 nm; whereas, when the aqueous content was lowered, the particle size increased up to the 300-400 nm range.

The solvent to buffer ratio has a significant effect ($p < 0.05$, ANOVA post hoc Dunnett's test) on the particle size as well as PDI. The smallest particle size observed was $81 \text{ nm} \pm 6 \text{ nm}$ with 15 mL/min TFR at 1:5 FRR, whilst the largest observed was $308 \text{ nm} \pm 17 \text{ nm}$ with the same process parameters 15 mL/min TFR at 1:1 FRR (Figure 5.3). A similar trend was observed with other TFRs, where at higher aqueous volume the size decreased, with increases seen at low aqueous volume.

Preliminary analysis of the DSPC:Cholesterol liposomes suggest the potential of a microfluidic device to produce size controlled liposomes; although the microfluidics method is relatively new, the process of nanoprecipitation involved is quicker compared to the multi-step process of the thin film hydration method described in chapter4 (Hood et al., 2014).

At high aqueous buffer content, the chaotic mixing of the phases was increased and it was presented previously that at higher TFR, the thickness of the solvent streams decreases and diminishes at a point (Kastner et al., 2014; Zook and Vreeland, 2010). Basically, FRR dictates the polarity of the fluid running in the microfluidic chamber, and this polarity is the basis of the precipitation reaction leading to liposome formation (Dong et al., 2012). Hence, it was observed that the smallest liposomes were produced at higher aqueous volumes. On the other hand, it was observed that FRR 1:1 produces the largest sized liposomes at any TFR (Figure 5.3 and 5.4). This is because increases in the aqueous portion of the FRR changes the polarity of solvent, which limits the production of large liposomes, resulting in the production of smaller sized liposomes (Jahn et al., 2010), whilst at lower FRR, the bilayer alcohol gets exhausted at a slower rate and, hence, produces larger liposomes as the bilayer gains more time to stabilise (Zook and Vreeland, 2010). In all cases, the liposome formulations were near neutral in zeta potential, as would be expected for such formulations. When comparing FRR at different TFRs, it was observed and concluded that higher TFR and FRR 1: 5 (organic to aqueous) are comparatively better process parameters as smaller liposomes are produced. Hence, TFR 15 mL/min and FRR 1:5 (organic to aqueous) was adopted for further experiments.

5.3.2 Separation of non-encapsulated drug and removal of residual solvent

In the formulation of liposomes using microfluidics, both the removal of non-entrapped drug and residual solvent (in this case methanol) is a requirement. The ICH limit for methanol in formulation is 3000ppm; therefore, maximum removal of solvent from the sample is very important. As such, initially two methods (dialysis and spin-column

separation) were investigated for their ability to remove both non-incorporated drug and residual solvent. Both systems were compared using liposomes containing either metformin (Table 5.2) or glipizide (Table 5.3).

Table 5.2 Analysis of metformin loaded liposomes subjected to dialysis as well as spin column filtration. All the experiments were performed in triplicates (n=3).

Parameter		Sample from dialysis	Sample from spin columns
Size, nm		64.6 ± 2.3	56.1 ± 3.5
PDI		0.151± 0.02	0.211± 0.05
Zeta Potential, mV		-8.52 ± 1.6	-5.95 ± 2.4
Metformin	% Encapsulation	19.3 ± 1	20.0± 1.8
	% Non encapsulation	79.9± 3.2	79.9± 2.5
	% Drug Recovery	99.2	99.9
Solvent (ICH limit: 3000ppm), ppm		17 ± 2	34418 ± 576

Table 5.3 Analysis of glipizide loaded liposomes subjected to dialysis as well as spin column filtration. All the experiments were performed in triplicates (n=3).

Parameter		Sample from dialysis	Sample from spin Columns
Size, nm		62.16± 2.6	73.04 ± 5.6
PDI		0.272± 0.01	0.181± 0.06
Zeta Potential, mV		-4.96 ± 1.5	-7.06 ± 4.5
Glipizide	% Encapsulation	43.1 ± 2.2	4.7 ± 1.1
	% Non-encapsulation	60.3 ± 3.5	14.6 ± 2.5
	% Drug Recovery	103.4	19.3
Solvent (ICH limit-3000ppm), ppm		25 ± 6	49696 ± 970

Considering the metformin-loaded liposomes (Table 5.2), there was no notable difference in size, PDI or zeta potential observed for the liposome formulations after dialysis or filtration, with liposomes being 60 – 70 nm in size, with PDI of 0.2 and near neutral zeta potential. Similarly, metformin drug loading (as determined by HPLC analysis of both the liposome fraction and the eluent) were similar at approximately 20% (Table 5.2). However, it was observed that, whilst dialysis was able to reduce residual solvent levels to within ICH limits, the spin column method failed to remove residual solvent from the sample, with solvent levels at 34418 ± 576 ppm, which was much higher than the ICH limit (Table 5.2).

Similar results were observed with liposomes incorporating glipizide, with no significant difference in the size (60 – 70 nm) and polydispersity (0.2 to 0.3) of the liposomes recovered after dialysis or spin column purification, and again the spin-column method was unable to remove residual solvent (Table 5.3). However, in the case of glipizide-loaded liposomes, only dialysis was able to give reliable information on drug loading. The results obtained from analysis of dialysed sample show drug loading of 43 % and approximately 100 % recovery of the drug. However, when liposomes were subjected to spin column filtration, a low (20 %) drug recovery was measured and, as such, the drug loading measurements could not be considered (Table 5.3). It may be possible that the glipizide was absorbed to the polyethersulfone (PES) membrane within the spin column instead of passing through along with eluted solution and, therefore, could not be adopted as a reliable method. Therefore, for all subsequent studies, removal of non-loaded drug was undertaken by dialysis.

5.3.3 Microfluidics assisted liposomal co-encapsulation of two divergent solubility drugs

As discussed in section 5.3.1, whilst TFR did not affect liposome size, FRR was shown to impact on the liposome attributes. Therefore, all formulations thereafter were prepared using TFR 15 mL/min and FRR 1:5 (organic to aqueous) and the effect of loading metformin and glipizide, both individually and in combination, was considered, with glipizide dissolved in the solvent phase and metformin in the aqueous stream. In terms of initial drug added, 300 µg of glipizide dissolved in methanol (the maximal amount soluble in the solvent phase used; 300 µg in 0.27 mL i.e. 1.2 mg/mL) along with the DSPC and cholesterol (2.7 mg and 1.1 mg, respectively), and 20 mg/mL of metformin was added to the PBS phase. Microfluidics had been previously used to prepare small unilamellar liposomes, but there is limited research performed on liposome preparation using long chain phospholipids (e.g. DSPC) (Young and Tabrizian, 2015) and no research has been reported regarding preparation of DSPC liposomes using Precision system's microfluidic device.

Results in Figure 5.5 show that drug loading of glipizide within the liposomal bilayer was approximately 40% and metformin entrapment was approximately 20%. In all cases, it was found that >90 % glipizide and >95 % metformin was recovered (results not shown). Furthermore, the results show that loading of the drug individually or in combination had no significant impact on the loading capacity of the liposomes. However, the presence of either drug in the formulation tended to push the vesicle size down by approximately 20 nm, with the measured z-average particle size being 50 to 60 nm.

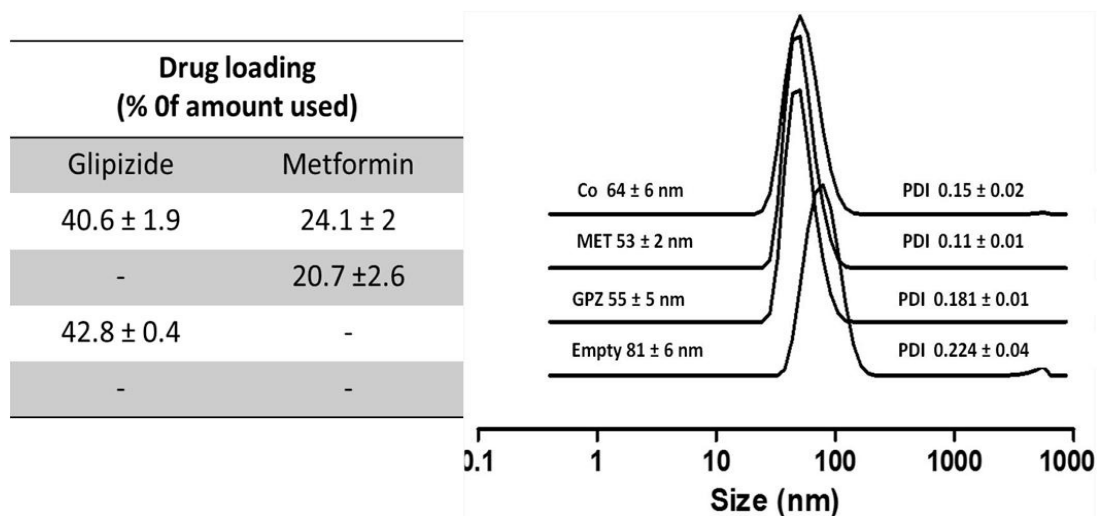


Figure 5.5 Comparison of DSPC:Cholesterol (5:2, w/w) liposomes z-average diameter, pdi and drug loading for liposomes with glipizide loading within the bilayer, with metformin loading within the aqueous phase, liposomes containing both glipizide and metformin and liposomes without drug present. Results represent mean ± SD, N=4.

In terms of drug loading within these vesicles prepared using microfluidics, the loading was based on the principle of passive loading, where both drug and lipids are co-dispersed in the aqueous phase. Generally, encapsulation efficiency for passive loading is less than 10% (Cullis et al., 1989), whilst these studies show notably higher hydrophilic (metformin) drug loading of approximately 20% was achieved (Figure 5.5); indeed, loading for both drugs was high, despite the large differences in Log P (Figure 5.6). The use of microfluidics has been suggested to improve hydrophilic loading; for example, Jahn et al. (2008) reported unexpectedly high entrapment efficiencies of a hydrophilic moiety (sulforhodamine B dissolved in PBS) within nanometer-scale liposomes prepared using a continuous-flow microfluidics system. The authors suggest that the high encapsulation efficiency may be due to a spatial concentration enhancement induced by viscosity anisotropy in the microchannel (Jahn et al., 2008). In terms of bilayer loading, the simultaneous packaging of the lipids and

glipizide within the bilayer can promote drug loading of approximately 40%, similar to previous studies with propofol (Kastner et al., 2015). The small decrease in size noted when liposomes were formed in the presence of metformin and/or glipizide may be a result of changes in viscosity, miscibility and/or mixing at the interphase as the liposomes form, as discussed by Jahn et al. (2008).

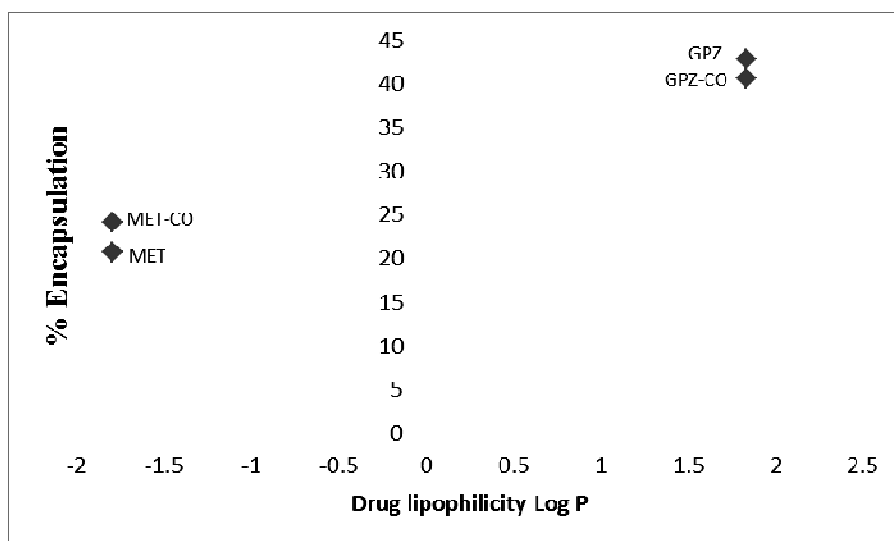


Figure 5.6 The relation between lipophilicity (log P) and drug encapsulation. Liposomal composition= DSPC:Cholesterol (5:2 w/w) with/without glipizide and metformin hydrochloride. (MET-CO: Metformin co-encapsulated, GPZ-CO: Glipizide co-encapsulated).

5.3.4 The role of drug concentration in drug loading

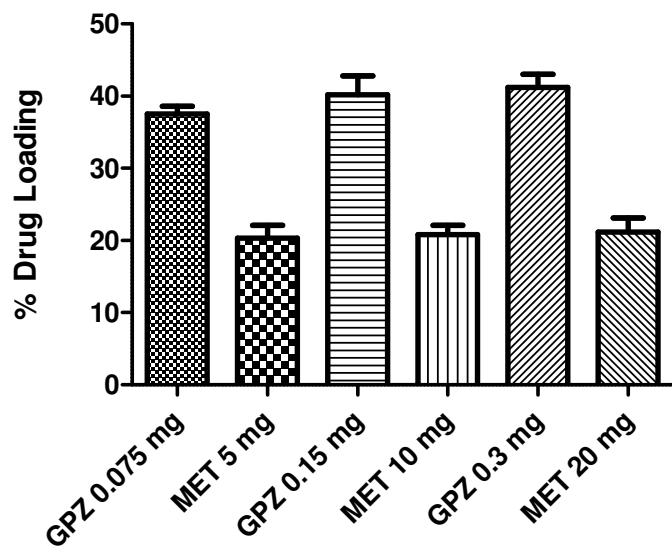
Considering the challenges associated with delivery of pharmacological agents, the possibility of liposomes as a carrier was coined more than four decades ago (Gregoriadis et al., 1971; Gregoriadis and Ryman, 1972a) and liposomal drug delivery systems became the first among the novel drug delivery systems to be commercialised. No such development with the plethora of commercialisation can be seen with other drug delivery systems, which

can be attributed to the innocuous nature of liposomes. As such, numerous updates have been made to extract the best from this outstanding drug delivery system.

With passive diffusion using traditional production methods, it can only be possible to encapsulate up to 50 % of the lipophilic drugs and upto 15 % of the hydrophilic drugs (Cullis et al., 1989).

Recently, it was reported that an increase in initial drug concentration increases encapsulation efficiency of liposomes (Kastner et al., 2015). Therefore, to study the maximum possible drug loading efficiency of the liposomes prepared using microfluidics, 3 different concentrations of both glipizide and metformin were tested. Due to limited solubility of glipizide in methanol, it was only possible to go up to 0.3 mg total drug in 0.27 mL organic phase of the aqueous to organic ratio 5:1 v/v. Therefore, solutions having 0.1, 0.2 and 0.3 mg of glipizide in 0.27 mL of organic phase was investigated in combination with metformin 5, 10 or 20 mg/mL in the aqueous phase were tested for escalation study. In both cases, the initial drug concentration did not significantly impact on the percentage drug loading (Figure 5.7a), demonstrating that increasing doses of drug could be delivered within the liposome formulation. Furthermore, it can be observed in Figure 5.7b that, although the percent of drug loading has not changed at any given concentration of drug, the amount of drug loaded into the liposomes (final volume 1.0 mL) was increased gradually with the increase in initial drug concentration.

a)



b)

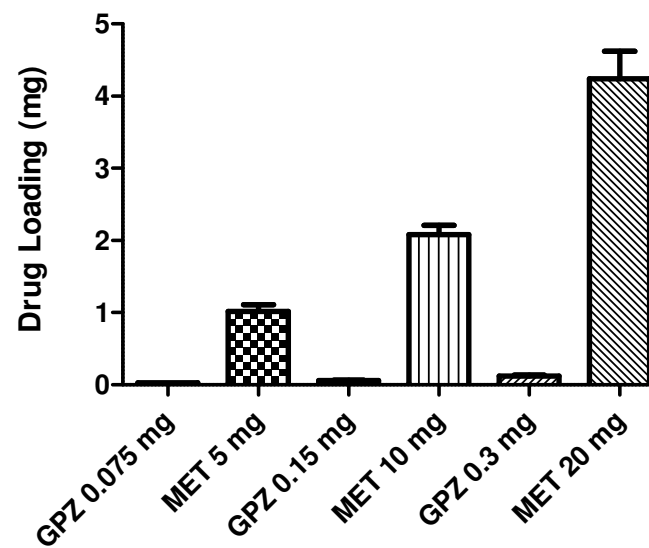


Figure 5.7 The role of drug concentration in drug loading for glipizide and metformin. Samples were prepared on microfluidic device and tested for percent loading using RP-HPLC (UV detector). a) % drug loading with respect to the drug concentrations. b) Drug loading presented as amount of drug loaded for respective drug concentration. (N=4, \pm SD).

5.3.5 Microscopic elucidation of small unilamellar liposomes

Cryo-TEM has significantly contributed to the understanding of complex structures like liposomes. Microscopy is usually used for liposomes to characterise their size and lamellarity. The liposomal bilayer can be spotted but, due to the limit of resolution, the arrangement of lipid within the bilayer cannot be spotted (Almgren et al., 2000). However, methods like small angle x-ray scattering (SAXS) or small angle neutron scattering (SANS) can be used for this purpose.

To consider the morphology of the liposomes prepared by microfluidics, 4 formulations were considered by cryo-TEM: liposomes without drug, liposomes incorporating either metformin or glipizide and also liposomes incorporating both drugs. As described in chapter 2 (section 2.3.7.1), the liposomal solution was applied to a microscopic grid, forming a thin film, which was then frozen by plunging into the cooling medium, such as ethane. Extra care was taken to avoid crystallisation during the process of freezing. Finally, the liposomal structures on the film were spotted and captured without dehydration.

No variation has been observed between DLS results and cryo-TEM results with respect to the size and PDI of liposomes, with the average size of liposome observed on cryo-TEM for all liposome samples being around 60 ± 10 nm (Figure 5.8).

Considering the speed of liposome preparation employed by the microfluidics system (i.e. 15 mL/minute) and high proportion of aqueous content, there was a possibility that the

shear may cause elongation of liposomes or possibly breakage (Richardson et al., 2007).

However, there was no such sign seen in any of the samples (Figure 5.8).

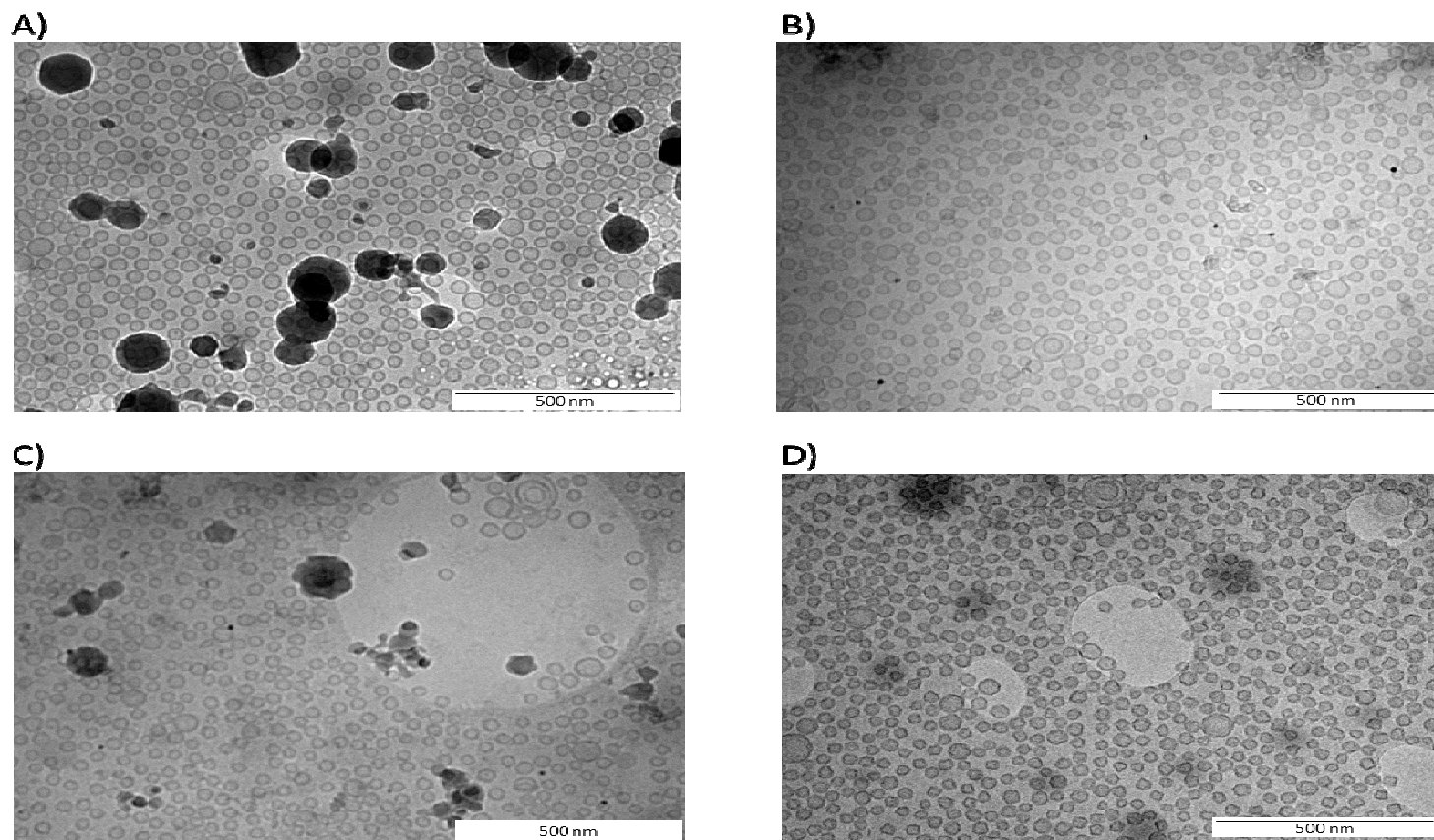


Figure 5.8 DSPC:Cholesterol (5:2, w/w) liposomes produced by microfluidics imaged by Cryo-TEM. A) Liposomes without drug incorporated, B) liposomes with glipizide loading within the bilayer, C) liposomes with metformin loading within the aqueous phase, D) liposome containing both glipizide and metformin.

5.3.6 *In-vitro* release study of liposome encapsulated and co-encapsulated glipizide and metformin.

In-vitro drug release was studied using USP-4 (SOTAX, SOTAX Ltd., London, UK). Liposomal drug release studies have often been performed using large amounts of buffer and it was also observed that excess buffer can result in inaccurate analysis due to leakage of drug (Shabbits et al., 2002). Therefore, the *in-vitro* drug release was studied using USP-4, flow through cell based closed loop system (SOTAX, SOTAX Ltd., London, UK). The USP-4 is well known for versatility, and has distinct advantages, such as requiring low volume of media, precise as well as auto-temperature control and most important is the adaptor, which is especially designed for the submicron sized delivery systems.

Drugs encapsulated into liposomes exhibit the pharmacokinetic properties of the liposome drug carrier. These properties may include long circulation, reticuloendothelial clearance pathway as well as greater permeability and tumour site drug accumulation (Lee, 2006). Enhanced drug safety and efficacy can be achieved after the liposomal encapsulation. Drug encapsulated into liposomes depends on the solubility of drug as well as components of liposomal system. Drugs co-encapsulated into liposomes may differ in the rate of release irrespective of region of encapsulation and/or drug solubility.

When drugs with divergent solubility are encapsulated into two distinct regions of liposomes, it can be expected that the release rate may vary (Lee, 2006). This difference in drug release rate from co-drug encapsulated liposomes often creates complications in

determination of released drug concentration. In this case, if the concentration falls below the limit of detection, then approaches like spiking can be used to achieve precision in the quantification. The drug release was observed in PBS flowing in closed loop system at flow rate of 8.0 mL/minute and at physiological temperature ($37^{\circ}\text{C} \pm 1^{\circ}\text{C}$). Released drug was quantified using RP-HPLC, as mentioned in chapter 2 (section 2.3.4.2). At predetermined intervals, a predetermined sample volume (1.0 mL) was taken and tested for drug release. The percent drug release was then calculated.

The release profiles of both drugs encapsulated individually or together were similar to the liposomes produced by thin film hydration method in chapter 4. However; from the R^2 values obtained from line of fit, it can be concluded that for metformin there is strong correlation observed with Higuchi model and for glipizide there is strong correlation observed with zero order kinetics (Figure 5.9 b & d and table 5.4). Comparitively, no strong correlation with first order kinetics was observed for any of the drug release. Metformin, due to its hydrophilic nature, was expected to be released faster; thus, almost 60 % metformin was released within the first 60 minutes and > 90 % released in 6 hours. On the other hand, it was observed that, within the initial stages of release, glipizide was very slow compared to metformin, but within 12 hours >90 % glipizide was released and quantified successfully (Figure 5.9).

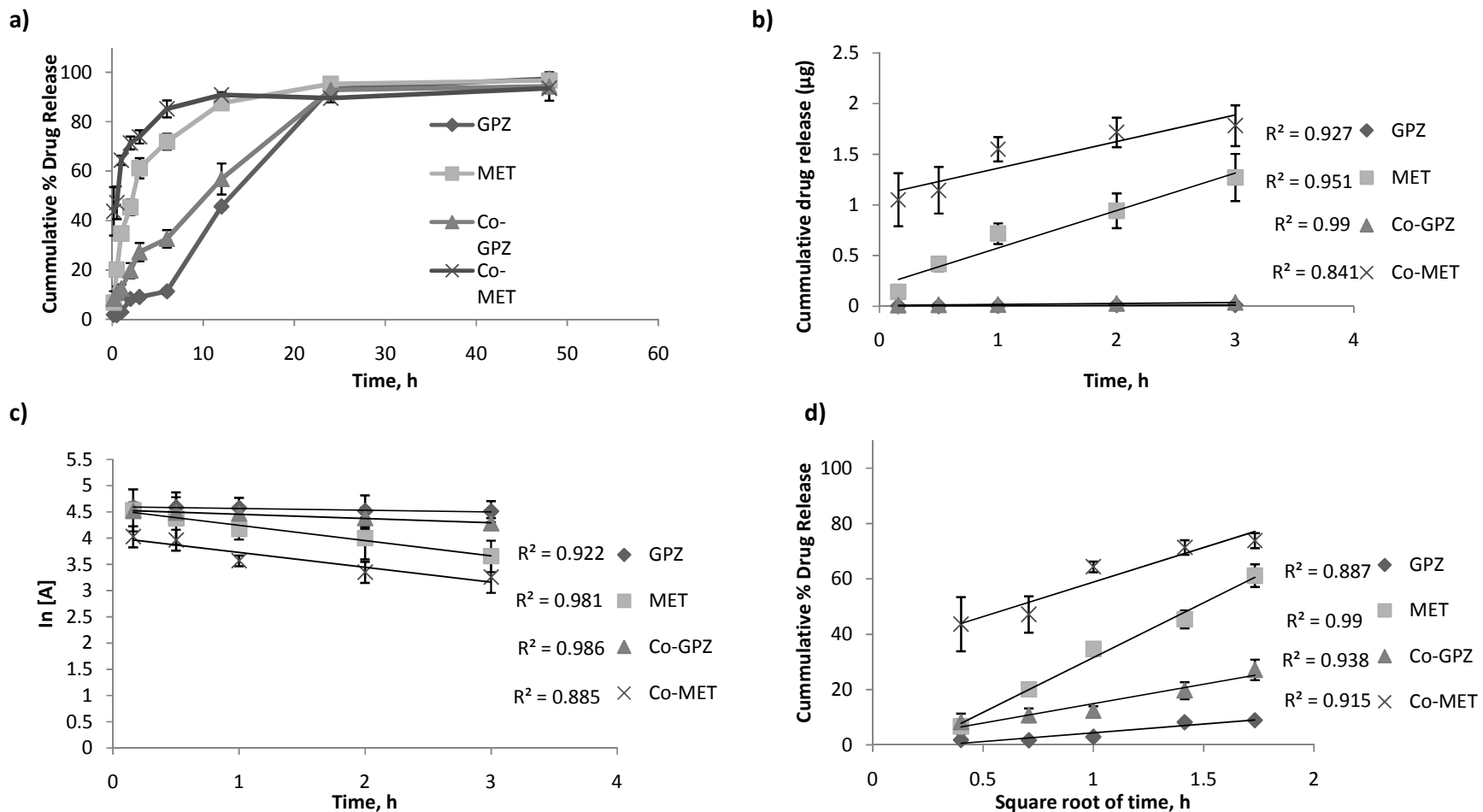


Figure 5.9 USP-4 aided study *in-vitro* release of glipizide and metformin in SUV. a) Drug release under physiological conditions from various formulations in aqueous buffer, pH = 7.4, at 37°C. b) Cumulative drug release (mg) representing data response under zero order model. c) Log cumulative percent drug remaining representing response under first order model. d) Cumulative percent drug release plotted using Higuchi model of drug release. (N=3, ± SD).

Table 5.4 Kinetic values of release of glipizide and metformin from liposomal formulations using the correlation coefficient parameter.

Glipizide						
	Zero Order		First Order		Higuchi Order	
	GPZ	GPZ-CO	GPZ	GPZ-CO	GPZ	GPZ-CO
TFH-MLV	0.797	0.913	0.867	0.934	0.917	0.947
TFH-SUV	0.976	0.946	0.971	0.929	0.904	0.981
MICF-SUV	0.927	0.99	0.922	0.986	0.887	0.938
Metformin Hydrochloride						
	Zero Order		First Order		Higuchi Order	
	MET	MET-CO	MET	MET-CO	MET	MET-CO
TFH-MLV	0.889	0.710	0.934	0.902	0.966	0.847
TFH-SUV	0.811	0.969	0.929	0.988	0.931	0.989
MICF-SUV	0.951	0.84	0.981	0.885	0.99	0.915
Based on the R ² values the applicable model is described in the table below						
	GPZ	GPZ-CO	MET	MET-CO		
TFH-MLV	Higuchi Order	Higuchi Order	Higuchi Order	First Order		
TFH-SUV	Zero Oder	Zero Order	Higuchi Order	Higuchi Order		
MICF-SUV	Zero Order	Zero Order	Higuchi Order	Higuchi Order		

TFH-MLV
TFH-SUV
MICF-SUV

*

Thin film hydration-Multi lamellar vesicles
Thin film hydration-Small Unilamellar vesicles
Microfluidics-Small Unilamellar vesicles
For all the 3 models only initial 3 hours were taken into consideration.

Release of drug is dependent on cholesterol concentration; relatively slow release was observed by *Ali et al.* (2010) when encapsulating propofol (lipophilic drug) within liposomes (*Ali et al.*, 2010). Therefore, the concentration of cholesterol could be a possible reason for slow release of glipizide.

Release of drug from a co-drug loaded liposomes is largely dependent of the water solubility of lipophilic drug. Recently published research on the release of co-encapsulated drug shows that the presence of lipophilic drug reduces the release rate of hydrophilic drug significantly (*Cosco et al.*, 2012). However in our case, it was observed that, when co-loaded, the initial release rate is increased for both drugs; in the case of metformin hydrochloride, the percent drug release was increased approximately 6 times that of release of individually entrapped metformin. Similarly, with glipizide the release was increased approximately 4 times that of release of individually entrapped glipizide. This may be a result of a burst effect (*Calvagno et al.*, 2007) i.e. initial release of glipizide increased fluidity of the bilayer, which in turn had a pronounced effect on metformin hydrochloride release, as well as glipizide release, to a lesser extent. The initial quick release of metformin is result of its solubility in PBS; which along with the driving forces made it to diffuse at higher rate compared to glipizide.

5.3.7 Influence of liposomal size on *in-vitro* drug release

Liposomal systems have been designed to control drug exposure, aid the drug in crossing biological barriers and protect the active ingredient from premature elimination (*Siegel and*

Rathbone, 2012). Liposomal formulations can be developed to deliver drug with controlled release and represent the sanctified as well as spatial presentation of the active pharmaceutical ingredients in the body. In the designing of controlled release systems, it is necessary to understand the kinetics of the drug release and factors affecting it.

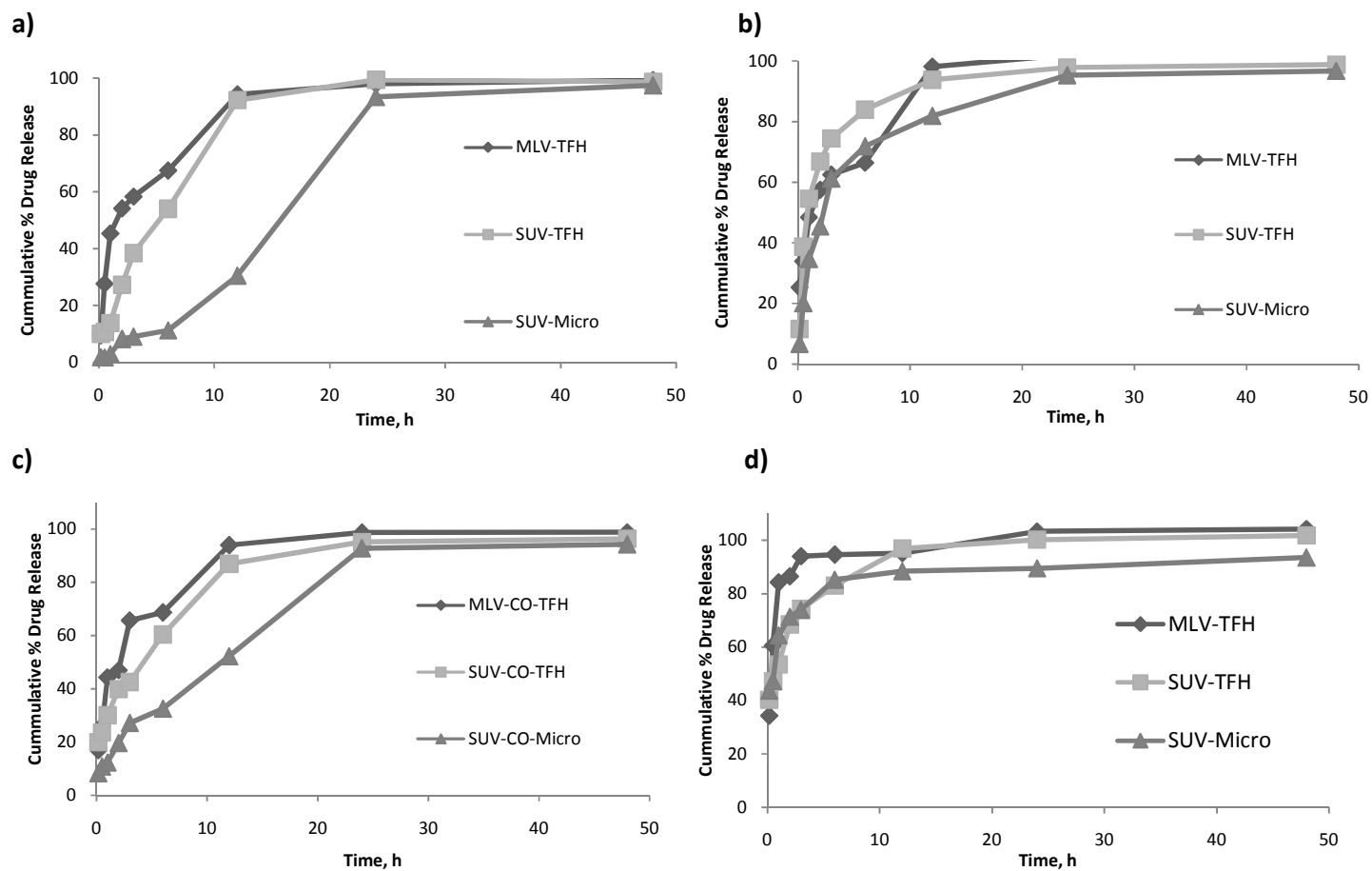


Figure 5.10 Drug release under physiological conditions from various formulations in aqueous buffer, pH = 7.4, at 37°C (n=4 ± SD). Comparison of drug release kinetics of the MV as well as SUV prepared by thin film hydration (TFH) and the SUV prepared by microfluidics. a) glipizide encapsulated individually, b) metformin encapsulated individually, c) glipizide co-encapsulated, d) metformin co-encapsulated.

The process of dissolution is the reverse of the precipitation (Rogers et al., 2004). Dissolution is a kinetic process dependent of the solubility and is a thermodynamic property of the drug.

As per Noyes-Whitney equation, the dissolution rate can be increased by increasing particle surface, but stern application of this law is unlikely as the surface area of the drug-encapsulating matrix changes over time and cannot be assumed constant (Perrie and Rades, 2012a). Also, recently *Siegel and Rathbone* (2012), *Hatzi et al.* (2007) as well as *Sridhar et al* (2008) have observed that the rate of dissolution decreases with increasing particle size and increases with increase in the solubility of the active ingredient.

Indeed, similar to the findings of *Siegel and Rathbone* (2012), it can be seen in figure 5.10 that the rate of release decreased as the particle size decreased (Release rate: MLV (approx. 10 μm) > SUV (approx. 150 nm) > SUV (approx. 70 nm). When comparing SUVs produced by thin film hydration versus SUVs produced by microfluidics, it was noticed that the dissolution rate did differ in both cases, but in the case of glipizide, the release rate was significantly slower ($p < 0.05$, t-test) for SUVs prepared by microfluidics (Figure 5.10). This is possibly due to the efficient mixing of aqueous and organic phase in microfluidics that resulted in the production of liposomes with a very rigid structure providing better drug encapsulation as well as slower release.

Along with factor of size of the liposomes, another important factor is the solubility of the encapsulated drug. It was seen that the rate of metformin release is faster in all cases suggesting that the release rate is dependent on diffusion. Moreover, it can be seen in Figure 5.10 that the rate of dissolution had more influence of size in the case of glipizide compared to metformin. This confirms that solubility of encapsulated drug is equally important in the process of dissolution.

5.4 Conclusions

For the first time, the co-encapsulation of divergent solubility drugs into liposomes prepared by microfluidics was investigated. Microfluidics was not only found to be efficient in producing co-drug encapsulated liposomes, but also was a rapid liposome production method; microfluidics is a simple, one step method for producing small unilamellar liposomes. Furthermore, to a degree, size may be controlled by consideration of the interplay between alcohol diffusion and laminar convection, in line with previous reports (Jahn et al., 2007; Kastner et al., 2014). With regards to developing a drug carrier system, it is particularly important that the carrier system's characteristics are reproducible and robust. This aspect can be achieved by use of microfluidics, which can reproduce formulation with robustness and in a limited amount of time. Microfluidics based liposomal encapsulation of a poorly water soluble drug was reported in past (Kastner et al., 2015) and the studies reported within this thesis demonstrate that high drug loading can be achieved with a range of drugs. Furthermore, for the first time, we have successfully prepared co-drug encapsulated liposomes using a microfluidic device, which may prove beneficial for drugs which are commonly used in combinational therapy and possess

divergent solubility, but also for the co-delivery of important anticancer drugs (Cosco et al., 2012). Overall, microfluidics offers several advantages over several other methods in use for liposome preparation; in particular, the ability to manufacture a precise, robust and scalable liposome product several times quicker than other production methods for liposomes.

Chapter 6: Liposomes for the inhibition of respiratory syncytial virus

Publication related to this chapter:

S Joshi, D Kirby, Y Perrie, S R Singh. Novel nano-biomaterials for inhibition of respiratory syncytialvirus. TechConnect World Innovation Conference and Expo, Technical Proceedings of the 2017, Volume 3, p. 75-78.

6.1 Introduction

Respiratory syncytial virus (RSV) as well as Rhinovirus (HRV) are the main causes of acute lower respiratory tract (LRTI) infections (Luchsinger et al., 2014), with noticeable increases in incidences of RSV infection during winter months, particularly in specific populations including foetus, infants, children and young adults (AR et al., 2005b; Borchers et al., 2013; JS and J, 2010; Rappuoli et al., 2011). RSV is a prominent cause of bronchitis and pneumonia, and it is widely recognised that there is need for vaccine against RSV; natural infection is not capable of inducing life-long immunity and patients are prone to suffer repeating RSV infection (Kamphuis et al., 2012).

RSV, which belongs to the *Paramyxo virus* community and *Pneumoviridae* subfamily (Wyde, 1998), is a distinct serotype having two major antigenic circulating subgroups, of which one dominates (Borchers et al., 2013). RSV has an RNA genome consisting of 15191 base pairs, which can be identified with 11 proteins, including 2-non-structural proteins (NS-1 and NA-2), 3-surface proteins (glycoprotein-G, fusion protein-F, and hydrophobic protein-HP), two overlapping frames of M2 mRNA producing 2 distinct matrix proteins (M-1 and M-2) and 4 other structural proteins (matrix protein-M, nucleocapsid-N, phosphoprotein-P and large protein-L) (Borchers et al., 2013) (Figure 6.1). Viruses of the *Pneumoviridae* subfamily fuse their membrane with the plasma membrane of the host, which results in cell fusion if added to the cell in large quantities (Haywood, 1978). The entry of RSV virus into the host cells happens with the aid of a fusion protein, which has two heptad-repeated regions that form a hairpin like structure, facilitating the entry of the virus into the cells (Zhao et al., 2000).

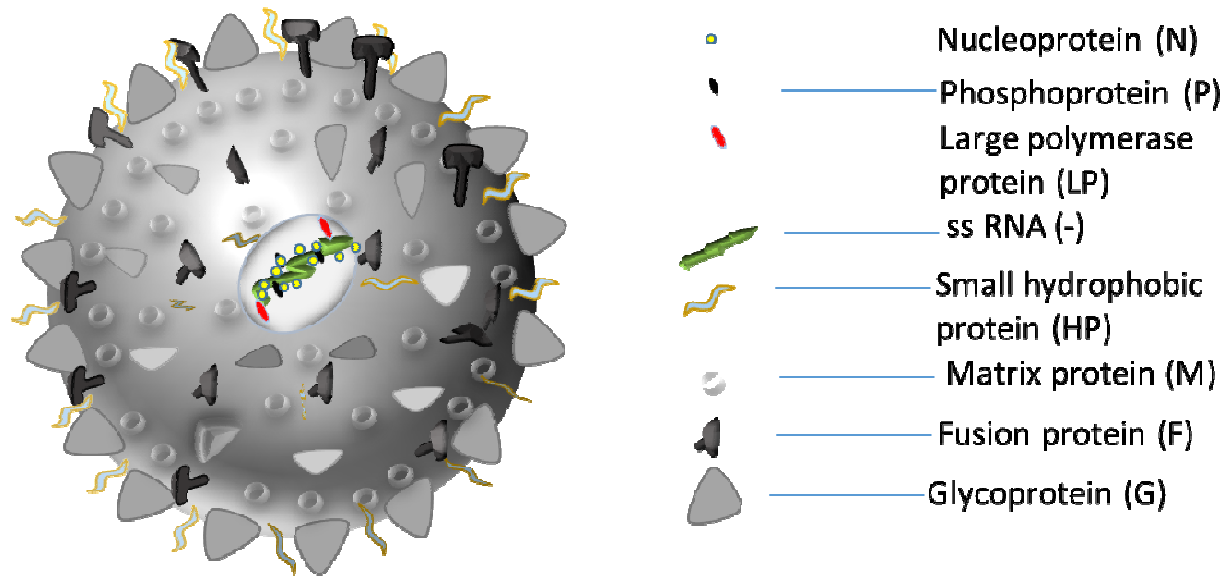


Figure 6.1 Diagrammatic illustration of the structure of respiratory syncytial virus (RSV), a member of the Paramyxo virus community and Pneumoviridae subfamily. (image modified from (Redmond, 2013)) .

Route cause analysis of any disease or disorder is at the foundation of treatment design. Infection of RSV can start with mild upper respiratory tract infection (URTI) and may lead to potentially precarious Lower respiratory tract infection (Borchers et al., 2013). RSV transmission happens person to person, directly or indirectly; an RSV infected person, upon sneezing or coughing, can leave viral droplets suspended in the air, which have the potential for transmission of infection by entering healthy individual through the mouth, nose or eyes (CDC, 2014; Diseases, 2014).

First line treatment of RSV infection is the use of bronchodilators, such as α and/or β adrenergic agonist (Borchers et al., 2013). For paediatrics, since corticosteroids are not approved for treating RSV infected individuals less than 1 year old due to safety concerns (Piedimonte and Perez, 2014), the use of vaporub and non-aspirin formulations, such as paracetamol, are the treatments of choice prior to clinical attention. Of the very few options available for the treatment of RSV, ribavirin, a broad spectrum antiviral drug, is used, although this too comes with limitations and drawbacks (Bawage et al., 2013); despite several concept studies claiming effectiveness of ribavirin in significantly reducing the RSV load and minimising disease severity, the disadvantages of mutagenicity, teratogenicity and carcinogenicity subsequently resulted in FDA denial (Simões et al., 2015). Active prophylaxis would be better than passive prophylaxis but, unfortunately, there is no current vaccine developed for RSV infection. Formalin inactivated vaccine was launched in the 1960s, but was later withdrawn due to poor

immunogenic response as well as an atypical T_H2-type response, increasing chances of reinfection with similar or deadly infections (Piedimonte and Perez, 2014).

Recently, a novel approach to inhibit RSV was the use of gold nanoparticles (GNPs). These GNPs can be functionalised with nucleic acid, antibodies, drugs as well as with peptides and these functionalised GNPs can then be applied in diagnosis or treatment (Tiwari et al., 2014). Indeed, anti-RSV fusion peptide RF-482 (Figure 6.2) has previously been used to functionalise GNPs, which resulted in significant RSV inhibition (Singh et al., 2014). Liposomes can also be conjugated in the same way, but very limited research has been performed using liposomes as a carrier system for the inhibition of RSV (Hendricks et al., 2015; Vabbilisetty and Sun, 2014). Therefore, considering the global need, the work in this chapter describes a combined approach; liposomes as a carrier system and conjugation of liposomes with the anti-RSV fusion peptide RF-482 for inhibition of RSV.

Peptide RF-482 is structure built of 39 amino acids (VFPSDEFDASISQVNEKIN QSLAFIRKSDLLHNVNAGKK) with a total of 611 atoms (atomic formula: C₁₉₂H₃₀₃N₅₃O₆₃, molecular weight: 4361.8, theoretical iso-electric point: 4.95), having a net charge of -2 (acidic to near neutral). RF-482 is derived from a precursor of RSV fusion protein F0 (Figure 6.2).

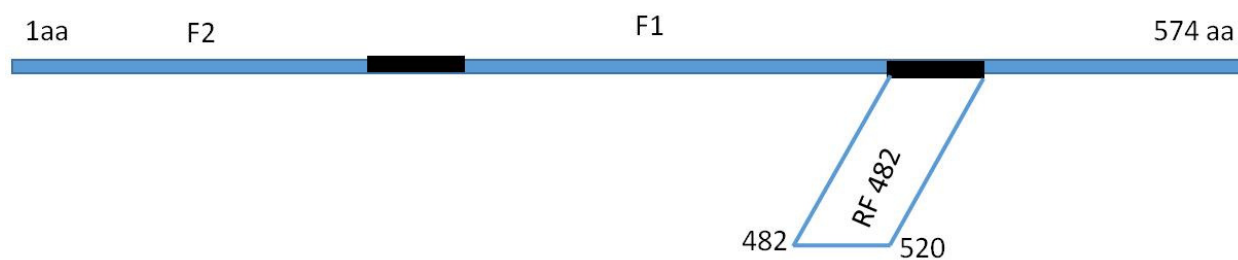


Figure 6.2 Diagrammatic illustration of the amino acid regions of the RSV fusion protein precursor F0 from which the peptide RF482 is derived.

Considering published outcomes related to treatment, as well as the impact of RSV on global healthcare, a promising treatment or vaccine development remains a priority. The genome of RSV codes immunogenic proteins, which creates scope for DNA vaccines, subunit vaccines and nano vaccines (Bawage et al., 2013). These vaccines can be designed as carrier based vaccines, through the use of nanoparticulate systems, such as liposomes, that can express adjuvant action by enhanced antigen delivery or inducing innate immune responses (Schwendener, 2014). The potential of liposomes as a carrier of active pharmacological agents was described decades ago (Gregoriadis et al., 1971; Gregoriadis and Ryman, 1972a, b), whilst liposomes have attracted much attention for their ability to carry antigens as well as immunomodulators (Perrie et al., 2013). Therefore, liposomes could be a potential candidate in vaccine development against the RSV.

6.2 Aim and objectives

The work in this chapter aimed to prepare liposomes < 100 nm using thin film hydration followed by sonication, to effectively conjugate the anti-RSV peptide RF-482 and investigate the efficiency of this formulation against RSV inhibition. To achieve this, the objectives were:

4. Preparation of RF-482 conjugated GNP as well as liposomes and separation of non-conjugated peptide.

5. Evaluate the toxicity of the formulations using HEP-2 cells.
6. Study and compare the liposomal RSV inhibition in presence and absence peptide RF-482, as well as with the GNP and RF-482 conjugated GNP.

6.3 Results and discussion

6.3.1 Conjugation of gold nanoparticles and peptide RF-482

Carboxyl-polymer coated spherical GNPs (Nanopartz™, Loveland, CO, USA), 50 nm in size, were functionalised with RF-482 (Bachem Americas Inc., Santa Clara, CA, USA) with the aid of 1-Ethyl-3-(3-dimethylaminopropyl) carbodiimide (EDC, Sigma Aldrich, St. Louis, MO, USA) chemistry.

Confirmation of conjugation of peptide with GNPs was made after the data analysis of DLS, and US/Visible spectrometry. It has previously been reported that peptide conjugation of the GNP can be confirmed by the increase in particle size and reduction in the surface potential (Tiwari et al., 2014). Similarly, DLS results here show that the hydrodynamic diameter of GNPs was changed from 58.14 ± 0.3 nm to 85.85 ± 1.5 nm after conjugation with RF-482 (Figure 6.3), whereas the zeta potential of GNPs changed from -66.5 ± 1.3 to -54.8 ± 0.4 mV ($n=3$, \pm SD). These changes in the particle characteristics confirm the conjugation of RF-482 with GNPs.

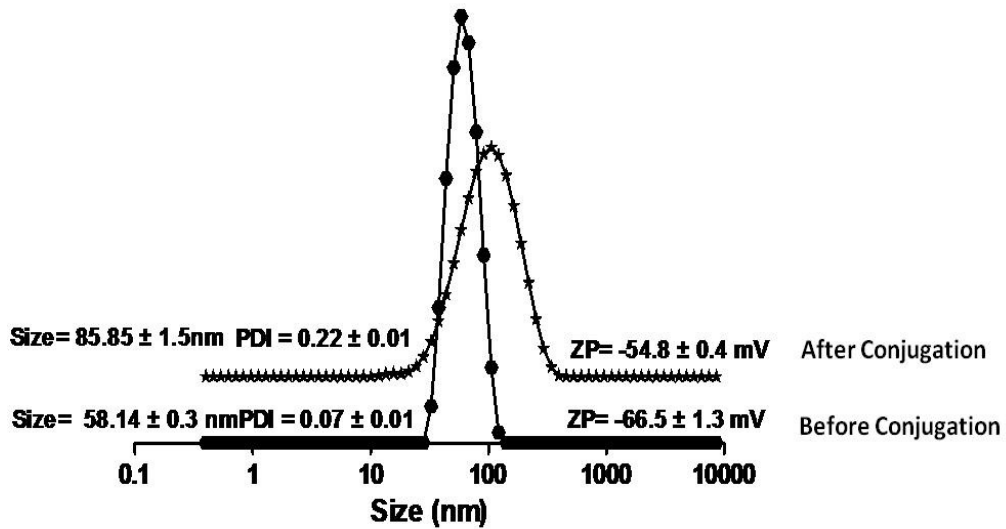


Figure 6.3 DLS analysis of non-functionalised and functionalised hours. The line at the bottom (size 85.85 ± 1.5 nm) represents non-functionalised nanoparticles; whereas top line (size 58.14 ± 0.3 nm) represents functionalised gold nanoparticles. ($n=3 \pm SD$).

For further evidence of peptide conjugation, previous studies have also shown that attachment of the peptide on the surface of the particle, including functionalisation of GNPs, can cause a shift in the surface plasma resonance (Chithrani et al., 2006a; Joshi et al., 2004; Stover et al., 2014). Similarly, the shift of spectra from 520 to 517 nm (Figure 6.4) was observed here after UV/Visible analysis of GNPs followed by FG NPs, further supporting the previous results confirming functionalisation of GNPs.

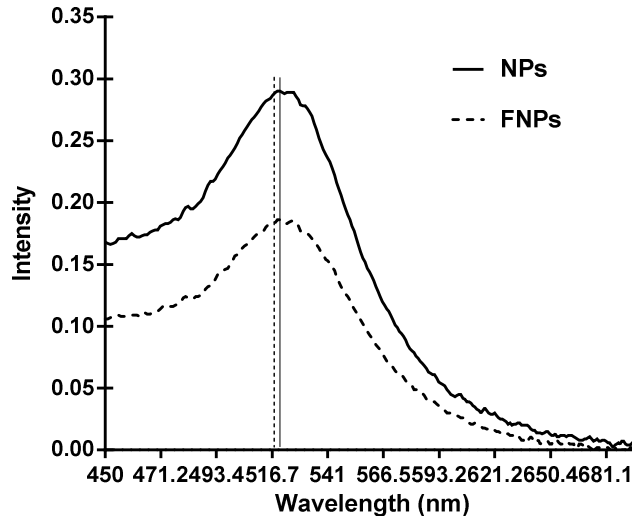


Figure 6.4 UV/Visible scan of GNPs and FGPs.

Furthermore, the supernatant obtained after FGPs washing was subjected to BCA assay and tested for quantification of the protein conjugated with GNPs, using an indirect approach. It was found that 53.6% ($n=3$, ± 1.3 %) was found not conjugated and, hence, it can be concluded that 46.4 % protein was conjugated.

6.3.3 Conjugation of liposomes and peptide RF-482

Liposomes are one of the most flexible structures that can conjugate moieties like lactose and peptide (Nahar et al., 2014; Vabbilisetty and Sun, 2014). As discussed earlier in this chapter (Figure 6.2), RF-482 is a very small peptide and, therefore, a slight increase in the size of liposomes can be expected to confirm the conjugation; indeed, it has previously been reported that the adsorption of protein to negatively charged liposomes can increase the size of

liposomes by >10 nm, but the phosphocholine liposomes can experience the change in size <10 nm (Brooksbank et al., 1993; Kozak et al., 2015).

Similarly, after the conjugation with RF-482, there is a slight change in the size of liposomes (91.78 ± 0.3 nm (PDI 0.2 ± 0.01) and 96.91 ± 0.6 nm (PDI 0.19 ± 0.03) before and after conjugation, respectively). However, unlike the FGNPs, there was little observed change in the zeta potential due to conjugation of RF-482 (-9.9 ± 1 mV and -12.2 ± 1.3 mV before and after conjugation, respectively) (Figure 6.5). This could be because the DSPC is neutral and the conjugation of RF-482 hasn't brought any charge shading effect on the particle. Unlike GNPs, there is no chemical process involved with the conjugation of RF-482 with liposomes and the conjugation is dependent on electrostatic or hydrophilic interaction of the RF-482 with liposome.

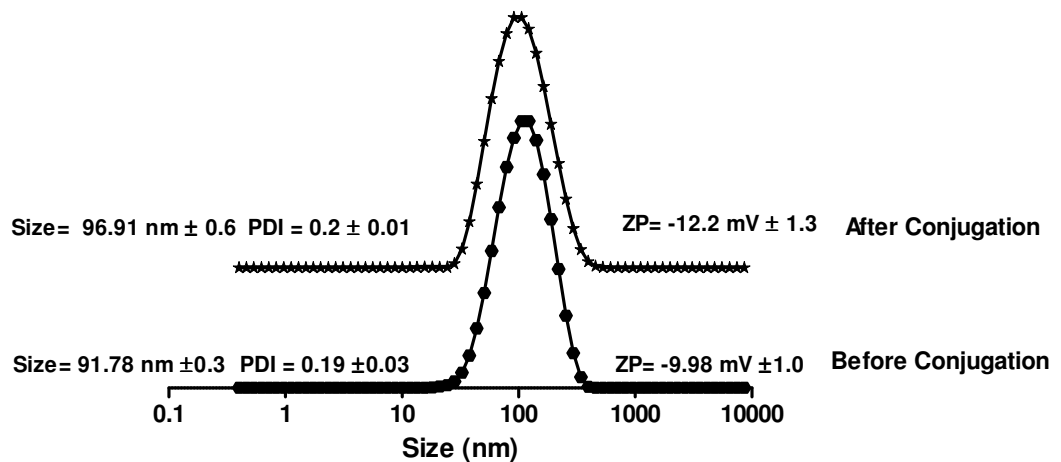


Figure 6.5 DLS measurement of liposomes before and after RF-482 conjugation. (n=3 \pm SD).

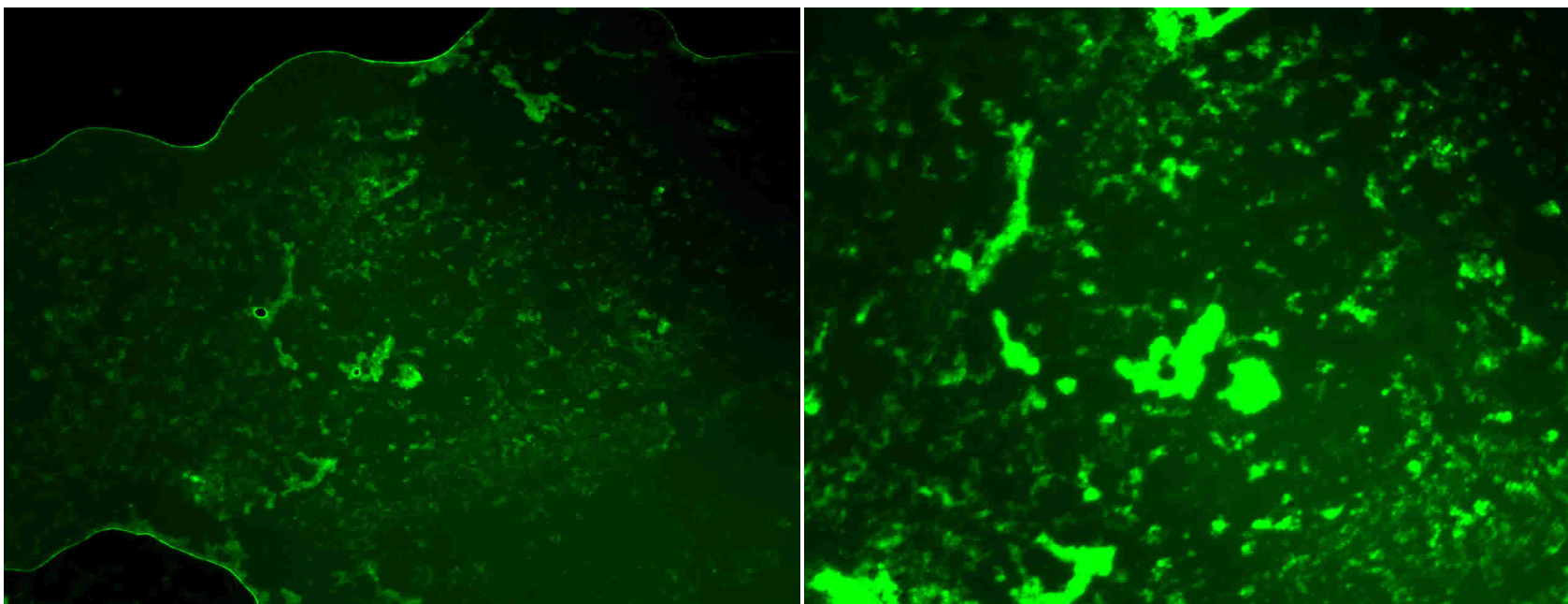
In order to support the results above indicating association of peptide with liposomes, further analysis employed fluorescent dye FITC labelled peptide RF-482 for the conjugation. After the separation of non-conjugated peptide, the liposomal suspension was dried, covered with phosphotungstic acid for better resolution and observed under the fluorescence microscope. After separation of non-conjugated peptide, the presence of peptide in the suspension suggests its association with the liposomes. The presence of RF-482 in the suspension was observed at low and high magnification (Figure 6.6a&b); the low magnification shows the omnipresence in the drop of the suspension, whereas at high magnification, the RF-482 appeared as clusters, possibly around the liposomes.

Indeed, this 'corona formation' phenomenon was described recently following adsorption of protein on the surface of liposomal nanoparticles; a protein corona formation was observed around the liposomes, with no significant effect on the size of liposomes (Hadjidemetriou et al., 2016; Hadjidemetriou et al., 2015). A similar phenomenon had also been reported for polymeric microparticles (Kirby et al., 2013).

Also, previous studies have reported that, whilst negatively charged liposomes have better protein adsorption due to high binding affinity, neutral liposomes could also have protein adsorption onto their surface due to some electrostatic interaction (Price et al., 2001).

It is described earlier in this chapter that the RF-482 is a fusion protein. Given the cohesive nature of the RF-482 and the resemblance of the liposomal bilayer to the cell surface, it is likely that some interaction has occurred between the protein and the lipid bilayer, resulting in its adsorption on the surface of the liposomes. Thereby, this whole conjugation resembles the phenomenon of the 'protein corona' formation, where protein is adsorbed on the surface of the liposomes forming a corona (Hadjidemetriou et al., 2016; Hadjidemetriou et al., 2015).

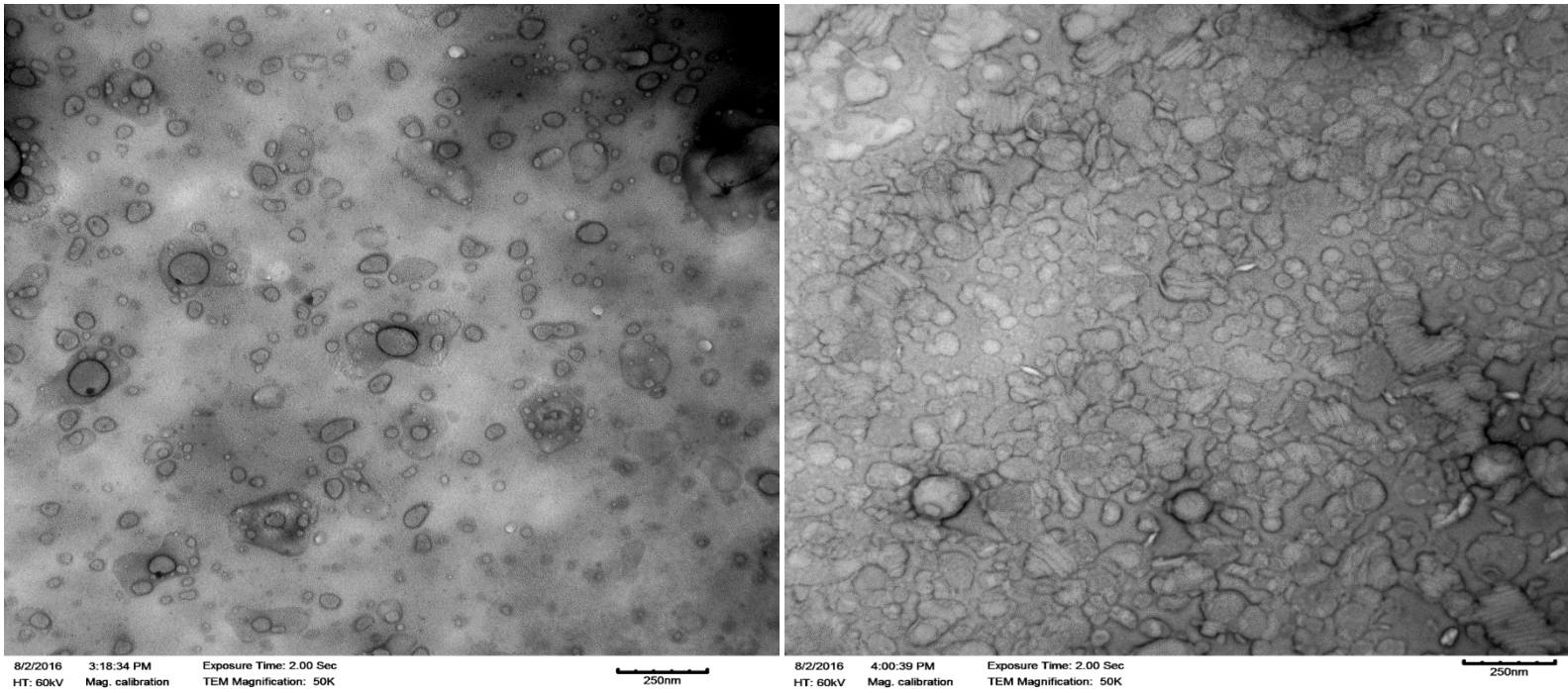
Knowing this, subsequently after the fluorescence microscopy, the empty liposomes as well as peptide conjugated liposomes were imaged under TEM. Presence of protein was again indicated by a cloudy environment observed around the conjugated liposomes and a change in morphology (Figure 6.7b), which was not observed in the case of empty liposomes (Figure 6.7a).



(a)

(b)

Figure 6.6 Fluorescence microscopy analysis liposomes conjugated with FITC labelled peptide RF-482 (Green). (a) 10X magnification and (b) at 40X magnification.



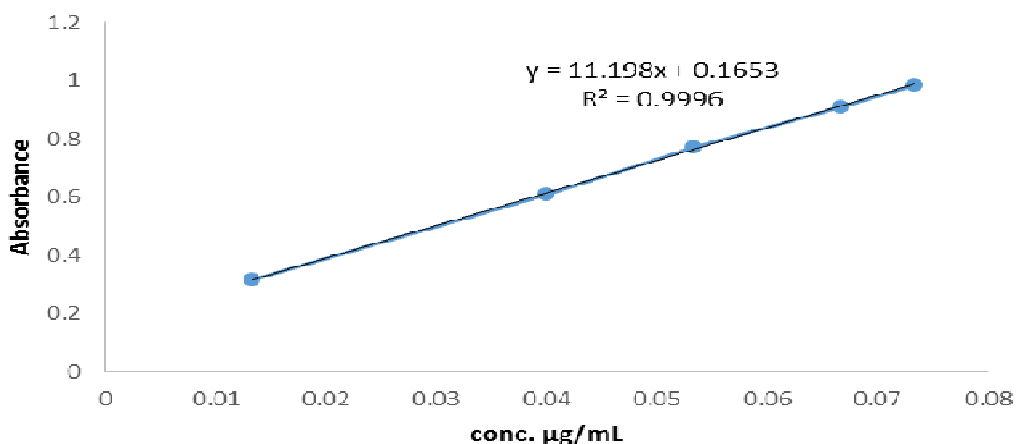
(a)

(b)

Figure 6.7 Transmission electron microscopy analysis. Comparison between (a) empty liposomes and (b) RF-482 peptide associated liposomes Images taken at 50X magnification and 60kv HT.

6.3.4 Evaluation of column efficiency to separate the non-conjugated protein

The efficiency of the column to separate the RF-482 was tested by running RF-482 solution. To achieve maximum removal, the solution was centrifuged at 18000g for 60 min. This non-separated protein may, thereby, be counted as conjugated protein. Also, to remove further doubt, three different concentrations of peptide RF-482 were ran through the same column for the same amount of time and the eluent was tested for recovery. It was observed that more than $97 \pm 1\%$ of protein passes through the column (Figure 6.8). This confirms that the column used to separate the non-conjugated protein is efficient for the purpose.



Sample	Absorbance	Conc.	Eluent Volume	Final Conc	Ini Conc	% Recovery
1	0.606	0.039355	1	0.983881	1	98.4
2	0.731	0.050518	1	1.262949	1.3	97.1
3	0.999	0.074451	1	1.86127	1.9	98

Figure 6.8 Analysis of column efficiency to separate non-conjugated protein.

Furthermore, this confirms that the liposomal sample obtained after separation of nonconjugated protein would have negligible amounts of non-conjugated protein present along with the liposomes in the suspension. In other words, only liposomes conjugated with the RF-482 can be present in the suspension as almost all the non-conjugated RF-482 separates out from the column after centrifugation.

6.3.5 Quantification of conjugation

The exact mechanism of protein-liposome association is still unknown, although results above indicate that RF-482 is associated with the liposomes. However, it was necessary to quantify the amount of protein conjugated with the liposomes, whilst being equally important to achieve the mass balance to confirm the actual amount of conjugation of peptide. Hence, the BCA assay was performed for the analysis of both eluent as well as liposome samples. It was confirmed that $81.7 \pm 0.1 \%$ ($n=3$) was not-conjugated and $19.1 \pm 0.4 \%$ ($n=3$) was conjugated (Figure 6.9). This also confirms 100 % recovery of initial amount of peptide.

The percent conjugation of GNPs was significantly higher than liposomes, since the conjugation of RF-482 and GNPs involves covalent bond formation, which contributes towards less loss of adsorbed (or conjugated) peptide upon centrifugation (Singh et al., 2014). Also, as mentioned in the previous section, the adsorption of peptides is higher in negatively charged particles than the neutral particles (Price et al., 2001). DSPC:cholesterol liposomes neither form any covalent bond with the peptide RF-482 nor have strong charges to absorb more peptide and, hence, the

percent conjugation of liposomes is significantly lower than GNPs. Factors such as cohesive nature of peptide RF-482, potential electrostatic and hydrophilic interaction between peptide RF-482 and liposomes as well as the resemblance of liposomes with the cell membrane contributes in making liposomes a potential carrier of anti-RSV peptide RF-482.

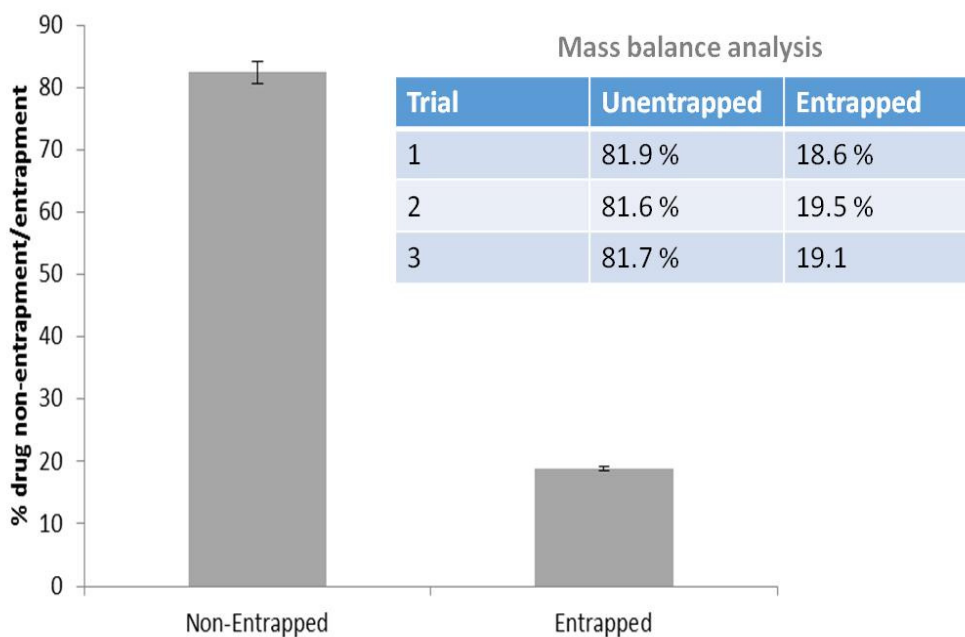


Figure 6.9 Liposomal conjugation with peptide RF-482 determined by BCA assay. Results presented as peptide conjugated determined after separation of non-conjugated peptide. (n=3 ±SD).

6.3.6 Cell toxicity analysis

The emerging problem of RSV treatment development is cell toxicity, as several compounds have failed to meet toxicity criteria in *in-vivo* testing, such as Pyrazofurin (Wyde et al., 1989), neplanocin (Shuto et al., 1992) and PALA (Wyde et al., 1995), which has made them unacceptable for clinical use. Peptide, GNPs and FGPs are proven to be non-toxic up to certain

levels of concentration (Tiwari et al., 2014), whilst liposomes can carry an extensive range of molecules, and have low toxicity for therapeutic requirements (Storm and Crommelin, 1998a).

A range of concentrations of peptide, GNPs, FGNPs, liposomes and peptide encapsulated liposomes were assessed for cell toxicity in human epidermoid type-2 (HEP-2) cells (American Type Culture Collection (ATCC), Manassas, VA 20110 USA). It was found that peptide up to 0.003 mg, as well as GNPs and FGNPs up to 3 nM concentrations were non-toxic to HEP-2 cells (Figure 6.10). It was also found that both empty and peptide encapsulated liposomes up to a volume of 150 μ L (150 μ L is approximately 0.03 mg RF-482) was non-toxic to HEP-2 cells (Figure 6.10).

Peptide, liposomes and peptide conjugated liposomes at two different concentrations were tested for their cell toxicity. There was no toxicity observed with both the concentrations of all samples. For all the chosen concentrations of all the samples, more than 80 % ($n=3 \pm$ SD) cell viability was observed after 72 hours of incubation (Figure 6.10).

Knowing that the toxicity is an emerging problem in RSV treatment (Wyde, 1998), it is one of the primary objectives when designing treatment for RSV infection. In this scenario, liposomes have shown their non-toxic nature for the chosen HEP-2 cells for 72 hours, reflecting their potential application in designing RSV treatment.

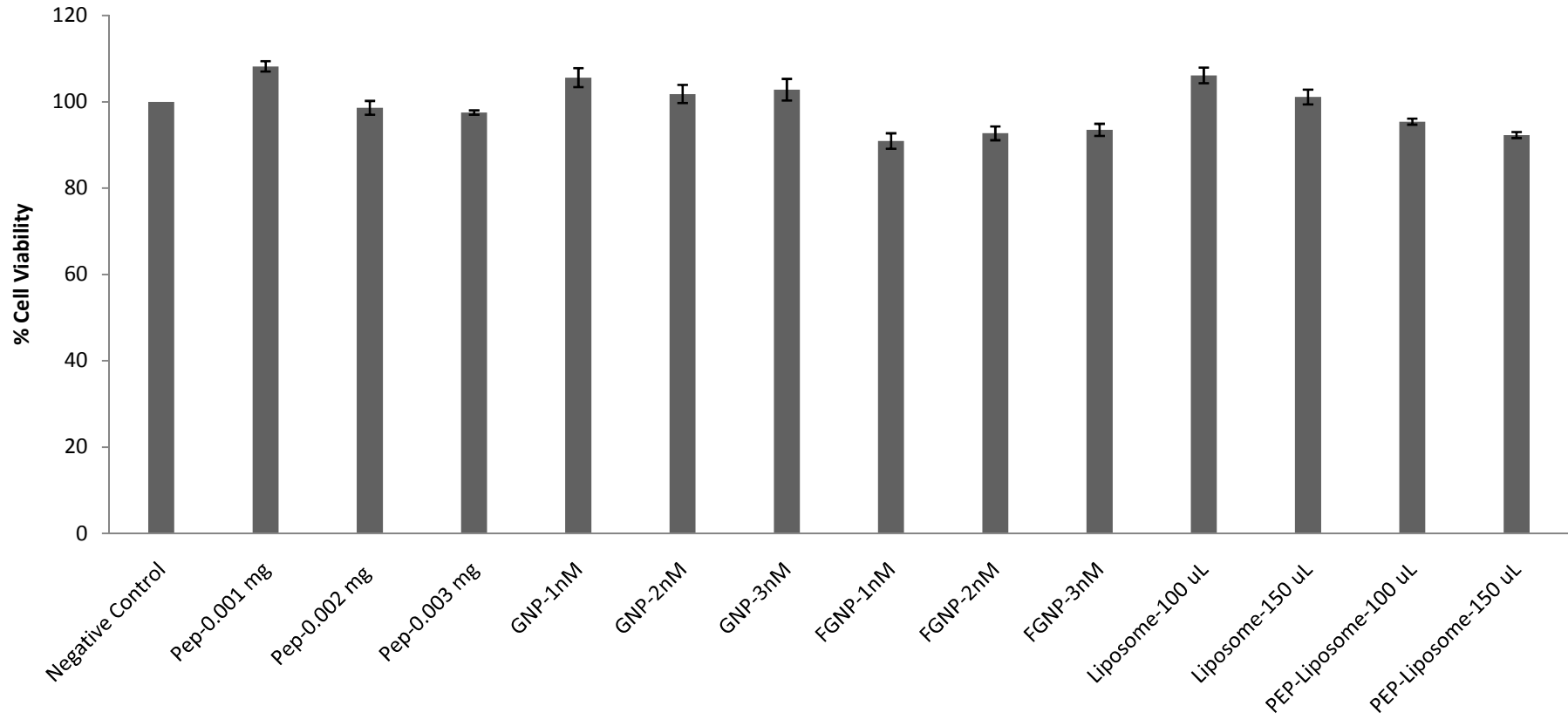


Figure 6.10 Toxicity profiling of peptide RF-482, Liposomes and RF-482 conjugated liposomes as well as GNPs and FG NPs presented through cell viability count performed using MTT assay (section 2.6.3). (72 hours, n=3 \pm SD).

6.3.7 Investigation of viral inhibition

The plaque assay is one of the most common and reliable methods of determination of viral/antiviral activity by counting plaques in the cell culture. Also, the plaque reduction assay is known as the optimum standard for antiviral activity analysis (Landry et al., 2000). The plaque assay was performed using HEP-2 cells (1.5×10^5 /well) proliferated in MEM-10 for 48 hours to achieve maximum confluence. During the plaque assay, the monolayer of HEP-2 cells was infected with the lytic RSV. The infected cells experience lytic cycles and eventually appear as plaques or, in other words, zones of cell death (Baer and Kehn-Hall, 2014). It was reported recently that surfactant phospholipids bound to RSV have markedly suppressed the infection through fusion inhibition (Numata et al., 2010).

Here, liposomes and nanoparticles with and without their conjugation product with the RSV fusion protein were tested against RSV infection to the HEP-2 cells. When these plaques were counted, it was observed that, in the presence of peptide RF-482/liposomes/peptide conjugated liposomes, the total number of plaques are significantly less than in the absence of the same (Figure 6.11; $p < 0.005$ ANOVA, post hoc-Dunnett's multiple comparison test). This confirms that liposomes/peptide RF-482 alone or as conjugation product is capable of inhibiting the virus.

Indeed, liposomes have recently gained attention for the treatment of viral infections (Hendricks et al., 2015); moreover, it has recently been shown that 1-stearoyl-2-arachidonoyl-

sn-glycero-3-phospho-L-serine (SAPS) liposomes can inhibit human rhinovirus (HRV) (Stokes et al., 2016). Thus, the findings presented here similarly confirming the inhibition of RSV in the presence of DSPC-cholesterol liposomes is of interest and corroborates research elsewhere in the field. The results also confirm that RSV percent inhibition is significantly increased (approximately 9 %, $p < 0.005$, ANOVA, post hoc-Dunnett's multiple comparison test) for RF-482 conjugated liposomes compared to RF-482 and liposomes alone (Figure 6.11).

On the other hand, GNPs as well as FGPNs were efficient in inhibiting virus and have shown more than 60 % viral inhibition through the plaque assay. However, when a comparison was made between functionalised gold nanoparticles and functionalised liposomes, it was found that the liposomes have a significantly greater RSV inhibitory effect ($P < 0.05$, t-test).

Although, the liposomes have less percent RF-482 conjugation compared to GNPs, it was observed that the toxicity index of liposome alone or functionalised liposomes is equal or better than the GNPs or FGPNs. Also, the plaque assay results represent a significant difference in RSV inhibition by liposomes compared to GNPs alone ($P < 0.05$, t-test) and there was also a significant difference in RSV inhibition by functionalised liposomes compared to GNPs and FGPNs ($p < 0.05$, ANOVA, post hoc-Dunnett's multiple comparison test). This suggests that liposomes are a better candidate for inhibiting RSV compared to GNPs alone, whilst functionalised liposomes are a better candidate for RSV inhibition compared to GNPs and FGPNs.

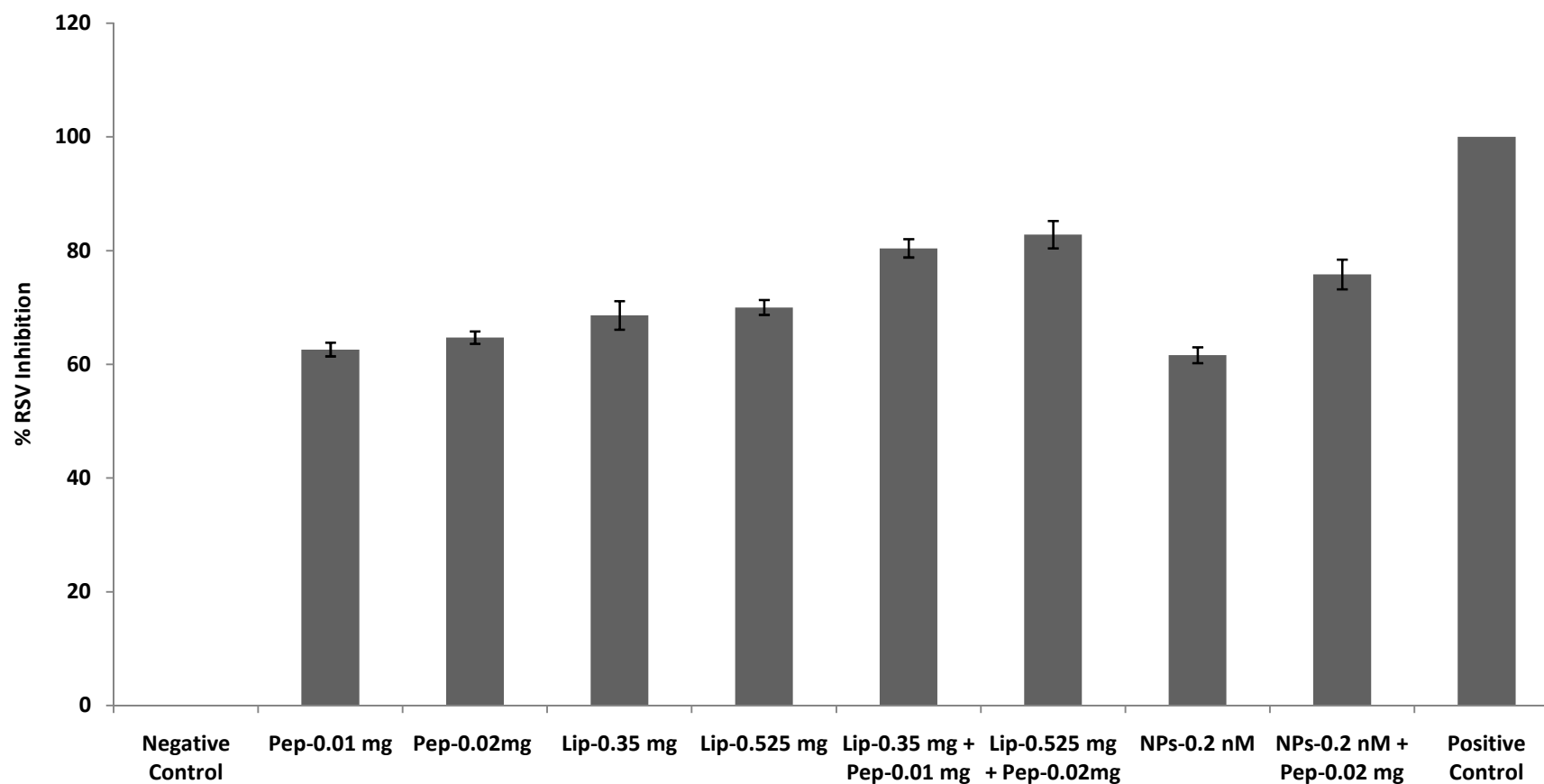


Figure 6.11 Screening of Peptide, Liposomes and gold nanoparticles with and without peptide conjugated against RSV. Plaques were counted and the mean count of each sample was compared against control to determine the percent inhibition. (n=3 ±SD).

It was important to post-investigate the findings of the plaque assay, in order to validate the results and provide a qualitative and quantitative assessment. Therefore, immunofluorescence imaging was used as a qualitative tool and PCR as a quantitative tool. For the immunofluorescence analysis, the HEP-2 cells were incubated for 48 h with peptide RF-482, empty liposomes and functionalised liposomes, as well as GNPs and FGPNs, followed by fixing in paraformaldehyde-glutaraldehyde and washing with buffer (1X PBS). An appropriate chamber from the 8-chambered slide was observed under the fluorescence microscope for the RSV activity. The observation made from this analysis matches the results obtained from the plaque assay and confirm that peptide RF-482, liposomes and peptide conjugated liposomes, as well as GNPs and FGPNs, are capable of inhibiting RSV (Figure 6.12).

Recently, reports have shown that phosphatidylinositol (PI) inhibits the respiratory syncytial virus (RSV), as the PI binds the RSV with high affinity, inhibiting its fusion to the epithelial cells (Numata et al., 2010; Numata et al., 2015). There are five derivatives of phospholipids including the PI and the phosphocholine (PC). Although the exact mechanism of RSV inhibition by PC is not confirmed, it is possible that, similarly to the PI, the PC could have affinity towards the RSV, inhibiting its fusion to the epithelial cells.

Presence of virus can be clearly marked with the green dye (FITC) and HEP-2 cells with the blue dye (DAPI). This microscopic investigation confirms that, not only GNPs and FGPNs, but also liposomes as well as functionalised liposomes are efficient in inhibiting RSV spread. With RF-482 alone, the effect is less prominent, as green dye (FITC) can still be observed in some places (Figure 6.12).

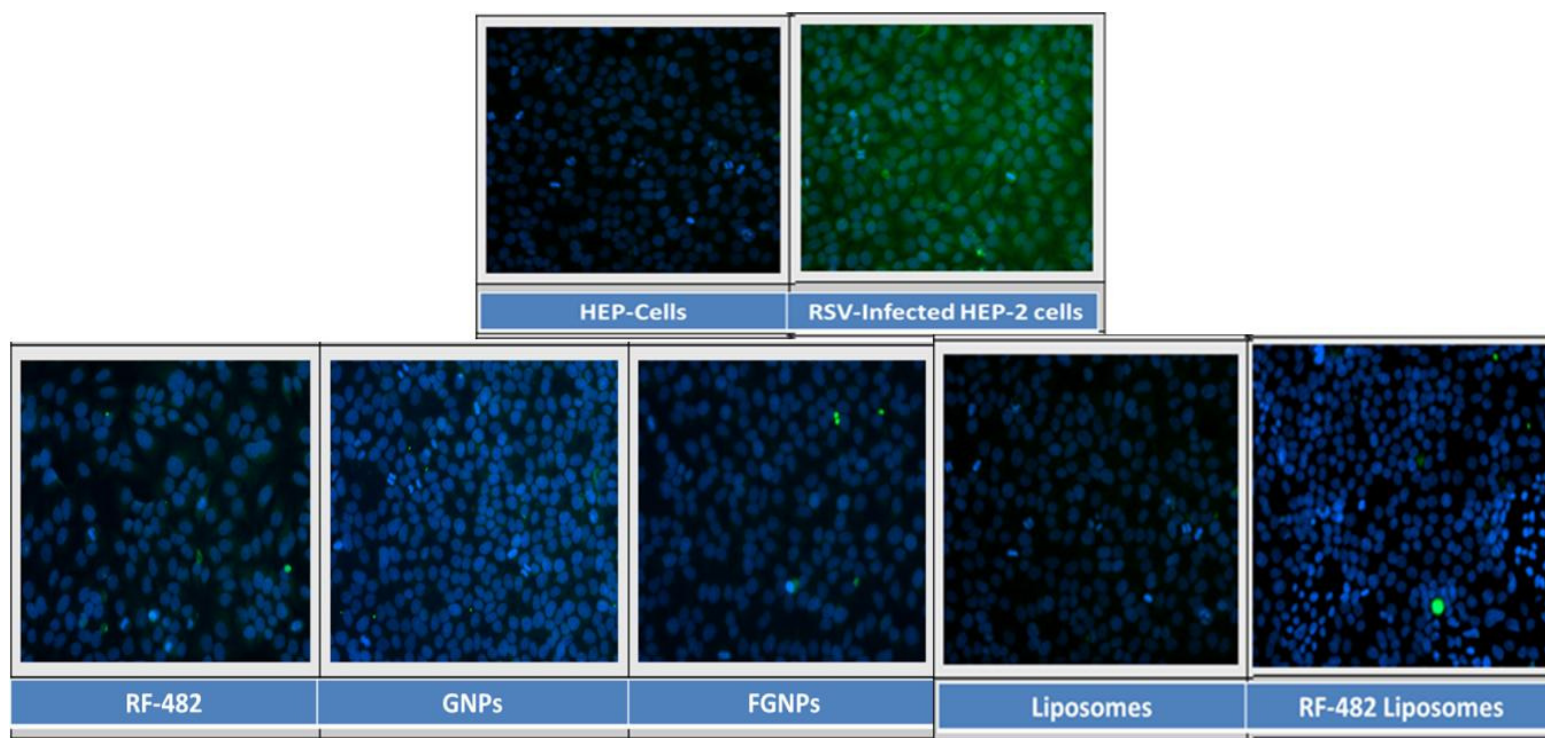


Figure 6.12 Fluorescence microscopy analysis. FITC (Green): RSV and DAPI (Blue): HEP-2 Cell nucleus. In liposomes and RF-482 liposomes the blue colour represents survived cells and green colour represents presence of RSV.

Polymerase chain reaction (PCR), one of the basic techniques available in the modern biological research, was employed for the quantification of the target sequence using real time, by detecting the number of amplicons generated at the end of every amplification cycle (Watzinger et al., 2006). The whole experiment was a set of small experiments starting from cell culture to gene quantification. Having confirmation from the microscopic observation of viral inhibition, it was necessary to validate, numerically, the plaque assay results.

qRT-PCR provides rapid and quantitative data for analysis of viral presence. However, prior to amplification of cDNA via RT-PCR, the RNA was extracted from the samples and cDNA was synthesised using the superscript. After amplification, the obtained cycle threshold 'Ct' values were used as a tool for the comparison between the samples.

Significant differences ($p < 0.005$, ANOVA, post hoc-Dunnett's multiple comparison test) were observed between the Ct value of virus samples and samples having peptide/liposomes/conjugated liposomes/GNPs/FGNPs (Figure 6.13). Although there is no significant difference ($p > 0.05$, t-test) observed between peptide/liposome alone and conjugated liposomes, the conjugated liposome samples displayed a slight trend for higher Ct values, further suggesting more inhibition when used in combination (Figure 6.13).

GNPs as well as FGNPs were efficient in inhibiting virus and have shown the cycle threshold significantly higher than the virus alone ($p < 0.05$, ANOVA, post hoc-Dunnett's multiple comparison test). This confirms the anti-RSV effect of GNPs and FGNPs observed through the plaque assay and immunofluorescence imaging. However, when a comparison was made

between GNPs and liposomes, it was found that the liposomes have a significantly increased inhibitory effect towards the RSV inhibition ($P < 0.05$, t-test) (Figure 6.13).

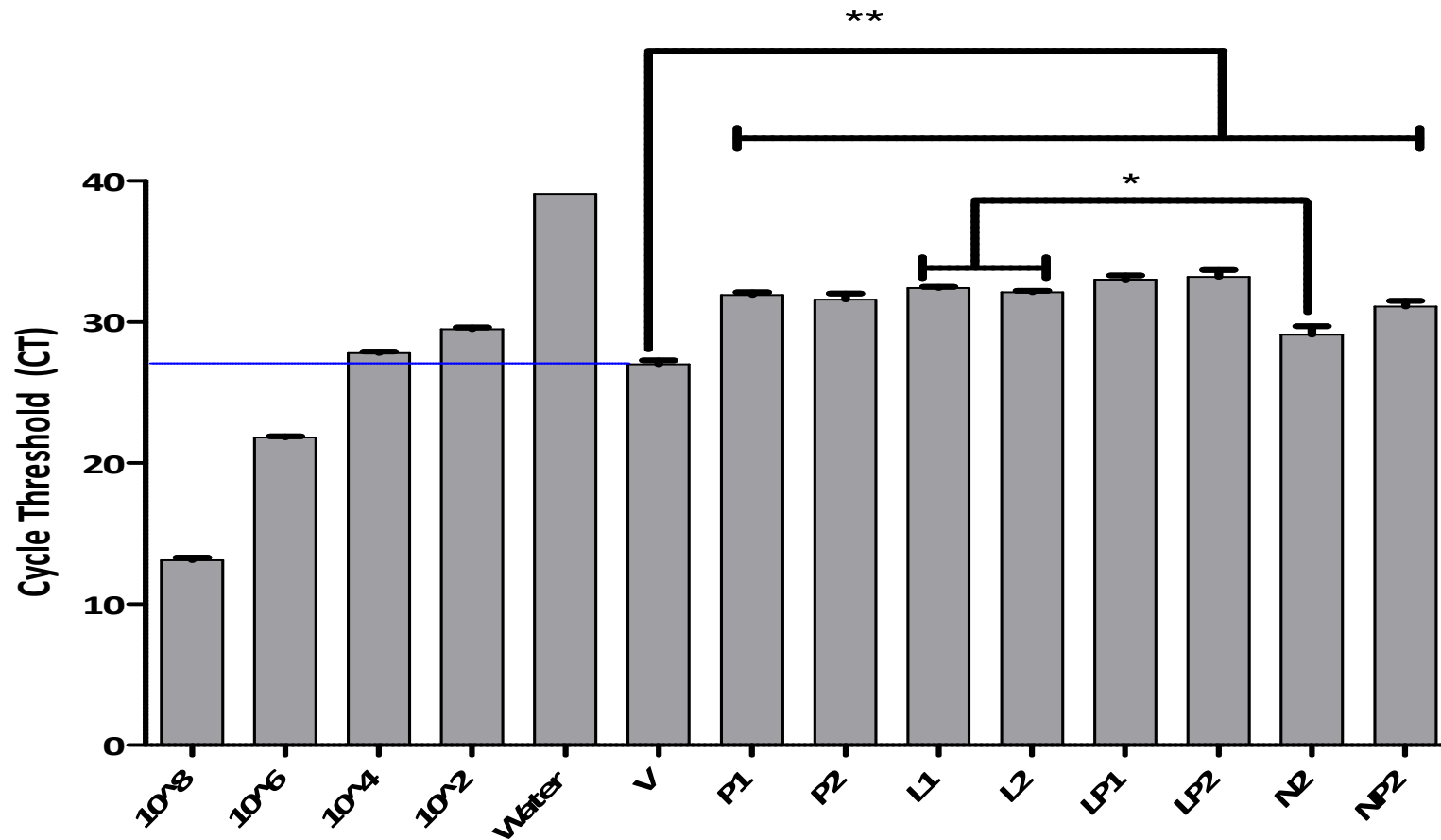


Figure 6.13 Screening of RSV-F gene amplicon dilution with water as negative control. Water represents blank or sample with no gene amplicon. Blue line: indicating the threshold of virus sample has higher gene amplicon than the gene amplicon of standard 10⁴. Comparison of viral gene amplicon (V) and Peptide (P1 & P2), Liposomes (L1 & L2), Functionalised liposomes (LP1 & LP2), gold nanoparticles (N2) and functionalized gold nanoparticles (NP2). (* and ** in the figure represents p<0.05 and p 0.01 respectively).

6.4 Conclusion

With the quest of finding an alternative carrier for delivering the anti-RSV peptide RF-482, a liposome formulation has been prepared and tested for the inhibition of RSV infection. Similar to the GNPs and FGPNs that have previously been reported (Singh et al., 2014; Tiwari et al., 2014), the functionalisation of liposomes was confirmed through dynamic light scattering (Figure 6.5), change in the surface charge, fluorescence imaging (Figure 6.6) and transmission electron microscopy (Figure 6.7). The cytotoxicity of various concentrations of these liposomes was tested by MTT assay and it was found that liposomes of two different concentrations of lipids with and without protein conjugation did not render any cytotoxic effect and molecular effect on the host HEP-2 cells (Figure 6.10). The anti-RSV effect was then confirmed in plaque assay (Figure 6.11), immunofluorescence imaging (Figure 6.12) as well as in qRT-PCR. In qRT-PCR, the cycle threshold (Ct) for liposomes of two different concentrations of lipids with and without protein conjugation was observed significantly higher ($P < 0.005$, t-test performed individually) than the virus cycle threshold (Ct) (Figure 6.13).

Overall, the observed potential of GNPs and FGPNs to inhibit RSV infection matches the past research (Tiwari et al., 2014). However, liposomes as a new candidate for RSV inhibition was tested and the inhibitory effect of liposomes was shown to be better compared to GNPs alone, whilst functionalised liposomes were shown to be a better candidate for RSV inhibition compared to both GNPs and FGPNs. However, this has generated another quest to unveil the exact mechanism of RSV infection inhibition by the use of liposomes or functionalised liposomes, which could lead to commercialisation of the formulation.

Chapter 7: Overall discussion and conclusion

7.1 RP-HPLC based simultaneous determination of metformin and glipizide

In this thesis, liposomes have been explored as a delivery vehicle to improve the delivery of drugs that require advanced strategies when considering their formulation. Consideration was given to improving the solubility and delivery of low-solubility drugs that could be co-encapsulated with hydrophilic drugs, and also liposomes were considered for their ability to deliver biopharmaceutical systems.

To achieve this, robust methods for drug quantification are required. Therefore, to determine drug encapsulation, as well as drug loss, an RP-HPLC based method was developed, where the separation was based on the affinity of the compound towards the stationary phase in the column and the quantification was performed using UV detection. This method was then evaluated using a range of parameters, such as specificity, accuracy, linearity, precision and intermediate precision, fulfilling ICH criteria for method validation (FDA, 1994). This method is based on isocratic elution, which makes the method simple and the retention time observed is less than 3 minutes. With this method, not only free drug, but also encapsulated as well as released drug was determined. The method was not compatible with the simulated medium used for drug release studies.

7.2 Production of liposomes co-encapsulating drugs of divergent solubility

As mentioned previously, the liposomal size is important given the possibility of clearance by RES (Gregoriadis, 1995), but size reduction to produce SUVs can lead to the formation of single compartment vesicles, thereby lowering internal volume, which directly affects the drug loading (Szoka and Papahadjopoulos, 1978). Therefore, both MLVs as well as SUVs were produced and evaluated for their potential of co-drug delivery.

Initially, the significance of cholesterol concentration was determined, where liposomes with two different concentrations of cholesterol were prepared. With low fractions of cholesterol in the formulations (below 33 mole %), no change in the size of the liposomes can be expected (Melzak et al., 2012) and the bulky appearance of cholesterol is responsible for the immobility of hydrophobic tails (Deol and Khuller, 1997), which can impact on drug loading within the bilayer. However, with the formulations tested within this thesis, no cholesterol concentration induced change was observed in size, surface potential, drug loading and retention capacity of liposomes. Simultaneously, the effect of drug encapsulation on particle characteristics was studied and it was found that neither metformin nor glipizide have any significant effect on MLV characteristics, irrespective of cholesterol concentration. Furthermore, the formulations were stable for 28 days, having particle sizes around 10 microns, surface charge $< \pm 10$ mV and $< 12\%$ drug loss of entrapped drug.

Knowing that the presence of cholesterol makes bilayers rigid (Eloy et al., 2014) and an increase in cholesterol concentration did not make any difference in particle characteristics – including drug loading or retention – DSPC:Cholesterol concentration of 5:2 w/w was finalised for further studies. Subsequently, co-encapsulation of two drugs simultaneously was evaluated. Here, no significant difference ($p > 0.05$, t-test) in drug loading was observed; however, the particle size of co-drug loaded MLVs was significantly increased ($P < 0.05$, t-test) compared to the single-drug loaded liposomes. To evaluate liposomes for the maximum possible encapsulation, a drug escalation study was performed. Although there was no difference observed in size or drug loading capacity of MLVs, there was a gradual increase in encapsulation efficiency observed for both metformin and glipizide.

MLVs can be transformed into SUVs by methods including sonication or extrusion, but sonication is broadly used because of ease of the method as well as cost effectiveness. However, during the course of sonication, the field of sonic energy ruptures the bilayer and forms SUVs. During this rupture process, the lipophilic drug becomes prone to leakage and the likelihood of loss of hydrophilic drug increases. To study this possibility, MLVs were transformed into SUVs by sonication and their particle size, drug loading as well as *in-vitro* drug release was compared with the MLVs. There was no significant difference ($p > 0.05$ ANOVA post hoc Dunnett's test) found in the particle characteristics (i.e. size and zeta potential) of empty, individual or co-drug loaded SUVs. However, the percent loading was significantly decreased (approximately 25 % for glipizide and 52 % for metformin, $p < 0.05$, t-test) in SUVs compared to

MLVs. However, drug release was comparatively slower in SUVs than MLVs and SUV are less prone to a burst effect, possibly due to the rigid bilayer packing achieved.

7.3 Microfluidics based simultaneous co-encapsulation of lipophilic and hydrophilic drugs

Unlike probe sonication, the microfluidics process of SUV production is less disruptive as well as less prone to contamination (Batzri and Korn, 1973; Wagner and Vorauer-Uhl, 2010). Moreover, it is a rapid, one step liposome production method. Use of microfluidics for the encapsulation of poorly water soluble drug propofol was reported recently (Kastner et al., 2015), but in this thesis, for the first time simultaneous encapsulation of lipophilic and hydrophilic drug was demonstrated.

Initially, the impact of FRR and TFR was studied on the formation of SUVs composed of the long chain lipid, DSPC, in combination with cholesterol (5:2, w/w). Decreased availability of solvent for lipid solubilisation as well as decreased distance for diffusion impacts vesicle closure time and results in production of smaller vesicles (Zook and Vreeland, 2010). At higher TFR (15 mL/min) and high aqueous volume (5:1 aqueous: organic), production of smaller liposomes was observed in comparison with lower TFR and high organic content. The solvent to buffer ratio has a significant effect ($p < 0.05$, ANOVA post hoc Dunnett's test) on the particle size as well as PDI.

Size and lamellarity are the main points that confirm the formation of SUVs. The less than 100 nanometer size range of liposomes produced by microfluidics was confirmed by DLS and, to examine the structure of liposomes closely, cryo-electron microscopy was also undertaken. No significant variations have been observed between DLS results and cryo-TEM results with respect to the size and PDI of liposomes; the average size for all liposome samples was around 60 ± 10 nm. The presence of organic solvent over the permitted limit may deteriorate the formulation; therefore, dialysis was used for the removal of organic phase of liposomes obtained after the chaotic mixing of aqueous phase and organic phase having lipids dissolved. Only 25 ± 6 ppm of organic solvent was found remaining in the sample, which was far below the ICH limit (3000 ppm).

In terms of drug loading within these vesicles prepared using microfluidics, the loading was based on the principle of passive loading, where both drug and lipids are co-dispersed in the aqueous phase. Generally, encapsulation efficiency for passive loading is < 50% for lipophilic drugs (Cullis et al., 1989) and 1 to 15 % for hydrophilic drugs (Cullis et al., 1989; Sharma and Sharma, 1997), whilst these studies have shown notably higher hydrophilic (metformin) drug loading of approximately 20% was achieved. Subsequently, the maximum possible encapsulation was determined through a drug escalation study. Here, similar to the MLVs, although there was no difference observed in size or drug loading capacity of SUVs, there was a gradual increase in encapsulation efficiency observed for both metformin and glipizide.

Finally, the release of drugs was performed using the USP-4 dissolution apparatus. There are various models reported in past literature and it can be expected that any drug subjected for drug release could have strong relation with these models (Ramteke et al., 2014), with both zero order and first order kinetics being common; zero order is independent of drug concentration (Costa and Lobo, 2001), whilst first order is directly proportional to the drug concentration (Jeong et al., 2000). However; from the R^2 values obtained from line of fit, it can be concluded that only when the metformin was co-entrapped with the glipizide has followed first order release but for all other samples there is strong correlation observed with Higuchi model compared to first order and zero order kinetics. However, in case of drug release from SUV obtained after sonication; where, all the metformin shown to fit good with Higuchi model but the glipizide shown to fit good with zero order having difference in R^2 values. The initial fast drug release is possibly due to the burst effect, where release of glipizide increased the fluidity of the bilayer, which in turn had a pronounced effect on metformin hydrochloride release, as well as glipizide release, to a lesser extent. Also, the hydrophilic nature of the metformin may be responsible for its initial quick release.

7.4 Liposomal inhibition of respiratory syncytial virus

RF-482 was reported as an inhibitor of RSV fusion and, to date, gold nanoparticles are the only reported carrier of RF-482 (Singh et al., 2014). Given the potential of liposomes and the studies conducted in chapters 4 and 5, liposomes were considered as an alternative carrier for delivering the anti-RSV peptide, RF-482.

RF-482 is a small fusion peptide with 39 amino acids with a total of 611 atoms. Since it is fusion peptide and hydrophilic in nature, it was expected that the RF-482 may get entrapped in the hydrophilic core as well as it may adsorb on the surface of liposomes. The exact mechanism of protein-liposome association is still unknown, although results presented in this thesis indicate that RF-482 is associated with the liposomes. The functionalisation was confirmed by a small increase in the size of liposomes from 91.8 ± 0.3 nm (PDI 0.2 ± 0.01) to 96.9 ± 0.6 nm (PDI 0.2 ± 0.03), whilst association of peptide with liposome was also observed when FITC labelled peptide RF-482 was used for the conjugation and when the empty liposomes as well as peptide conjugated liposomes were imaged under TEM; the presence of the peptide was confirmed by the cloudy environment observed around the conjugated liposomes. In the case of the GNPs, the conjugation of RF-482 happens through a covalent bond, making the protein less susceptible to separation upon centrifugation, but in the case of DSPC:Cholesterol liposomes, the adsorption of peptides could be result of electrostatic interaction due to small amount of negative charge (< -10 mV) present on the liposomes as well as due to the fusogenic nature of RF-482 and its interaction with the polar heads.

To test the drug delivery efficacy of the liposomes with the RF-482, a plaque assay was used. This is one of the most common and reliable methods of determination of viral/antiviral activity by counting plaques in the cell culture (Landry et al., 2000). The results suggest that, although the liposomes have less percent RF-482 conjugation compared to GNPs, the toxicity index of

liposomes alone or functionalised is equal or better than the GNPs or FG NPs and were also superior in RSV inhibition compared to GNPs and FG NPs ($p < 0.05$, ANOVA).

However, it is necessary to validate the results of the plaque assay and provide a qualitative as well as quantitative assessment. Therefore, immunofluorescence imaging was used as qualitative tool and PCR as quantitative. The microscopic investigation confirmed that, not only GNPs and FG NPs, but also liposomes as well as functionalised liposomes are efficient in inhibiting RSV spread. Furthermore, the q-RT-PCR results suggest that, upon comparing GNPs and liposomes, it was found that the liposomes have a significantly increased inhibitory effect towards the RSV inhibition ($P < 0.05$, t-test), where the cycle threshold observed is significantly higher than GNPs. Overall, the liposomes as a new candidate for RSV inhibition was tested and the inhibitory effect of liposomes was better compared to GNPs alone and functionalised liposomes were better candidate for RSV inhibition compared to both GNPs and FG NPs.

7.5 Overall conclusion

In relation to the aims and objectives in this thesis, the studies show that:

1. Appropriate analytical methods for the preparation, quantification and characterisation of a range of liposomal formulations were developed and validated.
2. The potential of liposomes as a carrier of hydrophilic, lipophilic (alone or co-entrapped) and peptide drugs were demonstrated.

3. A new high-throughput one-step process for the manufacture of liposomes simultaneously entrapping hydrophilic and lipophilic drugs was developed, and the formulations were evaluated in comparison with the formulations produced by the conventional thin film hydration method.
4. Liposomes were shown to effectively deliver peptides and act as an anti-RSV protein carrier.

7.6 Future work

1. Knowing the multifaceted potential of liposomes make it a versatile drug delivery system. Co-encapsulation can be utilised as one of the routes to deliver the drugs used in the combinational therapy. For example, glipizide and metformin, paclitaxel and doxorubicin, gemcitabine and tamoxifen etc.
2. In the quest for a time saving and easy approach of liposome production, microfluidics has brought a revolution. It will be interesting to study the scalability of liposomal co-drug encapsulation using microfluidics as a method of production. Here, use of continuous production through a series of microfluidic devices could help to achieve the target of scalability.
3. Adsorption of anti-RSV protein RF-482 was an example of the multifaceted nature of liposomes. Further development such as a potential vaccine against the respiratory syncytial virus infection possible. Whereas the system can apt for imaging, diagnostic and therapeutic applications and this can be achieved by using cell specific markers which could provide targeted as well as enhanced intracellular delivery. However, the

mechanism of interaction of the fusogenic RF-482 with liposomes, and the mechanism of liposomes to inhibit the RSV can be further explored using techniques like enzyme linked immunosorbent assay (ELISA), western blot, qRT-PCR; where factors like stress conditions etc can be explored.

References

1. Abdelgawad, M., Watson, M.W., Wheeler, A.R., 2009. Hybrid microfluidics: A digital-to-channel interface for in-line sample processing and chemical separations. *Lab on a Chip* 9, 1046-1051.
2. Aguilar, M.-I., 2004. Reversed-phase high-performance liquid chromatography. *HPLC of peptides and proteins: Methods and protocols*, 9-22.
3. Akbarzadeh, A., Rezaei-Sadabady, R., Davaran, S., Joo, S.W., Zarghami, N., Hanifehpour, Y., Samiei, M., Kouhi, M., Nejati-Koshki, K., 2013. Liposome: classification, preparation, and applications. *Nanoscale research letters* 8, 1.
4. Ali, M.H., Kirby, D.J., Mohammed, A.R., Perrie, Y., 2010. Solubilisation of drugs within liposomal bilayers: alternatives to cholesterol as a membrane stabilising agent. *Journal of pharmacy and pharmacology* 62, 1646-1655.
5. Ali, M.H., Moghaddam, B., Kirby, D.J., Mohammed, A.R., Perrie, Y., 2013. The role of lipid geometry in designing liposomes for the solubilisation of poorly water soluble drugs. *International journal of pharmaceutics* 453, 225-232.
6. Allen, T.M., Williamson, P., Schlegel, R.A., 1988. Phosphatidylserine as a determinant of reticuloendothelial recognition of liposome models of the erythrocyte surface. *Proceedings of the National Academy of Sciences of the United States of America* 85, 8067-8071.
7. Almgren, M., Edwards, K., Karlsson, G., 2000. Cryo transmission electron microscopy of liposomes and related structures. *Colloids and Surfaces A: Physicochemical and Engineering Aspects* 174, 3-21.

8. Anderson, M., Omri, A., 2004. The Effect of Different Lipid Components on the In Vitro Stability and Release Kinetics of Liposome Formulations. *Drug Delivery* 11, 33-39.
9. Antonietti, M., Förster, S., 2003. Vesicles and Liposomes: A Self-Assembly Principle Beyond Lipids. *Advanced Materials* 15, 1323-1333.
10. AR, F., Hennessey Pa Fau - Formica, M.A., Formica Ma Fau - Cox, C., Cox C Fau - Walsh, E.E., EE, W., 2005a. - Respiratory syncytial virus infection in elderly and high-risk adults. *N Engl J Med* 352, 1749-1759.
11. AR, F., Hennessey Pa Fau - Formica, M.A., Formica Ma Fau - Cox, C., Cox C Fau - Walsh, E.E., EE, W., 2005b. Respiratory syncytial virus infection in elderly and high-risk adults. *The new England journal of medicine* 352, 1749-1759.
12. Arvizo, R.R., Miranda, O.R., Moyano, D.F., Walden, C.A., Giri, K., Bhattacharya, R., Robertson, J.D., Rotello, V.M., Reid, J.M., Mukherjee, P., 2011. Modulating pharmacokinetics, tumor uptake and biodistribution by engineered nanoparticles. *PLoS ONE* 6, e24374.
13. Atyabi, F., Farkhondehfai, A., Esmaili, F., Dinarvand, R., 2009. Preparation of pegylated nano-liposomal formulation containing SN-38: in vitro characterization and in vivo biodistribution in mice. *Acta pharmaceutica* 59, 133-144.
14. AvantiPolar, 2014. Cholesterol.
15. Baer, A., Kehn-Hall, K., 2014. Viral concentration determination through plaque assays: using traditional and novel overlay systems. *Journal of visualized experiments*, e52065.

16. Bakker-Woudenberg, I.A.J.M., Schiffelers, R.M., Storm, G., Becker, M.J., Guo, L., 2005. Long-Circulating Sterically Stabilized Liposomes in the Treatment of Infections, in: Nejat, D. (Ed.), *Methods in Enzymology*. Academic Press, pp. 228-260.
17. Bally, F., Garg, D.K., Serra, C.A., Hoarau, Y., Anton, N., Brochon, C., Parida, D., Vandamme, T., Hadziioannou, G., 2012. Improved size-tunable preparation of polymeric nanoparticles by microfluidic nanoprecipitation. *Polymer* 53, 5045-5051.
18. Balmayor, E.R., Azevedo, H.S., Reis, R.L., 2011. Controlled delivery systems: from pharmaceuticals to cells and genes. *Pharmaceutical research* 28, 1241-1258.
19. Bangham, A.D., Standish, M.M., Watkins, J.C., 1965. Diffusion of univalent ions across the lamellae of swollen phospholipids. *Journal of Molecular Biology* 13, 238-IN227.
20. Batzri, S., Korn, E.D., 1973. Single bilayer liposomes prepared without sonication. *Biochimica et Biophysica Acta (BBA) - Biomembranes* 298, 1015-1019.
21. Bawage, S.S., Tiwari, P.M., Pillai, S., Dennis, V., Singh, S.R., 2013. Recent advances in diagnosis, prevention, and treatment of human respiratory syncytial virus. *Advances in virology* 2013.
22. Bayindir, Z.S., Yuksel, N., 2010. Characterization of niosomes prepared with various nonionic surfactants for paclitaxel oral delivery. *Journal of pharmaceutical sciences* 99, 2049-2060.
23. Belliveau, N.M., Huft, J., Lin, P.J., Chen, S., Leung, A.K., Leaver, T.J., Wild, A.W., Lee, J.B., Taylor, R.J., Tam, Y.K., 2012. Microfluidic synthesis of highly potent limit-size lipid nanoparticles for in vivo delivery of siRNA. *Molecular Therapy—Nucleic Acids* 1, e37.

24. Bernsdorff, C., Wolf, A., Winter, R., Gratton, E., 1997. Effect of hydrostatic pressure on water penetration and rotational dynamics in phospholipid-cholesterol bilayers. *Biophysical journal* 72, 1264.
25. Bhalerao, S., Raje Harshal, A., 2003. Preparation, optimization, characterization, and stability studies of salicylic acid liposomes. *Drug development and industrial pharmacy* 29, 451-467.
26. Bhandary, S., Basu, R., Das, S., Nandy, P., 2010. Comparison of the effect of anti-hyperlipidemic drugs from different groups on the phase profile of liposomal membrane—a fluorescence anisotropy study. *Phase Transitions* 83, 518-525.
27. Bhardwaj, U., Burgess, D.J., 2010. A novel USP apparatus 4 based release testing method for dispersed systems. *International journal of pharmaceutics* 388, 287-294.
28. Bibi, S., Kaur, R., Henriksen-Lacey, M., McNeil, S.E., Wilkhu, J., Lattmann, E., Christensen, D., Mohammed, A.R., Perrie, Y., 2011. Microscopy imaging of liposomes: from coverslips to environmental SEM. *International journal of pharmaceutics* 417, 138-150.
29. Blok, M., Van der Neut-Kok, E., Van Deenen, L., De Gier, J., 1975. The effect of chain length and lipid phase transitions on the selective permeability properties of liposomes. *Biochimica et Biophysica Acta (BBA)-Biomembranes* 406, 187-196.
30. Borchers, A.T., Chang, C., Gershwin, M.E., Gershwin, L.J., 2013. Respiratory syncytial virus—a comprehensive review. *Clinical reviews in allergy & immunology* 45, 331-379.
31. Bozzuto, G., Molinari, A., 2015. Liposomes as nanomedical devices. *International journal of nanomedicine* 10, 975.

32. Bramwell, V.W., Perrie, Y., 2005. Particulate delivery systems for vaccines. *Critical Reviews™ in Therapeutic Drug Carrier Systems* 22.
33. Briuglia, M.-L., Rotella, C., McFarlane, A., Lamprou, D.A., 2015. Influence of cholesterol on liposome stability and on in vitro drug release. *Drug delivery and translational research* 5, 231-242.
34. Brooksbank, D.V., Leaver, J., Horne, D.S., 1993. Adsorption of milk proteins to phosphatidylglycerol and phosphatidylcholine liposomes. *Journal of colloid and interface science* 161, 38-42.
35. Burgess, D.J., Crommelin, D.J.A., Hussain, A.S., Chen, M.-L., 2004. Assuring quality and performance of sustained and controlled release parenterals: EUFEPS workshop report. *AAPS PharmSci* 6, 100-111.
36. Çağdaş, M., Sezer, A.D., Bucak, S., 2014. Liposomes as Potential Drug Carrier Systems for Drug Delivery.
37. CDC, 2014. Respiratory Syncytial Virus Infection (RSV). Center for disease control and prevention (CDC), Center for disease control and prevention (CDC).
38. Chen, P.C., Mwakwari, S.C., Oyelere, A.K., 2008. Gold nanoparticles: from nanomedicine to nanosensing. *Nanotechnology Science and Applications* 1, 45-66.
39. Chithrani, B.D., Ghazani, A.A., Chan, W.C., 2006a. Determining the size and shape dependence of gold nanoparticle uptake into mammalian cells. *Nano letters* 6, 662-668.
40. Chithrani, B.D., Ghazani, A.A., Chan, W.C.W., 2006b. Determining the Size and Shape Dependence of Gold Nanoparticle Uptake into Mammalian Cells. *Nano Letters* 6, 662-668.

41. Chonn, A., Cullis, P.R., 1995. Recent advances in liposomal drug-delivery systems. *Current opinion in Biotechnology* 6, 698-708.
42. Chorachoo, J., Amnuaikit, T., Voravuthikunchai, S.P., 2013. Liposomal encapsulated rhodomirtone: a novel antiacne drug. *Evidence-based complementary and alternative medicine : eCAM* 2013, 157635.
43. Collier, R., 2012. Reducing the "pill burden". *Canadian Medical Association Journal* 184, E117-E118.
44. Connor, J., Huang, L., 1986. pH-sensitive immunoliposomes as an efficient and target-specific carrier for antitumor drugs. *Cancer research* 46, 3431-3435.
45. Cornier, J., Owen, A., Kwade, A., Van de Voorde, M., 2016. *Pharmaceutical Nanotechnology: Innovation and Production*, 2 Volumes. John Wiley & Sons.
46. Cosco, D., Paolino, D., Cilurzo, F., Casale, F., Fresta, M., 2012. Gemcitabine and tamoxifen-loaded liposomes as multidrug carriers for the treatment of breast cancer diseases. *Int J Pharm* 422, 229-237.
47. Costa, P., Lobo, J.M.S., 2001. Modeling and comparison of dissolution profiles. *European journal of pharmaceutical sciences* 13, 123-133.
48. Cullis, P., Mayer, L., Bally, M., Madden, T., Hope, M., 1989. Generating and loading of liposomal systems for drug-delivery applications. *Advanced drug delivery reviews* 3, 267-282.
49. Daneshpour, N., Griffin, M., Collighan, R., Perrie, Y., 2011. Targeted delivery of a novel group of site-directed transglutaminase inhibitors to the liver using liposomes: a new

- approach for the potential treatment of liver fibrosis. *Journal of drug targeting* 19, 624-631.
50. Dash, S., Murthy, P.N., Nath, L., Chowdhury, P., 2010. Kinetic modeling on drug release from controlled drug delivery systems. *Acta Pol Pharm* 67, 217-223.
 51. De Villiers, M.M., Aramwit, P., Kwon, G.S., 2008. *Nanotechnology in drug delivery*. Springer Science & Business Media.
 52. Deniz, A., Sade, A., Severcan, F., Keskin, D., Tezcaner, A., Banerjee, S., 2010. Celecoxib-loaded liposomes: effect of cholesterol on encapsulation and in vitro release characteristics. *Bioscience reports* 30, 365-373.
 53. Deol, P., Khuller, G., 1997. Lung specific stealth liposomes: stability, biodistribution and toxicity of liposomal antitubercular drugs in mice. *Biochimica et Biophysica Acta (BBA)-General Subjects* 1334, 161-172.
 54. Desai, M.P., Labhsetwar, V., Walter, E., Levy, R.J., Amidon, G.L., 1997. The mechanism of uptake of biodegradable microparticles in Caco-2 cells is size dependent. *Pharmaceutical research* 14, 1568-1573.
 55. Diljyot, K., 2012. Niosomes: A new approach to targeted drug delivery. *International Journal of Pharmaceutical and Phytopharmacological Research* 2, 53-59.
 56. Diseases, C.o.I., 2014. Updated guidance for palivizumab prophylaxis among infants and young children at increased risk of hospitalization for respiratory syncytial virus infection. *Pediatrics* 134, e620-e638.
 57. Dokken, B.B., 2008. The pathophysiology of cardiovascular disease and diabetes: beyond blood pressure and lipids. *Diabetes Spectrum* 21, 160-165.

58. Dong, Y., Ng, W.K., Shen, S., Kim, S., Tan, R.B., 2012. Solid lipid nanoparticles: continuous and potential large-scale nanoprecipitation production in static mixers. *Colloids and Surfaces B: Biointerfaces* 94, 68-72.
59. Douroumis, D., Fahr, A., 2012. Drug delivery strategies for poorly water-soluble drugs. John Wiley & Sons.
60. Dua, J., Rana, A., Bhandari, A., 2012. Liposome: methods of preparation and applications. *International Journal of Pharmaceutical Studies and Research* 3, 14-20.
61. Ebrahim, S., Taylor, F.C., Brindle, P., 2014. Statins for the primary prevention of cardiovascular disease. *Bmj* 348, g280.
62. Effenhauser, C.S., Bruin, G.J., Paulus, A., 1997a. Integrated chip-based capillary electrophoresis. *Electrophoresis* 18, 2203-2213.
63. Effenhauser, C.S., Bruin, G.J., Paulus, A., Ehrat, M., 1997b. Integrated capillary electrophoresis on flexible silicone microdevices: analysis of DNA restriction fragments and detection of single DNA molecules on microchips. *Analytical Chemistry* 69, 3451-3457.
64. Eloy, J.O., de Souza, M.C., Petrilli, R., Barcellos, J.P.A., Lee, R.J., Marchetti, J.M., 2014. Liposomes as carriers of hydrophilic small molecule drugs: strategies to enhance encapsulation and delivery. *Colloids and Surfaces B: Biointerfaces* 123, 345-363.
65. Erbacher, C., Bessoth, F.G., Busch, M., Verpoorte, E., Manz, A., 1999. Towards integrated continuous-flow chemical reactors. *Microchimica Acta* 131, 19-24.

66. Eroglu, E., Tiwari, P.M., Waffo, A.B., Miller, M.E., Vig, K., Dennis, V.A., Singh, S.R., 2013. A nonviral pHEMA+ chitosan nanosphere-mediated high-efficiency gene delivery system. *International Journal of Nanomedicine* 8, 1403-1415.
67. Essa, E., 2010a. Effect of formulation and processing variables on the particle size of sorbitan monopalmitate niosomes. *Asian Journal of Pharmaceutics* 4, 227.
68. Essa, E.A., 2010b. Effect of formulation and processing variables on the particle size of sorbitan monopalmitate niosomes. *Asian Journal of Pharmaceutics* 4, 227.
69. Fahy, E., Subramaniam, S., Brown, H.A., Glass, C.K., Merrill, A.H., Murphy, R.C., Raetz, C.R., Russell, D.W., Seyama, Y., Shaw, W., 2005. A comprehensive classification system for lipids. *Journal of lipid research* 46, 839-862.
70. Fallon, A., Booth, R., Bell, L., 1987. *Applications of HPLC in Biochemistry*. Elsevier.
71. Fang, J.-Y., Hong, C.-T., Chiu, W.-T., Wang, Y.-Y., 2001. Effect of liposomes and niosomes on skin permeation of enoxacin. *International journal of pharmaceutics* 219, 61-72.
72. FDA, R.G., 1994. *Validation of chromatographic methods*. Center for Drug Evaluation Research (CDER), Washington, USA.
73. Felgner, J.H., Kumar, R., Sridhar, C., Wheeler, C.J., Tsai, Y.J., Border, R., Ramsey, P., Martin, M., Felgner, P.L., 1994. Enhanced gene delivery and mechanism studies with a novel series of cationic lipid formulations. *Journal of Biological Chemistry* 269, 2550-2561.
74. Fotaki, N., 2011. Flow-Through cell apparatus (usp apparatus 4): operation and features. *Dissolution Technol* 18, 46-49.

75. Gallová, J., Uhríková, D., Islamov, A., Kuklin, A., Balgavy, P., 2004. Effect of cholesterol on the bilayer thickness in unilamellar extruded DLPC and DOPC liposomes: SANS contrast variation study. *General physiology and biophysics* 23, 113-128.
76. Giddings, J.C., 1991. *Unified separation science*. Wiley New York etc.
77. Gobby, D., Angeli, P., Gavriilidis, A., 2001. Mixing characteristics of T-type microfluidic mixers. *Journal of Micromechanics and microengineering* 11, 126.
78. Gohel, M.C., Panchal, M.K., Jogani, V.V., 2000. Novel mathematical method for quantitative expression of deviation from the Higuchi model. *Aaps Pharmscitech* 1, 43-48.
79. Gregoriadis, G., 1993. *Interactions of liposomes with the biological milieu*. CRC Press.
80. Gregoriadis, G., 1995. Engineering liposomes for drug delivery: progress and problems. *Trends in biotechnology* 13, 527-537.
81. Gregoriadis, G., Davis, C., 1979. Stability of liposomes *invivo* and *invitro* is promoted by their cholesterol content and the presence of blood cells. *Biochemical and Biophysical Research Communications* 89, 1287-1293.
82. Gregoriadis, G., Leathwood, P., Ryman, B.E., 1971. Enzyme entrapment in liposomes. *FEBS letters* 14, 95-99.
83. Gregoriadis, G., Ryman, B.E., 1972a. Fate of Protein-Containing Liposomes Injected into Rats. *European Journal of Biochemistry* 24, 485-491.
84. Gregoriadis, G., Ryman, B.E., 1972b. Lysosomal localization of β -fructofuranosidase-containing liposomes injected into rats. Some implications in the treatment of genetic disorders. *Biochemical Journal* 129, 123-133.

85. Gregoriadis, G., Saffie, R., Hart, S.L., 1996. High yield incorporation of plasmid DNA within liposomes: Effect on DNA integrity and transfection efficiency. *Journal of drug targeting* 3, 469-475.
86. Gregoriadis, G., Senior, J., Wolff, B., Kirby, C., 1984. Fate of Liposomes In Vivo: Control Leading to Targeting, in: Gregoriadis, G., Poste, G., Senior, J., Trouet, A. (Eds.), *Receptor-Mediated Targeting of Drugs*. Springer US, pp. 243-266.
87. Hąc-Wydro, K., Wydro, P., Jagoda, A., Kapusta, J., 2007. The study on the interaction between phytosterols and phospholipids in model membranes. *Chemistry and physics of lipids* 150, 22-34.
88. Hadjidemetriou, M., Al-Ahmady, Z., Kostarelos, K., 2016. Time-evolution of in vivo protein corona onto blood-circulating PEGylated liposomal doxorubicin (DOXIL) nanoparticles. *Nanoscale* 8, 6948-6957.
89. Hadjidemetriou, M., Al-Ahmady, Z., Mazza, M., Collins, R.F., Dawson, K., Kostarelos, K., 2015. In vivo biomolecule corona around blood-circulating, clinically used and antibody-targeted lipid bilayer nanoscale vesicles. *ACS nano* 9, 8142-8156.
90. Han, H.-K., Shin, H.-J., Ha, D.H., 2012. Improved oral bioavailability of alendronate via the mucoadhesive liposomal delivery system. *European journal of pharmaceutical sciences* 46, 500-507.
91. Harrison, D.J., Manz, A., Fan, Z., Luedi, H., Widmer, H.M., 1992. Capillary electrophoresis and sample injection systems integrated on a planar glass chip. *Analytical chemistry* 64, 1926-1932.

92. Hathout, R.M., Mansour, S., Mortada, N.D., Guinedi, A.S., 2007. Liposomes as an ocular delivery system for acetazolamide: in vitro and in vivo studies. *Aaps Pharmscitech* 8, E1-E12.
93. Haywood, A.M., 1978. Interaction of liposomes with viruses *. *Annals of the New York Academy of Sciences* 308, 275-280.
94. Hendricks, G.L., Velazquez, L., Pham, S., Qaisar, N., Delaney, J.C., Viswanathan, K., Albers, L., Comolli, J.C., Shriver, Z., Knipe, D.M., 2015. Heparin octasaccharide decoy liposomes inhibit replication of multiple viruses. *Antiviral research* 116, 34-44.
95. Hood, R., Vreeland, W., DeVoe, D., 2014. Microfluidic remote loading for rapid single-step liposomal drug preparation. *Lab on a Chip* 14, 3359-3367.
96. Hope, M.J., Nayar, R., Mayer, L.D., Cullis, P.R., 1993. Reduction of liposome size and preparation of unilamellar vesicles by extrusion techniques. *Liposome technology* 1, 123-139.
97. Hung, O., 2006. Drug transformation: Advances in drug delivery systems. *Canadian Journal of Anesthesia/Journal canadien d'anesthésie* 53, 1074-1077.
98. Hunter, D., Frisken, B., 1998. Effect of extrusion pressure and lipid properties on the size and polydispersity of lipid vesicles. *Biophysical journal* 74, 2996-3002.
99. Ihara, H., Shundo, A., Takafuji, M., Nagaoka, S., 2006. Polymer Grafting to Silica Surface for Highly Selective RP-HPLC, *Encyclopedia of Chromatography*, pp. 1-11.
100. Immordino, M.L., Dosio, F., Cattel, L., 2006. Stealth liposomes: review of the basic science, rationale, and clinical applications, existing and potential. *International journal of nanomedicine* 1, 297.

101. ISI Web of Science 2016, s.f.t.M., www.isiknowledge.com, ISI Web of Science, search for topic 'Microfluidics'.
102. Jahn, A., Stavis, S.M., Hong, J.S., Vreeland, W.N., DeVoe, D.L., Gaitan, M., 2010. Microfluidic mixing and the formation of nanoscale lipid vesicles. *Acs Nano* 4, 2077-2087.
103. Jahn, A., Vreeland, W.N., DeVoe, D.L., Locascio, L.E., Gaitan, M., 2007. Microfluidic directed formation of liposomes of controlled size. *Langmuir* 23, 6289-6293.
104. Jahn, A., Vreeland, W.N., Gaitan, M., Locascio, L.E., 2004. Controlled vesicle self-assembly in microfluidic channels with hydrodynamic focusing. *Journal of the American Chemical Society* 126, 2674-2675.
105. Jain, P., Jivani, H., Khatal, R., Surana, S., 2011. Development and validation of RP-HPLC method for estimation of ethacridine lactate in bulk and in pharmaceutical formulation. *Pharmaceutical methods* 2, 112-116.
106. Jamadar, S.A., Mulye, S.P., Karekar, P.S., Pore, Y.V., Burade, K.B., 2011. Development and validation of UV spectrophotometric method for the determination of Gliclazide in tablet dosage form. *Der Pharma Chemica* 3, 338-343.
107. Jeong, B., Bae, Y.H., Kim, S.W., 2000. Drug release from biodegradable injectable thermosensitive hydrogel of PEG-PLGA-PEG triblock copolymers. *Journal of controlled release* 63, 155-163.
108. Joshi, H., Shirude, P.S., Bansal, V., Ganesh, K., Sastry, M., 2004. Isothermal titration calorimetry studies on the binding of amino acids to gold nanoparticles. *The Journal of Physical Chemistry B* 108, 11535-11540.

109. JS, T., J, S., 2010. Respiratory viral infections in infants: causes, clinical symptoms, virology, and immunology. *Clinical Microbiology Reviews* 23, 74-98.
110. Kalepu, S., Nekkanti, V., 2015. Insoluble drug delivery strategies: review of recent advances and business prospects. *Acta Pharmaceutica Sinica B* 5, 442-453.
111. Kamphuis, T., Meijerhof, T., Stegmann, T., Lederhofer, J., Wilschut, J., de Haan, A., 2012. Immunogenicity and Protective Capacity of a Virosomal Respiratory Syncytial Virus Vaccine Adjuvanted with Monophosphoryl Lipid A in Mice. *PLOS ONE* 7, e36812.
112. Kar, M., Choudhury, P.K., 2009. HPLC Method for Estimation of Metformin Hydrochloride in Formulated Microspheres and Tablet Dosage Form. *Indian Journal of Pharmaceutical Sciences* 71, 318-320.
113. Karim, K.M., Mandal, A.S., Biswas, N., Guha, A., Chatterjee, S., Behera, M., Kuotsu, K., 2010. Niosome: a future of targeted drug delivery systems. *Journal of advanced pharmaceutical technology & research* 1, 374.
114. Kastner, E., Kaur, R., Lowry, D., Moghaddam, B., Wilkinson, A., Perrie, Y., 2014. High-throughput manufacturing of size-tuned liposomes by a new microfluidics method using enhanced statistical tools for characterization. *International Journal of Pharmaceutics* 477, 361-368.
115. Kastner, E., Verma, V., Lowry, D., Perrie, Y., 2015. Microfluidic-controlled manufacture of liposomes for the solubilisation of a poorly water soluble drug. *International Journal of Pharmaceutics* 485, 122-130.

116. Kazi, K.M., Mandal, A.S., Biswas, N., Guha, A., Chatterjee, S., Behera, M., Kuotsu, K., 2010. Niosome: A future of targeted drug delivery systems. *Journal of advanced pharmaceutical technology & research* 1, 374-380.
117. Kępczyński, M., Nawalany, K., Kumorek, M., Kobierska, A., Jachimska, B., Nowakowska, M., 2008. Which physical and structural factors of liposome carriers control their drug-loading efficiency? *Chemistry and physics of lipids* 155, 7-15.
118. Kirby, C., Clarke, J., Gregoriadis, G., 1980. Effect of the cholesterol content of small unilamellar liposomes on their stability in vivo and in vitro. *Biochemical Journal* 186, 591-598.
119. Kirby, D.J., Rosenkrands, I., Agger, E.M., Andersen, P., Coombes, A.G., Perrie, Y., 2008. Liposomes act as stronger sub-unit vaccine adjuvants when compared to microspheres. *Journal of drug targeting* 16, 543-554.
120. Kolusheva, S., Wachtel, E., Jelinek, R., 2003. Biomimetic lipid/polymer colorimetric membranes molecular and cooperative properties. *Journal of lipid research* 44, 65-71.
121. Kozak, D., Broom, M., Vogel, R., 2015. Accurate Size, Charge & Concentration Analysis of Liposomes using Tunable Resistive Pulse Sensing.
122. Lai, E.P., Feng, S.Y., 2006. Solid phase extraction—Non-aqueous capillary electrophoresis for determination of metformin, phenformin and glyburide in human plasma. *Journal of chromatography B* 843, 94-99.
123. Landfester, K., Ostafin, A., 2008. *Nanoreactor engineering for life sciences and medicine*. Artech House.

124. Landry, M.L., Stanat, S., Biron, K., Brambilla, D., Britt, W., Jokela, J., Chou, S., Drew, W.L., Erice, A., Gilliam, B., 2000. A standardized plaque reduction assay for determination of drug susceptibilities of cytomegalovirus clinical isolates. *Antimicrobial agents and chemotherapy* 44, 688-692.
125. Laouini, A., Jaafar-Maalej, C., Limayem-Blouza, I., Sfar, S., Charcosset, C., Fessi, H., 2012. Preparation, characterization and applications of liposomes: state of the art. *Journal of colloid Science and Biotechnology* 1, 147-168.
126. Lasic, D.D., 1993. *Liposomes: from physics to applications*. Elsevier Science Ltd.
127. Lasic, D.D., 1998. Novel applications of liposomes. *Trends in biotechnology* 16, 307-321.
128. Lasic, D.D., Barenholz, Y., 1996. *Handbook of nonmedical applications of liposomes: Theory and basic sciences*. CRC Press.
129. Lawrence, X.Y., 2008. Pharmaceutical quality by design: product and process development, understanding, and control. *Pharmaceutical research* 25, 781-791.
130. Lebovitz, H.E., 1985. Glipizide: A Second-generation Sulfonylurea Hypoglycemic Agent; Pharmacology, Pharmacokinetics and Clinical Use. *Pharmacotherapy: The Journal of Human Pharmacology and Drug Therapy* 5, 63-77.
131. Lee, J.N., Park, C., Whitesides, G.M., 2003. Solvent compatibility of poly (dimethylsiloxane)-based microfluidic devices. *Analytical chemistry* 75, 6544-6554.
132. Lee, R.J., 2006. Liposomal delivery as a mechanism to enhance synergism between anticancer drugs. *Molecular cancer therapeutics* 5, 1639-1640.
133. Lipowsky, R., Sackmann, E., 1995. *Structure and dynamics of membranes: I. from cells to vesicles/II. generic and specific interactions*. Elsevier.

134. Liu, Y., Fang, J., Kim, Y.-J., Wong, M.K., Wang, P., 2014. Codelivery of doxorubicin and paclitaxel by cross-linked multilamellar liposome enables synergistic antitumor activity. *Molecular pharmaceutics* 11, 1651-1661.
135. Lo, C.T., Jahn, A., Locascio, L.E., Vreeland, W.N., 2010. Controlled self-assembly of monodisperse niosomes by microfluidic hydrodynamic focusing. *Langmuir* 26, 8559-8566.
136. Luchsinger, V., Ampuero, S., Palomino, M.A., Chnaiderman, J., Levican, J., Gaggero, A., Larrañaga, C.E., 2014. Comparison of virological profiles of respiratory syncytial virus and rhinovirus in acute lower tract respiratory infections in very young Chilean infants, according to their clinical outcome. *Journal of Clinical Virology* 61, 138-144.
137. Mabrey, S., Sturtevant, J.M., 1976. Investigation of phase transitions of lipids and lipid mixtures by sensitivity differential scanning calorimetry. *Proceedings of the National Academy of Sciences* 73, 3862-3866.
138. Magarkar, A., Dhawan, V., Kallinteri, P., Viitala, T., Elmowafy, M., Róg, T., Bunker, A., 2014. Cholesterol level affects surface charge of lipid membranes in saline solution. *Scientific reports* 4.
139. Manojlovic, V., Winkler, K., Bunjes, V., Neub, A., Schubert, R., Bugarski, B., Lenewit, G., 2008. Membrane interactions of ternary phospholipid/cholesterol bilayers and encapsulation efficiencies of a RIP II protein. *Colloids and Surfaces B: Biointerfaces* 64, 284-296.
140. Mansoori, M., Agrawal, S., Jawade, S., Khan, M., 2012. A review on liposome. *International Journal Advance Research in Pharmaceutical and Bio Science* 2, 453-464.

141. Marianecci, C., Di Marzio, L., Rinaldi, F., Celia, C., Paolino, D., Alhaique, F., Esposito, S., Carafa, M., 2014. Niosomes from 80s to present: the state of the art. *Advances in colloid and interface science* 205, 187-206.
142. Marques, M.R., Loebenberg, R., Almukainzi, M., 2011. Simulated biological fluids with possible application in dissolution testing. *Dissolution Technol* 18, 15-28.
143. Melzak, K.A., Melzak, S.A., Gizeli, E., Toca-Herrera, J.L., 2012. Cholesterol organization in phosphatidylcholine liposomes: a surface plasmon resonance study. *Materials* 5, 2306-2325.
144. Mentel, R., Wegner, U., Bruns, R., Gürtler, L., 2003. Real-time PCR to improve the diagnosis of respiratory syncytial virus infection. *Journal of medical microbiology* 52, 893-896.
145. Mitra, A., Lee, C.H., Cheng, K., 2013. *Advanced drug delivery*. John Wiley & Sons.
146. Mizuguchi, C., Ogata, F., Mikawa, S., Tsuji, K., Baba, T., Shigenaga, A., Shimanouchi, T., Okuhira, K., Otaka, A., Saito, H., 2015. Amyloidogenic Mutation Promotes Fibril Formation of the N-terminal Apolipoprotein AI on Lipid Membranes. *Journal of Biological Chemistry* 290, 20947-20959.
147. Mody, V.V., Siwale, R., Singh, A., Mody, H.R., 2010. Introduction to metallic nanoparticles. *Journal of Pharmacy and Bioallied Sciences* 2, 282.
148. Moghaddam, B., Ali, M.H., Wilkhu, J., Kirby, D.J., Mohammed, A.R., Zheng, Q., Perrie, Y., 2011. The application of monolayer studies in the understanding of liposomal formulations. *International journal of pharmaceutics* 417, 235-244.

149. Mohammed, A., Weston, N., Coombes, A., Fitzgerald, M., Perrie, Y., 2004. Liposome formulation of poorly water soluble drugs: optimisation of drug loading and ESEM analysis of stability. *International journal of pharmaceutics* 285, 23-34.
150. Monteiro, N., Martins, A., Reis, R.L., Neves, N.M., 2014. Liposomes in tissue engineering and regenerative medicine. *Journal of the Royal Society Interface* 11, 20140459.
151. Muppidi, K., Pumerantz, A.S., Wang, J., Betageri, G., 2012. Development and stability studies of novel liposomal vancomycin formulations. *ISRN pharmaceutics* 2012.
152. Nagaraja, N.V., Paliwal, J.K., Gupta, R.C., 1999. Choosing the calibration model in assay validation. *Journal of Pharmaceutical and Biomedical Analysis* 20, 433-438.
153. Nahar, K., Absar, S., Gupta, N., Kotamraju, V.R., McMurtry, I.F., Oka, M., Komatsu, M., Nozik-Grayck, E., Ahsan, F., 2014. Peptide-coated liposomal fasudil enhances site specific vasodilation in pulmonary arterial hypertension. *Molecular pharmaceutics* 11, 4374-4384.
154. Nge, P.N., Rogers, C.I., Woolley, A.T., 2013. Advances in microfluidic materials, functions, integration, and applications. *Chemical reviews* 113, 2550-2583.
155. Nomura, S.-i.M., Mizutani, Y., Kurita, K., Watanabe, A., Akiyoshi, K., 2005. Changes in the morphology of cell-size liposomes in the presence of cholesterol: Formation of neuron-like tubes and liposome networks. *Biochimica et Biophysica Acta (BBA) - Biomembranes* 1669, 164-169.
156. Nounou, M.M., El-Khordagui, L.K., Khalafallah, N.A., Khalil, S.A., 2006. In vitro release of hydrophilic and hydrophobic drugs from liposomal dispersions and gels. *ACTA PHARMACEUTICA-ZAGREB* 56, 311.

157. Numata, M., Chu, H.W., Dakhama, A., Voelker, D.R., 2010. Pulmonary surfactant phosphatidylglycerol inhibits respiratory syncytial virus-induced inflammation and infection. *Proceedings of the National Academy of Sciences* 107, 320-325.
158. Numata, M., Kandasamy, P., Nagashima, Y., Fickes, R., Murphy, R.C., Voelker, D.R., 2015. Phosphatidylinositol inhibits respiratory syncytial virus infection. *Journal of lipid research* 56, 578-587.
159. O'Brien, M., Wigler, N., Inbar, M., Rosso, R., Grischke, E., Santoro, A., Catane, R., Kieback, D., Tomczak, P., Ackland, S., 2004. Reduced cardiotoxicity and comparable efficacy in a phase III trial of pegylated liposomal doxorubicin HCl (CAELYX™/Doxil®) versus conventional doxorubicin for first-line treatment of metastatic breast cancer. *Annals of oncology* 15, 440-449.
160. Ong, S.G.M., Ming, L.C., Lee, K.S., Yuen, K.H., 2016. Influence of the encapsulation efficiency and size of liposome on the oral bioavailability of griseofulvin-loaded liposomes. *Pharmaceutics* 8, 25.
161. Patil, Y.P., Jadhav, S., 2014. Novel methods for liposome preparation. *Chemistry and physics of lipids* 177, 8-18.
162. Paul, H., Katherine, H., Suzanne, S., 2013. Molecular weight cut-off (MWCO) specifications and rates of buffer exchange with Slide-A-Lyzer Dialysis Devices and Snakeskin Dialysis Tubing. Thermo Fisher Scientific.
163. Perrie, Y., Kastner, E., Kaur, R., Wilkinson, A., Ingham, A.J., 2013. A case-study investigating the physicochemical characteristics that dictate the function of a liposomal adjuvant. *Human vaccines & immunotherapeutics* 9, 1374-1381.

164. Perrie, Y., Mohammed, A.R., Kirby, D.J., McNeil, S.E., Bramwell, V.W., 2008. Vaccine adjuvant systems: enhancing the efficacy of sub-unit protein antigens. *International journal of pharmaceutics* 364, 272-280.
165. Perrie, Y., Rades, T., 2012a. *FASTtrack Pharmaceuticals: Drug Delivery and Targeting*. Pharmaceutical press.
166. Perrie, Y., Rades, T., 2012b. *Pharmaceutics: drug delivery and targeting*. Pharmaceutical Press.
167. Pharmacopoeia, J., 2002. *United States' Pharmacopeia*.
168. Piedimonte, G., Perez, M.K., 2014. Respiratory Syncytial Virus Infection and Bronchiolitis. *Pediatrics in Review* 35, 519-530.
169. Pons, M., Foradada, M., Estelrich, J., 1993. Liposomes obtained by the ethanol injection method. *International journal of pharmaceutics* 95, 51-56.
170. Pradhan, P., Guan, J., Lu, D., Wang, P.G., Lee, L.J., Lee, R.J., 2008. A facile microfluidic method for production of liposomes. *Anticancer research* 28, 943-947.
171. Prendergast, B., 1983. Glyburide and glipizide, second-generation oral sulfonylurea hypoglycemic agents. *Clinical pharmacy* 3, 473-485.
172. Price, M., Cornelius, R., Brash, J., 2001. Protein adsorption to polyethylene glycol modified liposomes from fibrinogen solution and from plasma. *Biochimica et Biophysica Acta (BBA)-Biomembranes* 1512, 191-205.
173. Quevedo, E., Steinbacher, J., McQuade, D.T., 2005. Interfacial polymerization within a simplified microfluidic device: capturing capsules. *Journal of the American Chemical Society* 127, 10498-10499.

174. Rahman, A., White, G., More, N., Schein, P.S., 1985. Pharmacological, toxicological, and therapeutic evaluation in mice of doxorubicin entrapped in cardiolipin liposomes. *Cancer research* 45, 796-803.
175. Ramteke, K., Dighe, P., Kharat, A., Patil, S., 2014. Mathematical models of drug dissolution: a review. *Sch. Acad. J. Pharm* 3.
176. Rappuoli, R., Mandl, C.W., Black, S., De Gregorio, E., 2011. Vaccines for the twenty-first century society. *Nat Rev Immunol* 11, 865-872.
177. Redmond, J., 2013. title., Oregon State University.
178. Repka, M.A., Battu, S.K., Upadhye, S.B., Thumma, S., Crowley, M.M., Zhang, F., Martin, C., McGinity, J.W., 2007. Pharmaceutical applications of hot-melt extrusion: Part II. Drug development and industrial pharmacy 33, 1043-1057.
179. Repka, M.A., Repka, S.L., McGinity, J.W., 2002. Bioadhesive hot-melt extruded film for topical and mucosal adhesion applications and drug delivery and process for preparation thereof. Google Patents.
180. Riahi, R., Tamayol, A., Shaegh, S.A.M., Ghaemmaghami, A.M., Dokmeci, M.R., Khademhosseini, A., 2015. Microfluidics for advanced drug delivery systems. *Current Opinion in Chemical Engineering* 7, 101-112.
181. Ricci, M., Sassi, P., Nastruzzi, C., Rossi, C., 2000. Liposome-based formulations for the antibiotic nonapeptide Leucinostatin A: Fourier transform infrared spectroscopy characterization and in vivo toxicologic study. *AAPS PharmSciTech* 1, 9-19.
182. Richardson, E.S., Pitt, W.G., Woodbury, D.J., 2007. The role of cavitation in liposome formation. *Biophysical journal* 93, 4100-4107.

183. Richter, F., Finegold, L., Rapp, G., 1999. Sterols sense swelling in lipid bilayers. *Physical Review E* 59, 3483.
184. Ristori, S., Oberdisse, J., Grillo, I., Donati, A., Spalla, O., 2005. Structural characterization of cationic liposomes loaded with sugar-based carboranes. *Biophysical journal* 88, 535-547.
185. Rogers, T.L., Gillespie, I.B., Hitt, J.E., Fransen, K.L., Crowl, C.A., Tucker, C.J., Kupperblatt, G.B., Becker, J.N., Wilson, D.L., Todd, C., 2004. Development and characterization of a scalable controlled precipitation process to enhance the dissolution of poorly water-soluble drugs. *Pharmaceutical research* 21, 2048-2057.
186. Rozet, E., Ceccato, A., Hubert, C., Ziemons, E., Oprean, R., Rudaz, S., Boulanger, B., Hubert, P., 2007. Analysis of recent pharmaceutical regulatory documents on analytical method validation. *Journal of Chromatography A* 1158, 111-125.
187. Sabin, J., Prieto, G., Ruso, J., Hidalgo-Alvarez, R., Sarmiento, F., 2006. Size and stability of liposomes: a possible role of hydration and osmotic forces. *The European Physical Journal E* 20, 401-408.
188. Sackmann, E., 1995. Physical basis of self-organization and function of membranes: physics of vesicles. *Handbook of Biological Physics* 1, 213-304.
189. Savva, M., Torchilin, V.P., Huang, L., 1999. Effect of Polyvinyl Pyrrolidone on the Thermal Phase Transition of 1,2 Dipalmitoyl-sn-glycero-3-phosphocholine Bilayer. *Journal of Colloid and Interface Science* 217, 160-165.
190. Sawant, R.R., Torchilin, V.P., 2012. Challenges in development of targeted liposomal therapeutics. *The AAPS Journal* 14, 303-315.

191. Schellinger, A.P., Carr, P.W., 2006. Isocratic and gradient elution chromatography: a comparison in terms of speed, retention reproducibility and quantitation. *Journal of Chromatography A* 1109, 253-266.
192. Schwendener, R.A., 2014. Liposomes as vaccine delivery systems: a review of the recent advances. *Therapeutic advances in vaccines* 2, 159-182.
193. Schwendener, R.A., Ludewig, B., Cerny, A., Engler, O., 2010. Liposome-based vaccines. *Liposomes: Methods and Protocols, Volume 1: Pharmaceutical Nanocarriers*, 163-175.
194. Seleci, D.A., Seleci, M., Walter, J.-G., Stahl, F., Scheper, T., 2016. Niosomes as Nanoparticulate Drug Carriers: Fundamentals and Recent Applications.
195. Setter, S.M., Iltz, J.L., Thams, J., Campbell, R.K., 2003. Metformin hydrochloride in the treatment of type 2 diabetes mellitus: a clinical review with a focus on dual therapy. *Clinical therapeutics* 25, 2991-3026.
196. Shabbits, J.A., Chiu, G.N., Mayer, L.D., 2002. Development of an in vitro drug release assay that accurately predicts in vivo drug retention for liposome-based delivery systems. *Journal of Controlled Release* 84, 161-170.
197. Sharma, A., Sharma, U.S., 1997. Liposomes in drug delivery: progress and limitations. *International Journal of Pharmaceutics* 154, 123-140.
198. Shuto, S., Obara, T., Toriya, M., Hosoya, M., Snoeck, R., Andrei, G., Balzarini, J., De Clercq, E., 1992. New neplanocin analogs. 1. Synthesis of 6'-modified neplanocin A derivatives as broad-spectrum antiviral agents. *Journal of medicinal chemistry* 35, 324-331.

199. Siegel, R.A., Rathbone, M.J., 2012. Overview of controlled release mechanisms, *Fundamentals and Applications of Controlled Release Drug Delivery*. Springer, pp. 19-43.
200. Siepmann, J., Peppas, N.A., 2011. Higuchi equation: derivation, applications, use and misuse. *International journal of pharmaceutics* 418, 6-12.
201. Siewert, M., Dressman, J., Brown, C.K., Shah, V.P., Aiache, J.-M., Aoyagi, N., Bashaw, D., Brown, C., Brown, W., Burgess, D., 2003. FIP/AAPS guidelines to dissolution/in vitro release testing of novel/special dosage forms. *AAPS PharmSciTech* 4, 43-52.
202. Simões, E.A., DeVincenzo, J.P., Boeckh, M., Bont, L., Crowe, J.E., Griffiths, P., Hayden, F.G., Hodinka, R.L., Smyth, R.L., Spencer, K., 2015. Challenges and opportunities in developing respiratory syncytial virus therapeutics. *Journal of Infectious Diseases* 211, S1-S20.
203. Singh, R., Lillard, J.W., 2009. Nanoparticle-based targeted drug delivery. *Experimental and molecular pathology* 86, 215-223.
204. Singh, S.R., Tiwari, P.M., Dennis, V.A., 2014. Anti respiratory syncytial virus peptide functionalized gold nanoparticles. U.S. Patent No. 8,815,295. 26 Aug. 2014.
205. Small, D., 1981. The behavior of biological lipids. *Pure and Applied Chemistry* 53, 2095-2103.
206. Snyder, L., Dolan, J., Gant, J., 1979. Gradient elution in high-performance liquid chromatography: I. Theoretical basis for reversed-phase systems. *Journal of Chromatography A* 165, 3-30.
207. Snyder, L.R., Kirkland, J.J., Glajch, J.L., 2012. *Practical HPLC method development*. John Wiley & Sons.

208. Socaciu, C., Jessel, R., Diehl, H.A., 2000. Competitive carotenoid and cholesterol incorporation into liposomes: effects on membrane phase transition, fluidity, polarity and anisotropy. *Chemistry and physics of lipids* 106, 79-88.
209. Song, J.-Z., Chen, H.-F., Tian, S.-J., Sun, Z.-P., 1998. Determination of metformin in plasma by capillary electrophoresis using field-amplified sample stacking technique. *Journal of Chromatography B: Biomedical Sciences and Applications* 708, 277-283.
210. Stokes, C., Kaur, R., Edwards, M., Mondhe, M., Robinson, D., Prestwich, E., Hume, R., Marshall, C., Perrie, Y., O'Donnell, V.B., 2016. Human rhinovirus-induced inflammatory responses are inhibited by phosphatidylserine containing liposomes. *Mucosal immunology*.
211. Storm, G., Crommelin, D.J., 1998a. Liposomes: quo vadis? *Pharmaceutical Science & Technology Today* 1, 19-31.
212. Storm, G., Crommelin, D.J.A., 1998b. Liposomes: quo vadis? *Pharmaceutical Science & Technology Today* 1, 19-31.
213. Stover, R.J., Murthy, A.K., Nie, G.D., Gourisankar, S., Dear, B.J., Truskett, T.M., Sokolov, K.V., Johnston, K.P., 2014. Quenched assembly of NIR-active gold nanoclusters capped with strongly bound ligands by tuning particle charge via pH and salinity. *The Journal of Physical Chemistry C* 118, 14291-14298.
214. Stroock, A.D., Dertinger, S.K.W., Ajdari, A., Mezić, I., Stone, H.A., Whitesides, G.M., 2002. Chaotic Mixer for Microchannels. *Science* 295, 647-651.

215. Subczynski, W.K., Wisniewska, A., Yin, J.-J., Hyde, J.S., Kusumi, A., 1994. Hydrophobic barriers of lipid bilayer membranes formed by reduction of water penetration by alkyl chain unsaturation and cholesterol. *Biochemistry* 33, 7670-7681.
216. Szoka, F., Papahadjopoulos, D., 1978. Procedure for preparation of liposomes with large internal aqueous space and high capture by reverse-phase evaporation. *Proceedings of the National Academy of Sciences* 75, 4194-4198.
217. Tadros, T., Izquierdo, P., Esquena, J., Solans, C., 2004. Formation and stability of nano-emulsions. *Advances in colloid and interface science* 108, 303-318.
218. Tardi, P.G., Gallagher, R.C., Johnstone, S., Harasym, N., Webb, M., Bally, M.B., Mayer, L.D., 2007. Coencapsulation of irinotecan and floxuridine into low cholesterol-containing liposomes that coordinate drug release in vivo. *Biochimica et Biophysica Acta (BBA)-Biomembranes* 1768, 678-687.
219. Taylor, F., Huffman, M.D., Macedo, A.F., Moore, T.H., Burke, M., Davey Smith, G., Ward, K., Ebrahim, S., 2013. Statins for the primary prevention of cardiovascular disease. *The Cochrane Library*.
220. Terada, T., Nishikawa, M., Yamashita, F., Hashida, M., 2006. Influence of cholesterol composition on the association of serum mannan-binding proteins with mannosylated liposomes. *Biological and Pharmaceutical Bulletin* 29, 613-618.
221. Timsina, M., Martin, G., Marriott, C., Ganderton, D., Yianneskis, M., 1994. Drug delivery to the respiratory tract using dry powder inhalers. *International journal of pharmaceutics* 101, 1-13.

222. Tinner, H., 2016. Analysis of Difficult Polar Compounds using Sigma-Aldrich Ion Pair Reagents and Supelco Ascentis HPLC Columns, p. AnalytiX Volume 6 Article 4.
223. Tiwari, P.M., Eroglu, E., Bawage, S.S., Vig, K., Miller, M.E., Pillai, S., Dennis, V.A., Singh, S.R., 2014. Enhanced intracellular translocation and biodistribution of gold nanoparticles functionalized with a cell-penetrating peptide (VG-21) from vesicular stomatitis virus. *Biomaterials* 35, 9484-9494.
224. Torchilin, V.P., Rammohan, R., Weissig, V., Levchenko, T.S., 2001. TAT peptide on the surface of liposomes affords their efficient intracellular delivery even at low temperature and in the presence of metabolic inhibitors. *Proceedings of the National Academy of Sciences* 98, 8786-8791.
225. Uchegbu, I.F., Florence, A.T., 1995. Non-ionic surfactant vesicles (niosomes): Physical and pharmaceutical chemistry. *Advances in Colloid and Interface Science* 58, 1-55.
226. Uchegbu, I.F., Vyas, S.P., 1998a. Non-ionic surfactant based vesicles (niosomes) in drug delivery. *International Journal of Pharmaceutics* 172, 33-70.
227. Uchegbu, I.F., Vyas, S.P., 1998b. Non-ionic surfactant based vesicles (niosomes) in drug delivery. *International journal of pharmaceutics* 172, 33-70.
228. Vabbilisetty, P., Sun, X.-L., 2014. Liposome surface functionalization based on different anchoring lipids via Staudinger ligation. *Organic & biomolecular chemistry* 12, 1237-1244.
229. van Dissel, J.T., Joosten, S.A., Hoff, S.T., Soonawala, D., Prins, C., Hokey, D.A., O'Dee, D.M., Graves, A., Thierry-Carstensen, B., Andreasen, L.V., 2014. A novel liposomal

- adjuvant system, CAF01, promotes long-lived Mycobacterium tuberculosis-specific T-cell responses in human. *Vaccine* 32, 7098-7107.
230. Van Slooten, M., Boerman, O., Romøren, K., Kedar, E., Crommelin, D., Storm, G., 2001. Liposomes as sustained release system for human interferon- γ : biopharmaceutical aspects. *Biochimica et Biophysica Acta (BBA)-Molecular and Cell Biology of Lipids* 1530, 134-145.
231. Vigneri, R., Goldfine, I.D., 1987. Role of metformin in treatment of diabetes mellitus. *Diabetes care* 10, 118-122.
232. Vora, B., Khopade, A.J., Jain, N., 1998. Proniosome based transdermal delivery of levonorgestrel for effective contraception. *Journal of controlled release* 54, 149-165.
233. Wagner, A., Vorauer-Uhl, K., 2010. Liposome technology for industrial purposes. *Journal of drug delivery* 2011.
234. Wang, X., Quinn, P.J., 2002. Cubic phase is induced by cholesterol in the dispersion of 1-palmitoyl-2-oleoyl-phosphatidylethanolamine. *Biochimica et Biophysica Acta (BBA) - Biomembranes* 1564, 66-72.
235. Wanjari, M., There, A., Tajne, M., Chopde, C., Umathe, S., 2008. Rapid and simple RPHPLC method for the estimation of metformin in rat plasma. *Indian journal of pharmaceutical sciences* 70, 198.
236. Washburn, A.L., Gunn, L.C., Bailey, R.C., 2009. Label-free quantitation of a cancer biomarker in complex media using silicon photonic microring resonators. *Analytical chemistry* 81, 9499-9506.

237. Waterhouse, D.N., Madden, T.D., Cullis, P.R., Bally, M.B., Mayer, L.D., Webb, M.S., 2005. Preparation, Characterization, and Biological Analysis of Liposomal Formulations of Vincristine, in: Nejat, D. (Ed.), *Methods in Enzymology*. Academic Press, pp. 40-57.
238. Watzinger, F., Ebner, K., Lion, T., 2006. Detection and monitoring of virus infections by real-time PCR. *Molecular aspects of medicine* 27, 254-298.
239. Webb, M.S., Boman, N.L., Wiseman, D.J., Saxon, D., Sutton, K., Wong, K.F., Logan, P., Hope, M.J., 1998. Antibacterial efficacy against an in vivo *Salmonella typhimurium* infection model and pharmacokinetics of a liposomal ciprofloxacin formulation. *Antimicrobial agents and chemotherapy* 42, 45-52.
240. Wyde, P.R., 1998. Respiratory syncytial virus (RSV) disease and prospects for its control. *Antiviral Research* 39, 63-79.
241. Wyde, P.R., Gilbert, B.E., Ambrose, M.W., 1989. Comparison of the anti-respiratory syncytial virus activity and toxicity of papaverine hydrochloride and pyrazofurin in vitro and in vivo. *Antiviral research* 11, 15-26.
242. Wyde, P.R., Moore, D.K., Pimentel, D.M., Blough, H.A., 1995. Evaluation of the antiviral activity of N-(phosphonoacetyl)-l-aspartate against paramyxoviruses in tissue culture and against respiratory syncytial virus in cotton rats. *Antiviral research* 27, 59-69.
243. Yang, W., Yu, M., Sun, X., Woolley, A.T., 2010. Microdevices integrating affinity columns and capillary electrophoresis for multibiomarker analysis in human serum. *Lab on a Chip* 10, 2527-2533.

244. Yoshioka, T., Sternberg, B., Florence, A.T., 1994. Preparation and properties of vesicles (niosomes) of sorbitan monoesters (Span 20, 40, 60 and 80) and a sorbitan triester (Span 85). *International journal of pharmaceutics* 105, 1-6.
245. Young, R.V.T.S., Tabrizian, M., 2015. Rapid, one-step fabrication and loading of nanoscale 1, 2-distearoyl-sn-glycero-3-phosphocholine liposomes in a simple, double flow-focusing microfluidic device. *Biomicrofluidics* 9, 046501.
246. Yu, B., Lee, R.J., Lee, L.J., 2009. Microfluidic methods for production of liposomes. *Methods in enzymology* 465, 129-141.
247. Yuan, W., Kuai, R., Dai, Z., Yuan, Y., Zheng, N., Jiang, W., Noble, C., Hayes, M., Szoka, F.C., Schwendeman, A., 2016. Development of a Flow-Through USP-4 Apparatus Drug Release Assay to Evaluate Doxorubicin Liposomes. *The AAPS Journal*, 1-11.
248. Zhang, J., Zhang, Z., Yang, H., Tan, Q., Qin, S., Qiu, X., 2005. Lyophilized paclitaxel magnetoliposomes as a potential drug delivery system for breast carcinoma via parenteral administration: in vitro and in vivo studies. *Pharmaceutical research* 22, 573-583.
249. Zhao, X., Singh, M., Malashkevich, V.N., Kim, P.S., 2000. Structural characterization of the human respiratory syncytial virus fusion protein core. *Proceedings of the National Academy of Sciences* 97, 14172-14177.
250. Zook, J.M., Vreeland, W.N., 2010. Effects of temperature, acyl chain length, and flow-rate ratio on liposome formation and size in a microfluidic hydrodynamic focusing device. *Soft Matter* 6, 1352-1360.